AD-A059 704 LOCKHEED-CALIFORNIA CO BURBANK F/G 1/3
NATURAL ICING FLIGHT TESTS AND ADDITIONAL SIMULATED ICING TESTS--ETC(U)
JUL 78 R H COTTON DAAJ02-77-C-0002
UNCLASSIFIED LR-28240 USAAMRDL-TR-77-36 NL

1 OF 3
ADA
059704

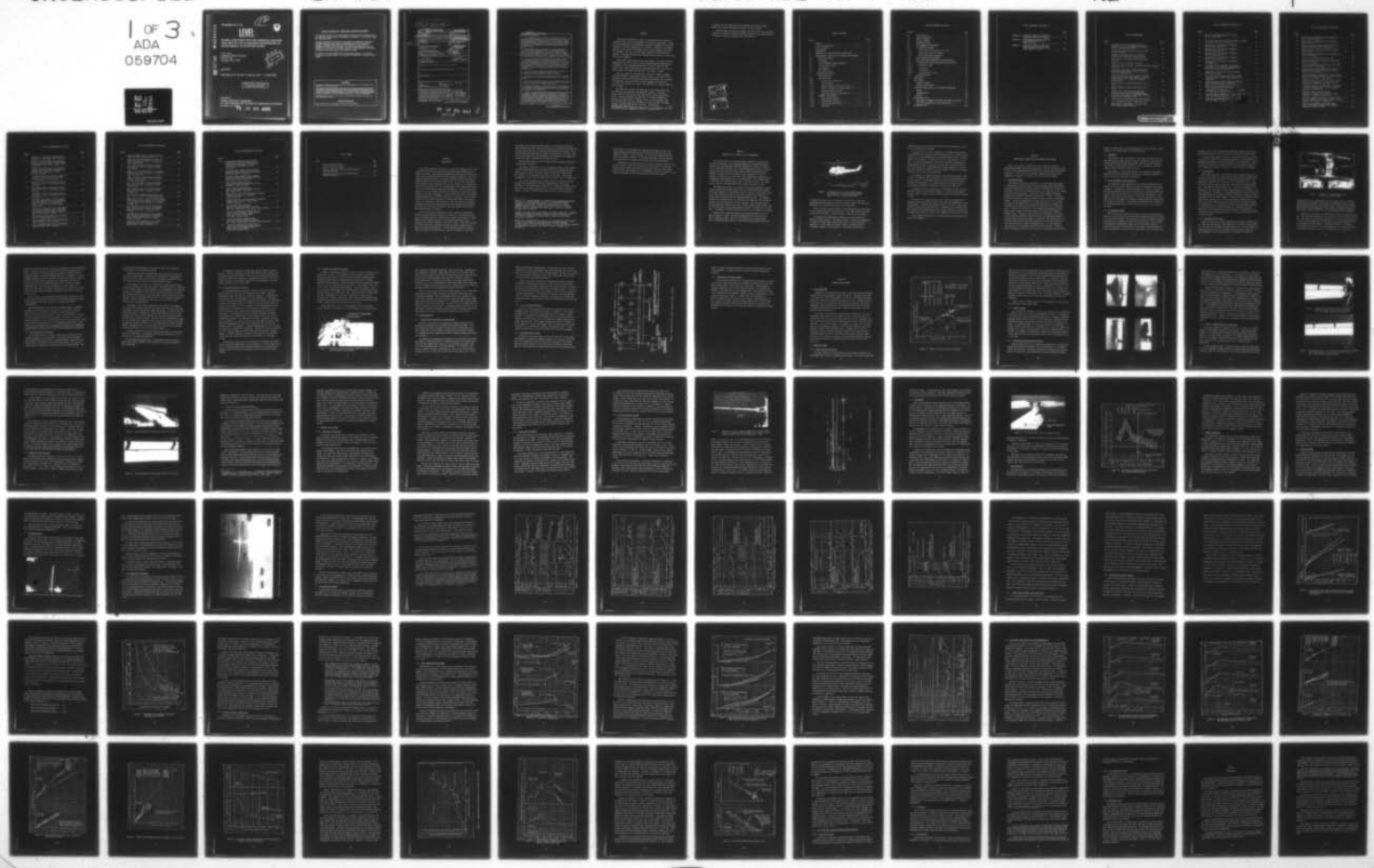

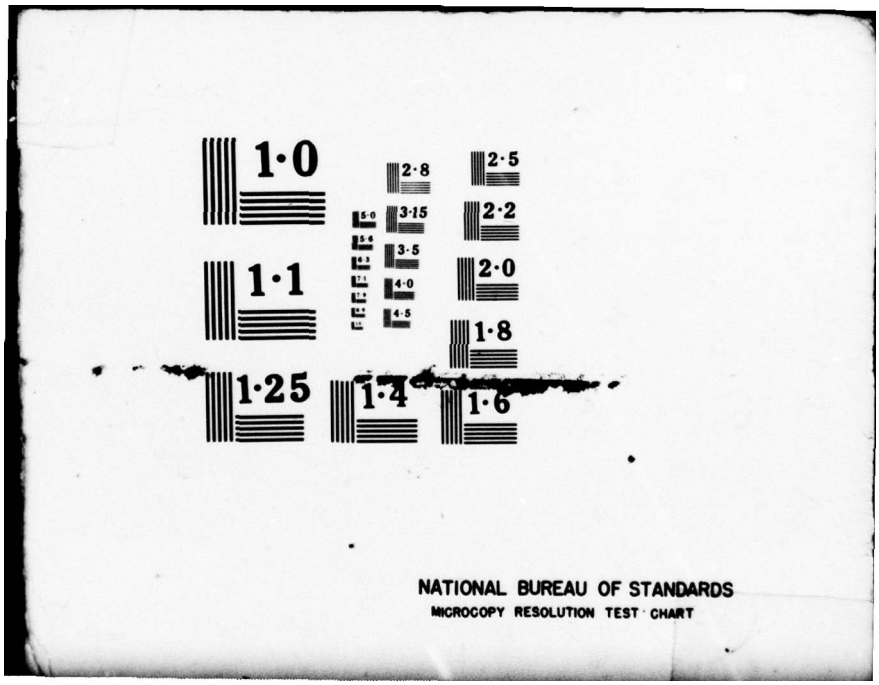
1·0
1·1
1·25
1·4
1·6
1·8
2·0
2·2
2·5
2·8
3·15
3·5
4·0
4·5
NATIONAL BUREAU OF STANDARDS
MICROCOPY RESOLUTION TEST CHART

12

USAAMRDL-TR-77-36

LEVEL II

NATURAL ICING FLIGHT TESTS AND ADDITIONAL SIMULATED ICING TESTS OF A UH-1H HELICOPTER INCORPORATING AN ELECTROTHERMAL ICE PROTECTION SYSTEM

R. H. Cotton
Lockheed-California Company
P.O. Box 551
Burbank, Calif. 91520

July 1978

Final Report for Period 17 February 1977 - 15 April 1977

Prepared for

APPLIED TECHNOLOGY LABORATORY
U. S. ARMY RESEARCH AND TECHNOLOGY LABORATORIES (AVRADCOM)
Fort Eustis, Va. 23604

APPLIED TECHNOLOGY LABORATORY POSITION STATEMENT

This Laboratory concurs in the findings presented in this report and recommends use of the information contained herein in the design and development of ice protection systems for rotary-wing aircraft.

This report documents the results of the first natural icing flight tests of the UH-1H electrothermal deicing system designed and developed by the Lockheed-California Company. Additional Ottawa Spray Rig tests, extending the work reported in USAAMRDL-TR-76-32, are also described. Due to the comparatively warm weather conditions, the test results are not entirely conclusive; further verification of the results in the spray rig and under natural icing conditions is needed.

Mr. Richard I. Adams was responsible for overall program guidance. Ms. Phyllis F. Kitchens was the project engineer. Both personnel are assigned to the Systems Support Division.

(14) LR-28240

Unclassified
SECURITY CLASSIFICATION OF THIS PAGE (When Data Entered)

REPORT DOCUMENTATION PAGE

READ INSTRUCTIONS BEFORE COMPLETING FORM

1. REPORT NUMBER: USAAMRDL-TR-77-36	2. GOVT ACCESSION NO.
3. RECIPIENT'S CATALOG NUMBER	
4. TITLE (and Subtitle): NATURAL ICING FLIGHT TESTS AND ADDITIONAL SIMULATED ICING TESTS OF A UH-1H HELICOPTER INCORPORATING AN ELECTROTHERMAL ICE PROTECTION SYSTEM	5. TYPE OF REPORT & PERIOD COVERED: Final Report for Period 17 Feb 1977 to 15 April 1977
6. PERFORMING ORG. REPORT NUMBER: Lockheed Report LR-28240	
7. AUTHOR(s): R. H. Cotton	8. CONTRACT OR GRANT NUMBER(s): DAAJ02-77-C-0002
9. PERFORMING ORGANIZATION NAME AND ADDRESS: Lockheed-California Company, P.O. Box 551, Burbank, California 91520	10. PROGRAM ELEMENT, PROJECT, TASK AREA & WORK UNIT NUMBERS: 63209A 1H263209D103 00 001 EK
11. CONTROLLING OFFICE NAME AND ADDRESS: Applied Technology Laboratory, U.S. Army Research and Technology Laboratories (AVRADCOM), Fort Eustis, VA 23604	12. REPORT DATE: July 1978 13. NUMBER OF PAGES: 204
14. MONITORING AGENCY NAME & ADDRESS (if different from Controlling Office): (12) 206 p.	15. SECURITY CLASS. (of this report): Unclassified 15a. DECLASSIFICATION/DOWNGRADING SCHEDULE

16. DISTRIBUTION STATEMENT (of this Report)

Approved for public release; distribution unlimited.

17. DISTRIBUTION STATEMENT (of the abstract entered in Block 20, if different from Report)

18. SUPPLEMENTARY NOTES

19. KEY WORDS (Continue on reverse side if necessary and identify by block number)

Ice	UH-1H	Flight Tests
Snow	Electrothermal Deicing	
Deicing System	Ice Protection	
Advanced Rotary Wing Aircraft	Ice Prevention	

20. ABSTRACT (Continue on reverse side if necessary and identify by block number)

Natural icing flights and additional simulated icing tests were accomplished with a UH-1H helicopter equipped with an advanced ice protection system. This testing was the third icing test program accomplished with the test aircraft, but the first to include natural icing conditions. The simulated icing tests were conducted in the National Research Council (NRC) spray rig at Ottawa, Canada. The natural icing flights were made from the Ottawa International Airport. → next page

DD FORM 1 JAN 73 1473 EDITION OF 1 NOV 65 IS OBSOLETE

Unclassified
SECURITY CLASSIFICATION OF THIS PAGE (When Data Entered)

209970

20. Abstract (continued)

The ice protection system incorporates an ac electrical system for operation of electrothermal main and tail rotor blade deicing and electrically heated windshields and stabilizer bar. Main rotor blade deicing is accomplished by heating each of six zones from tip to root in a spanwise sequence. The system can operate automatically at three different voltages controlled as a function of liquid water content (LWC) and has provisions for adjusting the heater-on time for each zone as a function of LWC and/or outside air temperature (OAT).

Seven tests in the spray rig and ten natural icing flights were made totaling 30.4 flight hours of icing testing. Icing was encountered on five of the natural icing flights. The icing conditions ranged from 0.15 gram per cubic meter ~~(g/m^3)~~ liquid water content at -18°C to 0.30 g/m^3 at -2°C. The aircraft operated in icing conditions on each of the flights from 40 minutes to a little over one hour. The number of main blade deicing cycles required under the conditions experienced varied from three to five.

The deicing and anti-icing systems performed satisfactorily under all conditions and no difficulty was experienced in operating the aircraft in the natural icing environment. The windshields remained clear of ice at all times. Although the engine air inlet screens collected some ice, there was no increase in the measured pressure drop across the screens. At altitudes near and above 10,000 feet, pilot workload was increased while flying on instruments with ice on the blades. An increase and decrease in 6 per rev vibration was noted also at these higher altitudes with the accretion and shedding of ice.

All of the previously experienced problems with the ice protection system appear to have been eliminated and further testing can be accomplished without any configuration changes to the system.

The results of the icing flights are discussed and data and information included that should aid others in the design and testing of ice protection systems.

Three different types of ice detection and rate measuring systems were utilized. Data were obtained from these systems that permitted an evaluation of the use of their output in scheduling blade deicing.

Data were obtained also that aid in defining the rotor blade spanwise surface temperature distribution in and out of an icing cloud, blade heating characteristics, heater-on time required, and the effects of inboard blade ice and runback on autorotational rpm.

Because of the comparatively limited ranges of liquid water concentration and outside air temperature encountered on the natural icing flights, it is recommended that additional icing tests be accomplished. This additional testing should include both simulated and natural icing to obtain more data needed to establish the correlation between these two modes of testing. In order to accomplish this objective, it is recommended that efforts be continued to develop a positive means of establishing the blade ice condition before and after deicing. Ideally such a system would provide for real time in-flight viewing but at least should provide for photographic recording.

PREFACE

The natural and simulated icing test program described herein was conducted under the direct management of the Eustis Directorate, U.S Army Air Mobility Research and Development Laboratory (USAAMRDL),* Fort Eustis, Virginia. From this organization, Mr. Richard I. Adams was the program manager and Ms. Phyllis F. Kitchens was the project engineer and onsite test manager. Both are from the Flight Controls and Subsystems Area, Applied Aeronautics Technical Area, Systems Support Division of the Eustis Directorate, USAAMRDL.

Three pilots participated in the test program: Mr. David W. Thomas, Engineering Test Pilot from the FAA New England Regional Headquarters; LT Michael L. Hill, Engineering Test Pilot from U.S. Naval Air Test Center (NATC); and CPT Eugene Mace, Operational Test Pilot from the U.S. Army Aircraft Development Test Activity, Fort Rucker, Alabama.

The test program was directed by Mr. Richard H. Cotton, Lockheed-California Company. Other onsite Lockheed support in the form of ice-protection system and instrumentation system maintenance, test planning, data analysis, and incorporation of design changes was provided by L.C. Macy, T.H. Oglesby, S.L. Kiser, W.A. Maynard, H.D. Carr, R. Metcalf, and R. Lennert.

The UH-1H test aircraft was maintained by SP6 Vernon Taylor from the 101st Airborne Division, Fort Campbell, Kentucky. The crash/rescue UH-1H aircraft and crew were also from the 101st Airborne Division. The crew consisted of pilots CW2 T. G. Beatty and WO1 W. C. Aylikci; crew chief SP4 T. G. Krause; SP5 W. A. Collier, medic, from HHC, 326th Medical Battalion; and SGT B. A. Kline and PFC H. M. Auman, firemen, from HHC 101st Airborne Division. Both the test

*Redesignated Applied Technology Laboratory, U.S. Army Research and Technology Laboratories (AVRADCOM), effective 1 September 1977.

and chase aircraft operated from the Canadian Forces Base (South), Hangar 12, at Ottawa International Airport, Ontario, Canada.

Program support at Ottawa for hangar and office facilities, logistics support and fabrication shop services was provided by the Canadian Forces at Hangar 12 under the command of MAJ John McTavish.

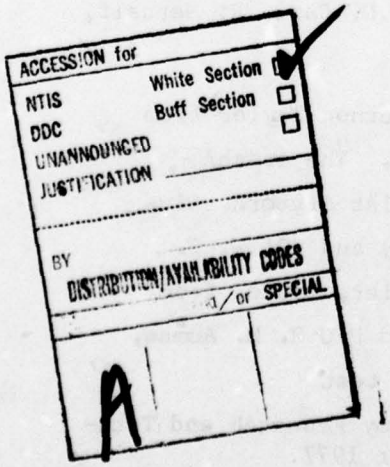

TABLE OF CONTENTS

TABLE OF CONTENTS (Continued)

TABLE OF CONTENTS (Continued)

LIST OF ILLUSTRATIONS

LIST OF ILLUSTRATIONS (Continued)

LIST OF ILLUSTRATIONS (Continued)

LIST OF ILLUSTRATIONS (Continued)

LIST OF ILLUSTRATIONS (Continued)

LIST OF ILLUSTRATIONS (Continued)

LIST OF TABLES

SECTION 1

INTRODUCTION

This report presents the results of natural and simulated icing tests conducted with an Army UH-1H helicopter equipped with an advanced ice-protection system. The system was designed and installed on the test aircraft by the Lockheed-California Company, Burbank, California. The test program described herein was a follow-on program to previous testing conducted in March 1975 and February/March 1976. The previous testing was under simulated icing conditions with the test objective of progressing to natural icing conditions as soon as satisfactory functioning and reliability of the ice-protection system were established. The 1975 program was conducted in forward flight using the CH-47 Helicopter Icing Spray System (HISS) at Moses Lake, Washington. Blade deicing and other ice-protection system performance was considered satisfactory. However, electrical short problems in the conductor wiring to the main blade heaters were experienced. The testing was terminated when it was found that the standpipe carrying the electrical wiring inside the rotor shaft had failed and had been the source of other intermittent electrical grounds that had been experienced during the program.

The 1976 program was conducted at Ottawa, Canada in the National Research Council's (NRC) icing spray rig facility. Satisfactory performance was demonstrated and a flight safety release was obtained to conduct natural icing flights but natural icing weather conditions did not materialize during the remainder of the test season. During this testing, electrical shorts were experienced between the heater element and the main rotor blade erosion shield. A blade teardown inspection conducted after the program indicated that the cause of the failures could have

been small voids between the bonded layers of the heater installation. Other possibilities were that the insulating later between the heater and the shield was too thin, or that there had been moisture ingress. Prior to the testing reported here, the heater installations on the main rotor blades were replaced and design changes were incorporated to improve the installation and to eliminate these suspect causes.

The detailed results of the two previous test programs are reported in References 1 through 3.

The primary objective of the 1977 program was natural icing testing. Ottawa was selected as the test location because it provided the opportunity for both natural icing and additional simulated icing testing and therefore for the maximum utilization of test time. The program encompassed a 55-day span at Ottawa from 17 February 1977 to 12 April 1977.

The aircraft preparation and flight checkout activity for the test program was accomplished at the Naval Weapons Center, China Lake, California. After satisfactory checkout of all systems including the new TACAN and ILS glideslope additions, the aircraft was flown to Ottawa, Canada. In order to minimize operating time on the limited quantity of

---

[1]Werner, J.B., THE DEVELOPMENT OF AN ADVANCED ANTI-ICING/DEICING CAPABILITY FOR U.S. ARMY HELICOPTERS, VOLUME II - ICE PROTECTION SYSTEM APPLICATION TO THE UH-1H HELICOPTER, Lockheed-California Company; USAAMRDL Technical Report 75-34B, Eustis Directorate, U.S. Army Air Mobility Research and Development Laboratory, Fort Eustis, Virginia, November 1975, AD A019049.

[2]USAAEFA Project No. 74-13, Final Report, ARTIFICIAL ICING TESTS, LOCKHEED ADVANCED ICE PROTECTION SYSTEM INSTALLED ON A UH-1H HELICOPTER, U.S. Army Aviation Engineering Flight Activity, Edwards Air Force Base, California, June 1975.

[3]Cotton, R.H., OTTAWA SPRAY RIG TESTS OF AN ICE PROTECTION SYSTEM APPLIED TO THE UH-1H HELICOPTER, Lockheed-California Company; USAAMRDL Technical Report 76-32, Eustis Directorate, U. S. Army Air Mobility Research and Development Laboratory, Fort Eustis, Virginia, November 1976, AD A034458.

test hardware, the sliprings were removed and the main and tail rotor blades replaced with standard ones for the ferry flight and then reinstalled at Ottawa. At the conclusion of the program, the aircraft was placed in storage at Ottawa. It is anticipated that additional natural icing testing will be conducted during the 1977/1978 winter season.

Presented and discussed herein are the test procedures used, the overall test results, data on the operation of three types of ice detector systems, blade surface temperature measurements, heater-on time optimization results, and general data and information that will be useful in the design and planning of other ice protection systems and testing.

SECTION 2

DESCRIPTION OF THE TEST UH-1H CONFIGURATION

The test aircraft is a UH-1H helicopter modified to incorporate an ice protection system. The system was designed by Lockheed-California Company and installed under a previous contract to evaluate an advanced anti-icing/deicing system concept. The modifications provide for electro-thermal deicing of the main and tail rotor blades, heated glass windshields, and heated anti-ice blankets on the stabilizer bar and tip weights. Electrical power for each of these components is supplied by an ac generator installed as part of the modification. The system includes a controller that utilizes inputs from an ice detector and an air temperature sensor to program blade deicing cycles and heater-on time.

The heated rotor blades are standard UH-1H blades modified by replacing the leading edge erosion shield with a new one incorporating etched-foil heater elements and associated electrical wiring. The inboard portion of the main blade span which has structural doublers was faired and a heated shield installed over the smoothed surface contour. The outboard section of the erosion shield is .030-inch steel material, and the inboard portion over the doublers is .016-inch aluminum. The tail rotor blade erosion shield was replaced with one of electro-formed nickel material that is .030 inch thick at the leading edge and tapers to .010 inch at the trail-edge. The inboard or doubler portion of the tail rotor blade is not heated.

The main rotor blade incorporates six separately heated zones, as shown in Figure 1, that are activated sequentially from tip to root to effect spanwise deicing. The tail rotor blades have a single heated zone. The heating power density of the main blade varies with zone from

Figure 1. In-flight Photo of the Test UH-1H Showing the Boundaries of the Six Spanwise Deicing Heater Zones on the Main Rotor Blade

26 watts/in^2 at the root to 12 watts/in^2 at the tip to utilize the aerodynamic heating generated by blade rotational speed. The tail rotor blade heats at a uniform power density of 20 watts/in^2.

The ac electrical power leads are routed inside the main rotor shaft to slip rings installed on top of the hub. Slip rings are also provided on the tail rotor shaft to route the power to the tail rotor blades.

For research and development purposes, the deicing system can operate at three voltages - 160, 200, or 230 Vac - which are programmed as a function of liquid water concentration (LWC). This provides the capability to cycle through the heater zones at different rates to accommodate changes in icing severity. The system controller also

includes provisions for adjusting the heater-on and heater-off times to aid in optimizing blade deicing.

The stabilizer bar and tip weights are continuously heated during icing conditions to provide an anti-icing capability at 5 watts psi with 200 volts, ac. The windshields are of laminated glass with a tin oxide (NESA) film in between. At 200 volts, ac, they are heated at 3.3 watts psi. The total power demand of the various ac-operated components is approximately 25.4 kVA at 200 Vac or 16.3 kVA and 33.6 kVA at 160 and 230 Vac, respectively. The distribution is approximately 13.2 kVA for main rotor blades, 4.0 kVA for tail rotor blades, 3.0 kVA for the stabilizer bar, and 5.2 kVA for the windshield.

The outside air temperature input to the deicing controller is provided by a flush-type surface temperature sensor located under the nose of the aircraft. Two different types of ice detectors were installed initially for evaluation: an infrared type and an ultrasonic type. A third system utilizing the inferential principle was added later.

The engine air inlet configuration is unmodified and does not incorporate any special ice protection features. In addition, the engine air inlet filter screens were left installed during all testing conducted to date.

The lateral tilt angle of the FM radio antenna was increased 15 degrees per the standard UH-1H modification work order (MWO) prior to any icing testing to provide more clearance from the tail rotor plane based on previous Army icing test experience. Subsequent test experience with this configuration showed more tilt was needed; therefore, an additional 15 degrees were added for a total of 42.5 degrees from the vertical plane.

A more complete description of the system and the modifications can be found in Reference 1.

SECTION 3

CONFIGURATION CHANGES FOR THE CURRENT TEST PROGRAM

Since the initial installation of the ice protection system, developmental changes have been incorporated to improve function and reliability. Those made between the previous test programs were described in Reference 3. This section of this report describes the changes made subsequent to Reference 3 and prior to the current test program.

3.1 MAIN ROTOR BLADES

New heater installations were made to the outer blade with changes to eliminate the electrical short-to-ground problems experienced between the heater element and the erosion shield, to eliminate the surface discontinuity at station 83 between the steel and the aluminum, and to provide for better moisture sealing. The outboard erosion shield and heater elements were removed and replaced with new ones. The new installation had thicker insulation material between the erosion shield and the heater element. The heater elements were shifted inboard 0.25 inch to reduce the width of the unheated band at the manufacturing joint between the aluminum and the steel erosion shields at blade station 83 (29 percent span). A better fit between all of the leading edge components (steel shield, heater element, and blade contour) was achieved to minimize possible voids. A positive moisture seal was incorporated in the form of more heater edge distance and application of a polysulfide sealing material under and around all edges. In addition, the inboard end of the .030-inch steel erosion shield was chem-milled in five .003-inch-deep x .50-inch-wide steps to reduce the thickness over a 2.5-inch length to .015 inch thick, to mate flush with the .016-inch aluminum. This was done to eliminate the surface discontinuity at the station 83 joint that

caused ice hangup and as a design improvement to reduce stresses in the bonding at the inboard edge of the erosion shield.

3.2 CONTROLLER

The problem of heater zone skip in the deicing controller that had been experienced during testing to date was eliminated. Although this problem was experienced only during hangar checkout and was associated with heating during extended operation, it was considered a potential flight problem and therefore was corrected.

Improvements in the internal wiring of the controller were made to eliminate all of the unsupported runs that were considered potential strain conditions on the solder connections.

3.3 UH-1H INSTRUMENT FLIGHT CAPABILITY

The instrument flight capability of the UH-1H was augmented by the addition of Tactical Air Navigation (TACAN), ILS glideslope and a radar altimeter. The TACAN was considered necessary to be able to operate in the designated ICECAP test area at Ottawa without requiring ground radar control. The ILS glideslope was to facilitate an IFR recovery to the airport in the event it was necessary. The radar altimeter was for possible use to aid an engine-out emergency landing under low ceiling and/or low visibility conditions. These systems were installed and checked out at the Naval Weapons Center in China Lake, California, prior to going to Ottawa.

3.4 AC ELECTRICAL SYSTEM

The ac electrical system incorporated a floating electrical ground feature to provide positive protection against shorts-to-ground that could cause rotor blade damage. This protection system, as originally designed, was voided when an external ac power unit was connected to the aircraft in the hangar for maintenance checks of the blade heater system. An isolation transformer was installed in the aircraft wiring between the ac circuit breakers and the main and tail rotor power relays to provide the

protection from a rotor blade short during hangar checkout and to gain operational experience with the system incorporating this modification.

Although changes based on laboratory tests had been made to correct the problem of a delay in the ac generator coming on the line under low temperature conditions, the problem continued to be experienced. Prior to this year's testing, an arbitrary reduction in the generator regulator trip frequency was made in an attempt to further evaluate the problem.

3.5 ICE DETECTION

One of the objectives of the UH-1H icing test program has been to evaluate various types of ice detector and icing ratemeter systems which are needed to supply a LWC input to the blade deicing controller. Two systems have been installed during most of the testing to date. These were both accretion-type ice detectors. One was the infrared-occlusion type. The other was the ultrasonic type. Last year a nonaccretion or inferential type was added but proper functioning was not obtained. All three systems are considered in a development state at least as applied to helicopter operations, and have undergone configuration changes by their manufacturers for each test program. The detectors are mounted on 12-inch high pylons or masts on top of the forward cabin as shown in Figure 2. The 12-inch high location was selected based on previous UH-1H testing that indicated it to be necessary to assure a high impingement probability from the flow aft of the windshield top. Simulated icing test experience to date has indicated that this height is excessive but any changes have been deferred until natural icing with smaller droplet sizes has been evaluated.

3.5.1 Infrared-Occlusion Type

This ice detector system was designed by the supplier specifically for helicopter application. The sensing unit or probe is located inside of a duct that is anti-iced with engine bleed air. It also utilizes the engine bleed air to create a jet-pump action and induce a high rate of flow of ambient air over the sensing unit to provide an icing rate

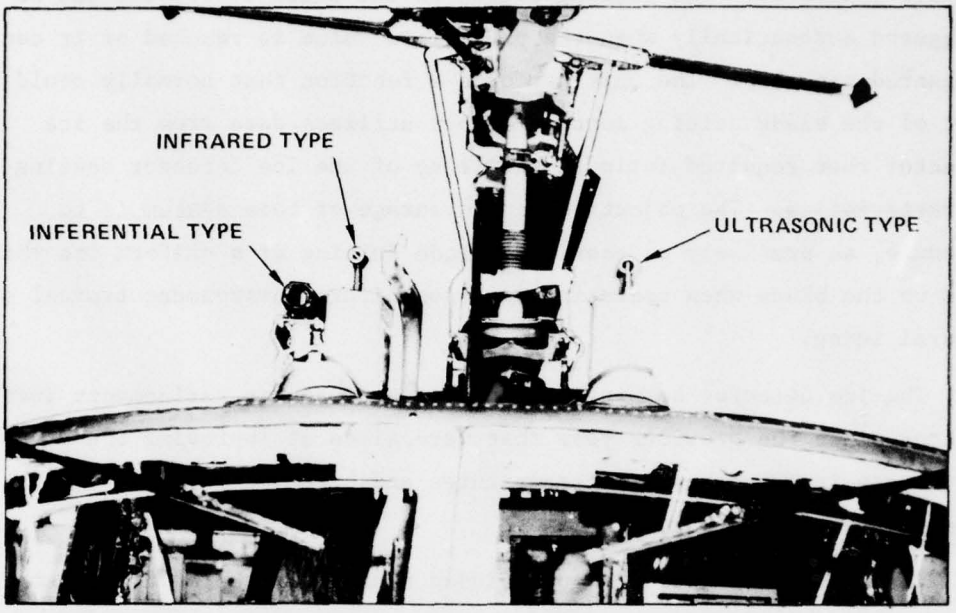

Figure 2. Ice Detector Installations on the Top of the Forward Fuselage

indication in hover. Calibrations show flow velocity over the sensing element with 50 psig bleed pressure is approximately 140 knots at hover and 175 knots at a 90-knot cruise speed. The thickness of ice accreted on the probe between icing cycles was .013 inch. The cycle time of this probe varies from 75 seconds at low LWC values to 8 seconds or less for LWC values of $1.0 g/m^3$ or greater. Thus, in heavy icing the LWC display, which updates every time the probe is deiced, changes every 8 seconds.

Another feature added to the system this year was an Integrating Rate Unit (IRU) which would provide a deicing signal to the rotor blade controller. The output is based on the integration of icing rate with respect to time and the IRU signals when the equivalent to a given thickness of ice on the blades has been accreted. The system provides for a display of the incremental buildup of ice on the sensing probe, a totalizing counter for display of the sum of accreted ice thickness, and a selector for

inserting the value of the sum at which it is desired to have blade deicing occur. A calculated value was used initially and then adjusted as test results indicated. The deicing signal to the blade controller can be triggered automatically when the prescribed value is reached or it can be triggered manually. The unit performs a function that normally could be part of the blade deicing controller but utilizes data from the ice detector that requires intimate knowledge of the ice detector sensing characteristics. The objective and advantage of this system is to schedule, as precisely as possible, blade deicing at a uniform ice thickness on the blade when operating in a nonuniform environment typical of natural icing.

The ice detector sensing head had several design refinements incorporated since the previous year that were aimed at improving the accuracy of the sensing at near zero temperatures and high liquid water concentrations.

The test installation also included a digital counter to register the number of ice detector cycles that occur. One cycle is the time interval for the ice detector to accrete a fixed thickness of ice, electrothermally deice, and recover to start another accretion. The number of ice detector cycles that correspond to the time to accrete the desired thickness of ice on the rotor blade can be used to provide a signal to the blade deicing controller and thus schedule blade deicing. This method is not as precise as a true integrating system; cycle counting may be sufficiently accurate but more extensive testing over a wide range of conditions will be necessary before this can be established conclusively.

3.5.2 Ultrasonic-Type Ice Detector

The ultrasonic-type ice detector utilizes a vibrating probe which changes frequency as ice is accreted. For application to helicopter zero airspeed operations (hover), a separate aspirator shroud that uses engine bleed air was added to the basic configuration. The jet pump action induces a high-velocity airflow over the ice sensing probe. The

flow velocity over the sensor is 110 knots at hover and 155 knots at cruise speed with 40 psig bleed pressure.

The system includes a ratemeter that outputs an analog voltage signal that is proportional to liquid water concentration. During probe deice and recovery time, a hold circuit is utilized to maintain the last rate output until the sensor is functioning normally again.

The thickness of ice that is accreted on the probe between deicing cycles was increased from .040 inch, used in previous testing, to .080 inch for the current program. This adjustment was accomplished by the supplier to reduce the percentage of time that the probe was deicing and recovering and thus result in an icing severity (LWC) readout closer to full time. The cycle time of this probe varied from 0.7 to 5.0 minutes from high to low LWC. This was considerably longer than the cycle time for the .040-inch ice thickness setting.

In addition to the longer cycle time for the probe, the ratemeter hold circuit that retains the last LWC reading while the probe deices and cools down to start measuring rate again was changed. Originally the hold circuit was based on a fixed time. Under some conditions, it was found that the hold circuit was insufficient, and the rate indication would go to zero until the probe recovered. The hold circuit was modified to sense the rate voltage output signal from the probe and hold from the time probe deicing was initiated (.080 inch of ice buildup) until the output voltage reached a threshold value that would ensure that the probe had recovered and was indicating the rate of ice accretion properly.

A digital counter in the cockpit displayed the number of probe deice cycles, for evaluation in scheduling blade deicing, the same as for the infrared type as mentioned previously.

A rate integrating system could be implemented using this detector system based on the ratemeter output voltage, but it was not done during this program.

As originally configured, the aspirator shroud blocked the lower portion of the vibrating probe and thus affected the proper operation of the sensor under some conditions. For this test program, the aspirator had been modified by the supplier by incorporating a notch in the shroud, thereby permitting the original length of the sensing probe to be completely exposed to the icing airflow.

3.5.2 Inferential-Type Ice Detector

The inferential-type ice detector consists of two heated sensing probes located in line, with one downstream of the other. Both are electrically heated to maintain a constant temperature. The leading one is exposed to the icing environment and the trailing one is shielded in a way to separate the moisture particles from the airflow. The difference in electrical current necessary to maintain the leading probe (which is cooled by any moisture in the air stream) at the same temperature as the shielded probe, is converted to a signal which is processed by a rate-meter and outputted as a liquid water concentration value (grams per cubic meter). The sensing head of this system incorporates a temperature switch that is combined with the LWC signal to infer that icing conditions are present. For this year's testing, the supplier incorporated an aspirator to provide for airflow over the sensor in hover. This detector was mounted on the side of the same pylon (RH) on which the infrared detector was mounted. A separate engine bleed air line was used to provide an air supply for this system. The bleed air used was from the line that normally feeds the sand and dust particle separator scavenge system. A pressure regulator, provided by the supplier, was installed in the line that limited the airflow to the detector to 18 psig and 5 scfm.

An electronic control unit was furnished by the supplier that generated a blade deice signal based on the integration of the LWC signal with time. A cockpit display of the computed accumulation of ice was incorporated as well as provisions for adjusting the trip value for blade deicing.

3.5.4 Visual Ice Accretion Indicator

A means of providing the flight crew with a visual indication of ice buildup was utilized. It consisted of a short section of an airfoil mounted on struts about 12 inches above the copilot's overhead window. Extending forward from the leading edge of the airfoil was a small diameter probe graduated in .2-inch increments for use in gaging the thickness of ice on the leading edge of the airfoil. The indicator was viewed by the copilot through the overhead window. After one flight, it was found that the window fogged under some conditions, which prevented viewing the detector, and there was no way to deice the airfoil between blade deicings. Subsequently, the visual indicator was relocated to the copilot's door adjacent to eye level. This proved very satisfactory and was easily deiced in flight with the aid of a stick through the copilot's window. Figure 3 shows the installation on the door.

The thickness ratio (t/c) of the miniature airfoil section was within 1 percent of the main rotor blade thickness and thus resulted in a

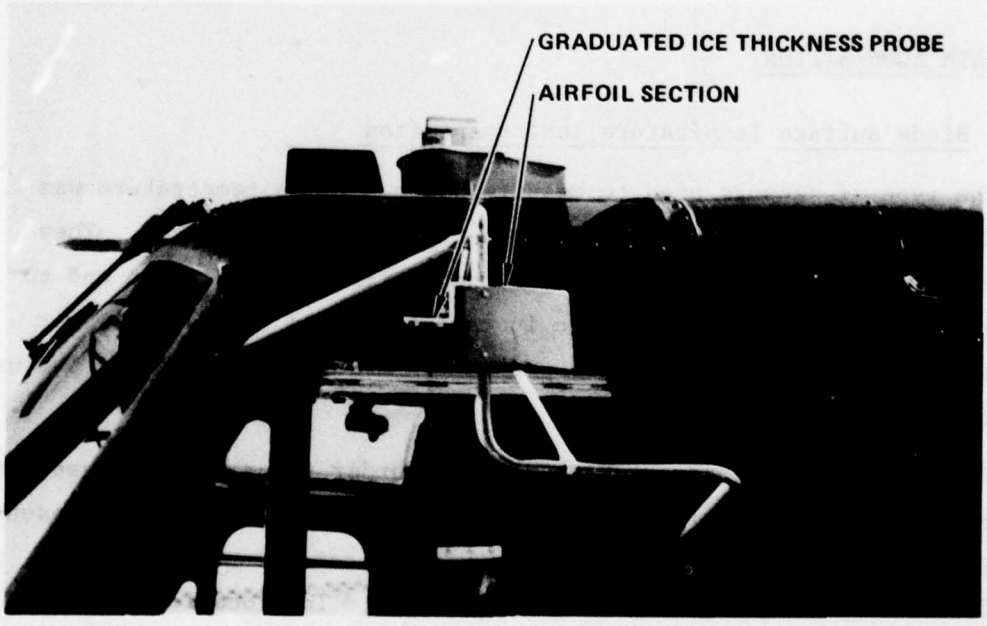

Figure 3. Visual Ice Accretion Indicator Mounted on Copilot's Door Following a Spray Rig Test

catch efficiency reasonably comparable to the rotor blade. Accounting for the difference in velocity (flight speed for the airfoil section versus rotor rotational speed at the 50 percent span point on the blade) the ice thickness on the probe between deice cycles was planned to provide a simple indication of probable ice thickness on the blade leading edge (velocity at R = 0.5 is approximately three times flight speed; therefore, the ice thickness on the main blade would be approximately three times the thickness accreted on the fuselage-mounted airfoil section).

The ice on the airfoil section was deiced manually on each main rotor blade deice cycle in order to maintain an accurate indication of the ice thickness buildup. The ice thickness increase on a component is not linear due to changes in catch efficiency as the size and/or shape changes under various LWC and OAT conditions (i.e., mushroom shape versus pointed shape and/or clear versus rime ice). Usually the ice was removed from the airfoil section only on one side of the graduated probe and the ice on the other side allowed to accumulate in order to provide a rough indication of the maximum ice buildup on unprotected components of the aircraft.

3.6 DATA ACQUISITION

3.6.1 Blade Surface Temperature Instrumentation

The type of sensors used to measure blade surface temperature was changed from thermocouples to resistance-type temperature gages. They were changed in order to provide a smoother surface installation and to improve accuracy. The thermocouple installations had tended to impair ice shedding and had an unresolved problem in absolute temperature measurement accuracy.

In addition, more sensors were added in order to provide at least one measurement in each heater zone. A temperature sensor was located essentially at the midspan point of each of the six heater zones and 1 inch back from the leading edge on the lower surface. The location 1 inch back was chosen to provide a measurement as close to the leading edge as possible and thus be under the ice accreted on the blade but aft of the

erosion area along the leading edge. It was found that the 1 inch aft location was too near the leading edge at the 89 percent span location in zone 1 and the gage was lost due to erosion damage. The next one, inboard at 70 percent span, also showed erosion wear and required repair along the leading edge of the gage periodically.

Figure 4 shows the locations of the temperature sensors and their relationship to heater zone boundaries. Note that the erosion shield material is .016-inch-thick aluminum over the inboard "doubler" portion of the blade and .030-inch-thick steel over the outboard portion. The junction of these materials falls in the center of zone 5, which is heated at a uniform power density. The difference in material type and thickness results in different heating rates, which compromises the determination of optimum heater-on time for this zone as will be discussed later in this report.

3.6.2 Data Quick-Look Capability

The small portable ground station used for onsite strip-out of the FM magnetic tape was modified to increase its capability. The previous configuration was limited to 10 discriminators and utilized a six-pen recorder. An additional 10 discriminators were incorporated, as well as replacing the pen recorder with a 50-channel oscillograph equipped with a Data Rite magazine. These changes considerably reduced the number of passes required to extract the pertinent data from the tape and provided the capability to review high frequency vibration-type data. A voice channel was added also to record in-flight radio and intercom comments.

3.6.3 Hub-Mounted Blade Camera

The built-in electrical heater of the 16 mm main rotor blade camera was modified to increase the internal heating. An additional heater was added, the temperature control switches were relocated to the outside case, and the air sealing of the insulating hood around the camera was improved. Unfortunately, the heated viewing window in the lens enclosure

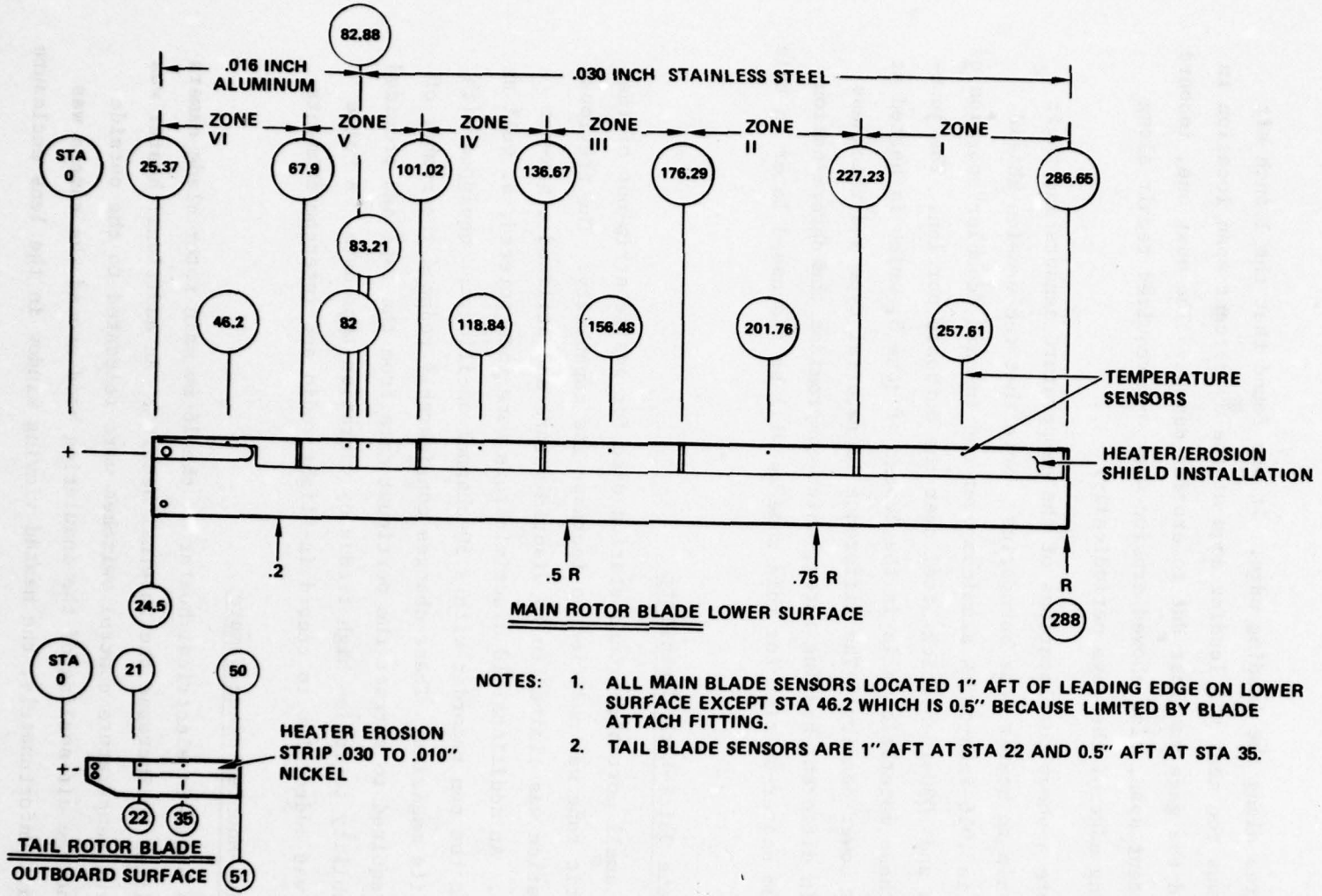

NOTES:
1. ALL MAIN BLADE SENSORS LOCATED 1" AFT OF LEADING EDGE ON LOWER SURFACE EXCEPT STA 46.2 WHICH IS 0.5" BECAUSE LIMITED BY BLADE ATTACH FITTING.
2. TAIL BLADE SENSORS ARE 1" AFT AT STA 22 AND 0.5" AFT AT STA 35.

Figure 4. Main and Tail Rotor Blade Temperature Sensor Locations

failed to operate and went unnoticed due to the long turnaround time for film processing. No usable pictures of blade ice and/or deicing were obtained.

3.6.4 Fuselage-Mounted Blade Camera

A second camera installation to photograph main rotor blade ice condition from the nonrotating system was designed and fabricated this year but never reached flight status during the program span. The government-supplied system was to use a 35 mm camera installed in an enclosure and mounted on the right-hand external armament rack. The camera was to face the aft right-hand rotor quadrant, viewing up, and be synchronized to photograph the blade lower surface. A strobe light was incorporated to provide illumination of the blade's lower surface. The capability to be able to assess in-flight icing and deicing conditions on the rotor blade is considered extremely desirable and almost mandatory; therefore, the development of this type of an installation should be continued for future testing.

SECTION 4

DISCUSSION AND RESULTS

4.1 TEST CONDITIONS

A summary of the simulated and natural icing test conditions obtained during the 1977 test program is shown in Figure 5. Simulated icing tests in the NRC spray rig were conducted in the $-2^{o}C$ to $-9^{o}C$ temperature range with most of the runs at temperatures warmer than $-5^{o}C$. Although the primary objectives of the spray rig testing were accomplished, this limited temperature range and especially the predominately near $0^{o}C$ conditions precluded the satisfactory completion of some of the secondary but technically valuable objectives.

The natural icing conditions encountered were generally in the same temperature range except for one flight at $-18^{o}C$. The liquid water concentrations found on the natural icing flights were also considerably lower than the desired test criterion representing the continuous maximum icing condition. Also shown on Figure 5, to present the range of all testing to date, are the conditions evaluated in the previous simulated icing flight programs of March 1975 and February 1976. Although a broad range of conditions has been covered, additional natural and simulated testing is considered highly desirable to increase the LWC range of natural icing testing so as to cover the continuous and intermittent maximum conditions and to complete specific investigations that can only be done in the spray rig.

4.2 SPRAY RIG TESTS

4.2.1 Spray Rig Test Objectives

The tests conducted in the NRC spray rig had specific objectives for this program and others to supplement previous data. The initial objectives

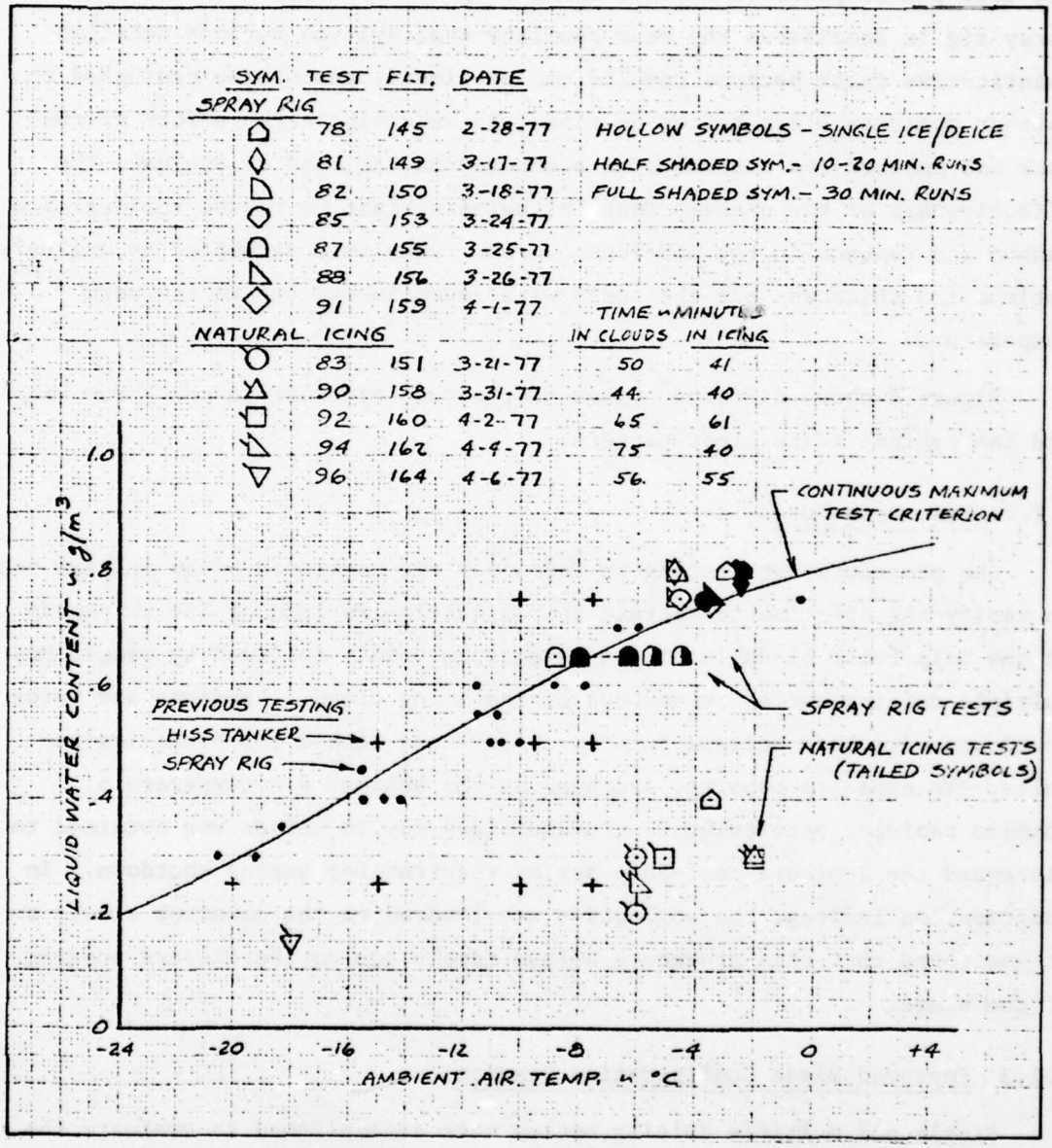

Figure 5. Summary of UH-1H Icing Test Conditions

were to verify that the overall main rotor blade deicing effectiveness was unaffected by the extra thickness of insulating material incorporated in the heater installation, and to provide icing testing indoctrination for the test pilots prior to natural icing flights. In addition, since the spray rig is considered the best facility available to perform detailed quantitative tests because results can be viewed, tests were conducted to further evaluate blade heater-on times, to investigate the effect of runback and inboard ice accretion on autorotation rpm, and to evaluate the effectiveness of the changes made in the main blade to reduce residual ice hangup and runback in the mid-zone 5 area. Runs were attempted to evaluate optimum ice thickness but the tests were inconclusive due to the warm temperature.

Figure 6 shows different views of the test aircraft in the spray rig and the typical icing cloud pattern.

4.2.2 Test Procedure

The procedure for testing in the spray rig consisted of an initial run to verify the off-time to accrete approximately 1/4 inch of ice thickness at the main rotor blade leading edge midspan point, followed by single and multiple deicing cycles in and out of the icing cloud. Landings and rotor shutdowns were made between runs to observe and record the blade ice results. To expedite testing, and because the ambient air temperature changes rapidly, particularly on a cloudless day, a waiver was obtained to disregard the 2-minute cool-down period required for engine shutdown. In addition, on landing, the collective was lowered to the downstop slowly as it was found that this procedure helped retain ice on the inboard portion of the blade.

4.2.3 Improved Blade Configuration Results

Single and multiple deicing cycles were accomplished to evaluate the improved main blade heater/erosion shield installation of the reworked blades used this year. The amount of residual ice hangup on the leading edge at the station 83 junction between the steel and aluminum erosion

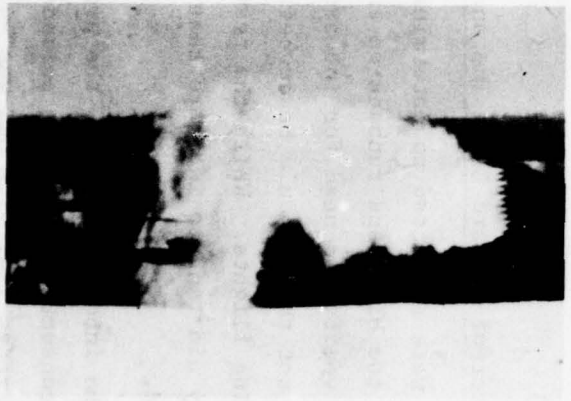

Figure 6. Different Views of the Test Aircraft Operating in the NRC Spray Rig

shield material was considerably reduced but not completely eliminated by the smoother joint of the new blades. It was apparent that any surface discontinuity can impair blade deicing to some degree and therefore should be avoided. For example, on occasions where a marginal heater-on time was used, ice would be retained on the blade which had the temperature sensors and strain gages installed whereas the other blade would be perfectly clean.

There was still repeated evidence of runback from the inboard heated area (zones 4, 5, and 6) even on the short heater-on time runs. The magnitude of the runback is not considered to be particularly severe since it appears that the number of deicing cycles, and therefore the amount of runback, that will occur on a typical natural icing flight will probably not be significantly different than viewed in the spray rig testing. Runback does imply an imperfect and undesirable blade deicing characteristic, however. The analysis of the blade surface temperature data obtained this year, as discussed in Section 4.11, indicates that the runback probably cannot be entirely eliminated because of the difference in erosion shield material covering zone 5, which is heated at a uniform power density, as described previously. Figures 7 and 8 show the excellent deicing results experienced this year, marred only by the runback from the inboard half of zone 5.

4.2.4 Effect of Inboard Blade Ice and Runback

Tests were conducted to determine the effect of ice on the inboard portion of the blade and runback on autorotation. This was done in an attempt to verify the need for inboard blade deicing and to establish whether or not there should be concern over probable runback during the natural icing flights. While the results were not as conclusive as desired, they did tend to indicate that safety of flight was not compromised.

For the inboard ice test, the procedure was to enter the spray cloud for three consecutive off-time periods, accreting ice on the blade and deicing only zones 1-4. The OAT was $-4.5^{o}C$ and the cloud LWC was 0.75 g/m^3.

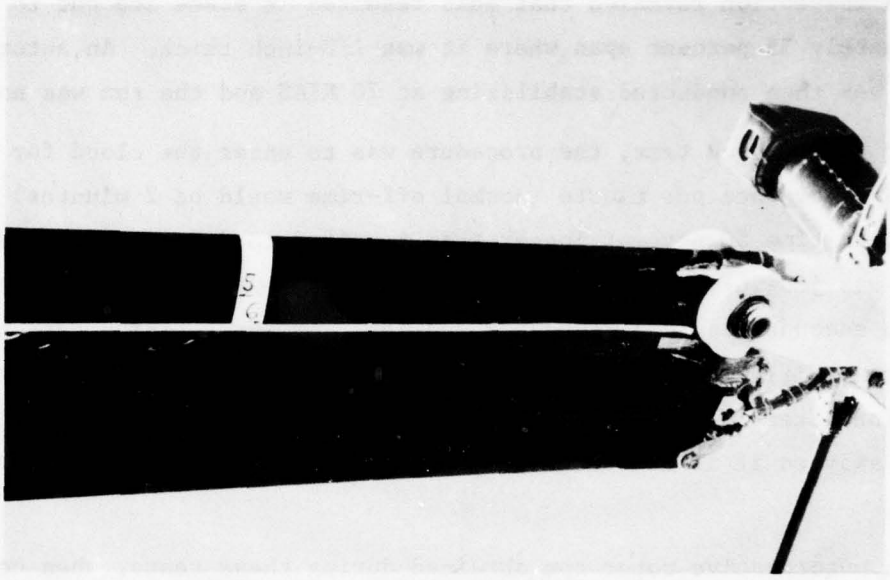

FLT 155 B

Figure 7. Satisfactory Main Rotor Blade Deicing Results, Zone 6 and Inboard Zone 5 on Spray Rig Test 5 ($-7^{o}C$, 0.65 g/m^3, 30-Minute Spray Rig Run)

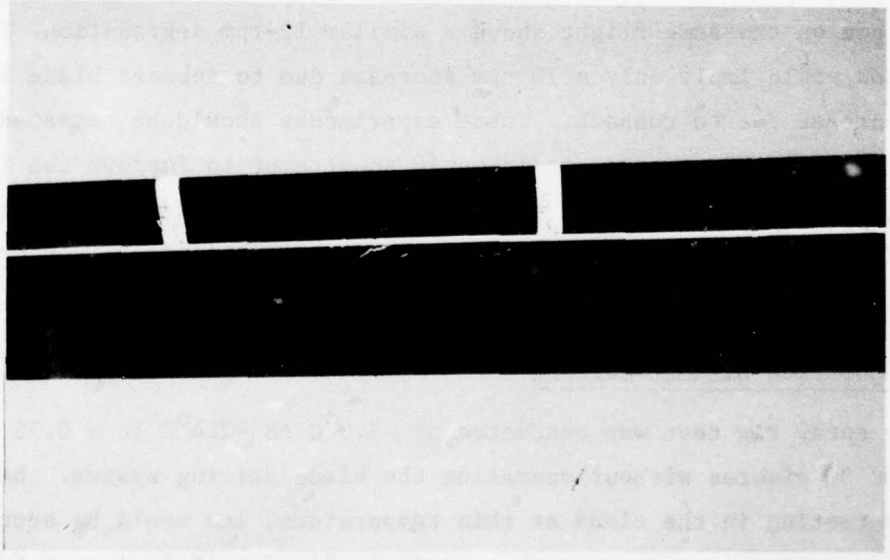

FLT 155 A

Figure 8. Satisfactory Zone 6, 5, and Inboard 4 Deicing Results Showing Only Slight Runback from Zone 5 Aluminum Area ($-7^{o}C$, 0.65 g/m^3, 30-Minute Spray Rig Run)

Post-run inspection revealed that this resulted in blade ice out to approximately 35 percent span where it was 1/8-inch thick. An autorotation descent was then conducted stabilizing at 70 KIAS and the rpm was noted.

For the runback test, the procedure was to enter the cloud for 10 minutes and deice once per minute (normal off-time would be 2 minutes) using a heater-on time 50 percent longer than required to deice. The resulting runback was judged to be severe by the spray rig operator and as much as would be encountered (see Figures 9 and 10). An autorotation descent was made as expeditiously as possible following the ice accretion. Post-flight inspection after the descent showed that all of the runback ice had sublimated away so it is not known exactly what the condition was during the descent.

The autorotative rotor rpm obtained during these tests, when compared with data from another flight without ice on the blade but at the same aircraft gross weight, indicated a 22 rpm decrease due to inboard blade ice and approximately a 12 rpm decrease due to runback. Some doubt is placed on the accuracy of the data because another descent with no ice on the blades made on the same flight shows a similar 12-rpm degradation. This comparison would imply only a 10 rpm decrease due to inboard blade ice and 0 rpm decrease due to runback. These experiments should be repeated under a lower ambient temperature condition in an attempt to improve the ice retention. It is felt, however, that the results that were obtained tended to verify the need for inboard blade deicing and to eliminate concern for runback that might be experienced during natural icing flights.

4.2.5 Operation Without Deicing

One spray rig test was conducted at $-3.5^{\circ}C$ to $-2.4^{\circ}C$ in a 0.75 g/m^3 cloud for 30 minutes without operating the blade deicing system. Based on previous testing in the cloud at this temperature, ice would be accreted out to approximately midspan with a nominal off-time of 2 minutes for 1/4-inch ice at R = 0.5. Blade ice was observed to self-shed at 8 to 10-minute intervals. There were no vibration changes noted; therefore, the

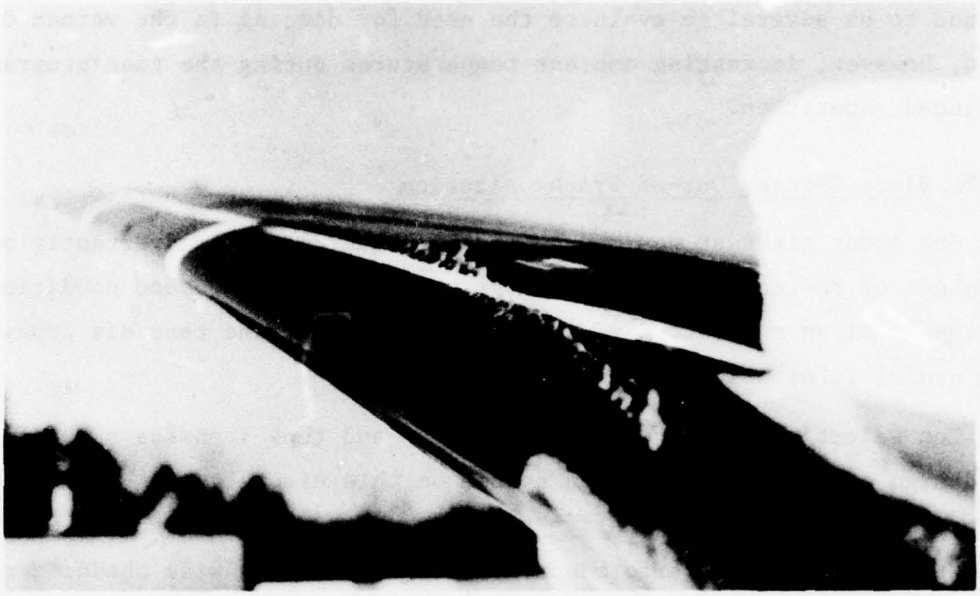

Figure 9. Induced Runback on Upper Blade Surface from Zone 6

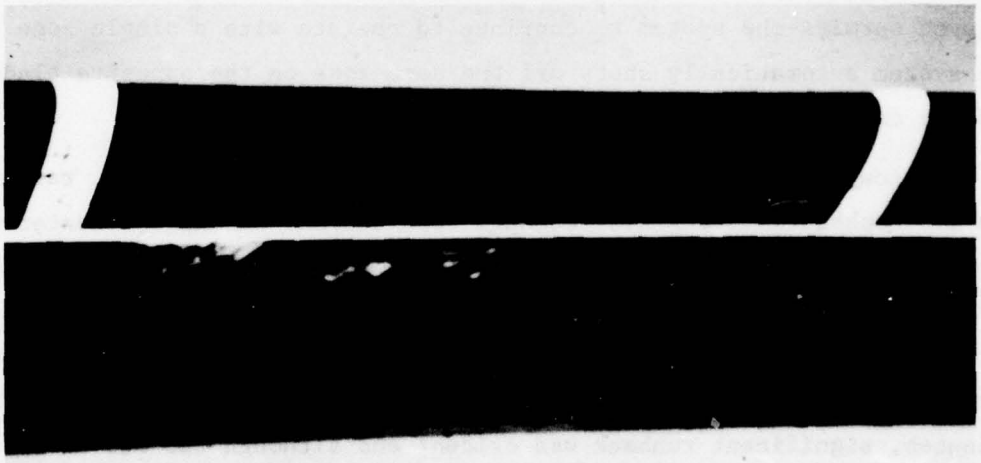

Figure 10. Induced Runback on Lower Blade Surface Aft of Zone 5

shedding was symmetrical from both blades. This test was one of what was planned to be several to evaluate the need for deicing in the warmer OAT range, however, increasing ambient temperatures during the test program span precluded repetition.

4.2.6 Blade Deicing Out-of-Synchronization

One spray rig test was made with the heater zones inadvertently operating out of the design sequence. The out-of-design sequence condition was the result of an undetected wiring hookup error but the test did provide some useful information on failure mode operation.

The selection of spanwise-heated zones and thus spanwise shedding for the design of the ice protection system on this aircraft was based partially on the results of the comparative testing reported in Reference 4 which demonstrated a decided performance advantage for a spanwise shedding system. Another consideration was that only a relatively limited percentage of the total blade span would be affected aerodynamically in the event of a single zone failure. In turn, this led to the conclusion that a single zone failure could be tolerated; therefore, the design controller logic that was employed permits the system to continue to operate with a single zone failed. (The system automatically shuts off the same zone on the opposite blade to preclude asymmetric shedding.)

The zone heating sequence on the test was 5, 6, 1, 2, 3, 4, rather than 1-6 consecutively. This sequence resulted in the inboard heaters (zones 5 and 6) being cycled while there was still ice on the adjacent outboard zone (zone 4). A shorter-than-normal on-time was used for zone 4. For single ice accretion and deicing cycles, the blade deiced properly; however, after a 15-minute immersion with deicing cycles activated every 2 minutes, significant runback was evident and although the mid-chord ice

---

[4] Stallabrass, J. R., and Gibbard, G. A., A COMPARISON BETWEEN SPANWISE AND CHORDWISE METHODS OF HELICOPTER ROTOR BLADE DE-ICING, National Research Council of Canada Aeronautical Report LR-270, January 1960.

was gone, the leading edge ice on all three inboard zones remained. The 15-minute immersion was repeated using a longer off-time to increase the ice thickness prior to deicing and a shorter on-time to reduce the runback but no change in deicing effectiveness was noted. Post-test analysis indicates that the runback was caused by the excessive heater-on time for zones 5 and 6 which were being heated for the time normally programmed for zones 1 and 2. It also appears that the presence of zone 4 ice prevented zones 5 and 6 from shedding. This makes the design philosophy of permitting the system to continue to operate with one heater zone inoperative questionable, at least for the inboard portion of the blade where centrifugal shedding forces are lower. More testing of simulated single zone failures appears necessary to verify the validity of the single zone failure design philosophy as applied to the spanwise shedding blade deicing concept.

4.3 NATURAL ICING FLIGHTS

4.3.1 Operational Procedures

The natural icing flights were conducted in the ICECAP test area south of Ottawa International Airport. The ICECAP test area is a reserved airspace controlled by the Canadian Ministry of Transportation that is bounded by the 110° and the 210° radials and ranges of 15 nmi and 28 nmi from the Ottawa TACAN station.

A crash/rescue UH-1H helicopter accompanied the test aircraft on all natural icing flights. While the test aircraft was operating in the clouds, the chase UH-1H would remain at approximately 1000 feet above ground level (AGL) under visual flight conditions on the 15-mile edge of the ICECAP area. Upon termination of a natural icing flight, a VFR rendezvous would be accomplished with the test aircraft to permit external visual observation and photography of ice accretions on the test aircraft. When conditions permitted, the rendezvous was accomplished at altitudes higher than 1000 feet, if the temperature was lower, in an attempt to retain as much ice as possible for documentation.

Initially, base weather station information was used to decide when to launch a natural icing flight. However, it was found that the best procedure was to have the aircraft available as much of the time as possible and to launch whenever there were clouds in the ICECAP area and suitable departure and enroute conditions were present.

The test aircraft would attempt to search out the darkest cloud area in the ICECAP area, enter it and climb to the desired OAT and/or LWC condition. It was soon evident that when icing was encountered, it existed within an extremely limited airspace. After finding icing conditions, it was necessary to climb or turn frequently in order to stay in the icing environment. A running plot of altitude, air temperature, and TACAN location was maintained by the flight crew to aid in predicting where icing might be expected and to define the boundaries once it was encountered. Typical plots are included as supplemental information (see Figures 37 and 38 in Section 6.2).

The safety-of-flight release that governed the program required a 1500-foot ceiling and 1-mile visibility conditions from the Ottawa airport to and including the ICECAP test area and also required a planned VFR return. These limitations resulted in missing several good natural icing test opportunities. It was found that by the time the ceiling lifted to the required 1500 feet at the airport and the test aircraft reached the test area, the storm passage was almost complete and the weather was improving rapidly. The result was that the test area would have a broken cloud condition with limited icing for a first flight of the day and usually scattered clouds to clear by the time a second turnaround flight was attempted. During the program, 10 natural icing flights were launched. Icing was found on five and none was found on the second flight of the day.

The test crew consisted of a pilot, copilot, and two flight test engineers. The pilots alternated the task of flying and operating the aircraft in the IFR environment as well as evaluating the ice protection system functioning and performance. The engineers monitored the various indications from the ice detection systems, operated the ice protection system,

maintained running logs of pertinent test data parameters utilizing a special test instrumentation console that extended aft of the pilot's station, and assisted the pilots in assessing the flight situation.

In order to accomplish a gradual buildup approach to the ice accumulation on the unprotected portions of the aircraft, natural icing flights were limited initially to a maximum time exposure in the icing environment between visual observations by the chase helicopter, equivalent to four rotor blade deice cycles. Subsequent exposures were to be limited to progressive increases in the number of blade deice cycles. This method of using blade deice cycles rather than a time buildup was designed to allow for variations in LWC that might be encountered. During the program the maximum exposure never exceeded the four blade deicing cycles, because of fuel limitations of the aircraft and the low levels of LWC that were encountered.

4.3.2 Deicing Test Procedure

One of the objectives of the natural icing testing was to evaluate several methods or systems for programming blade deicing with a consistent ice thickness on the blade. For this purpose, the test instrumentation included ice detector cycle counters for both of the two accretion-type detectors, and two rate integrating systems. Both rate integrating systems included cockpit readouts of the accumulative total of ice buildup. In addition, a visual ice accretion probe was monitored.

All blade deicings were to be initiated manually by the flight crew until the estimated trip-point values based on counts or integrated rate units were verified or different experimental values established. The controller was capable of receiving either a manual or an automatic deice signal. Completely automatic operation was not attempted until the last natural icing flight due to the difficulty in identifying and correcting the problem with the OAT signal which was being affected by cabin temperature changes. (Section 4.8 discusses this problem in more detail.)

During the blade ice accretion periods (heater-off time), the indications of all of the ice detector systems were monitored and the deicing cycle initiated when the crew judged the appropriate point had been reached. Sample flight test cards used on the natural icing flights including the various indications on which the judgement was based are presented as supplemental data in Tables 3 and 4 in Section 6.2. Engine torque was monitored but the concept of a change in torque required was found to be relatively useless as a deicing cue because of the constantly changing conditions utilized to maintain flight in the icing environment.

4.3.3 Main Rotor Blade Deicing

Blade deicing was accomplished in natural icing each time the blades had accreted an estimated 1/4 inch of ice on the midspan leading edge. This point was determined from the indications of the ice detector systems as explained previously. Normally, the deicing cycle was completed without any detectable change in vibration or aircraft handling qualities apparent to the flight crew. In fact, there was no in-flight means of positively assessing blade deicing effectiveness. A hub camera was installed and operated in an attempt to photograph the blade ice condition but unfortunately there were no satisfactory or useable pictures obtained.

As mentioned previously, a typical icing flight in 0.2 to 0.3 g/m^3 liquid water concentration resulted in only 3 or 4 deicing cycles. After return to base and landing, the blades were found to be clear of ice except on the one flight at $-18^{o}C$ OAT. On this flight, there was some residual leading-edge ice on the stepped portion of the steel erosion shield approximately from station 83 to 89 (Figure 11). There was no evidence of runback.

On two natural icing flights, an increase and decrease in amplitude of the 6-per-rev (6P) vibration was noted during blade ice accretion and deice shedding. These were the only times that the 6P vibration change was apparent on any of the deicing cycles accomplished to date, including the simulated icing tests behind the Helicopter Icing Spray System (HISS)

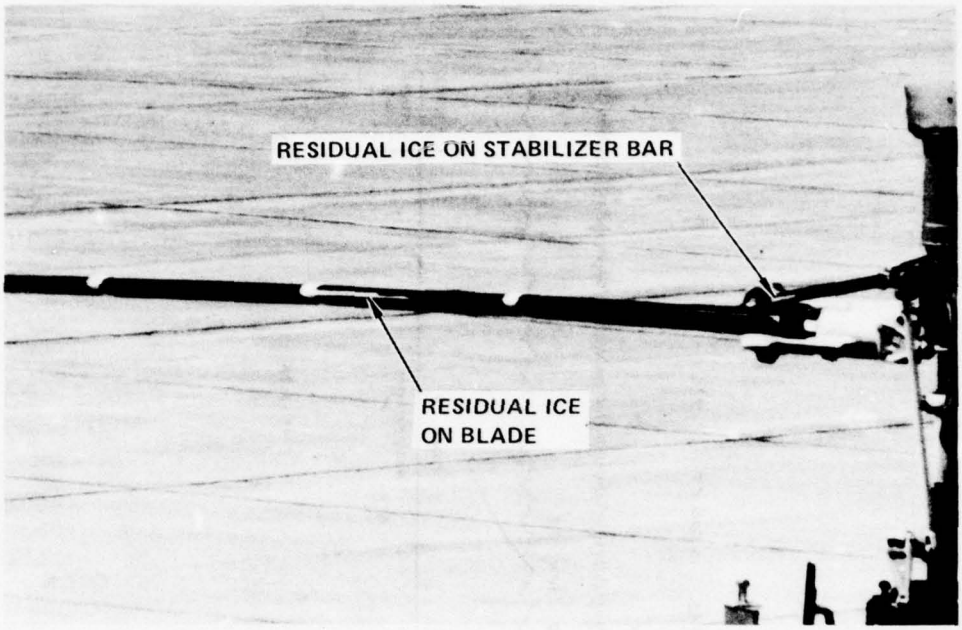

Figure 11. Residual Ice on the Stepped Leading Edge Surface of Zone 5 and on the Stabilizer Bar on Return from a Natural Icing Flight through a Broken Cloud Condition at -18°C

tanker or in the spray rig. The instrumentation test records showed the 6P vibration change in the cg vertical acceleration and in main rotor blade flapwise bending measurements. Figure 12 shows typical tracings. The reduction in amplitude occurs immediately following zone 2 heater-on time application, indicating the ice in the 60 to 80 percent span area was the cause. The condition occurred during the only two icing encounters at 9500 feet and 10,500 feet pressure altitude and was more pronounced at 10,500 feet. The OAT was -5 and -6°C, respectively. Examination of the blade response curves indicates that the third flapwise bending mode probably was affected. If the phenomenon were to occur all of the time, it would provide a good natural indication that the blades were icing and the deicing system was operating effectively. Unfortunately, it appears that it only occurs at the higher collective blade angle setting, as no amplitude change was noted or apparent on the test records at

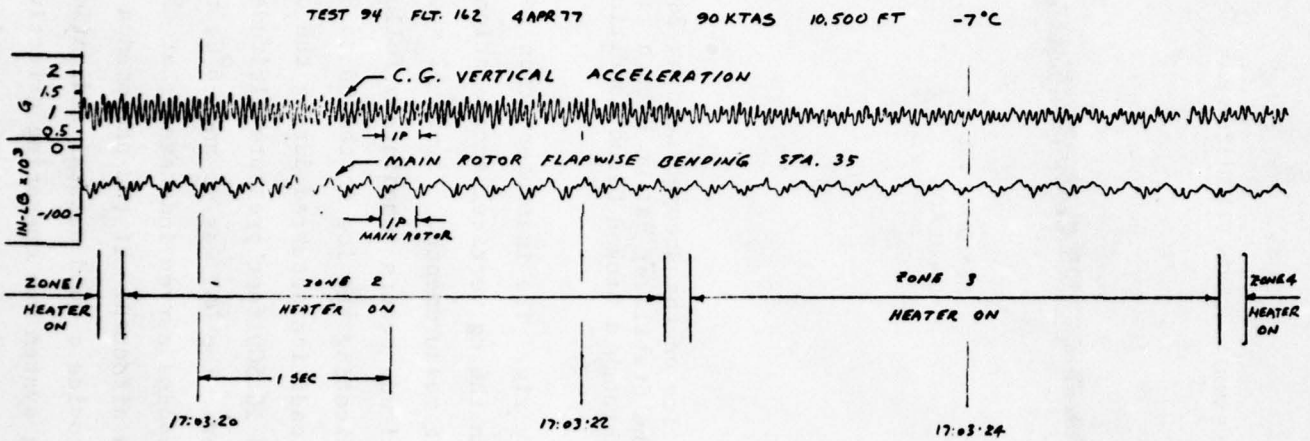

Figure 12. 6-Per-Rev Vibration Change During Blade Deicing

7500 feet or below. It also points out that blade stresses can be affected by operation in icing conditions. The pilots reported an increase in workload was experienced flying under these increased vibration periods.

4.3.4 Tail Rotor

Early in the testing at Ottawa and prior to any of the natural icing flights, failure of the tail rotor slipring bearings was experienced. Because the time to refurbish the installation was estimated to be excessive for the remaining test program span and prior test experience with the UH-1H did not indicate a positive need for tail rotor blade deicing, the sliprings were removed and left off. A safety-of-flight release to operate in the spray rig and in natural icing without blade deicing capability was obtained with some OAT limitations. The release was based on the evidence that the air temperature at the tail rotor with the infrared (IR) suppressor installed is above 0°C due to engine exhaust heating.

To supplement this information and to provide a direct indication of tail air temperature to the flight crew, a total air temperature probe was installed on the fin adjacent to the tail rotor plane at blade spanwise station 23 or 0.45 R (Figure 13). Clear air flight investigation showed that the exhaust plume with the infrared suppressor installed apparently rode to the left of the fin on the side of the tail rotor and slightly high. The tail air temperature could be increased with left sideslip and/or a pushover and decreased by the reverse.

A survey of the variation of tail air temperature with sideslip angle as measured by the sensing probe is shown in Figure 14. Sideslip is presented in terms of ball displacement of the turn-and-slip indicator. A calibration check using a RH windshield-located yaw string indicated that a one-quarter ball displacement was equivalent to 10 degrees of sideslip angle. This data shows good agreement between the measured air temperature and blade surface temperature which verifies accuracy and indicates that the air temperature at the tail rotor is approximately 20 degrees warmer than ambient in clear air due to exhaust heating. The abrupt decrease in indicated temperature to the left probably indicates that the

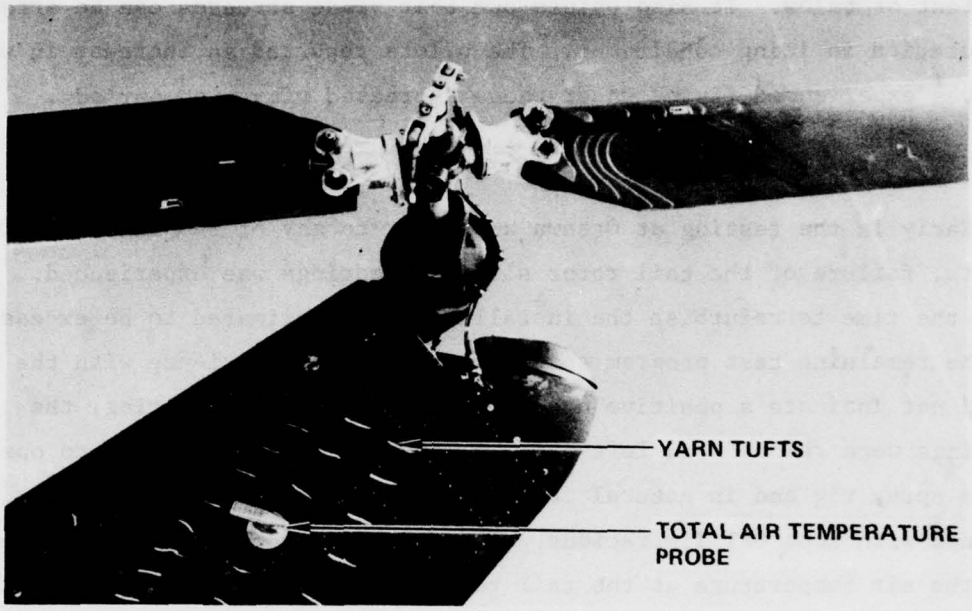

Figure 13. Tail Fin-Mounted Total Air Temperature Probe

maximum sensing angle of the temperature sensor was exceeded (approximately 30 degrees of sideslip).

On natural icing flights, if the tail air temperature was to decrease below 0°C, the aircraft would be sideslipped to increase the temperature periodically. No evidence of blade ice or runback was noted following any of the flights.

There was no data collected without the IR suppressor installed but the indications from icing testing to date, in which the tail rotor blades remained clear but the hub and the fin collect ice, are that the heat plume is much lower but still to the left side.

4.4 STABILIZER BAR

The stabilizer bar anti-icing effectiveness has been demonstrated in previous spray rig testing. No evidence to the contrary was apparent on the natural icing flights except on the flight at -18°C which was made in

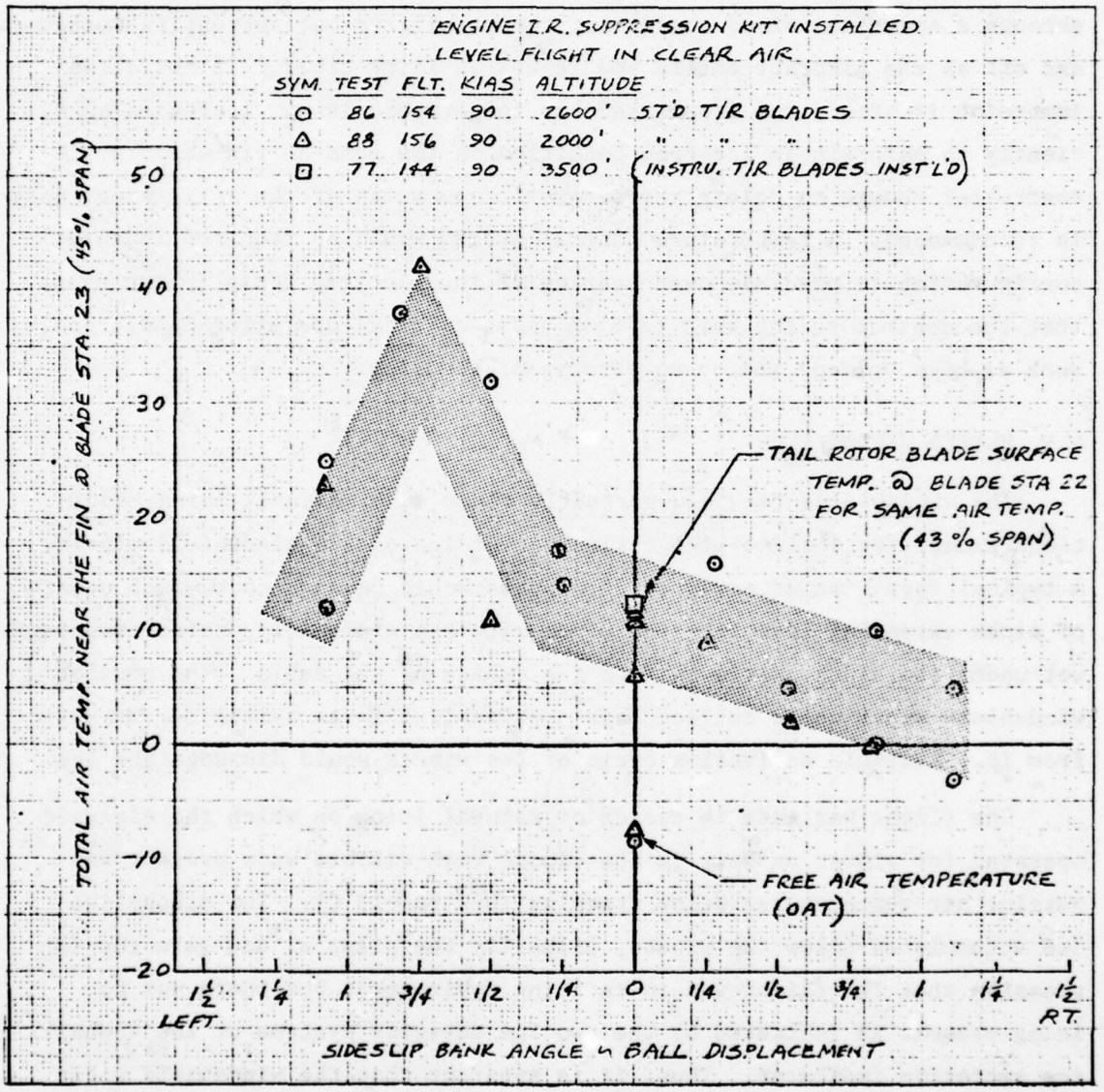

Figure 14. Increased Air Temperature at the Tail Rotor Due to Engine Exhaust Heating

a broken-to-scattered cloud condition. On this flight, some residual ice was present on the outer portion of the bar upon return to the airport (Figure 11). This is the result of the present logic in the ice protection system controller. Currently, the stabilizer bar is not heated unless icing conditions are sensed by the system. Thus, in a flight such as this one through a scattered cloud condition, the stabilizer bar current is turned on and off as the aircraft enters and leaves an icing cloud. If the cloud immersion is brief, the stabilizer bar temperature is not increased sufficiently to maintain an ice-free condition on the arms or tip weights. A controller change to delete the automatic operation of the anti-icing system is recommended. A temperature control system would be required in this configuration to preclude over-heating of the electric boots in the event that the control switch were left on under critical operating conditions, such as high voltage and/or no aerodynamic cooling.

4.5 HEATED WINDSHIELDS

The windshields remained perfectly clear under natural icing conditions except for a slush-like collection of ice on the windshield wipers. A typical formation after 40 to 50 minutes would be an 8-to 10-inch square of slush extending down from the wiper with the windshield surface running wet under the slush as viewed from the inside of the cabin. The copilot's windshield wiper would collect less - probably a 5- to 6-inch square down from it. A single activation cycle of the wipers would dislodge the ice.

One flight was made in search of natural icing on which the aircraft operated for almost an hour in the clouds with visible snow present and outside air temperatures below freezing ($0^{\circ}C$ to $-13^{\circ}C$). The slush-like ice accumulated below the wipers, primarily the pilot's, and gave the impression that the flight was in an icing environment but there was no icing present as indicated by the two ice detector systems or the visual ice accretion indicator. Thus, it is apparent that the windshield wiper icing cannot be used as an icing indicator.

Testing to determine the minimum windshield heating requirements was attempted by operating in natural icing with the voltage reduced from 200 Vac which gives 3.3 watts psi to 80 Vac. The test was inconclusive, however, because even at the reduced voltage no appreciable ice formed on the three-inch unheated bordering edge of glass around the heated portion of the windshield. This characteristic was experienced in all of the spray rig testing to date also. It appears that under some conditions cabin heat is sufficient to keep the windshield reasonably warm and clear. This condition agrees with UH-1H experience reported by the U.S. Army Aviation Engineering Flight Activity (USAAEFA). They reported that prior use of cabin heat (preheating) can significantly delay the formation of ice on the windshield after entering a natural icing cloud. Apparently, cabin heat will have to be left off or at least treated as a test variable in future testing and zero voltage to the windshield used initially to establish a baseline for a particular flight evaluation.

In previously conducted spray cloud tests behind the CH-47 HISS, minimum cabin heat was used for other reasons but the unheated edges of the windshield always collected appreciable amounts of ice (see photos in References 1 and 2). This condition must be attributable to the larger droplet size of the HISS cloud (150 microns vs 20 microns), and points out the conservatism of HISS testing results.

4.6 FM RADIO ANTENNA

Previous test experience has shown that ice accumulation on the tail-mounted FM whip antenna results in an oscillation of the antenna that can reach an amplitude sufficient to strike the tail rotor blades. This has occurred even with the maintenance work order (MWO) wedge installed that increases the lateral tilt of the antenna from 12.5 degrees to 27.5 degrees from the vertical. The test aircraft incorporated an additional 15 degrees of tilt or a total of 42.5 degrees. On the icing flight at -18°C, the chase aircraft noted the antenna tip oscillating laterally in a 36-inch arc. A rime ice formation extended approximately 1 inch forward on the outboard 12 inches of antenna span. Tail rotor plane clearance with this tilt angle

was approximately 18 inches. On another flight at -15°C, 4 inches of ice were observed on the antenna with no abnormal motions occuring. Figure 15 shows the antenna after landing with a portion of the ice still attached. The 42.5-degree configuration appears adequate for future testing.

There has been no formal avionics evaluation made of the effect of this increased tilt on FM antenna performance. This will be necessary for a final configuration determination.

4.7 UNPROTECTED AREAS

The natural icing flights did not reveal any problem with the unprotected areas of the aircraft for the conditions encountered. As described previously, the test procedure was to increase the exposure time incrementally so that the ice buildup on the unprotected areas could be monitored. Visual observations from the chase UH-1H reported ice on the skid crosstubes, engine inlet air filter side screens, synchronized elevator, VOR antenna, 42-degree gearbox fairing and the vertical fin. There was more ice on these areas on the right side of the aircraft than on the left

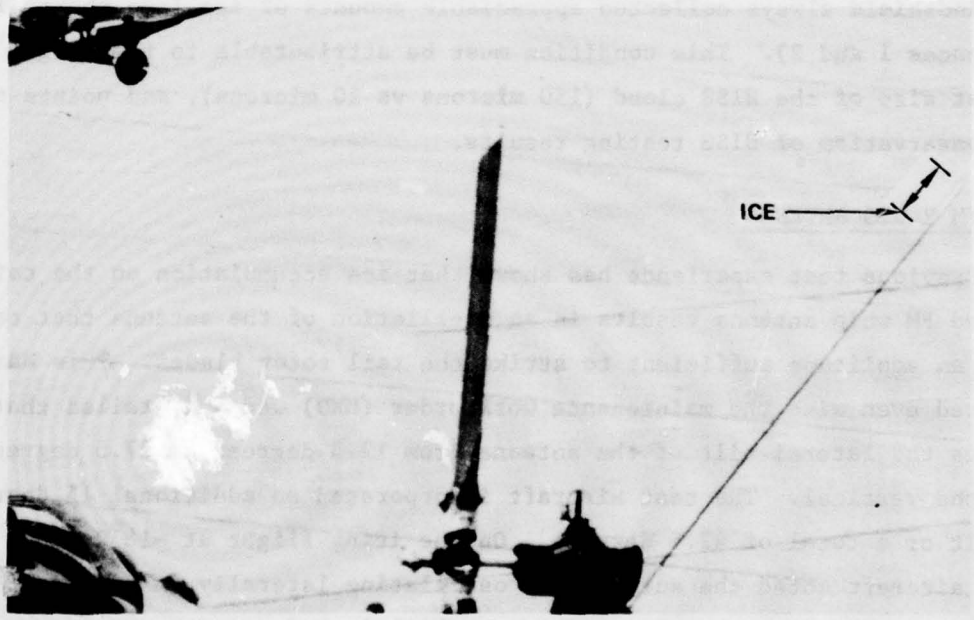

Figure 15. Ice on the FM Radio Antenna After -18°C Natural Icing Flight

side. Exposure time on these flights ranged from 35 to 60 minutes with liquid water concentrations varying in the 0.15 to 0.30 g/m^3 range.

The ice on the engine inlet air filter screens built forward from the aft end, generally in a vertical line on the right side screen and in a diagonal line on the left side screen, starting from the lower rear corner. The maximum coverage on the right-hand screen extended to within 2 inches of the forward edge and approximately one-half of the left-hand screen area. There was no ice formation noted on the top, horizontal screen. No increase in differential pressure across the screens was measured by the test aircraft instrumentation under these conditions.

The ice on the synchronizing elevator was a maximum of 1/2 inch thick on the leading edge. It was generally full span on the right-hand surface and was tapered in thickness on the left-hand surface, decreasing in thickness from the tip to the root.

There was ice of much less prominence on the other protuberances of the aircraft. Figure 16 shows the test aircraft in flight after a natural icing encounter and points out some pertinent features.

The exposure time to icing on the test flights is considered reasonably typical of the maximum for a 2-hour flight. More significant ice buildup can be expected on flights of the same duration with higher liquid water concentrations present.

4.8 AIR TEMPERATURE MEASUREMENT

One input needed for operation of the blade deicing system is outside air temperature for programming heater-on time. The sensor used for this purpose is a flush-type electrical resistance bulb. The flush-type sensor was selected because it would not require ice protection as is required for some probe-type sensors. In addition, the flush installation did not add another external protuberance on the aircraft to interfere with ground maintenance. Problems have been experienced in testing to date, however, in obtaining accurate and consistent air temperature data with the flush sensor.

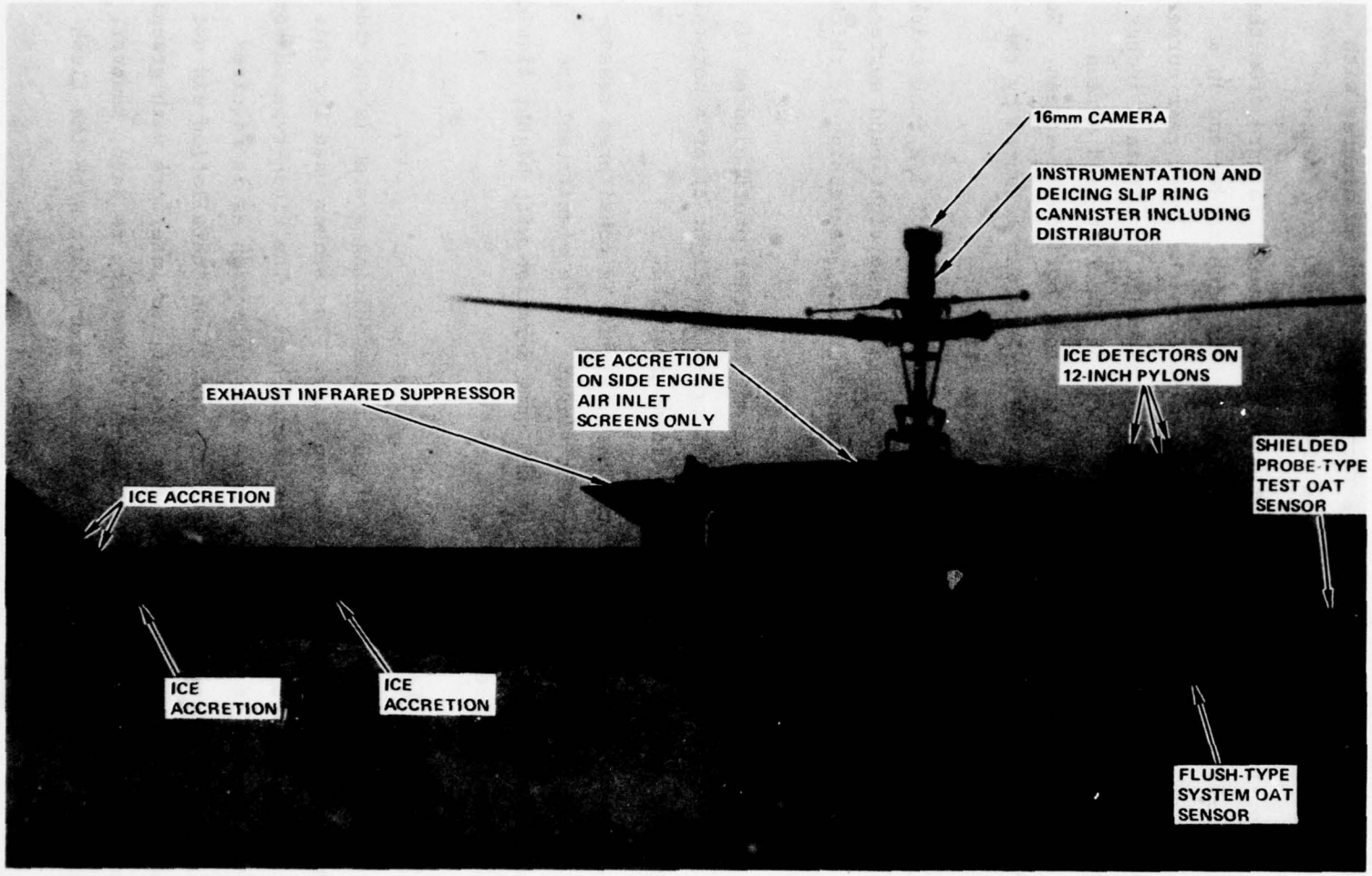

Figure 16. Test UH-1H Aircraft Following 21 Minutes in Natural Icing (FLT 162, $-8^{o}C$, 0.3 g/m^{3})

It was found during this year's testing that the readings from the sensor were being affected by cabin heat. This phenomenon had been suspected previously but a cursory investigation had indicated that there was no correlation. A more detailed check was made which established a definite effect of internal compartment or "backside" heating on the sensor. This was verified on the ground by applying heat with a heat gun to the electrical connector.

Inspection of the aircraft installation revealed that air from a cabin heat outlet for the chin window was probably responsible. An alternate location under the nose was not readily available so the sensor was moved to an externally-mounted bracket on the forward nose just below the battery compartment. Satisfactory readings were obtained with this location on the later flights. This location would probably result in the sensor becoming covered with ice under higher liquid water concentration conditions and therefore being in error. The standard UH-1H windshield probe collects ice and eventually becomes encased in ice (see Figure 39 in Section 8.1 and Figure 102 of Reference 1). Although a specific accuracy investigation has not been made, the readings from this probe generally appear to agree very well with the test instrumentation sensor even after the standard probe is iced up. This suggests that for the flight speed of the UH-1H, the effect of being iced up is negligible for practical purposes.

Post-test investigation revealed that the MS 28038-2 type sensor used is the wrong type for installation in a location where internal temperature changes. There is another MS 28038-2 sensor that is not affected by internal temperature changes. That model is not a hermetically sealed unit and should be used for the UH-1H installation.

4.9 ICE DETECTION SYSTEMS

As described previously three ice detection systems were installed and planned for use in the test program. However, due to conflicting bleed air pressure requirements for the detectors that were not known

previously and because of testing priorities, the inferential-type system had to be removed after limited spray rig testing and only one natural icing flight had been accomplished.

On the natural icing flight on which the inferential-type detector was operational, the system appeared to function properly for a period of 5 to 10 minutes and then displayed very high values of LWC; later ice was observed on the lip of the aspirator unit. This experience agrees with a post-test icing tunnel calibration (Appendix C) that showed that icing on the aspirator duct was the cause of the high and erroneous readings. The aspirated configuration is new and only had a minimum of development testing by the supplier prior to delivery. Obviously the bleed air heating of the aspirator duct was inadequate.

Time histories of pertinent data for the ultrasonic-type detector and the infrared-type system during flight in icing clouds are shown in Figures 17 through 21. These data are for four of the natural icing flights and one spray rig run.

Shown on these figures are the indicated liquid water concentrations for each system, plus the analog output from the ultrasonic-type probe and the integrated rate of the infrared-type. The LWC indication for ultrasonic-type system is essentially the slope of the analog output signal with respect to time and utilizes a hold circuit to keep the indication from dropping to zero during the probe deice and recovery portion of each cycle. The LWC indication for the infrared-type system is a calculated value of LWC for each ice accretion cycle of its probe.

The cycles for each type of detector can be seen on the time histories from the analog signal trace for the ultrasonic and from the step updates to the infrared readings. A long time interval between cycles generally reflects a low LWC and a shorter time interval generally reflects a higher LWC. The variation in the natural icing LWC environment during flight can be seen on Figures 17 through 20 and illustrates the need for some type of an integrating system to permit the scheduling of rotor blade deicing at intervals of a uniform amount of ice buildup on the blades.

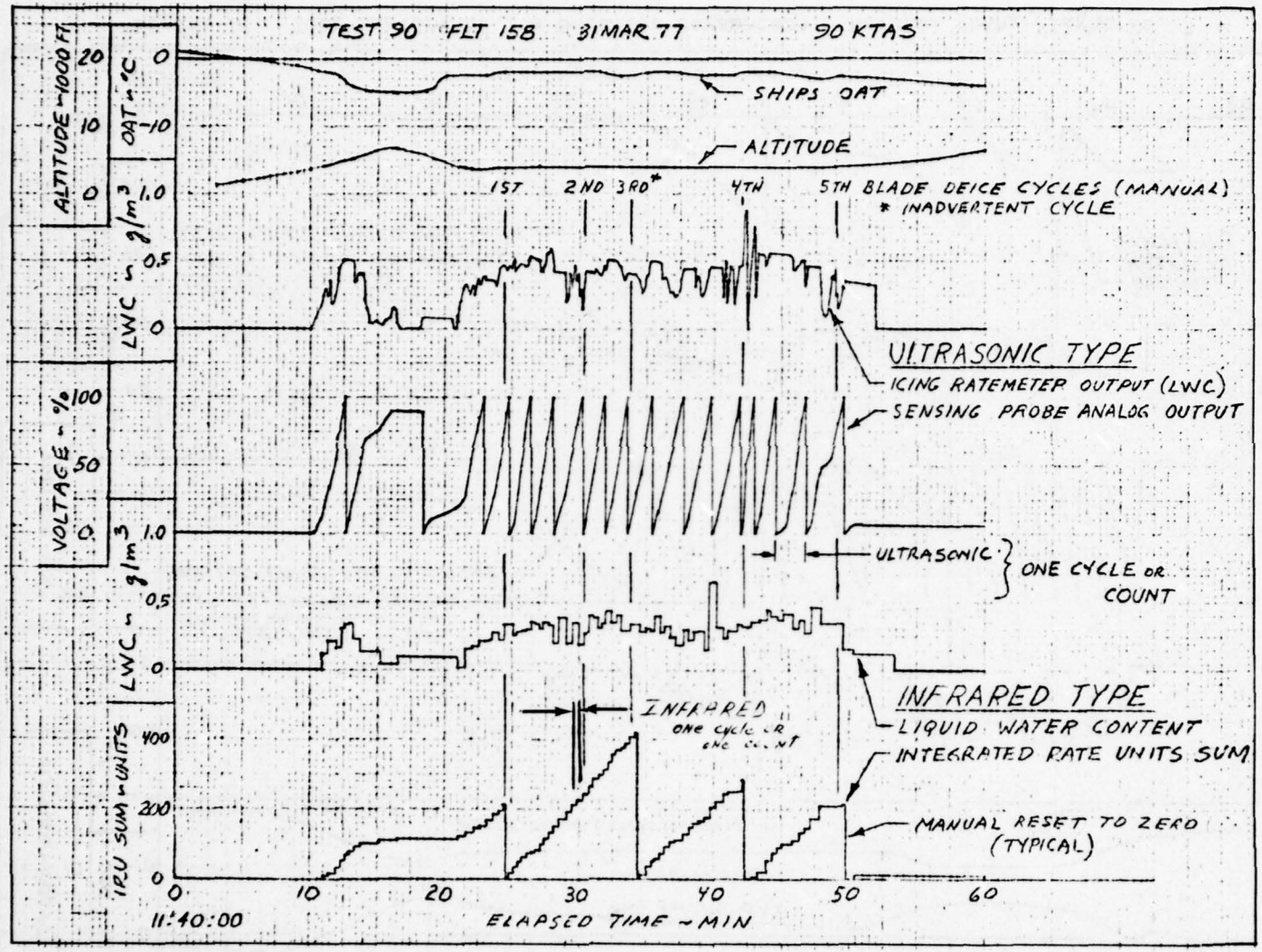

Figure 17. Time History of Ice Detector Parameters - Natural Icing Flight No. 2

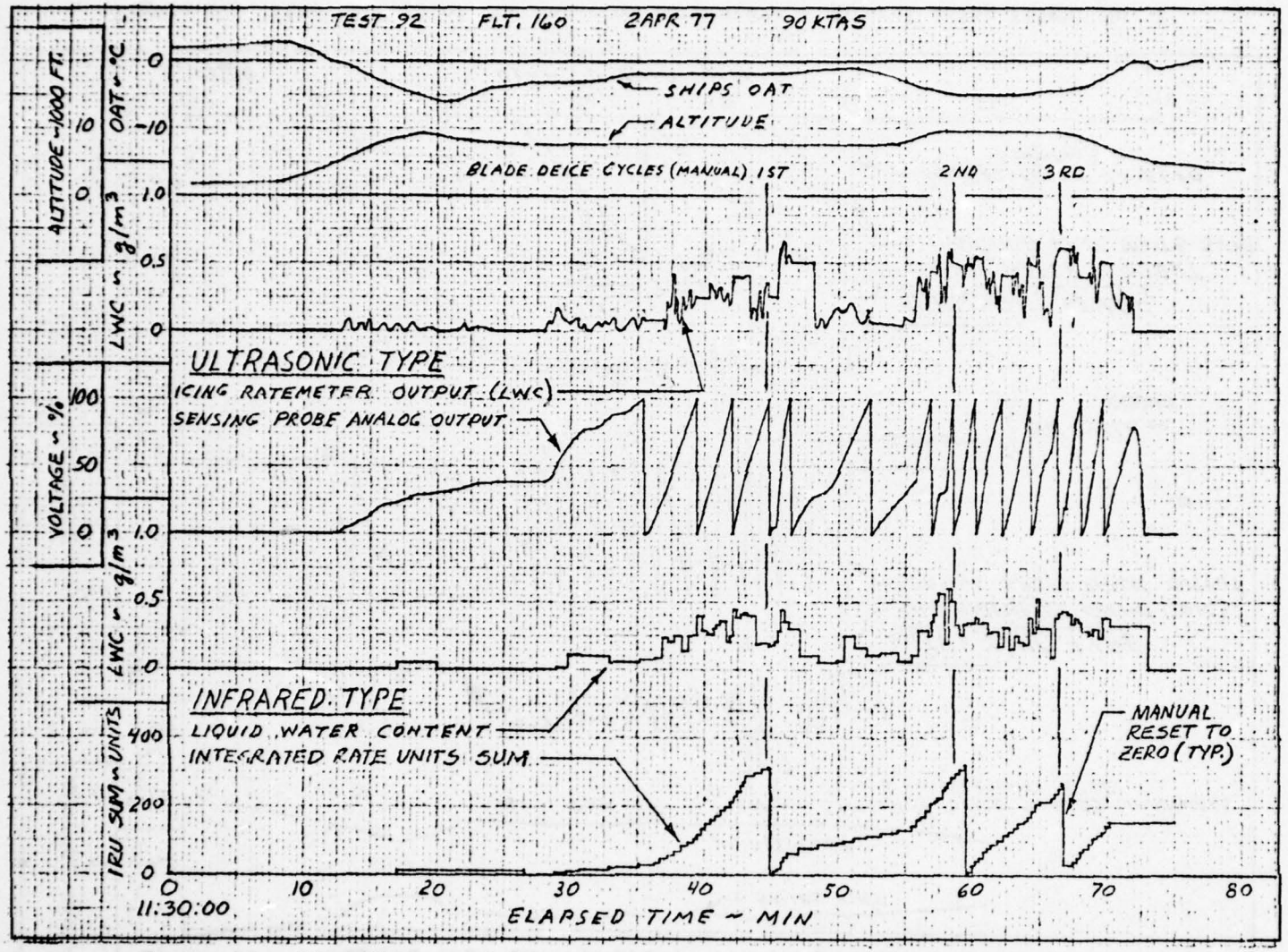

Figure 18. Time History of Ice Detector Parameters - Natural Icing Flight No. 3

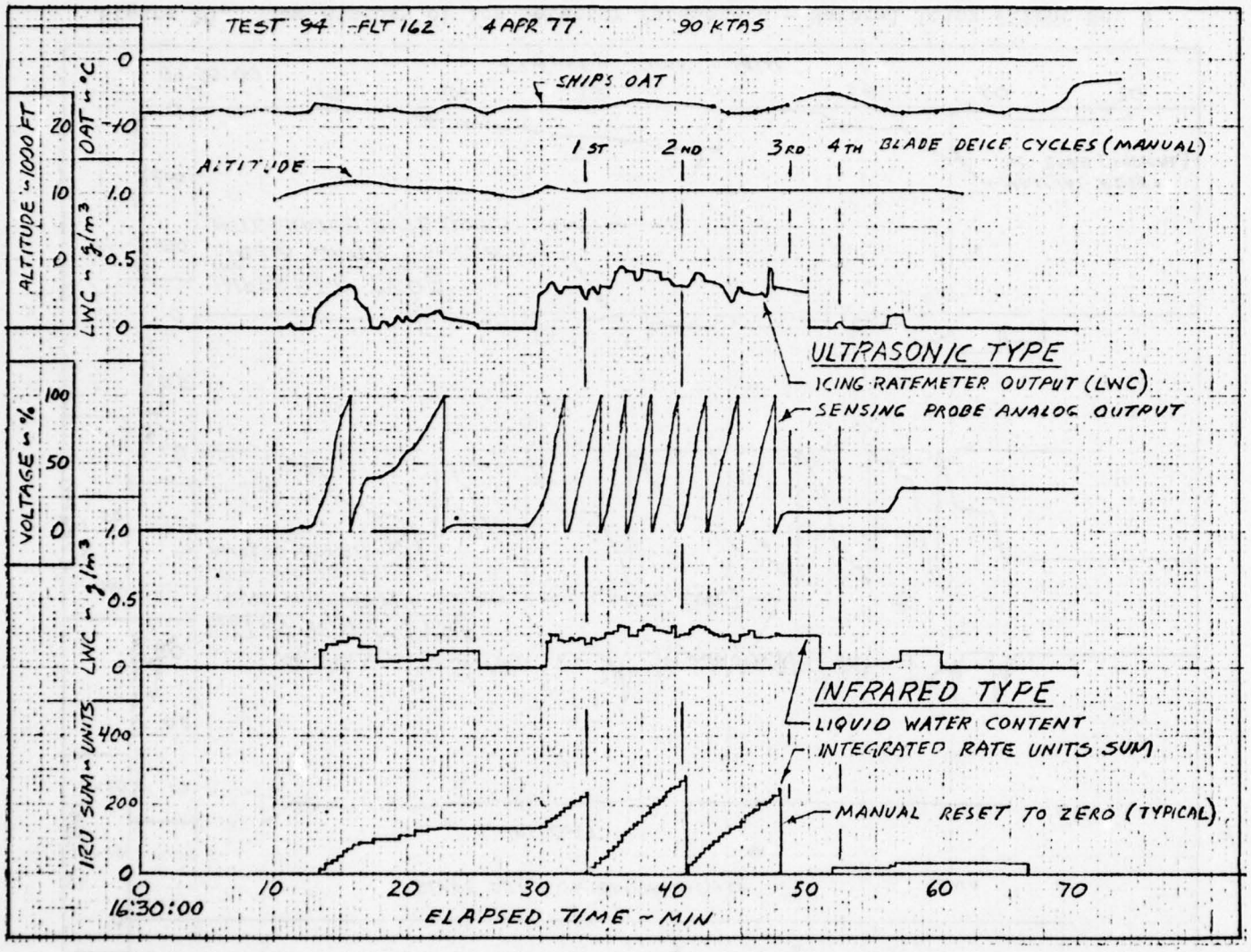

Figure 19. Time History of Ice Detector Parameters - Natural Icing Flight No. 4

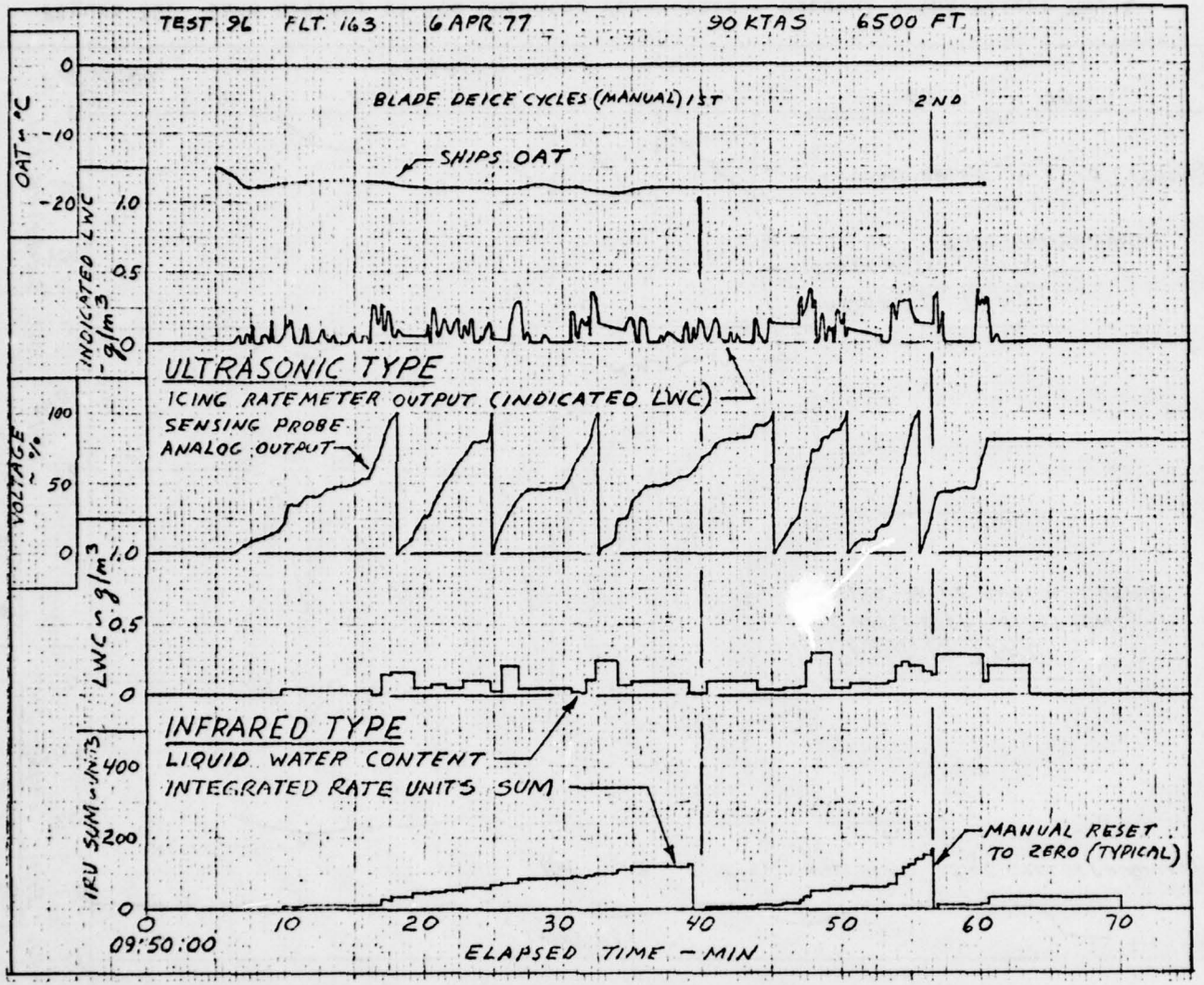

Figure 20. Time History of Ice Detector Parameters - Natural Icing Flight No. 5

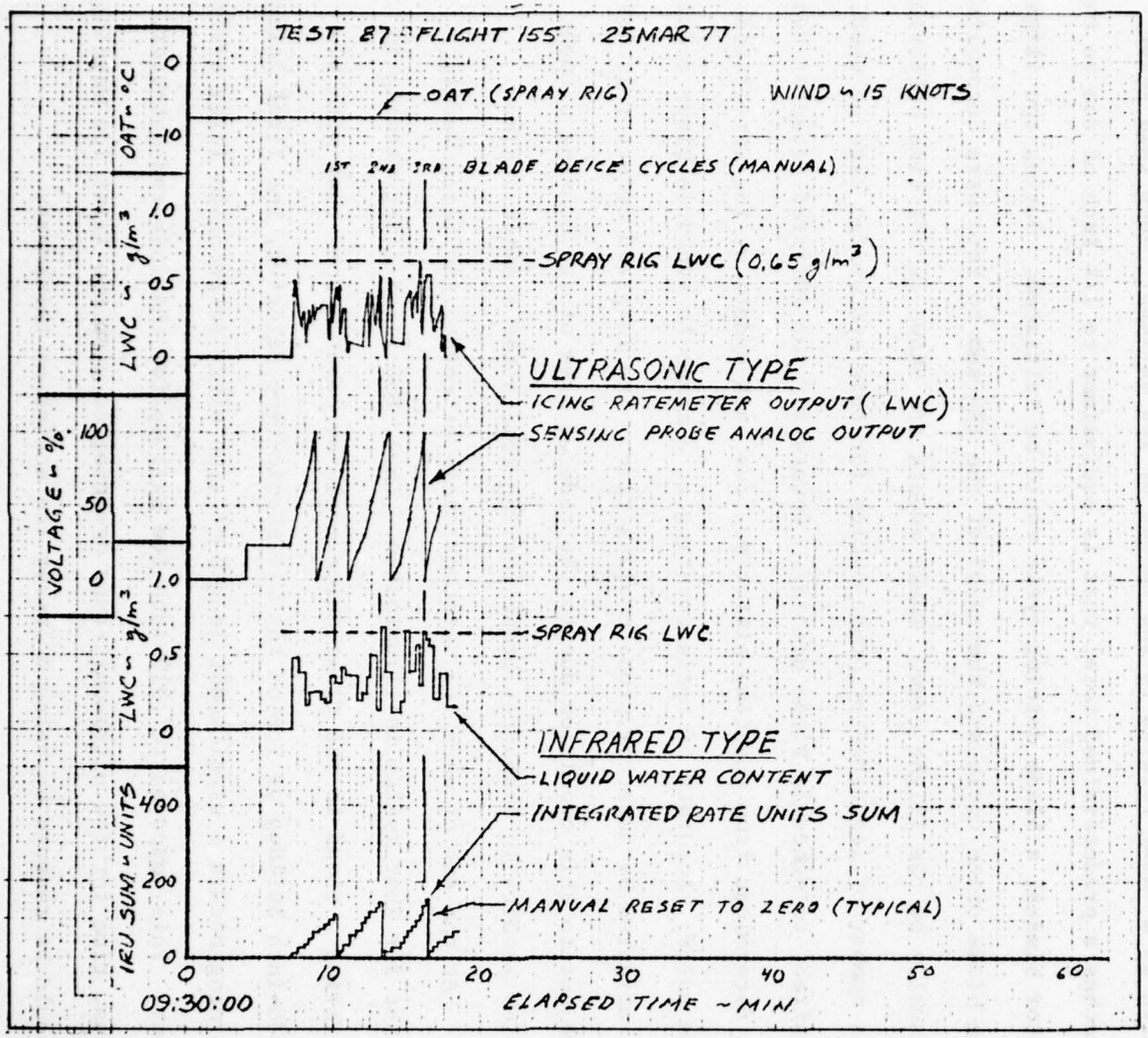

Figure 21. Time History of Ice Detector Parameters - Spray Rig Cloud

The integration of icing rate as accomplished by the infrared-type system's IRU is presented on the time histories as an integrated rate sum which is a value related to the amount of ice buildup. When this value reaches a predetermined total that is equivalent to 1/4 inch of ice on the rotor blades, a blade deicing cycle would be initiated. During the flights, the blade deice cycle and the reset of the IRU sum to zero were accomplished manually by the flight crew. These events are shown on the time histories. The number of ice detector probe cycles for this system can also be used, if desired, to schedule blade deicing. Counts for the infrared detector can be determined from the time histories from each update of the integrated sum value. Accuracy of cycle counting as a means to schedule blade deicing is affected by detector probe cooling time. The infrared detector is less subject to this condition due to the reduced mass of its sensing element which results in a shorter probe cooling time after a deice cycle.

At the end of each ice detector cycle or count, the icing warning light for that system is illuminated. Thus, the first icing warning on entering a cloud is the first deice cycle or count. Note that with the .080-inch buildup of ice on the ultrasonic-type detector, the first icing warning occurs a significant length of time after entering an icing environment. This compares to .013-inch ice buildup for the infrared detector. Thus, time for the ultrasonic-type detector to give the first ice warning should be reduced by using a lesser ice accretion thickness.

4.9.1 Liquid Water Concentration Indications

The agreement between the two systems for LWC measurement of the icing environment was, in general, found to be good. The time histories

show possibly a $0.1 g/m^3$ difference between the two systems some of the time, which may be due to differences between the bleed pressure used for the calibration and actual installation bleed pressure. For the spray rig run presented, Figure 21, both systems indicated about one-half of the cloud LWC. This may be due partly to sensing inaccuracy at low airspeed, but is more likely due to the fact that the sensors, which are located on the forward portion of the cabin roof, are not fully immersed in the cloud during spray rig operation. This is because the pilot must keep the nose of the aircraft relatively clear of the cloud in order to maintain visual reference for flying. It should be noted that system peak LWC indications accurately reflected cloud LWC during hover. This tends to confirm that the ice detectors are only immersed in the cloud on an intermittent basis. The spray rig run shown is in one of the better cloud conditions found during this year's testing. The gusty and relatively strong winds experienced this year resulted in generally useless indications of cloud LWC from the ice detectors (systems indicated near zero most of the time). This points out the fact that considerable judgment is necessary to use on-board instrumentation to determine the LWC of the spray cloud.

4.9.2 Blade Deicing Control Signals

Figure 22 presents data attempting to evaluate the relative accuracy of using counts or integrated rate units from the different systems to schedule rotor blade deicing. Shown are counts from both the ultrasonic and the infrared-type systems plotted versus infrared integrated rate units and against each other. This data is from the natural icing flight time histories of Figures 17 through 20. For any given flight, the relationship

appears linear although Flight 96 has two different slopes. This is most likely due to the fact that the first accretion cycle occupied over 15 minutes because of an intermittent LWC condition and was subject to sublimation. The relationship between counts from one system to counts from the other system and/or integrated rate units does not remain the same for different flights. This is possibly due to differences between the detectors relating to catch efficiencies, Ludlam limits, probe thermal inertias (cooling times), etc. A consistent relationship between detector outputs can be established only when sufficient data points have been accumulated. An integrating rate system avoids the inaccuracies due to varying probe cooling times by measuring the LWC value and multiplying it by the time between LWC updates to give an integrated value.

Further data is necessary before one can judge whether the relationship between detector output and blade ice thickness for any of the counting methods could consistently provide a blade deicing signal at a fixed ice thickness on the blade. The ability to establish an accurate and repeatable ice thickness on the blade immediately before deicing would depend on the degree of resolution of the measuring system. The ratio of the number of counts produced by one system versus the other relates directly to its resolution capability. These ratios are shown on Figure 22 as numbers noted adjacent to the characteristic curve for each test.

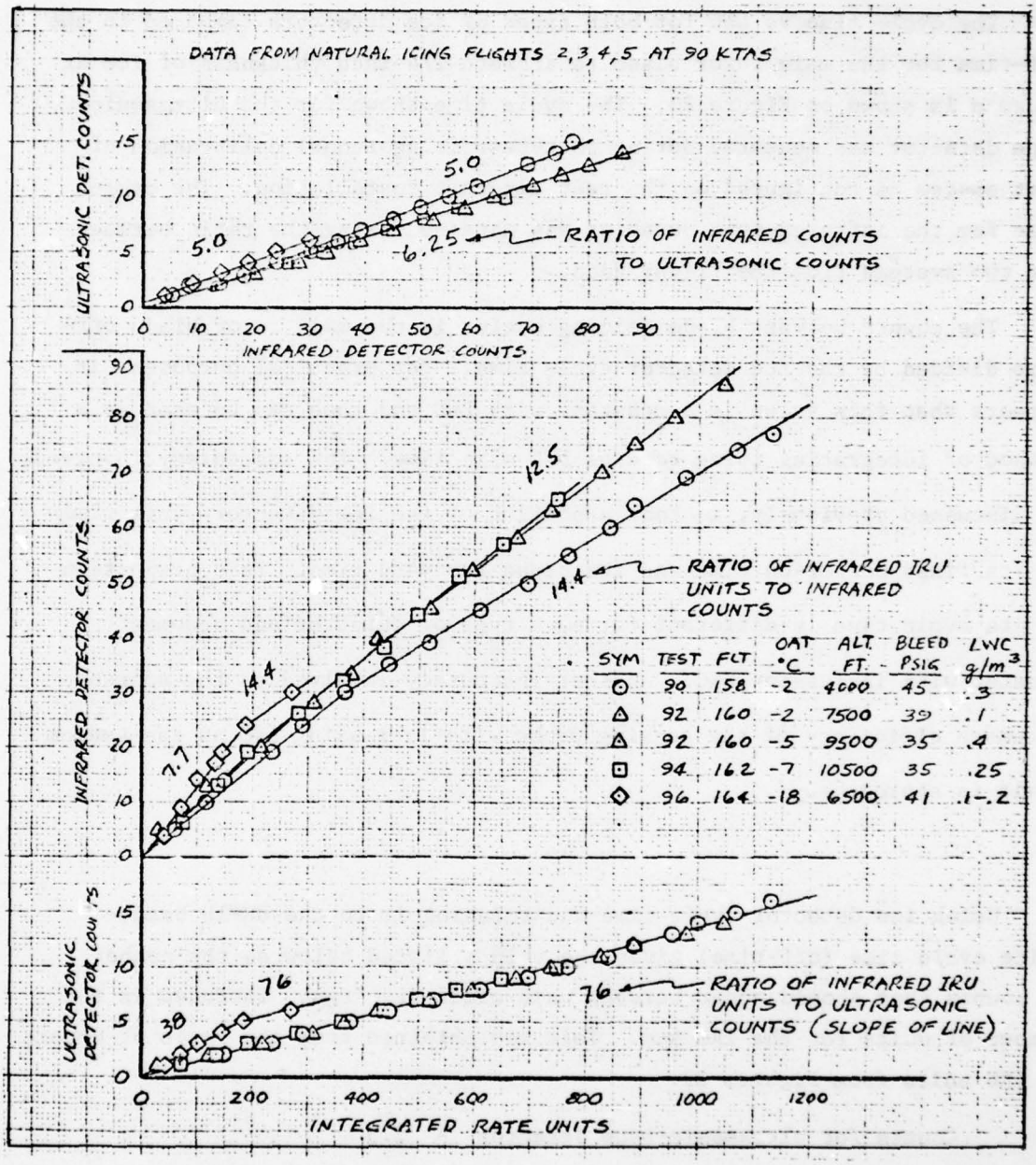

Figure 22. Ice Detector Cycle Counts from Ultrasonic-Type Detector Versus Counts and Integrated Rate Units from Infrared-Type Detector

The cycle time vs LWC for both types of ice detectors compared to the off-time for the main rotor blade to accrete 1/4-inch thickness of ice at midspan is shown on Figure 23. The cycle time shown for the ultrasonic-type detector was measured during post-test icing tunnel calibration of that system as configured on the test aircraft installation. The cycle time for the infrared-type detector was obtained using the ratio between the two systems from the flight data.

The counts between blade deicing cycles is the main rotor blade off-time divided by the ice detector cycle time. For practical purposes, it appears that this value is a constant with LWC and thus can be used as a method of integrating icing rate or LWC with time. The inaccuracy involved, as discussed previously, is that a portion of the ice detector cycle time is its fixed heater-on time and its probe recovery time. This proportion of its cycle time is different for each type of detector and becomes greater with increasing LWC. Another inaccuracy involved is the decrease in catch efficiency of the sensing probe with increasing LWC as the Ludlam limit is approached.

Using ice detector cycle time and relating it to the UH-1H blade-deice cycle time (off-time) gives the values listed below as the number of counts that should occur between main blade deicings. Included is the number of units for the IRU sum. This was obtained from the ratio of counts to IRU units from Figures 22.

Counts for ultrasonic-type detector - 2.3

Counts for infrared-type detector - 13

Sum from the infrared IRU system - 180

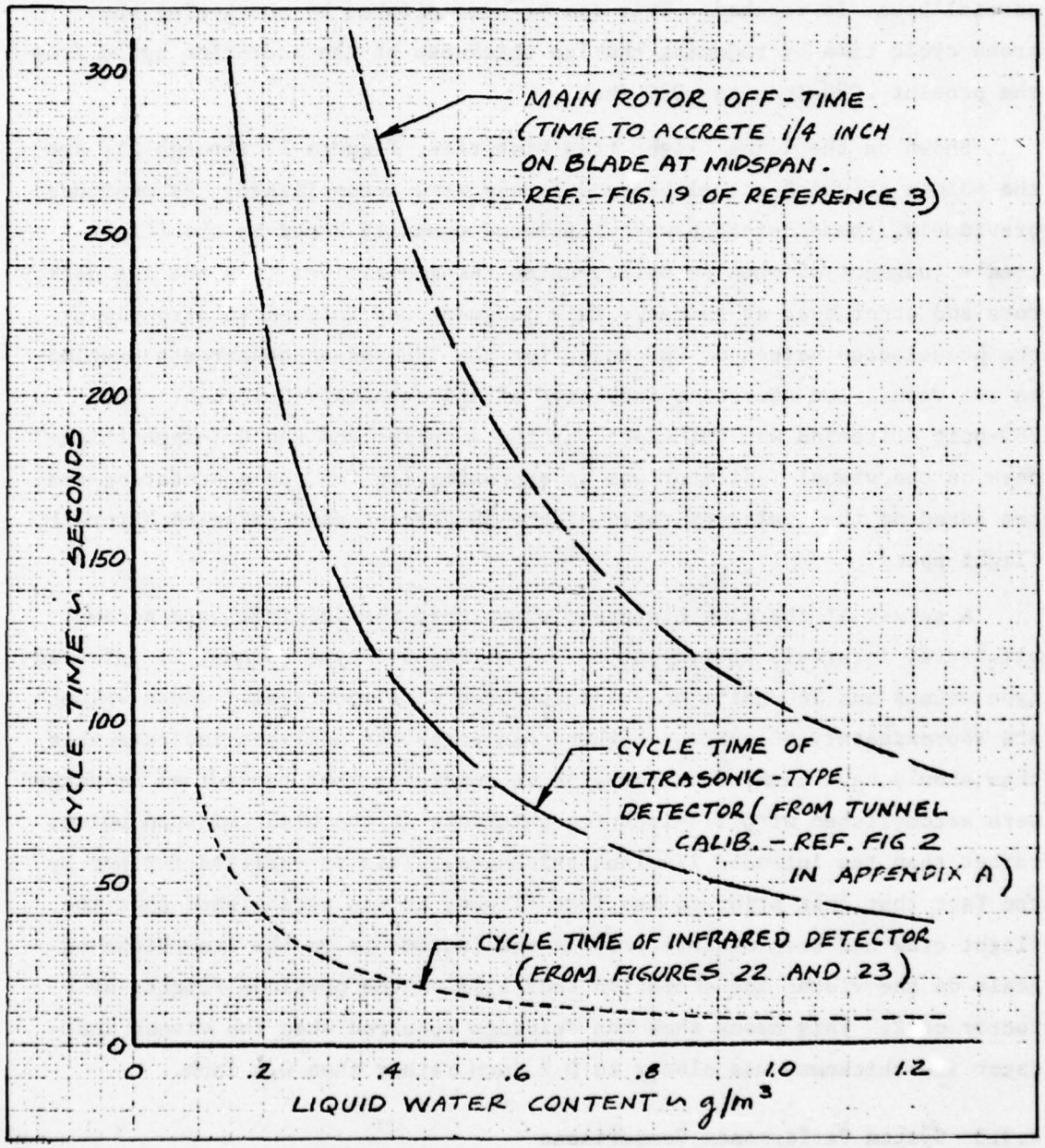

Figure 23. Comparison of Ice Detector Cycle Time with Main Rotor Off-Time

The number of counts for the ultrasonic type needs to be increased in order to provide a whole number as there is no way to ascertain the point when a partial count is reached. This can be accomplished by shortening the probe cycle time by reducing the ice thickness of the accretion cycle from the present .080 inch to .020 inch

Shown on the icing flight time histories, Figures 17 through 21, are the points at which actual blade deicings were accomplished. As mentioned previously, these deicings were initiated manually based on the flight crew's judgment of when to deice, using the indications from the ice detectors and other cues as guides. This judgment was influenced strongly by the preselected values of 260 units for the IRU and an observed accretion on the visual ice accretion indicator of approximately 0.1 inch. The 260-unit criterion was calculated by the supplier and the 0.1-inch thickness on the visual indicator was an approximation for the nonrotating system based on the velocity ratio of the 50-percent span point to aircraft flight speed.

A survey of the time histories shows that the deicings were accomplished at intervals equivalent to 3.5 ultrasonic-type counts, 21 infrared-type counts and 260 units on the integrated rate totalizer. These values are approximately 50 percent higher than post-test analyses indicate that they should have been; therefore, it is concluded that the actual deicings were accomplished with 3/8-inch ice thickness at the blade midspan point, rather than the intended 1/4-inch thickness. This is verified further by the fact that just prior to the last flight, it was established that the flight crew had been misinterpreting the increments on the ice-thickness scale on the visual ice accretion indicator on the previous flights by a factor of 2. This means that the deicings occurred when the visual indicator ice thickness was closer to 0.2 inch rather than 0.1 inch.

4.9.3 System Performance Comparisons

The range of test conditions in terms of LWC and OAT encountered during the program was relatively limited and thus precluded a comprehensive

evaluation of ice detector performance. To supplement the flight data, a review of tunnel calibration data available from the suppliers was made and additional calibrations were conducted in the Canadian NRC Low Temperature Laboratory. These tests were conducted by NRC personnel, but sponsored and witnessed by a U.S. Army engineering observer. The hardware tested was that removed from the test aircraft at the conclusion of the flight program and was, therefore, configured exactly as flight tested. The bleed air temperature and pressure for the calibrations were set to the same values as measured on the test aircraft installation. This evaluation provided the following information and conclusions:

- Even though all three systems are aspirated in order to provide sensing capability at hover, they all remain sensitive to airspeed changes and to bleed pressure. The detectors have been optimized to provide essentially zero error at 90/100 KTAS, the flight speed of the UH-1H. Presumably, this can be deone for any desired speed. Because of the sensitivity to airspeed, an electronic signal conditioning switching arrangement would be required to provide zero error for different speeds such as hover and cruise speed. The hover case is further complicated by wind velocity effects.

- The accuracy of any of the systems or the ability to continue to indicate LWC above 0.8 to 0.9 g/m^3 at 90 knots has not been verified by icing tunnel calibration data except for the infrared-type detector. Icing tunnel calibrations show the infrared-type is linear to 2.4g/m^3 at -21°C and to 1.8g/m^3 at -11°C.
- The present bleed air anti-icing of the duct lip of the aspirator is inadequate at lower temperatures for both the ultrasonic and inferential type detectors. The aspirator icing condition results in large inaccuracies in LWC indication. The ultrasonic-type-system experienced icing problems below -9 to -10°C and the inferential type at -5°C. The aspirator of the infrared-type detector is adequately anti-iced, as shown during flight tests and icing tunnel calibrations.
- The icing indicator light of the inferential system does not operate at liquid water concentrations below about 0.5 g/m^3.

Copies of the reports describing the detailed results of post-test calibrations for the three ice detectors are included in this report as Appendixes A, B, and C.

It is recommended that users of ice detection systems be aware of state-of-the-art limitations and/or shortcomings of the available systems in order to properly interpret their operational functioning or to

design a system that depends on their sensing accuracy and reliability. It is also recommended that further natural icing testing be accomplished to establish whether there is a practical requirement for accurate indication or measurement of liquid water concentrations greater than 1.0 gram per cubic meter. For example, LWC primarily affects off-time (the time between deice cycles). It is possible that since these high concentrations will be experienced in the relatively warm (near $0^{\circ}C$) range, the Ludlam effect will result in a single off-time being adequate for LWC in excess of 1.0 g/m^3.

4.10 BLADE TEMPERATURE MEASUREMENT

Measurements of main rotor blade surface temperatures were evaluated to aid in the determination of the optimum heater-on time. One factor needed in this determination was to establish the temperature of the blade surface prior to initiating a blade heater cycle. This temperature is the combined effect of kinetic heating due to blade rotational speed and the cooling of the icing environment.

Spanwise temperature variations were evaluated with and without ice on the blade and in or out of an icing cloud. Although individual comparisons showed changes in surface temperature with different environmental conditions, the exact level for specific temperatures and/or liquid water concentrations could not be established. This is attributed to the relatively limited spread in data available and the measuring accuracy required. It is felt, however, that the data obtained during this year's program was considerably better than previous results. This was indicated by the close agreement between the independently measured outside air temperature measurement used for plotting at blade station zero and the outboard blade surface temperature measurements.

Figure 24 presents individual data comparisons in and out of an icing cloud at three different air temperatures. Also presented on these distributions is the known spanwise extent of ice coverage on the blade for the spray rig tests. For the natural icing flight at $-18^{\circ}C$, the spanwise ice coverage should have been 100 percent.

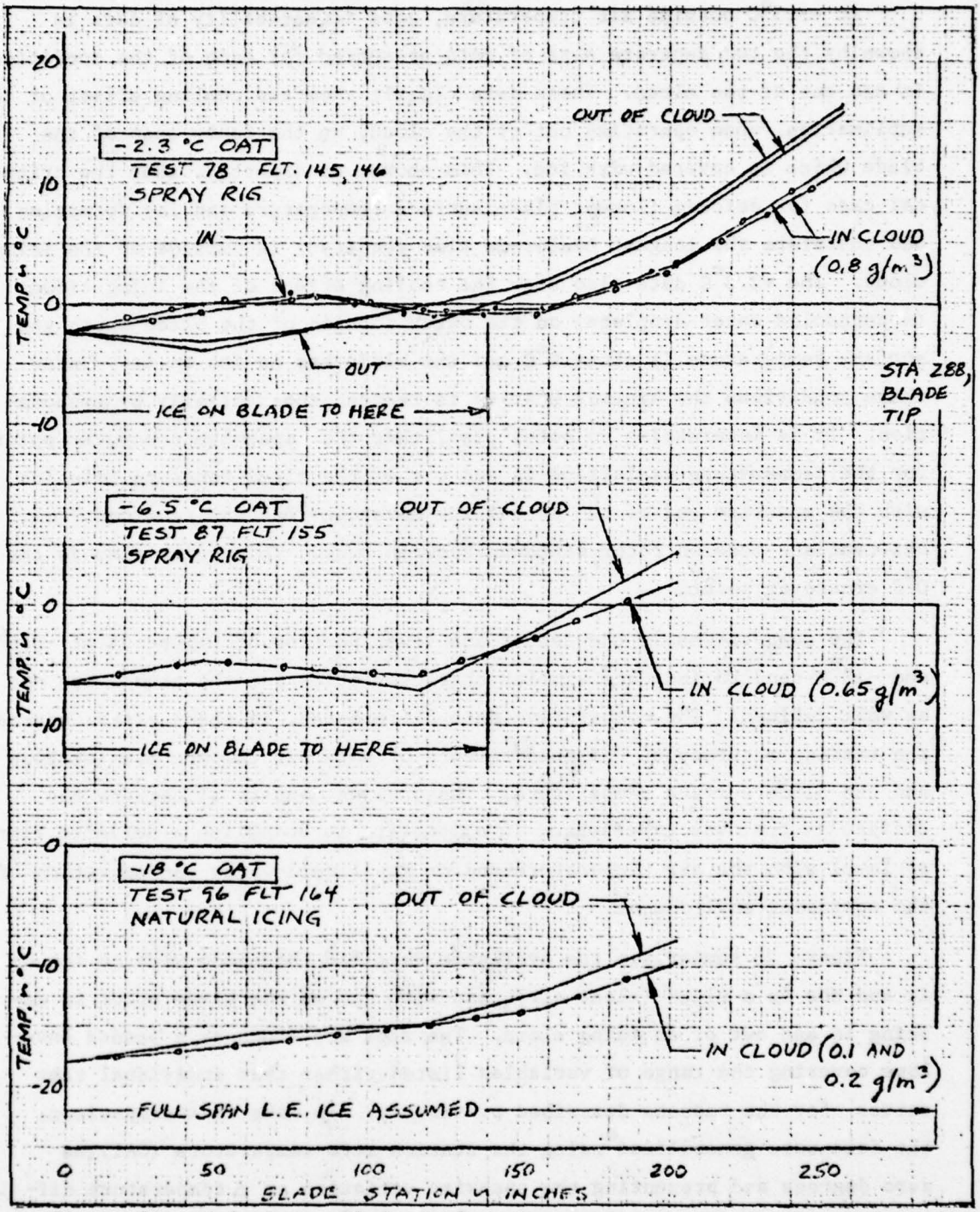

Figure 24. Main Rotor Blade Surface Temperature vs Span, In and Out of an Icing Cloud at Various Air Temperatures

At -2.3°C outside air temperature, good repeatability of data is shown by the two separate sets of data presented for each of the conditions in and out of the cloud. These data clearly show the cooling effect of ice sublimation, when operating out of the cloud, on the inner span of the blade which is covered with ice. This shows, as expected, that the critical case for deicing (lowest blade surface temperature and ice formation and therefore the longest heater-on time required) is outside of the icing cloud. The -2.3°C data also show the cooling effect of the icing cloud (supercooled water droplets) on the outer portion of the blade where the surface temperature is above 0°C and the blade has no ice on it. Under these conditions the kinetic heating is reduced substantially by evaporation. It is interesting to note, also, that the spanwise crossover point for the temperature variations in and out of the cloud tends to coincide with the spanwise end of the actual ice coverage that was recorded from observations made on rotor shutdown between runs. This point also is the 0°C crossover point.

The comparisons in the center and lower portion of Figure 24 at -6.5°C and -18°C tend to indicate similar characteristics but the trends are not as well defined. The comparative data differences, in these cases, approach the reading accuracy of the measurements of both air temperature (station 0) and the blade surface temperature. These cases tend to illustrate the difficulty that was experienced in attempting to establish a definite trend or level with the air temperature and/or the liquid water concentration of the operating environment.

Figure 25 summarizes the available data for the blade with no ice on it and not in a cloud (clear air), and with ice on the blade prior to deicing in and out of an icing cloud. The data are shown as a shaded envelope covering the range of variables listed rather than individual test curves, for the reasons described previously. To make this comparison, the data were generalized using the station zero temperature (OAT) as zero degrees and presenting the spanwise variation as Δ temperature difference from the air temperature. It can be noted that even for the most

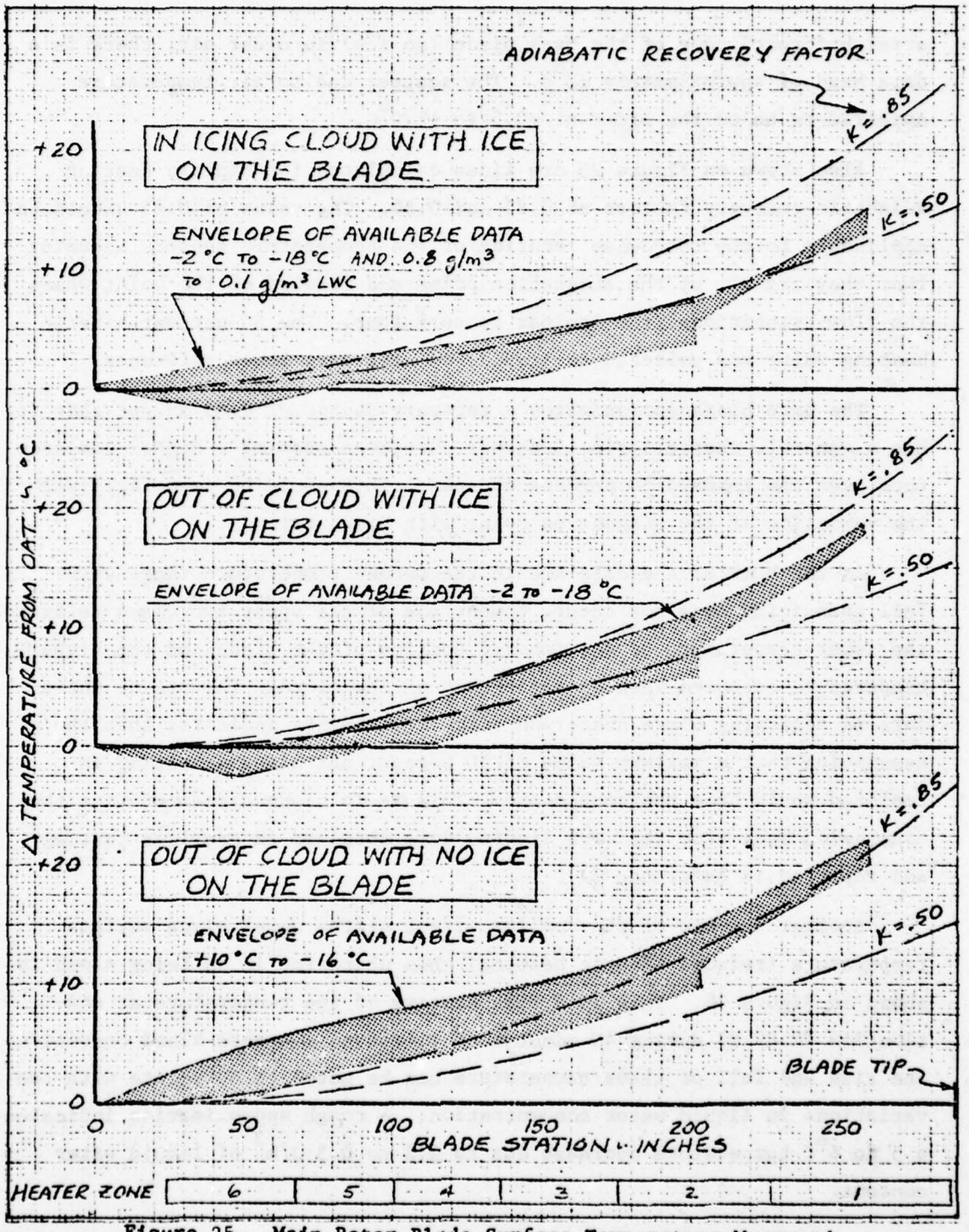

Figure 25. Main Rotor Blade Surface Temperature Measured Under Different Operating Conditions

straightforward case of the bare blade (no ice) in clear air, there is a data band of approximately $\pm 2^{\circ}C$. The scatter due to air temperature appeared to be on the order of ± 0.5 to $\pm 1.0^{\circ}C$.

Also shown on Figure 25 are lines calculated for kinetic heating adiabatic recovery factors of 0.85 and 0.50. The value of 0.85 should be applicable to the chordwise location of the temperature sensors assuming that they are aft of the stagnation point and forward of the point where the flow transitions from laminar to turbulent. The 50-percent kinetic heating value was selected to provide an arbitrary lower reference.

The bare blade approximates a recovery factor of 0.85 except that it has a general, charactistic, S-shaped curvature showing a higher temperature over the inboard 50 percent of span. This could be associated with the variation of the stagnation point with blade twist.

As the bulk of the data are in the warmer temperature range where full span icing does not occur, comparison of the upper two cases reflects the lower temperature of the inboard portion of the blade and the higher temperature outboard when operating out of the cloud. The use of these data in assessing blade heater-on time requirements indicates that the assumption that a maximum value of 50 percent net kinetic heating is realized would be a reasonable one. This is in close agreement with the conclusion made from the more limited data obtained in previous testing and reported in Reference 3.

Another example of the cooling effect on the outer blade surface temperature (reduced kinetic heating) when operating in an icing cloud is shown in Figure 26. This is a time history of the temperature at station 258 (0.89 R) during 40 minutes of flight in a broken cloud condition. The rise and fall of blade temperature can be noted to correlate with the variations in liquid water concentration. A rough approximation indicates a 5 to $6^{\circ}C$ temperature decrease due to 0.2 to 0.3 g/m^3 of liquid water content.

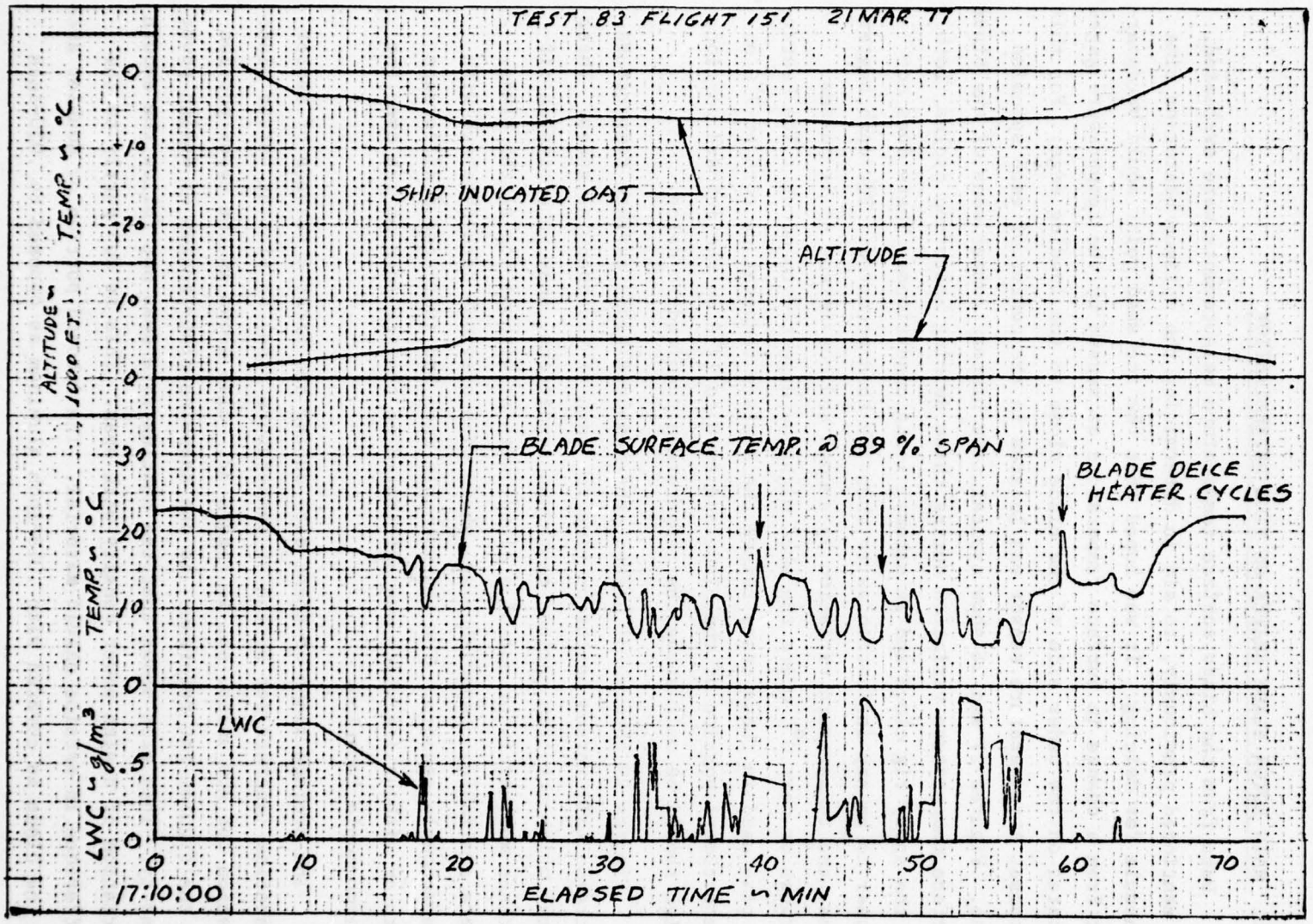

Figure 26. Main Rotor Blade Surface Temperature During Flight Through Broken Icing Clouds

4.11 MAIN ROTOR BLADE HEATER-ON TIME DETERMINATION

Data from the blade surface temperature measurements were evaluated, as mentioned previously, to aid in determining the optimum heater-on time schedule for deicing. It was hoped that the ice shed point would be apparent from a change in surface temperature as sensed by the temperature gages located on the under side of the blade close to the leading edge. For this purpose, a temperature sensor was located in the center of each spanwise zone. Figures 27 and 28 show typical time history comparisons of the blade surface temperature variation during three deicing heater-on cycles, both in the spray rig cloud and in natural icing conditions. There does not appear to be any indication as to when the shed occurred. For each heater zone, the temperature variation is smooth and consistent as it passes through or near $0^{o}C$ where the shed might be expected to occur. The heater-on time used in these cases raised the surface temperature to 6 or $7^{o}C$ on the outboard portion of the blade and to 8 to $12^{o}C$ on the inboard portion, which should be well above the temperature required to deice.

Figures 29 through 31 present the measured blade surface temperature increase (ΔT) versus heater-on time for each of the spanwise zones. These data, which are from various tests and conditions, show no definable difference whether in or out of a cloud, with or without ice on the blade. Where available, comparisons are shown with previous data obtained with thermocouple sensors. The thermocouple data had indicated a difference with or without ice which was attributed to the presence of ice over the thermocouple location.

The average slope of these data during the first 4 seconds of heater operation (degrees per second of temperature rise) is plotted versus blade station for 200 volts, ac, in Figure 32. Also shown in the upper portion of the figure, for reference, is the spanwise distribution of design power density. This plot shows that the heating rate does not follow the smooth variation of design power density with span. This is due partly to the difference in erosion shield material. The inboard portion or doubler area of the blade is covered with .016-inch aluminum as opposed to .030-inch

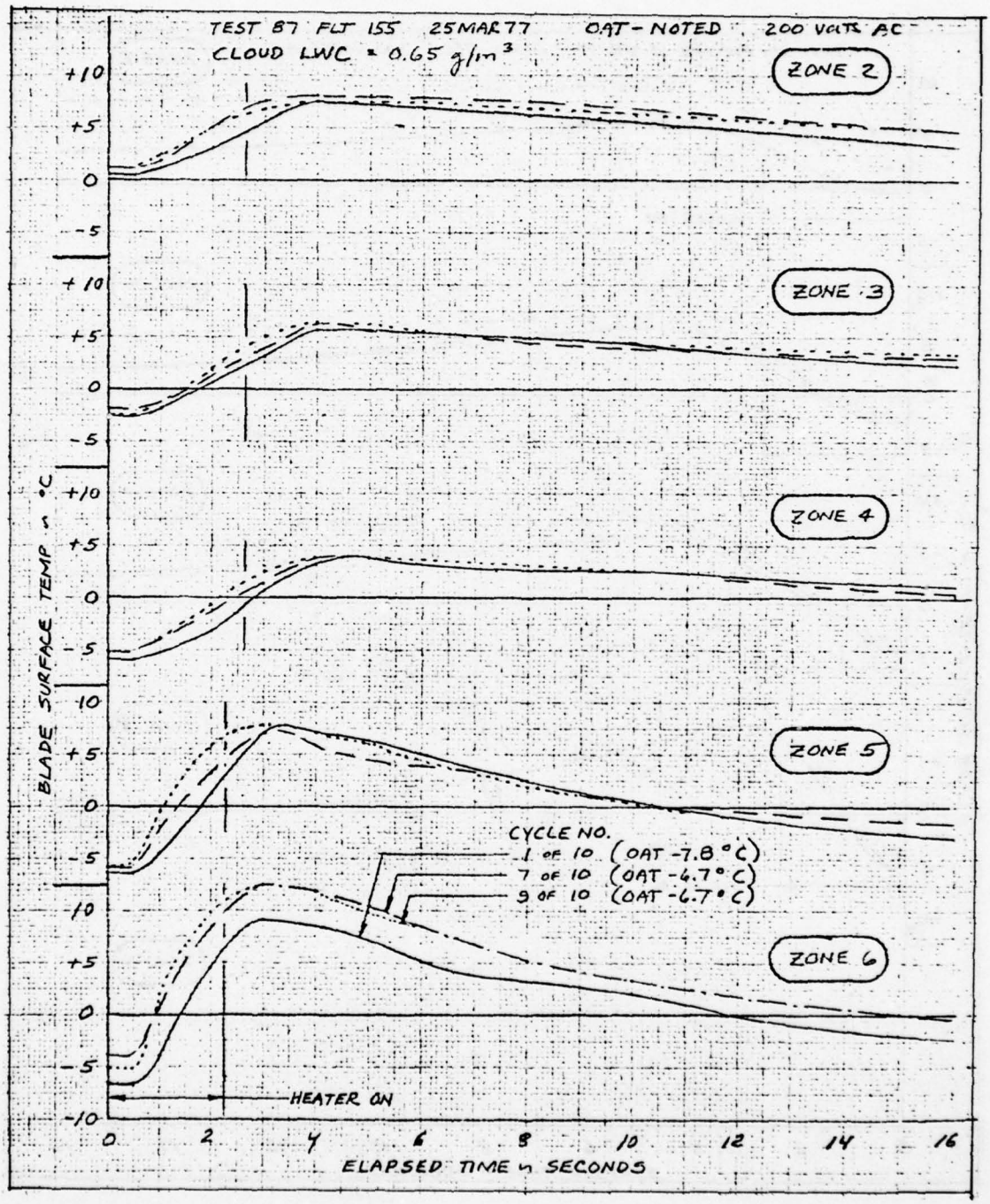

Figure 27. Time Histories of Main Blade Surface Temperature for Three Deicing Cycles in Spray Rig Cloud

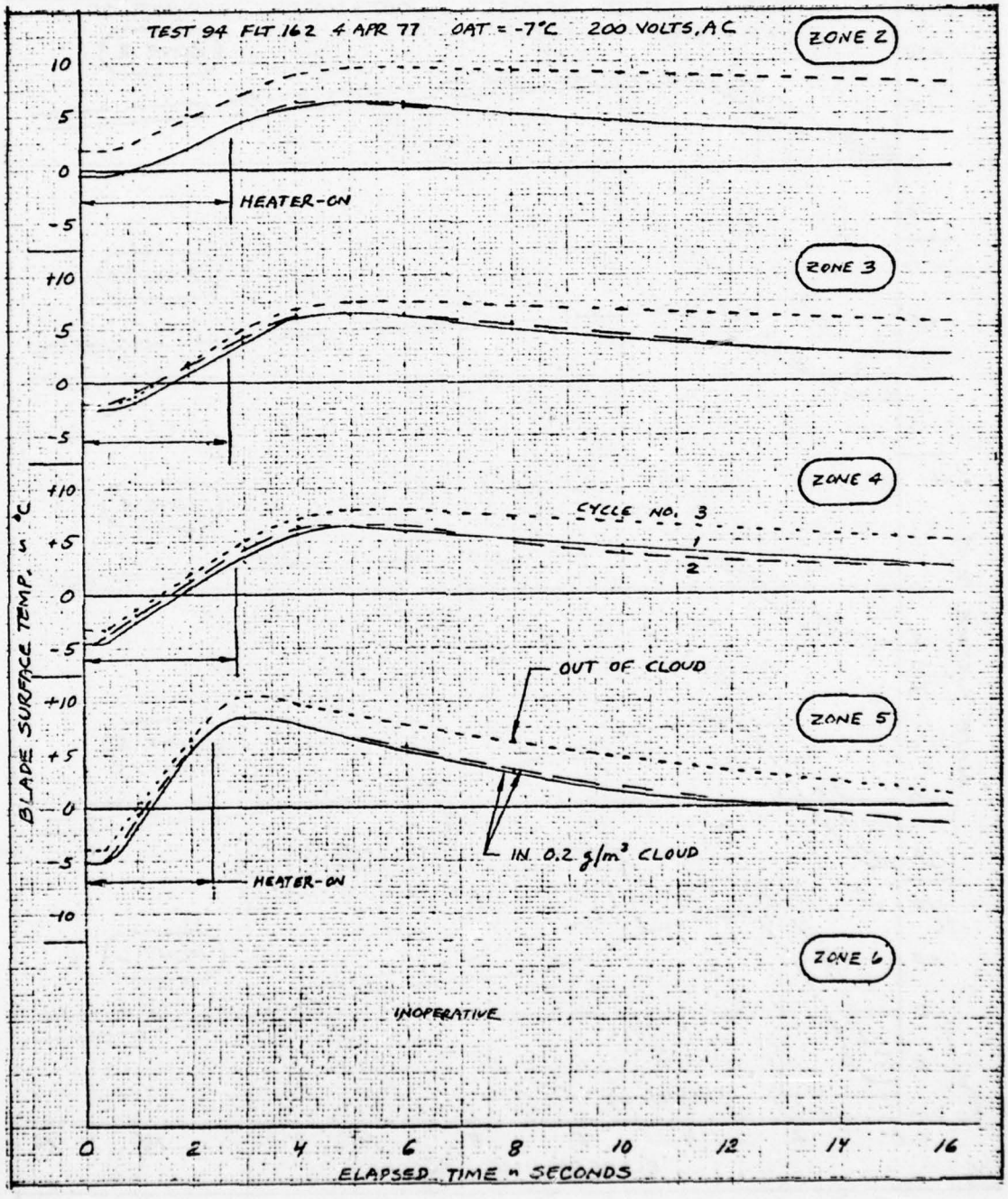

Figure 28. Time Histories of Main Blade Surface Temperature for Three Deicing Cycles in Natural Icing

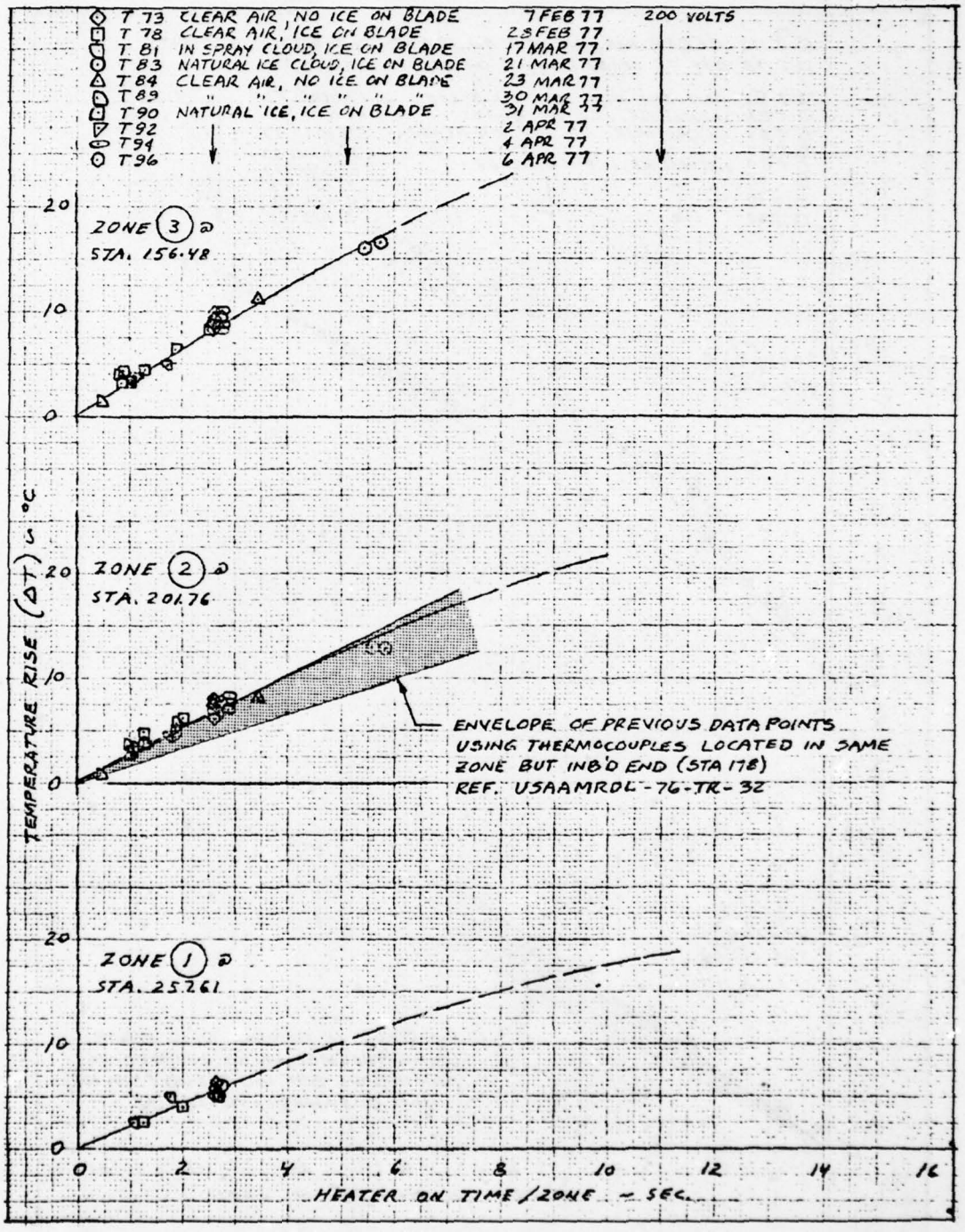

Figure 29. Blade Surface Temperature Rise vs Heater-On Time for Zones 1, 2, and 3

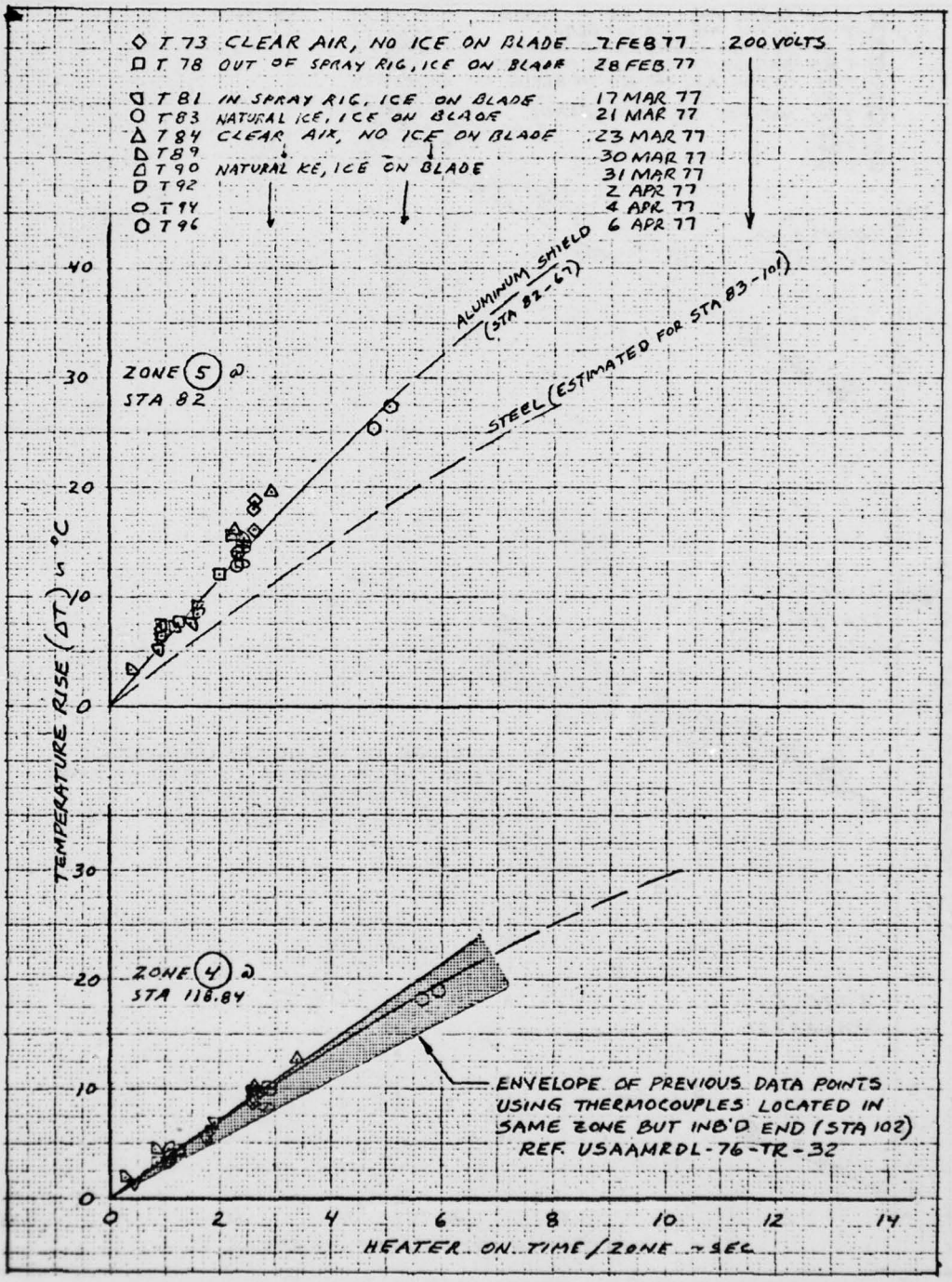

Figure 30. Blade Surface Temperature Rise vs Heater-On Time for Zones 4 and 5

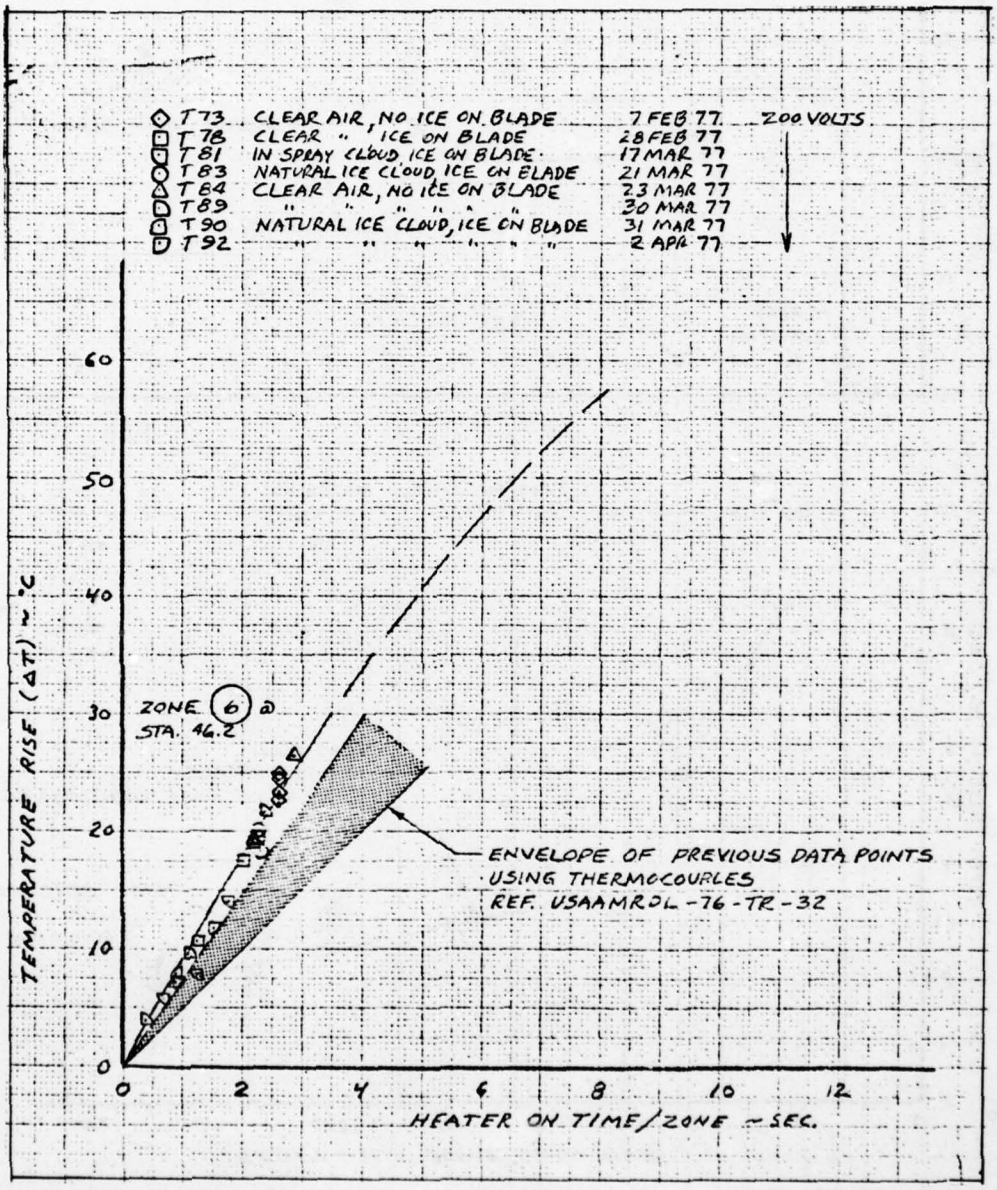

Figure 31. Blade Surface Temperature Rise vs Heater-on Time for Zone 6

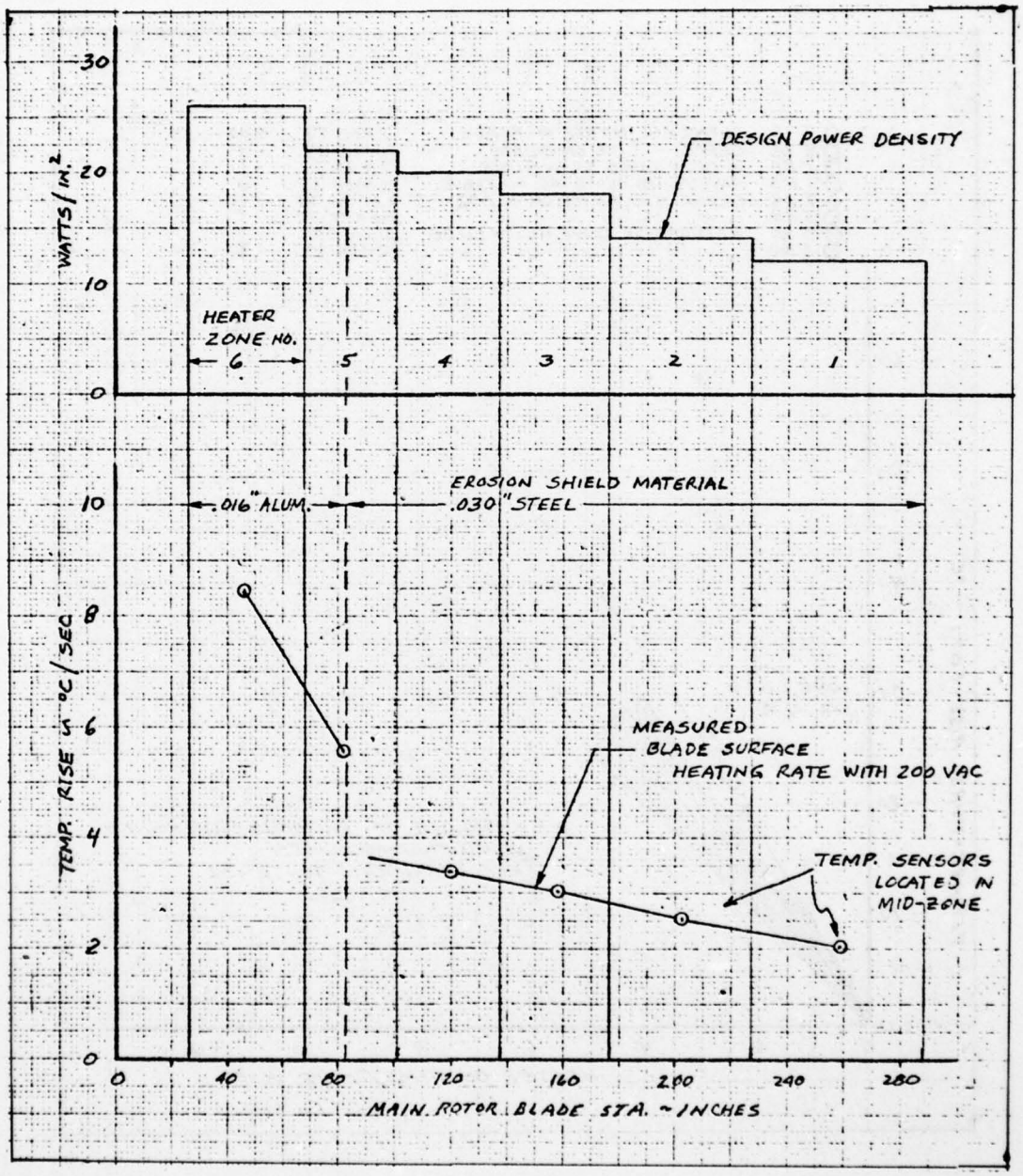

Figure 32. Main Rotor Blade Surface Temperature Rise per Second of Heater-On Time vs Blade Span

steel over the outboard or constant thickness part of the blade. The change occurs in the middle of heater zone 5. The aluminum material was used inboard for ease of manufacture, but results in a problem in setting the heater-on time for zone 5 which heated at a single power density. The heater-on time must be based on the time to heat the steel. This will heat the aluminum surface on the inboard half of zone 5 more than necessary. This overheating is undoubtedly responsible for the runback from this area of the blade that has been experienced during spray rig testing to date. The runback from the inboard half of zone 5 is clearly evident in photographs of blade deicing results (see Figure 9 of Reference 3 and Figures 76 through 79 in Section 8.1 of this report).

Figure 33 shows the rate of temperature increase for each spanwise zone plotted versus design power density. It is apparent that the slope of heating rate versus power density does not pass through zero for the aluminum. This suggests that the actual power density for zone 6, at least along the leading edge in front of the root end fittings where the sensor is located, might be higher than the design 26 watts/in^2 - possibly as high as 33 watts/in^2. This was not obvious from previous data due to the limited number of temperature sensors used in previous testing. This higher power density is probably the cause of the runback experienced from the zone 6 area (see Figures 52 and 53 in Section 8.1 of this report).

Using the data from Figures 29 through 31, the heater-on time that would be required to raise the blade surface temperature to 0^{o}C for the six spanwise zones was determined and plotted versus span in Figure 34. These data are for the ideal case and show a spanwise variation within each zone, whereas a single on-time must be used for each zone to simplify controller design. The higher heating capability of the inboard aluminum section discussed previously is reflected by the drastic reduction in on-time shown for zone 6 and the aluminum portion of zone 5. The importance of defining the actual kinetic heating realized for the outer blade is made apparent in this figure by the large difference in required on-time depending on the kinetic heating realized. Reports of natural icing

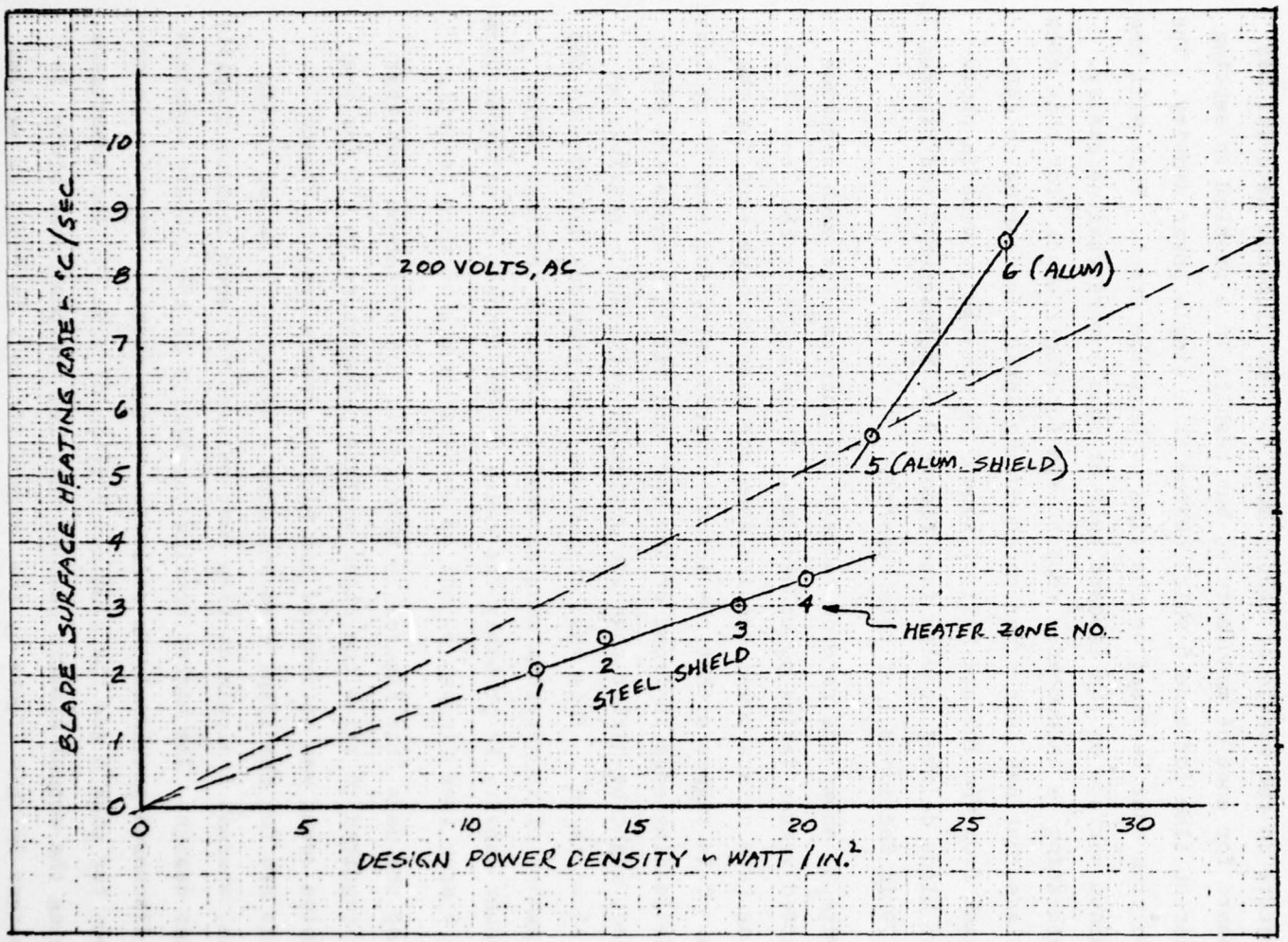

Figure 33. Measured Blade Surface Heating Rate vs Design Power Density

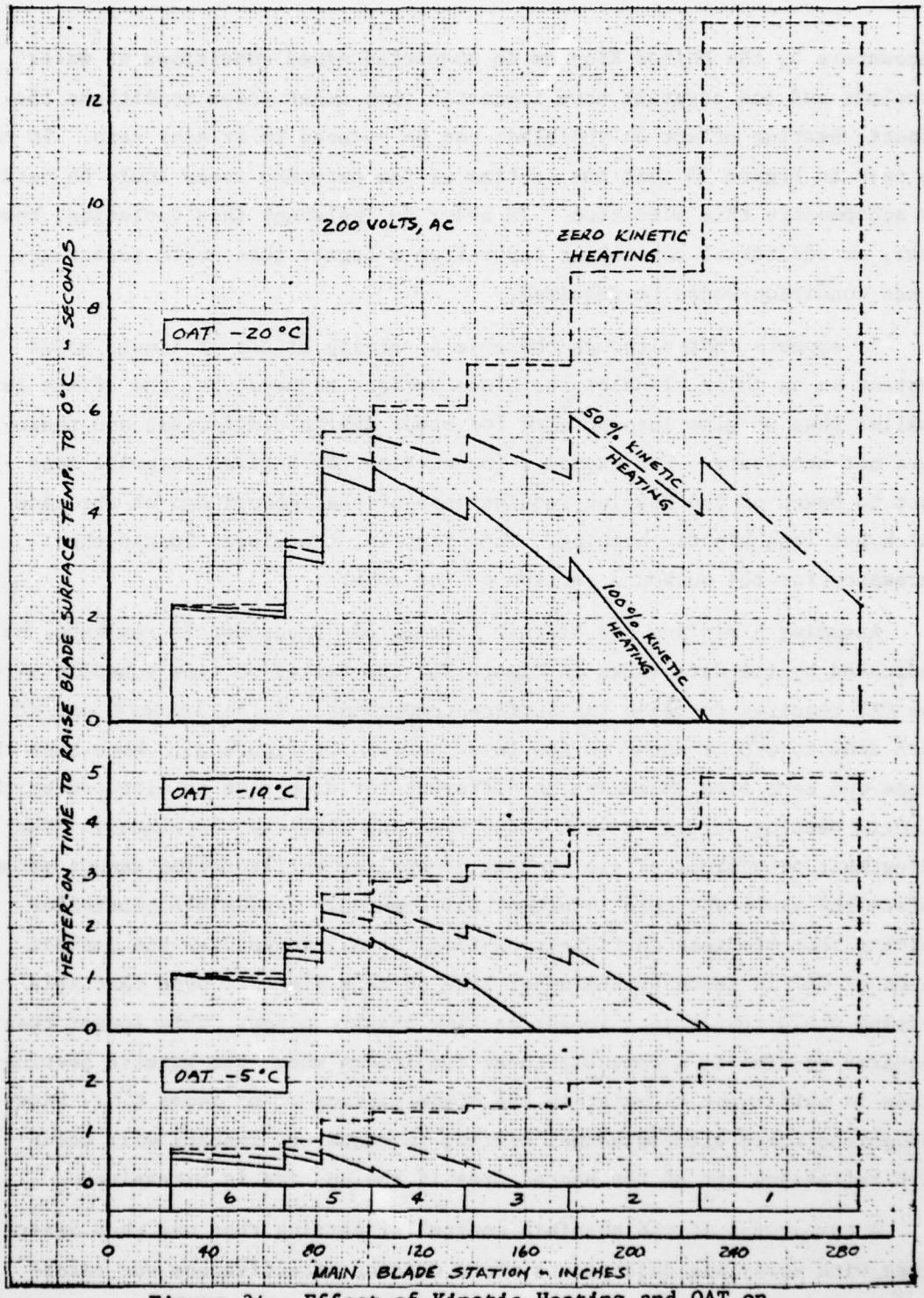

Figure 34. Effect of Kinetic Heating and OAT on Heater-On Time vs Blade Span

encounters by the United Kingdom in suspected mixed conditions of water droplets and ice crystals have indicated that under these conditions the kinetic heating effect on the blade can be reduced to or near zero. It can be seen in Figure 34 that the on-time of the outboard zones could be varied to accommodate this situation. In order to implement this variation, however, an additional controller input from a sensor that could detect the mixed condition would be required.

It appears that although there is a varying effect of liquid water content in an icing cloud on the blade surface temperature, the effect is smaller than margins incorporated for other design compromises and therefore not necessary. For example, the on-time for a given spanwise zone must be based on the heating requirements of the inboard end of the zone which has less kinetic heating. This time is, therefore, longer than necessary for the outboard portion of the zone.

Assuming a minimum net kinetic heating of 50 percent is realized, as indicated by the data shown in Figure 25, the heater-on time schedule versus OAT required to raise the surface temperature of the inboard end of each zone to $0^{o}C$ is shown in the lower portion of Figure 35. Note that the slope and zero time intercept is different for each zone as dictated by the kinetic heating variation with blade span and absolute temperature. The adjustment provisions of the present controller configuration cannot accommodate the slope and zero intercept differences. A possible controller setting that provides sufficient on-time for all zones over the desired range of OAT is shown by the upper line on this figure. Note that this setting would result in a longer on-time than required. This longer than required on-time is acceptable under conditions where the kinetic heating alone is sufficient to maintain the blade surface at or above $0^{o}C$. Under conditions where electrothermal heating is required, runback will occur with refreezing aft of the heated area if the on-time is excessive.

A comparison of the possible controller setting that was thus determined with spray rig data points where deicing effectiveness was established by test is shown on the upper half of Figure 35. This comparison

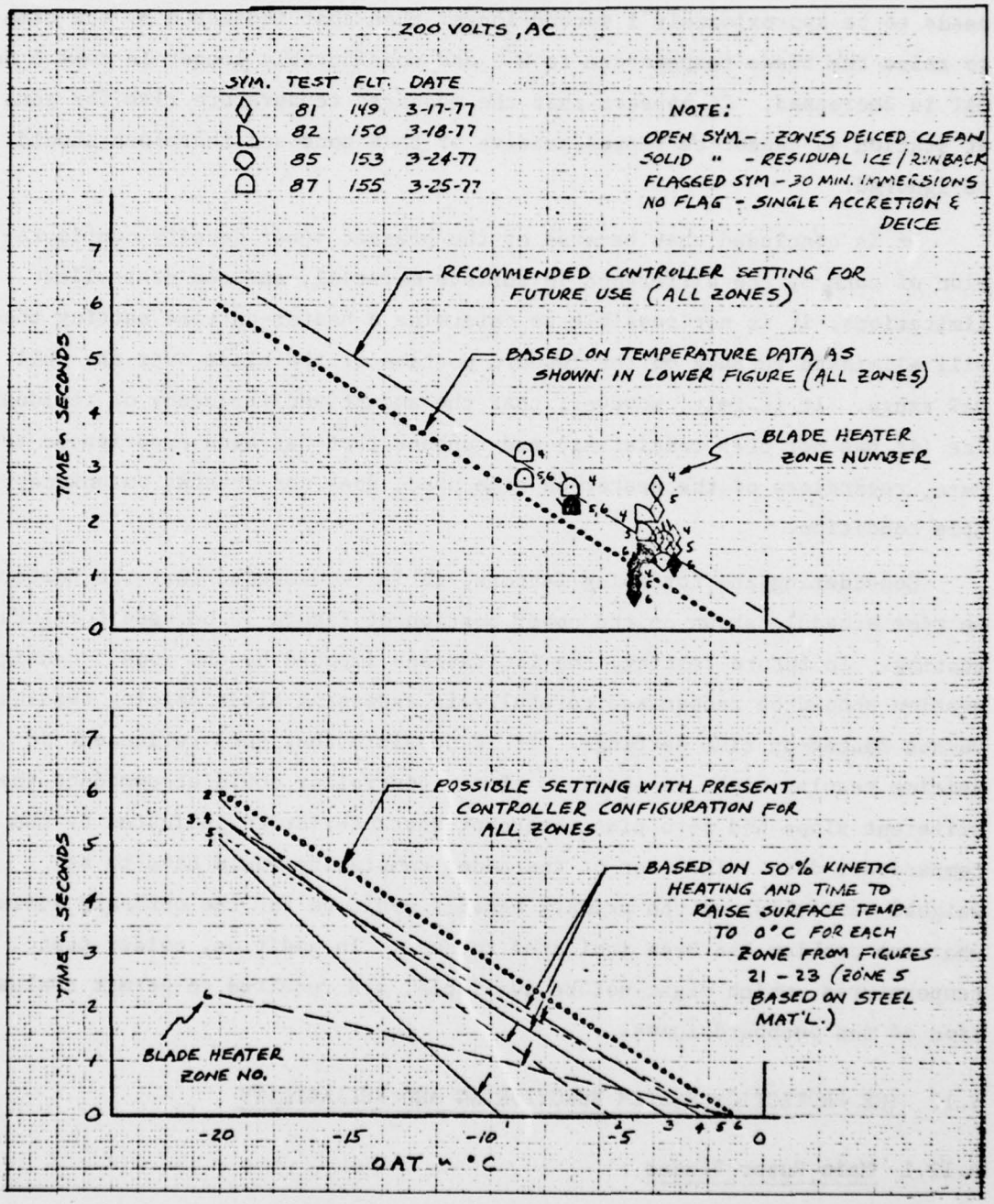

Figure 35. Main Rotor Blade Heater-On Time vs OAT

indicates that for acceptable inboard blade deicing, the heater-on time needs to be approximately 1 second longer than that indicated by the time to raise the blade temperature to $0^{o}C$ and considerably longer in zone 6 as OAT is decreased. It appears that the measured temperature rise for zone 6 at station 46 cannot be representative of that zone and therefore should be ignored.

It is concluded that because of the present power density configuration of zone 5, the difference in surface material, and the controller limitations, it is not possible to determine a heater-on time setting that will eliminate runback on the inboard portion of the blade over the full OAT range. It is felt, however, that the amount and frequency of residual ice (it has not been consistent) and runback that has been experienced to date, regardless of the heater-on time used, does not present an unacceptable condition.

Considering the foregoing factors, it is recommended that the heater-on time schedule shown on the upper portion of Figure 35 be used for future testing. In future testing, the limitations imposed by the zone 5 configuration should be recognized carefully in assessing blade deicing results versus heater-on time settings. It is possible that some refinement in deicing results might be obtained if the controller could accommodate the different slope and zero time intercept characteristics indicated by the temperature data. The cost of the added complexity would have to be weighed carefully, as the primary benefit would be for the outboard zones, where no problem has been indicated to date. In addition, colder test temperatures, which might not be available, are required to permit evaluation of the outboard zones.

4.12 ICE PROTECTION SYSTEM FUNCTIONING AND RELIABILITY

4.12.1 Main Rotor Blades

There were no functional problems experienced with the main rotor blades during this program. Apparently the design improvements incorporated in the new heater installation were effective, although more flight

hours of use are required to be absolutely conclusive with respect to the electrical shorts between the heater element and the erosion shield that were experienced previously. Failures were experienced previously at 25.6 and 37.9 hours on one blade and 43.4 hours on another. The total flight time to date on the improved blade configuration is 43.5 hours.

It is interesting to note that the original blades, which were reworked for this test program by removing and replacing the outboard leading edge erosion strip, did not require any aerodynamic tracking adjustment (tab changes) on reinstallation.

There was a decrease in the measured dielectric strength of the main rotor blades during the period at Ottawa but the decrease is not believed to be attributable to moisture ingress. This conclusion is based on the fact that a comparable decrease was measured on the blade that was never removed from the shipping box during the Ottawa program span and also was measured on the tail rotor blades. This suggests the possibility of an inconsistency in the readings from the measuring device - a 500-volt megohmmeter.

4.12.2 Controller

The ice protection system controller also functioned flawlessly during the entire program. A problem was experienced following the initial wiring reinstallation after the aircraft arrived at Ottawa. This problem, which was due to a wiring error and not a controller fault, caused damage to several of the ice protection system electronic components and required considerable time to troubleshoot and repair, but was not associated with the system design. During this troubleshooting and repair period, an old controller problem, known as "zone skip," was experienced. The cause was identified and a design change was made which eliminated it.

4.12.3 Ice Detection

As described previously, three different types of ice detectors were installed for evaluation. All three systems utilize engine bleed air for

anti-icing and aspirator operation. It was found that the bleed air requirements were significantly different for each system and could not be accommodated satisfactorily. Originally a single bleed air line was installed for the ice detectors that tapped into the line from the engine port that supplies air to the cabin heat system. With this arrangement cabin heating demands would result in an inadequate airflow for the two detectors under some conditions and thus affect the detector functioning. This problem was resolved on a test basis by not using cabin heat.

When a third detector was added, a separate bleed air supply was obtained by using the air that normally operates the scavenge system of the engine inlet air sand and dust particle separator.

During the test program, it was learned that development changes had been made by the supplier to the infrared-type detector to increase its ice detection capability at near $0^{o}C$ temperatures, imposing a high temperature limit to the bleed air supply to this detector. In addition, icing tunnel calibrations were available at only one bleed air pressure which was not the same as in the aircraft installation. In order to satisfy these requirements a separate bleed supply to this detector was needed to assure the high pressure and a cooling radiator was incorporated in the line to reduce the bleed air temperature.

The other detector that originally shared the bleed supply from the cabin heat line was found to have inadequate anti-icing capability with the air temperature provided and required hotter air. This required a more complicated change than practical at the test site or during the program span.

It was also apparent that the normal engine bleed pressure variation with altitude and power setting results in a variation in aspirator bleed flow, and therefore affects aspirator performance which may consequently affect the LWC sensed by the system. Additional icing tunnel tests conducted after the flight program showed the infrared-type detector was insensitive to changes in bleed air pressure within the range of 30-65 psi.

Problems such as those discussed above serve to point out that the proper functioning and accuracy of aspirated ice detectors necessitates careful attention to the temperature and pressure requirements. Ideally the

detector should be insensitive to the normal bleed air variations or incorporate features to control them.

4.12.4 Air Temperature Sensor

As described previously, it was determined during the program that the seemingly random error in the sensing of air temperature by the flush-type OAT sensor used for the deicing control system was caused by internal cabin heat effects on the sensor. The sensor was located where the temperature of the compartment would change with cabin heat cycling and the sensor was a type that must be mounted in an unpressurized or unheated portion of the aircraft. This was not known when the sensor was selected. There is another model of the flush-type sensor that is not affected by the internal temperature of the aircraft. This type should replace the existing one for future test and evaluation.

4.13 STRUCTURAL LOADS

The simulated testing conducted on the test UH-1H previously had shown that blade icing and/or deicing had no measurable effect on rotor structural loads or vibration. The requirement for real-time monitoring of structural loads that had been maintained during testing was deleted for the 1977 test program. Measurement and recording of key structural bending moments and pitch link loads for the main and tail rotors was retained, however, and reviewed after each test flight.

Data from the checkout flights prior to departure for Ottawa showed no difference in main rotor blade structural loads with the improved deicer installation or during deicing operations. As described previously, there was a vibration change noted this year that had not been experienced previously. This was an increase and decrease in 6-per-rev (6P) amplitude with ice accretion and deicing under high altitude operating conditions. This was reflected in the measured blade root flapwise bending moment and in the cg vertical acceleration measurement. Refer to 4.3.3 for a more detailed discussion.

SECTION 5

CONCLUSIONS

The changes made in the main rotor blade deicer installation appear to have eliminated the electrical short problem between the erosion shield and the heater element. More service hours are necessary to be conclusive, but the experience to date with the modified configuration has exceeded previous failure conditions.

The changes made to eliminate the residual ice and runback experienced at the station 83 erosion shield joint have improved but not eliminated the condition. It is apparent that the leading edge surface needs to be completely smooth in order to deice perfectly clean. Deicing of the station 83/zone 5 area is complicated because the zone is heated at a uniform power density (watts per square inch) but is covered with .016-inch aluminum inboard of station 83 and .030-inch steel outboard which results in different heating rates. This precludes optimizing the heater-on time for this zone. In order to aid future optimization testing, a temperature sensor should be added to measure the zone 5 steel material temperature and the station 46 (zone 6) sensor should be relocated to outboard of the blade attach fittings.

Spray rig testing appears to be the only way to identify detailed problem areas of blade deicing as HISS tanker and/or natural icing testing has not indicated any deficiencies. Some method of determining the blade icing/deicing condition during HISS tanker or natural icing testing is necessary if no spray rig tests are accomplished.

The runback experienced to date does not appear to cause any significantly detrimental effect on aircraft operation. An autorotational RPM check indicated a 0 to 12 RPM decrease with severe runback.

More testing of failure modes is necessary to establish whether the design philosophy of continuing to operate with one heater zone inoperative is acceptable. Indications from one test during this program were that the inboard zones 5 and 6 would not shed with ice on the adjacent outboard zone 4.

The use of the number of cycle counts of an accretion-type ice detector appears to be a simple method of scheduling rotor blade deicing, but further investigation under widely varying conditions is necessary before this method can be confirmed as being satisfactory. A more sophisticated system that actually integrated icing rate (LWC) with respect to time which inherently is more accurate than a cycle counting system was evaluated in this program.

The data scatter and accuracy problem that has been experienced with the flush-type OAT sensor used for deicing system inputs in testing to date is due to the particular type of unit used. The unit used was a hermetically-sealed model and was found to be sensitive to aircraft interior heat. Another model is available that is not sealed; it should be used in future testing.

The present ice protection system controller logic that requires icing conditions to be present as sensed by OAT and LWC before the stabilizer bar heater operates is unsatisfactory. During operation in broken or scattered cloud conditions the intermittent heating that results is inadequate for anti-icing of the unit. The stabilizer bar heater power circuit should be modified to a simple on/off circuit.

Additional spray rig tests are needed to better define the effect of runback and inboard blade ice on autorotation RPM. Low temperatures are required for these tests to aid ice retention. In addition, zone failure effects, power density effects, and ice thickness variations should be evaluated.

More natural icing flight testing is necessary to evaluate the ice protection system over a wider range of conditions. Conditions of higher liquid water concentrations, both for blade deicing and exposure of the unprotected areas, are needed, as well as more data in the temperature range of -9^{o} to $-20^{o}C$.

AD-A059 704 LOCKHEED-CALIFORNIA CO BURBANK F/G 1/3
NATURAL ICING FLIGHT TESTS AND ADDITIONAL SIMULATED ICING TESTS--ETC(U)
JUL 78 R H COTTON DAAJ02-77-C-0002
UNCLASSIFIED LR-28240 USAAMRDL-TR-77-36 NL

2 OF 3
ADA
059704

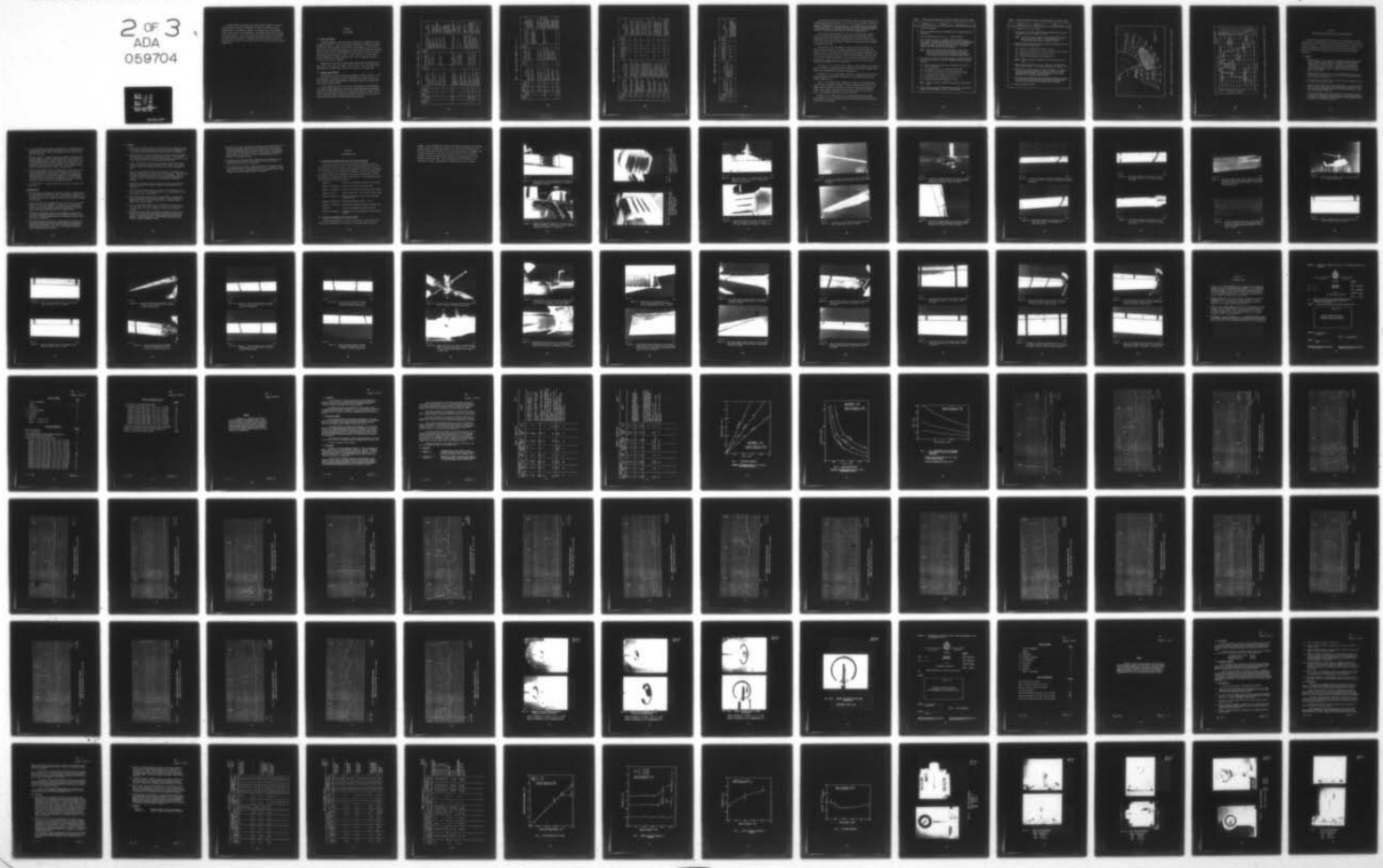

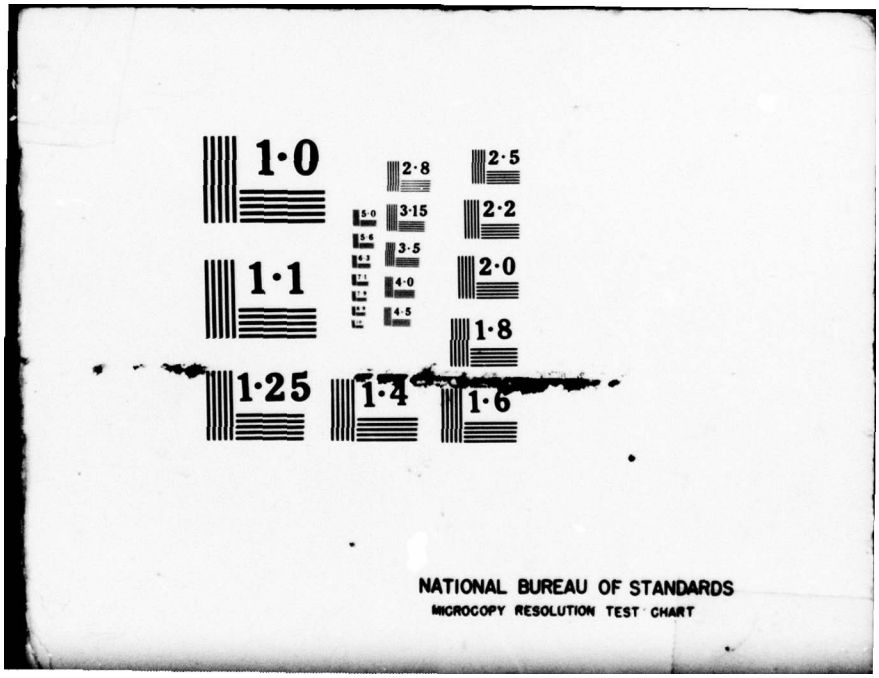
1·0
1·1
1·25
1·4
1·6
1·8
2·0
2·2
2·5
2·8
3·15
3·5
4·0
4·5
5·0
NATIONAL BUREAU OF STANDARDS
MICROCOPY RESOLUTION TEST CHART

A flight release to operate under lower weather minimum for natural icing testing at Ottawa is recommended in order to increase the cost-effectiveness of the testing. Based on the experience of this program, flight safety would not be compromised. The onboard TACAN and ILS systems functioned reliably. The airport radar surveillance service was excellent and demonstrated the ability to identify and track both the test and the chase helicopters easily at altitudes below 1,000 feet AGL within the entire ICECAP area.

SECTION 6

TEST SUMMARY

6.1 SPRAY RIG TESTING

A log-type summary of the seven tests conducted in the NRC spray rig is presented in Table 1. Each test represents essentially a session of testing in the spray rig that started first thing in the morning or as soon as temperature and wind conditions suitable for testing were available and continued that day until either a problem developed or the weather conditions changed, precluding further productive testing. Shown for each of the seven tests are the individual runs made during the test, the run objective, primary results, and pertinent comments.

Seventeen test runs were conducted with varying LWC, deicing heater-on time, time in the cloud, and number of deice cycles. The total flight time involved was 13.1 hours with a total of 4.4 hours in the icing cloud.

6.2 NATURAL ICING FLIGHTS

The details of the ten natural icing flights are shown in Table 2. The test plan was to decrease the test OAT progressively by test but after the first encounter the available weather conditions resulted in accepting the OAT at which icing was found.

A total flight time of 17.3 hours were accumulated on the ten flights. The flight time was generally two hours per flight (maximum fuel endurance) unless it was obviously fruitless to continue the search for icing. On the five flights during which icing was encountered, the total time in the overcast was 5.0 hours with 4.0 hours under icing conditions.

TABLE 1. SPRAY RIG TESTING SUMMARY (Sheet 1 of 2)

SPRAY RIG TEST NO.	1977 DATE	OUTSIDE AIR TEMP- °C	CLOUD LWC- g/m³	RUN NO.	RUN OBJECTIVE	MINUTES IN CLOUD	BLADE ICE COVERAGE PRIOR TO DEICING	NO. OF DEICE CYCLES	BLADE DEICING RESULTS	REMARKS
1	28 Feb	-3.5	0.4	1	Verify on-time from last year's data.	4.4	Ice on Zones 4, 5, 6 (1.8" max thickness)	1	Blades clean except on instrumentation at Station 46	Self shed beyond .47 R
		-3.0	0.8	2	Increase LWC in attempt to get better ice accretion.	2.0	Ice on Zones 4, 5, 6 about same as Run 1	1	Blades clean except on instrumentation at Station 46	Single deice OK. Instru. causes ice hang-up.
		-2.4	0.8	3	Check multiple deicing results.	14.0	-	7	L.E. didn't deice. Mid-chord clean, lots of runback.	Mr. Ron Price says runback is moderate to severe.
				-	Repeat deice in attempt to clean blades	-	Residual from Run 3 on L.E. of Zones 4, 5, 6.	1	Clean except strip of L.E. ice on outb'd Zone 4.	Cleaned runback off manually.
		-2.3	0.8	4	Repeat multiple deicing but using shorter on-time	15.0	-	6	L.E. ice still on Zone 5 and 4. Runback from Zone 6.	Controller was operating out-of-sync for entire test - Deice sequence for zones was 5-6-1-2-3-4 instead of 1-2-3-4-5-6.
2	17 Mar	-4.8	0.8	1	Deice Zone 1-4 only to observe Sta 83 wraparound strip effects on Zone 5 runback.	2.0	Ice on Zones 6, 5 and 1/3 of Zone 4 (Self-shed beyond).	1	Zone 4 didn't deice so all ice still on blades.	No adverse effect of wraparound strip was evident.
		-	-	-	Deice all blade ice.	-	Ice still on Zones 6, 5, and 4 from Run 1.	1	Blades didn't deice.	Heater-on time may be too short.
		-4.0	-	-	Repeat deice cycle using on-time increased ΔT = 3.5°C.	-	Ice still on Zones 6, 5, and 4 from Run 1.	1	Blades clean	Longer on-time is OK.
		-3.5	0.8	2	Multiple deicing to check results with on-time bias = 3.5°C ΔT.	30.0	-	15	Blades almost perfectly clean. Some ice on Zone 6 instru. blade. Slight runback.	Appears 1 second longer on-time is req'd.
3	18 Mar	-4.8	0.8	1	Verify 1 sec longer on-time needed.	2.0	Ice on Zones 6, 5, 4, and 1/3 of Zone 3.	1	Both blades clean except 1/3 - 1/2 of Zone 6 had residual ice.	Tail rotor slipring bearing failure terminated the testing.
4	24 Mar	-4.5	0.75	1	Try shorter on-time (Bias = 2.0°C ΔT).	2.5	Ice on Zones 6, 5, 4 - none on top surface.	1	Didn't land to check single cycle results.	Spray cloud coverage poor.
		-3.5	0.75	2	Multiple deicing with the shorter on-time (OAT warming rapidly).	30.0	-	12	Blades clean with very little runback.	Poor cloud - Δ OAT setting of -2°C looks OK.

TABLE 1. SPRAY RIG TESTING SUMMARY (Sheet 2 of 2)

SPRAY RIG TEST NO.	1977 DATE	OUTSIDE AIR TEMP- °C	CLOUD LWC- g/m^3	RUN NO.	RUN OBJECTIVE	MINUTES IN CLOUD	BLADE ICE COVERAGE PRIOR TO DEICING	NO. OF DEICE CYCLES	BLADE DEICING RESULTS	REMARKS
5	25 Mar	-8.8	0.65	1	Verify Δ OAT of -2°C is satisfactory on-time	3.0	Ice on Zones 6, 5, 4, 3, and 1/4 of Zone 2 (0.25" at 0.5 R).	1	Blades clean - best yet.	Self-shed beyond .65 R on-time OK for single cycle.
		-8.0 to -6.3	0.65	2	Multiple deicing with the on-time bias = 2.0°C.	30.0	-	10	Red blade had Zone 6 & 5 ice still on and runback. White blade was clean with minor runback from Zone 5.	Δ OAT Bias of -2°C appears adequate.
		-5.8 to -5.3	0.65	3	Effect of inboard blade ice on auto rpm.	3.0	Ice had self-shed to 1/2 of Zone 6.	4	-	Ice accretion may be too thick.
		-4.7 to -4.2	0.65	4	Collect inb'd ice only for auto rpm check.	3.0	Zone 4 had ice but 5 and 6 had self-shed.	3	-	Zone 5 & 6 ice shed on shutdown. Should be colder.
6	26 Mar	-4.8 to -4.5	0.75	1	Effect of inb'd ice on auto rpm.	2.0	Didn't land to check to avoid self-shed.	1	Deiced 1-4 only to leave ice on 5 & 6.	308 - 310 rpm with 950 lb fuel remaining.
		-4.3 to -4.2	0.75	2	Induce runback for effect on auto rpm. Use 3 sec on-time, 1 min off.	10.0	Upper surface had ice ridges aft of Zone 6. Lower surface had Zone 5 runback.	10	-	318 - 308 rpm. All ice had sublimated off after auto descent.
		-3.8 to -3.5	0.75	3	Multiple deicing cycles with 50% longer off-time.	20.0	Retained last 5 min of ice to check - only 1/8" thick at 0.4 R.	5	-	OAT too warm for conclusive test. Not much ice for long off-time.
7	1 Apr	-3.5 to -2.4	0.75	1	30 min. immersion w/o deicing.	30.0	-	-	-	Blades self-shed each 8-10 min.

TABLE 2. NATURAL ICING TEST SUMMARY (Sheet 1 of 2)

NAT. ICING FLT. NO.	1977 DATE	WEATHER CONDITIONS	FLIGHT PROFILE	ICING TEST CONDITIONS			MIN. IN CLOUDS	NO. OF DEICE CYCLES	REMARKS
				ALTITUDE-FT	OAT °C	LWC			
1	21 Mar	Broken clouds with base at 3200 feet.	Climbed to OAT of approx. -5°C for first encounter.	5,000	-6	0.2 to 0.3	56	3	Off-time based on 0.1" ice on visual indicator
2	23 Mar	Ceiling 2,000' with light snow. Visibility 5 mi.	Climbed in overcast to limit OAT of -13°C at 8,500' but found no icing. Searched within this limit.	-	-	-	70	-	Windshield wipers collected slush even under non-icing conditions.
3	31 Mar	2,000-ft ceiling with tops around 7,000 ft. OAT +2°C on ground to -6°C at 7,000'.	Climbed up through clouds to 6,700' on top. Descended to 4,000' for best LWC.	4,000	-2	0.3	40	4-5	Classic double horn ice formations. Deiced on 0.1" on visual and ≈ 260 counts on IRU.
4	2 Apr	5,000-ft ceiling with tops at 9,000 - 10,000'. 0°C at 5,200'.	Climbed to near tops at 9,200 ft and -5°C with only icing indication at 8,000'.	7,500	-2	0.3	58	1	Deicing time based on visual and IRU counts of 260.
			Descended to 7,500' until found ice, then climbed to 9,500' to maintain icing.	9,500	-5	0.3		2	Pilots felt vib. level improved after deicing.
5	2 Apr	2,500 ft scattered with base of overcast at 3,500'.	Climbed to 11,000' (1,500' on top) but found no ice. Descended back into clouds and searched.	-	-	-	40	-	No icing found. Minimum OAT was -1°C at 5,000'. +1°C at 8,000'.
6	4 Apr	3,000 ft ceiling with top above 12,000 ft.	Climbed to 12,000 ft. 11,300' first icing indication. Isothermal at -7°C from 4,500' to 12,000'.	10,500	-6	0.25	75	3	Descended to 10,500' because of roughness at 12,000'. Definite vib. increase and decrease with ice/deice.
7	5 Apr	High clouds in east ICECAP area only.	Climbed to 12,000' where encountered scatter clouds but only got brief "trace" icing indication.	-	-	-	-	-	Weather had passed by the time flight was launched.
8	6 Apr	Thin layer of broken clouds at 5,500 - 7,500'.	Climbed to 6,500' and flew in and out of broken cloud layer.	6,500	-18	0.15	50	2	Rime ice obscured visual ice accretion indicator scale. FM antenna whipping observed by chase.

TABLE 2. NATURAL ICING TEST SUMMARY (Sheet 2 of 2)

NAT. ICING FLT. NO.	1977 DATE	WEATHER CONDITIONS	FLIGHT PROFILE	ICING TEST CONDITIONS			MIN. IN CLOUDS	NO. OF DEICE CYCLES	REMARKS
				ALTITUDE-FT	OAT	LWC			
9	6 Apr	Thin layer of scattered clouds at 6,500'.	Climbed to approx. 6,500' and flew through as many clouds as possible.	-	-	-	-	-	No icing found.
10	8 Apr	Scattered clouds 2,500' to 5,000'.	Found intermittent light icing of short durations.	2500 to 4500	-15	0.1	-	-	Not enough ice for a deicing cycle. Ice sublimated between encounters. 4-inch length of ice on FM antenna but no abnormal oscillations.

The flight test card used on the initial flights on which the main rotor blade deicing interval (off-time for 1/4-inch ice on the blade) was based on estimated information as shown in Table 3. The integrating rate unit (IRU) reading of 260 shown for the infrared-type ice detector system was suggested by the manufacturer as a suitable starting value. This value needs to be adjusted as required to match specific aircraft characteristics.

The 0.1-inch thickness shown for the visual ice accretion indicator (airfoil section with a graduated leading edge probe) was based on the approximation that the aircraft flight speed was one-third of the velocity of the main rotor blade at midspan; therefore, 0.1-inch was used or roughly one-third of 0.25 inch.

The value of 13 for the number of cycles of the infrared-type ice detector was obtained from the previous determination of 10 counts in the spray rig cloud. This value was corrected to the in-flight condition by the ratio of the counts per minute at a given LWC experienced in the spray rig to the counts per minute obtained in the icing tunnel calibration runs of the detector. Based on data at two values of LWC, this ratio was established as approximately a 1.3:1 count ratio.

The value of 1 to 2 counts for the number of the ultrasonic-type detector cycles was based on supplier-furnished calibration data which, however, was based on the unaspirated ice detector configuration.

The value of 5 psi torque change was based on results of previous Army icing testing and successfully used during previous HISS testing of this aircraft (Reference 1).

Later in the program, after preliminary analysis of the various data sources showed a disparity between the various expected off-time cues, the flight card was modified to include an in-flight evaluation of different values in an attempt to optimize the off-time at least on a qualitative basis. The modified flight card is shown in Table 4.

Figures 36 and 37 show typical plots maintained during the natural icing flights to aid in defining the location and extent of the icing conditions found on the flight.

TABLE 3. TYPICAL FLIGHT CARD USED FOR INITIAL NATURAL ICING TEST FLIGHT

TEST NO. _____ FLIGHT _____ DATE _____

1. Start per checklist.

2. Proceed to ICECAP area per operations plan following specified procedures.

3. Turn LH windshield volts to _____. (Test variable)

4. Enter clouds and climb to altitude that will have icing at ___°C (Test variable that started at -5°C and then progressively was lowered. The LWC was not specified as the use of a progressive increase in exposure time was felt to be adequate control over the effects of this variable.)

   NOTE: Start ice accretion time (off-time) at first icing indication from infrared-type detector (shortest cycle time) or as soon as a positive icing condition is identified any other way, whichever occurs first.

5. Fly level at the IAS for 90 KTAS and deice periodically basing the off-time interval on the best judgement of the following criteria:

   (a) The off-time versus LWC curve from spray rig tests (if g/m^3 is constant).

   (b) An integrating rate unit (IRU) reading of 260.

   (c) A visual ice thickness of 0.1 inch on airfoil probe.

   (d) An infrared-type detector cycle count of 13.

   (e) An ultrasonic-type detector cycle of 1 to 2.

   (f) An engine torque rise (change) of 5 psi.

   NOTE: Clear all counters immediately after each blade deice cycle.

6. After a total of 4 (test variable) deice periods, descend and rendezvous with CHASE for visual check and photos.

TABLE 4. MODIFIED FLIGHT CARD USED FOR LATER NATURAL ICING TEST FLIGHTS

TEST NO. _____ FLIGHT _____ DATE _____
1 - 4. Same as for initial flights. 5. Fly level at IAS for 90 KIAS and deice automatically using the integrating rate unit (IRU) set at 260. NOTE: Turn M and T rotor switches ON and MODE switch to AUTO prior to entering clouds. A deicing cycle will be initiated when mode switch is moved to AUTO. 6. Monitor the below listed off-time cues for correlation with the 260 value and with each other. (a) Off-time vs LWC curve from spray rig data. (b) Visual ice thickness of 0.2 inch on airfoil probe (1 band). (c) Infrared-type detector cycle counts of 19. (d) Ultrasonic-type detector cycle counts of 3. NOTE: Clear all counters immediately after each blade deice cycle. 7. After the first blade deice cycle, change the IRU setting to 180 (Infrared counts = 13, ultrasonic counts = 2, visual = 0.1). 8. Based on test crew evaluation of step (5) versus (7), select a new IRU setting and continue in icing conditions for 4 more cycles (unless judgement of unprotected area ice accretion indicates the total time should be less). 9. Exit the icing environment and rendezvous with CHASE as rapidly as possible and at the altitude with coldest VFR temperature (to aid in ice retention) for visual check and photos. 10. Return to base and land.

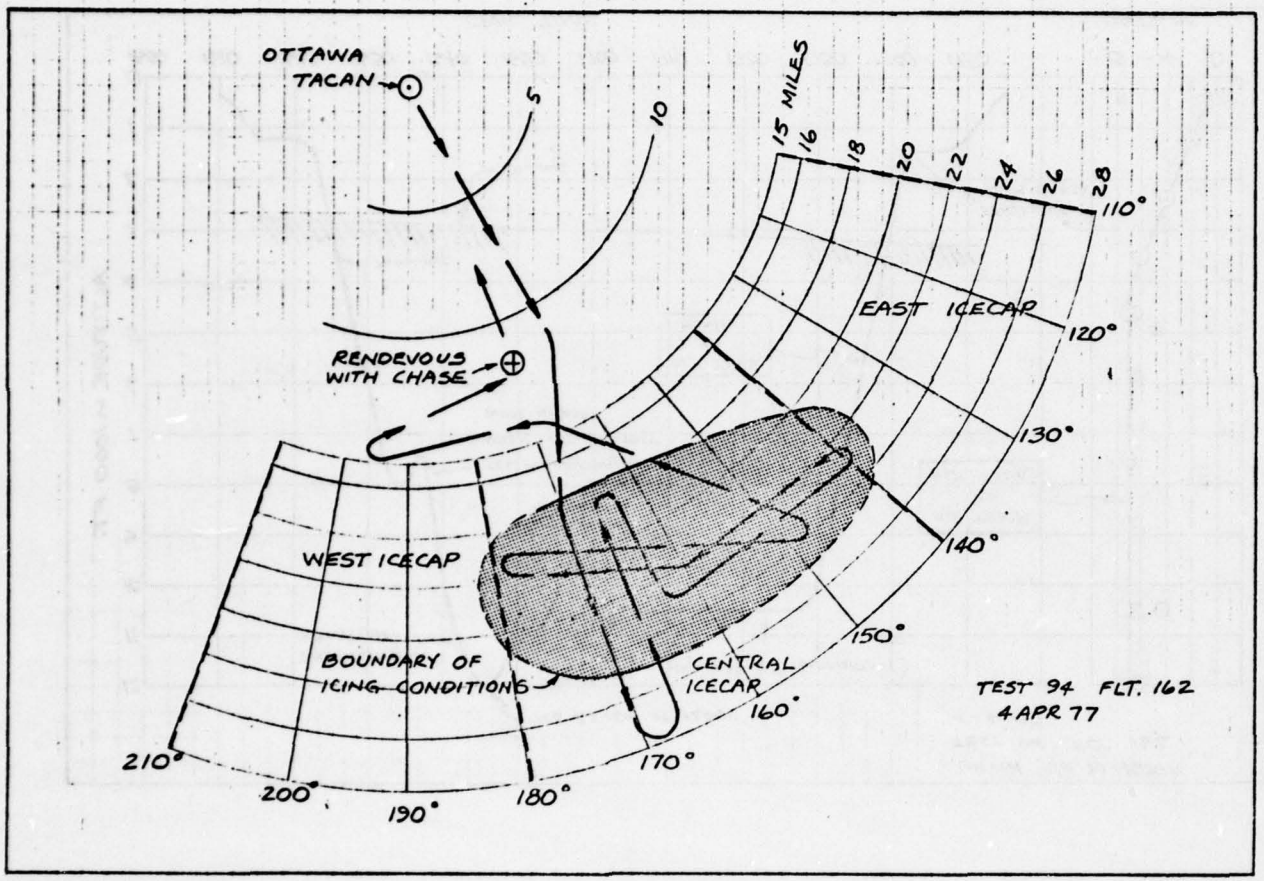

Figure 36. Typical Running Plot of TACAN Data Made During Natural Icing Flight

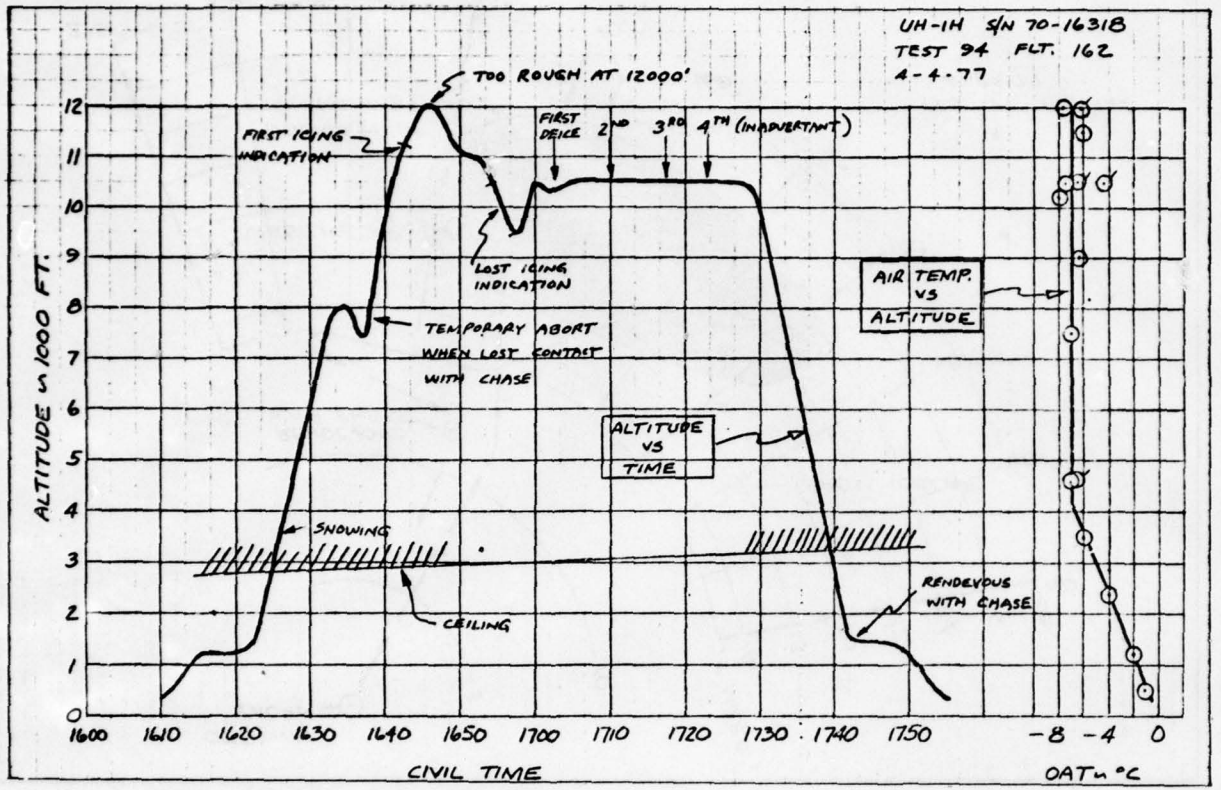

Figure 37. Typical Altitude and Air Temperature Plots Made During Natural Icing Flight

SECTION 7

ICING TEST NOTES BASED ON UH-1H PROGRAM EXPERIENCE

Included in this section are some icing test observations, opinions, conclusions and recommendations that have been noted from the UH-1H program experience to date. It is hoped that the information will be useful in the design, planning, and testing of other ice protection systems. They are grouped under different categories although the grouping is somewhat arbitrary.

7.1 DESIGN

- Unheated bands or cold spots in the otherwise deiced leading edge portion should be kept as small as possible because they will impair blade deicing and result in residual ice, especially at temperatures of -10°C and below. The UH-1H had problems with a 0.5-inch wide band at 0.3 R. The band was caused by heater element edge distance under the erosion shield at a production joint in the shield.

- Blade surface discontinuities of the leading edge surface of any magnitude will collect ice and retain ice after deicing especially at the colder temperatures.

- An icing light for the ice detector needs to have a dimming control the same as any cockpit light.

- Vents can get encased in ice and become blocked. The UH-1H battery vent on the nose was almost closed during HISS testing but at the LWCs and smaller droplet sizes of the natural icing tests to date, no problem has been indicated.

- If a voltage change to the heaters is used to provide more rapid cycling time under heavy icing conditions, an LWC averaging system will have to be employed to avoid frequent voltage cycling and yet accommodate a varying LWC atmosphere.

- A fully automatic ice protection system needs to consider the case of operating in broken cloud conditions as far as system on-off operation and final deicing after emerging from an icing environment are concerned.

- Heater-on time as a function of OAT only appears satisfactory and does not appear to require an LWC input but the mixed condition of water droplets and ice crystals should be a real concern. The United Kingdom relates a definite concern and is desirous of an ice detector that can sense the condition. The solution to the problem of encountering ice crystals that melt on impact and cool the outer blade, resulting in icing, is not defined.

- Engine exhaust heating should be considered in tail rotor ice protection requirements. On the UH-1H the exhaust plume does not reach the tail rotor in hover with or without the IR suppressor installed, due to the strong rotor downwash. In cruising flight, the plume appears to pass over the lower half of the rotor disk outboard of the hub without the IR suppressor installed and over the entire tail rotor with the suppressor installed.

- An icing light of 5 seconds duration is too short for normal scan detection.

INSTRUMENTATION

- The installation of temperature sensors and wiring to measure blade surface temperature should be as small and smooth a protuberance as possible to avoid ice retention. Any electrical insulation under the sensor also acts as thermal insulation and thus affects measurement accuracy.

- Blade ice should be photographed on the lower surface of the blade because there is more chordwise coverage to see, more problems to deice it, and more runback. The test UH-1H main blades have runback along the transition fairing that smoothes the trailing edge of the raised erosion shield to the lower surface.

- Temperature measurement should be done chordwise, especially if the structure under the heater offers different heat sink characteristics. Deicing problems may not be understood properly without this type of information.

- Photographing blade ice along the leading edge is complicated by the lack of contrast between the ice and snow-on-the-ground backgrounds and winter skies. The clear ice formed at the temperatures near zero cannot be seen aft of the leading edge because of its transparent characteristic.

7.3 TESTING

- Rotor blade structural loads on the UH-1H were not affected by blade ice except at high blade angles and with an excessive amount of ice on the blade (6P experienced with 3/8-inch blade ice at midspan).

- The spray rig is the best place to test and have positive confidence that the system is actually operating as desired. It is the only test mode that offers the ability to stop and look, as well as to test over a wide range of the icing variables (OAT and LWC).

- In the testing of an ice protection system in natural icing conditions or in the HISS cloud, the system either works or it doesn't. Without extensive instrumentation there is no way to ascertain in why.

- The UH-1H tests behind the HISS were successfully completed using heater-on times that later were found to be excessive. They must have resulted in considerable runback that was not apparent. The ice retention problem at station 83 was not apparent during the HISS testing. Good in-flight blade icing photography is obviously required.

- Qualitative testing to optimize heater-on times is very time consuming. Adequate blade surface temperature instrumentation is invaluable.

- It is difficult-to-impossible to evaluate an ice detector in the spray rig even if it is aspirated unless it is located where it will be immersed in the cloud properly.

- Wind velocity and the gust factor are significant variables that must be considered in spray rig operations. These variables can significantly affect the off-time required to accrete a given amount of ice on the blades.

- Once the proper off-time has been determined for a given LWC, it can be extrapolated with confidence to any mean LWC using the formula mean LWC x off-time = constant, at least up to an LWC of $0.8 g/m^3$.

- For natural icing testing, operations in and out of the test site airport under low ceiling and visibility minimums and with snow falling is necessary in order to get maximum utilization of the weather. Frontal passages are usually fairly rapid; therefore, the test window is relatively short.

- The test pilot needs some kind of a visual icing indicator that can be deiced when desired. Something like a miniature airfoil that has the same thickness/chord ratio as the rotor blade is ideal because it will have the same catch efficiency as the blade. Ice thickness can be related by the velocity ratio. This is needed primarily during testing, at least until it has been established that the ice detector is operating properly.

- In natural icing testing, weather observations and changes to the weather need to be recorded for correlation with data results. A detailed flight event log is essential.

- In the spray rig, tail rotor icing is difficult to evaluate because of the same immersion problem described for the ice detector. Tests where the tail rotor is intentionally and fully immersed even at the expense of main rotor immersion may be required.

SECTION 8

SUPPLEMENTAL DATA

8.1 PHOTOGRAPHIC DOCUMENTATION FROM 1976 SPRAY RIG TESTING

This section contains previously unpublished photographs from the test program in the NRC spray rig conducted during February and March 1976. The test results from that program are presented and discussed in Reference 3. Presented herein are additional photographs of details and comparisons that might provide useful background and reference information for other test programs of similar objectives and interests. The photographs reflect the following general subject matter:

Figure 38	- Icing of the standard OAT probe on the UH-1H
Figures 39 through 43	- Engine air inlet filter screen icing
Figures 44 through 49	- Typical ice accretion on the main rotor blade
Figures 50 and 51	- Runback from zones 5 and 6 after 9 deice cycles
Figures 52 through 57	- Main blade deicing results with insufficient heater-on time
Figures 58 through 63	- Main blade deicing results at -11°C
Figures 64 through 68	- Aircraft and component icing in freezing rain
Figure 69	- Intentional runback near main blade tip
Figures 70 through 79	- Comparison of deicing results for the two main blades

8.2 POST-TEST CALIBRATION OF THE ICE DETECTORS

Included as Appendixes A, B, and C to this report are the post-test icing tunnel calibrations of the three ice detectors used in the test

program. These Appendixes are copies of the reports prepared by the National Research Council of Canada who conducted the tests on the ultrasonic-type and the inferential-type detectors for the Eustis Directorate, USAAMRDL. The infrared-type detector tests were conducted by NRC for the ice detector supplier. Consent to publish these reports was obtained from each of the suppliers and from the NRC. These calibrations were conducted on the detectors in the same configuration as installed on the test aircraft.

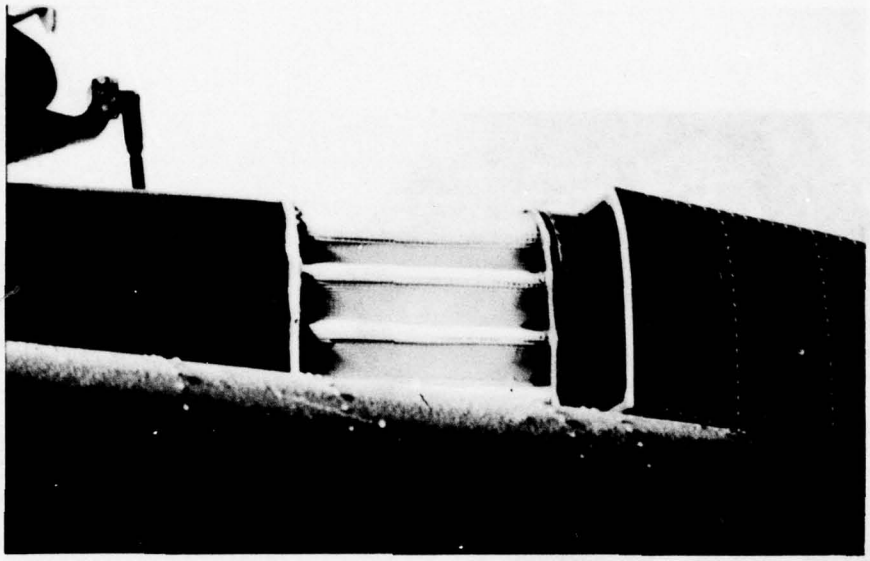

Flt. 72 93

Figure 38. Ice Accretion on the Standard UH-1H Outside Air Temperature Probe After 30 Minutes in Spray Rig at -6.8°C, 0.70 g/m^3

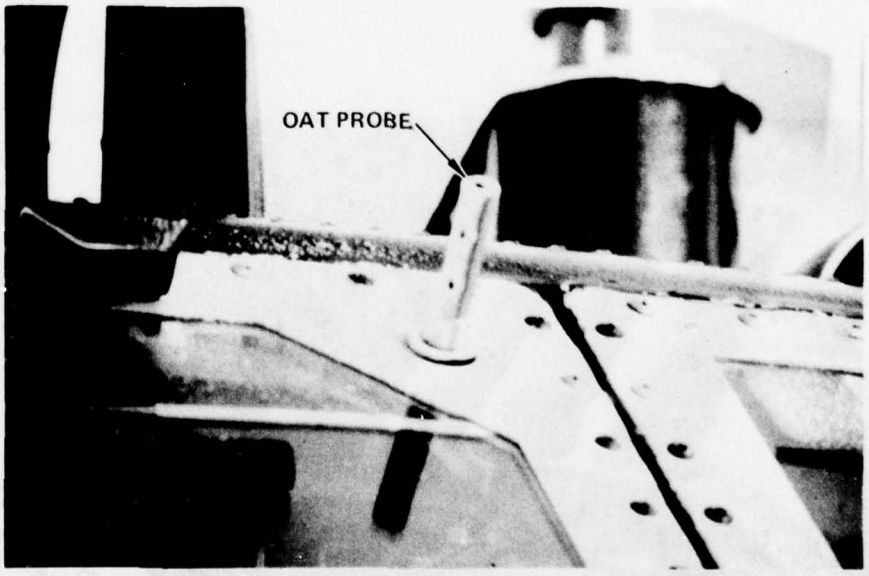

Flt. 86 583

Figure 39. Closeup of Engine Air Inlet L.H. Screen Icing After 30 Minutes in Spray Rig at -11°C, 0.30 g/m^3 (Measured ΔP Change = 5 inches H_2O)

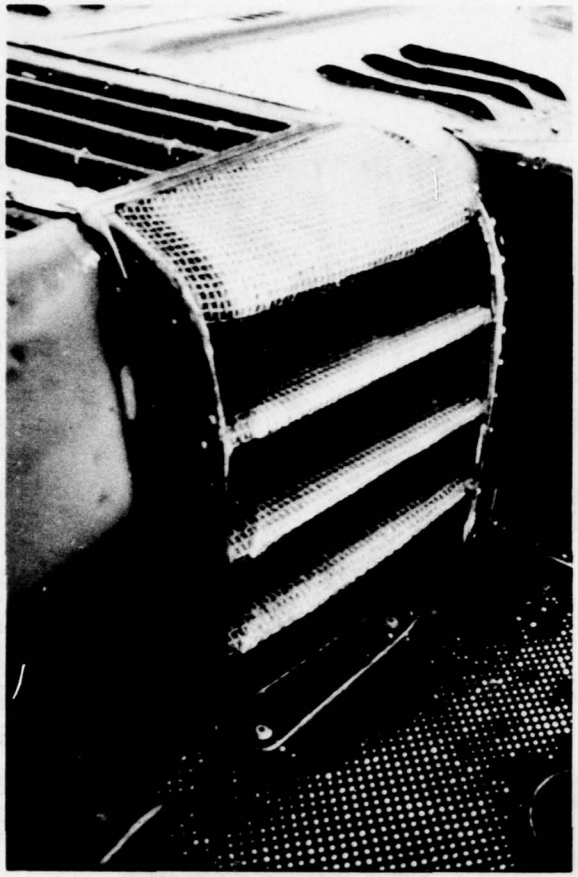

Flt. 155 C

Figure 40. Close-Up Of Engine Air Inlet L.H. Screen Icing, 30 Minutes in Spray Rig At -7.3°C, 0.65 g/m^3 (Measured ΔP Change = 1 inch H_2O)

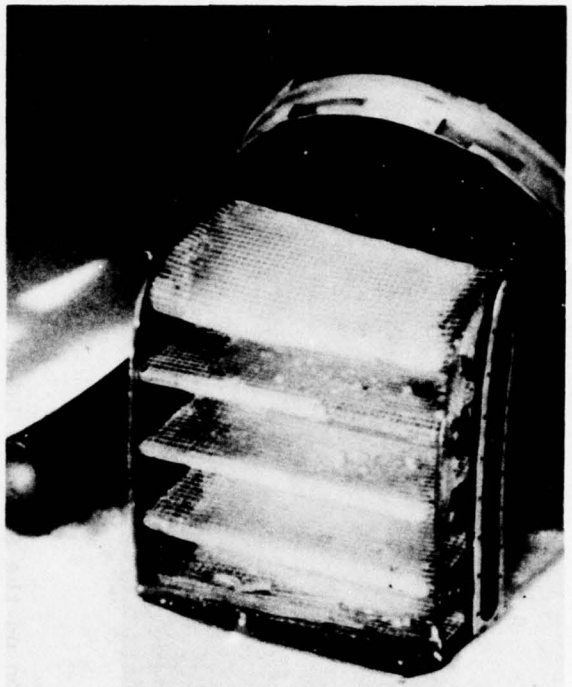

Flt. 80 291

Figure 41. Close-Up Of Engine Air Inlet Screen Icing After 2.5 Minutes in Spray Rig at -3.5°C, 0.80 g/m^3 (Measured ΔP Change = 0)

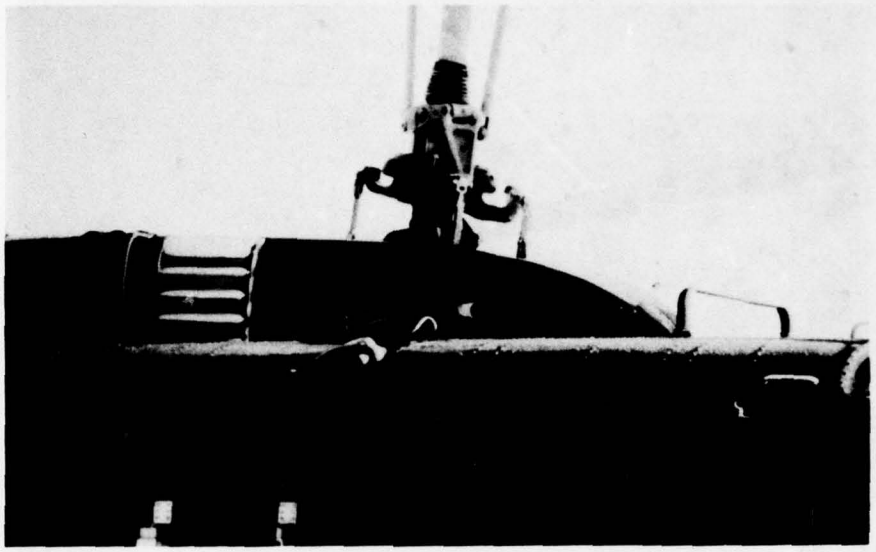

Flt. 72 83

Figure 42. Engine Air Inlet L.H. Screen Icing, 30 Minutes in Spray Rig at -6.8°C, 0.70 g/m^3 (Measured ΔP Change = 2 Inches H_2O)

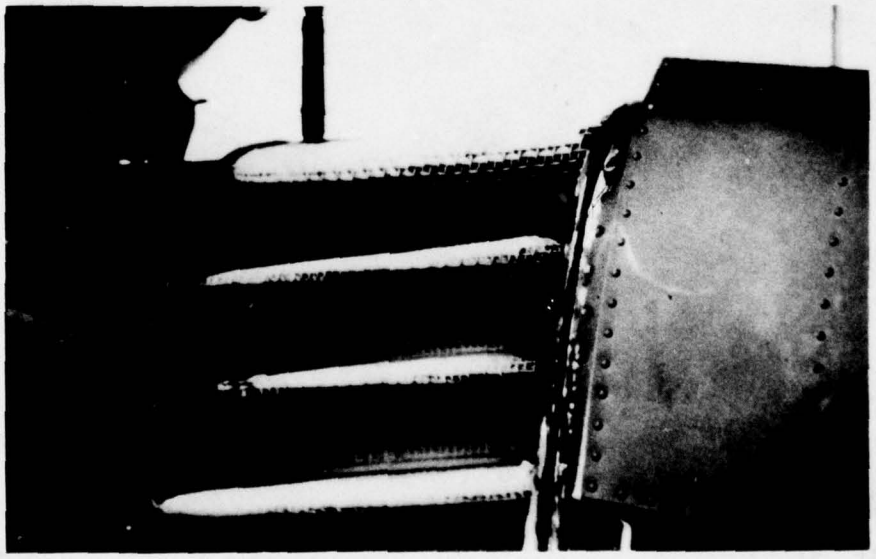

Flt. 72 84

Figure 43. Close-Up of Engine Air Inlet L.H. Screen Icing After 30 Minutes in Spray Rig at -6.8°C, 0.70 g/m^3 (Measured ΔP Change = 2 Inches H_2O)

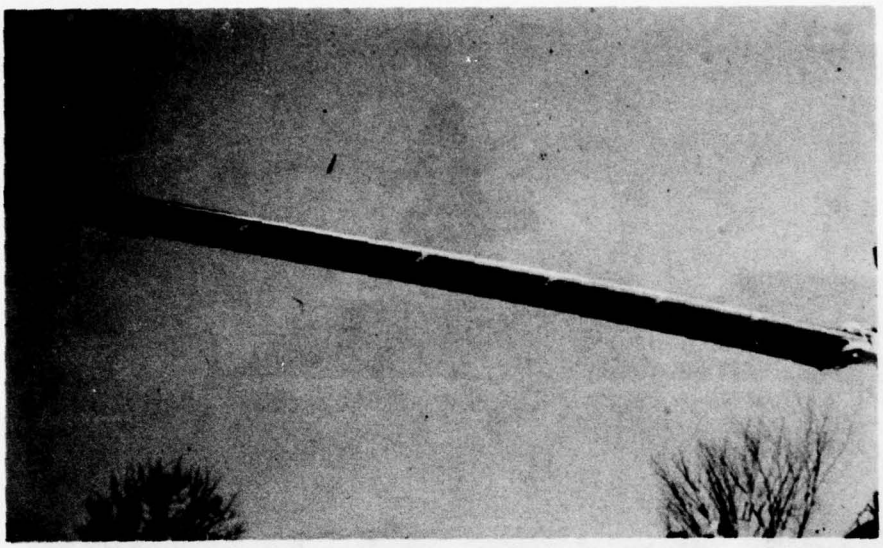

Flt. 81 331

Figure 44. Typical Ice Accretion on Main Rotor Blade Illustrating Maximum Ice Thickness Near Midspan (Spray Rig, -20°C, 0.3 g/m^3)

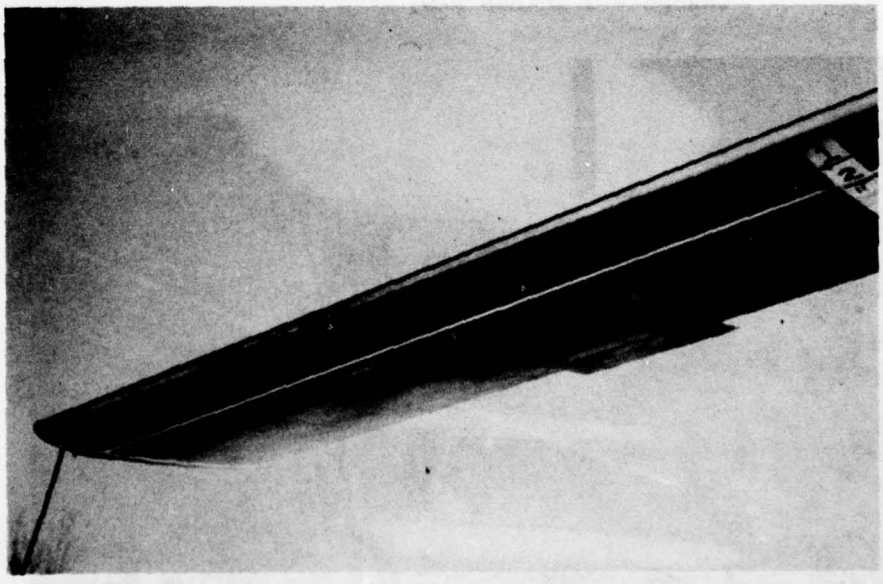

Flt. 81 326

Figure 45. Close-Up of Ice Accretion on Main Rotor Blade Zone 1 (Spray Rig -20°C, 0.3 g/m^3)

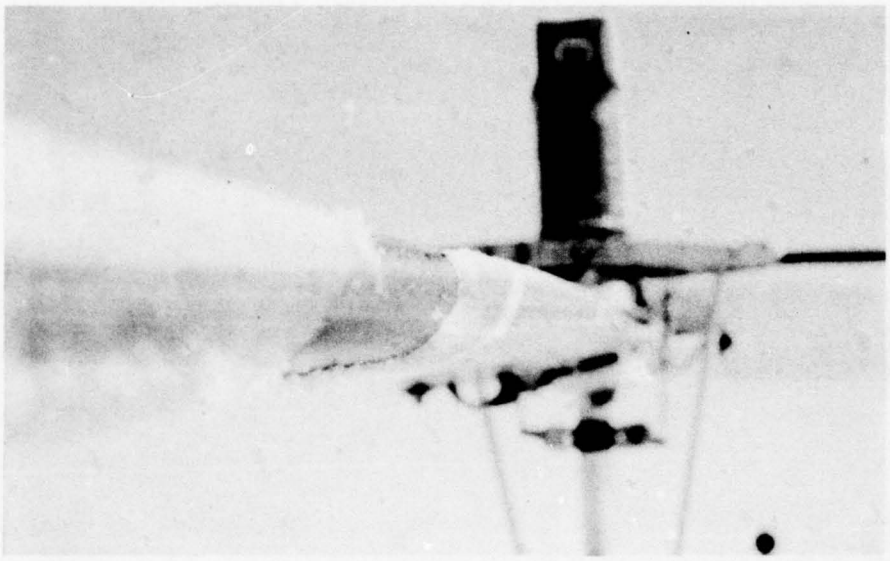

Flt. 89 748

Figure 46. Close-Up of Leading Edge Ice Accretion at Midspan After Ice Thickness Determination Had Been Made (Spray Rig, 1/4-Inch, -11°C, 0.55 g/m^3)

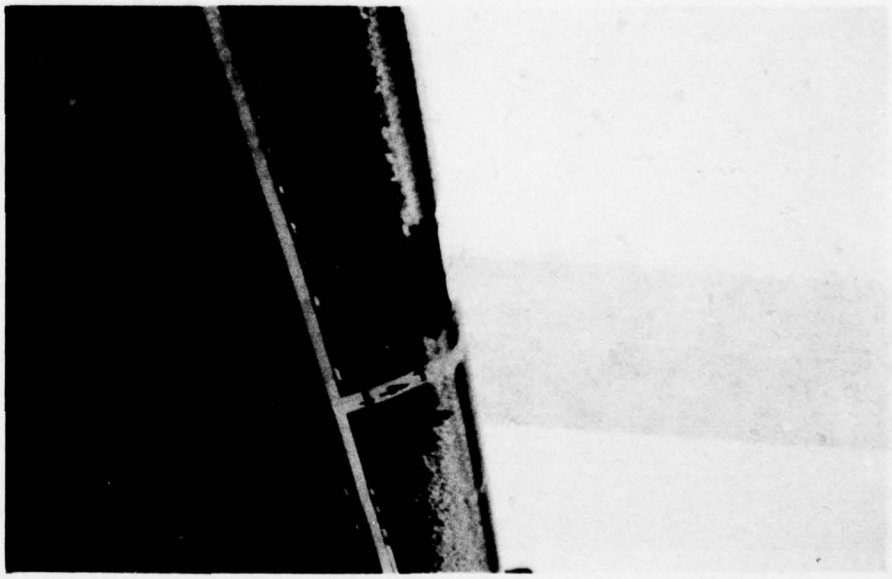

Flt. 86 515

Figure 47. Close-Up of Leading Edge Ice Accretion at Midspan After Ice Thickness Determination Had Been Made (Spray Rig, 1/2-Inch, -12.2°C, 0.3 g/m^3)

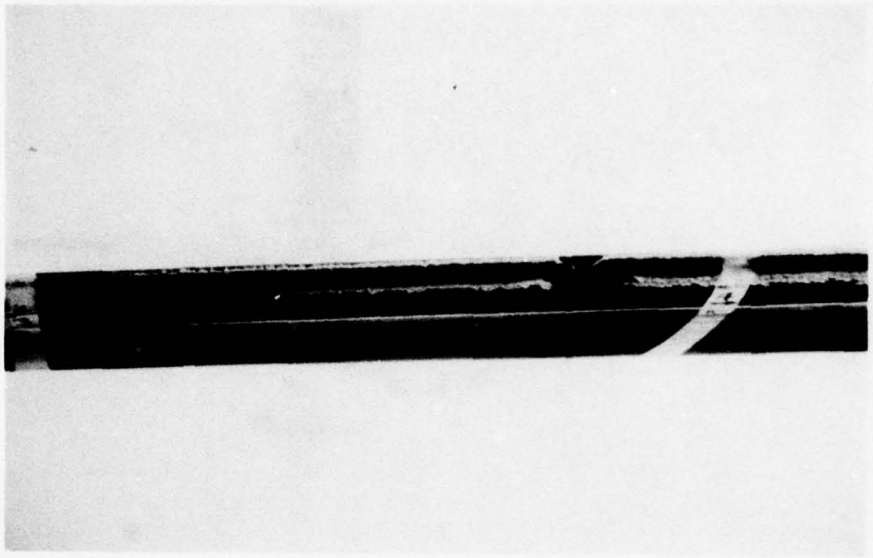

Flt. 86 501

Figure 48. 1/2-Inch Thickness of Main Rotor Blade Ice Accretion at Zone 3 (-12.2°C, 0.3 g/m^3, 3-1/2 Minutes in Spray Rig Cloud)

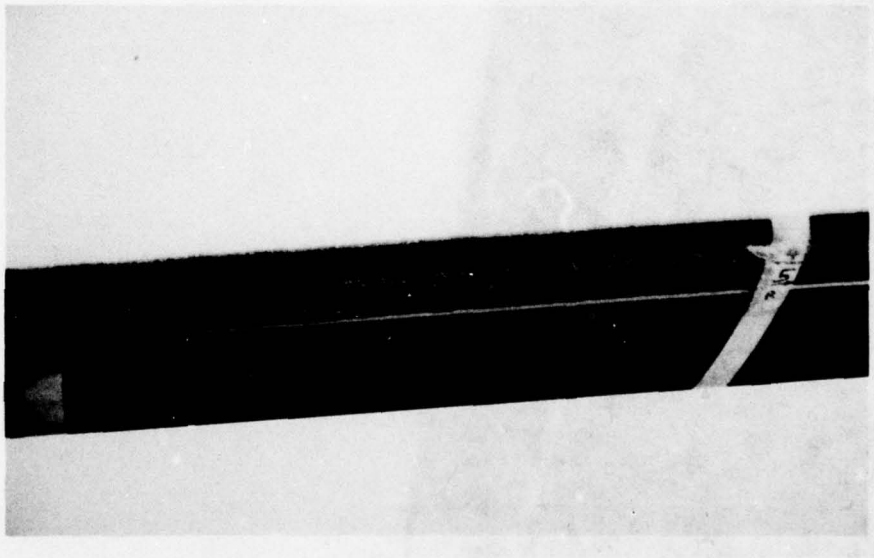

Flt. 86 502

Figure 49. Main Rotor Blade Ice Accretion at Zone 4 (-12.2°C, 0.3 g/m^3, 3-1/2 Minutes in Spray Rig Cloud)

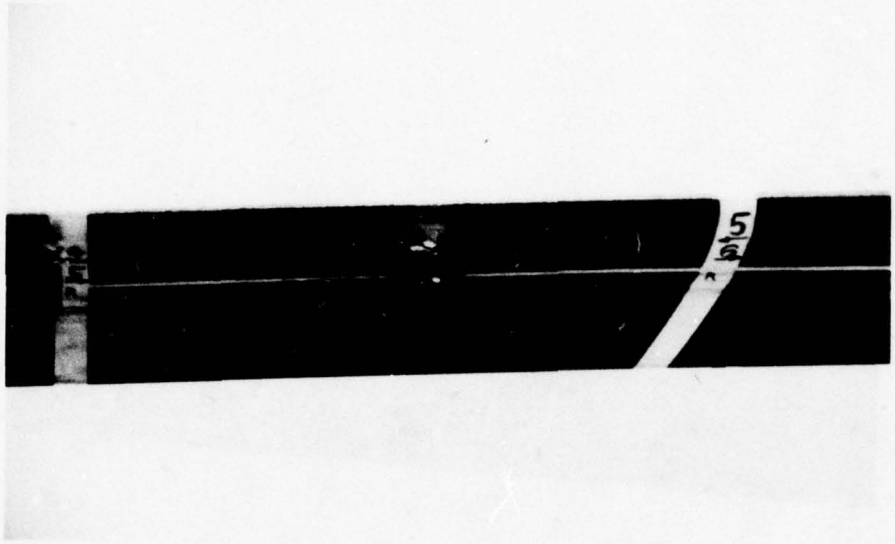

Flt. 86 503

Figure 50. Main Rotor Blade Ice Accretion at Zone 5 (-12.2°C, 0.3 g/m^3, 3-1/2 Minutes in Spray Rig Cloud)

Flt. 86 504

Figure 51. Main Rotor Blade Ice Accretion at Zone 6 (-12.2°C, 0.3 g/m^3, 3-1/2 Minutes in Spray Rig Cloud)

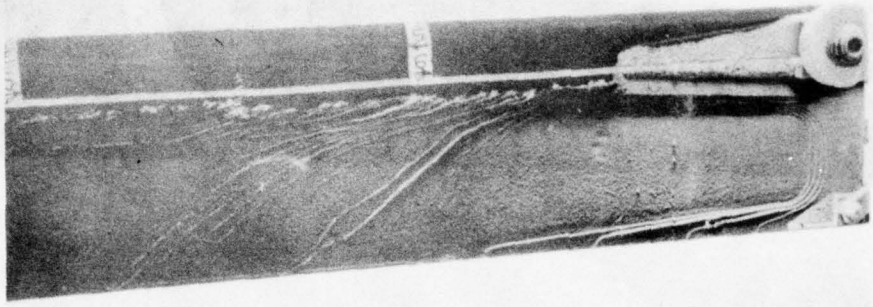

Flt. 86 552

Figure 52. Main Rotor Blade Zones 5 and 6 Condition Following 30-Minute Spray Rig Run Deicing Each 3-1/2 Minutes for 9 Deice Cycles (-12°C to -8°C, 0.3 g/m^3, Snow Falling During Test)

Flt. 86 550

Figure 53. Close-Up of Runback From Zone 6 and Inboard Half of Zone 5 (Doubler Area) Following 9 Deicing Cycles During 30-Minute Spray Rig Run (-12°C to -8°C, 0.3 g/m^3)

Flt. 87 676

Figure 54. Test Aircraft During -11°C, 0.5 g/m^3 Spray Rig Run in Light Freezing Rain

Flt. 87 602

Figure 55. Zone 3 Incomplete Deice Due to Insufficient Heater-On Time (-11°C, 0.5 g/m^3)

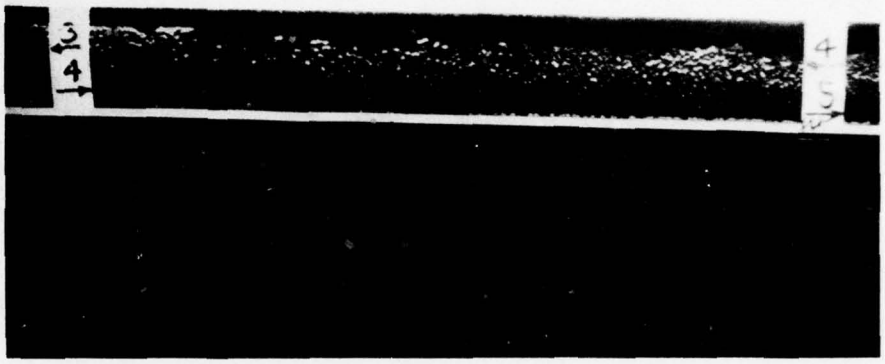

Flt. 87 603

Figure 56. Zone 4 Incomplete Deice Due to Insufficient Heater-On Time (-11°C, 0.5 g/m^3)

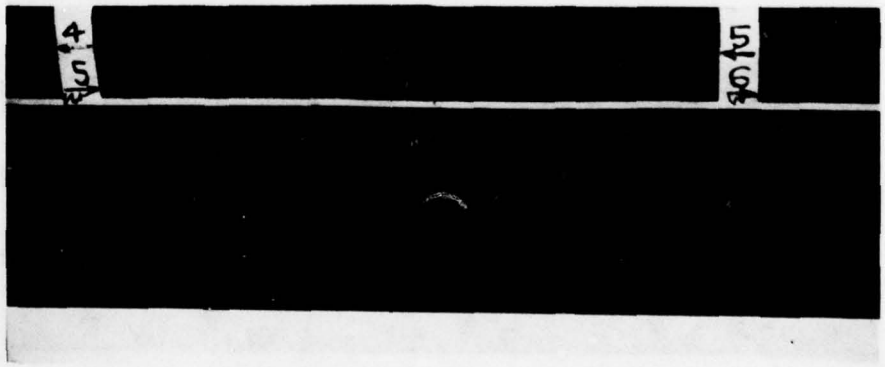

Flt. 87 604

Figure 57. Zone 5 Incomplete Deice Due to Insufficient Heater-On Time (-11°C, 0.5 g/m^3)

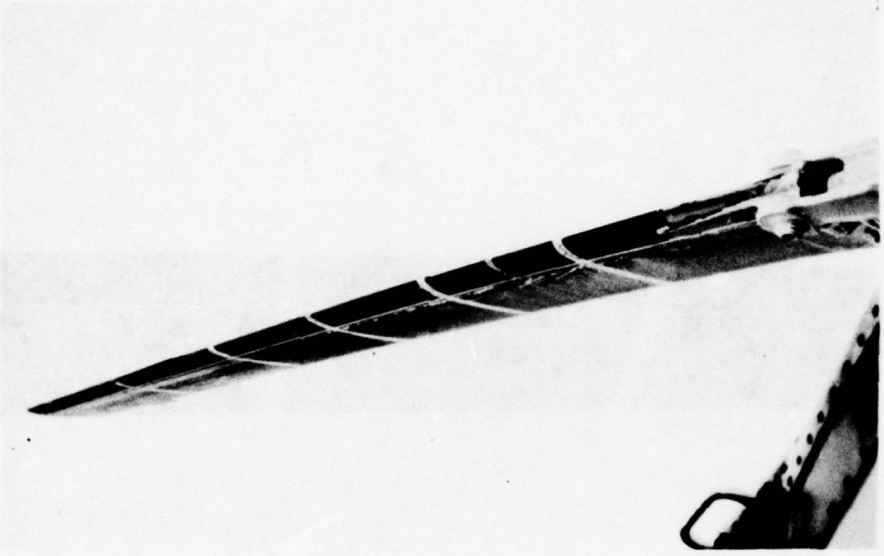

Flt. 87 625

Figure 58. Overall Blade Deicing Results Following 30-Minute Spray Rig Run (-11°C, 0.5 g/m^3) in Light Freezing Rain

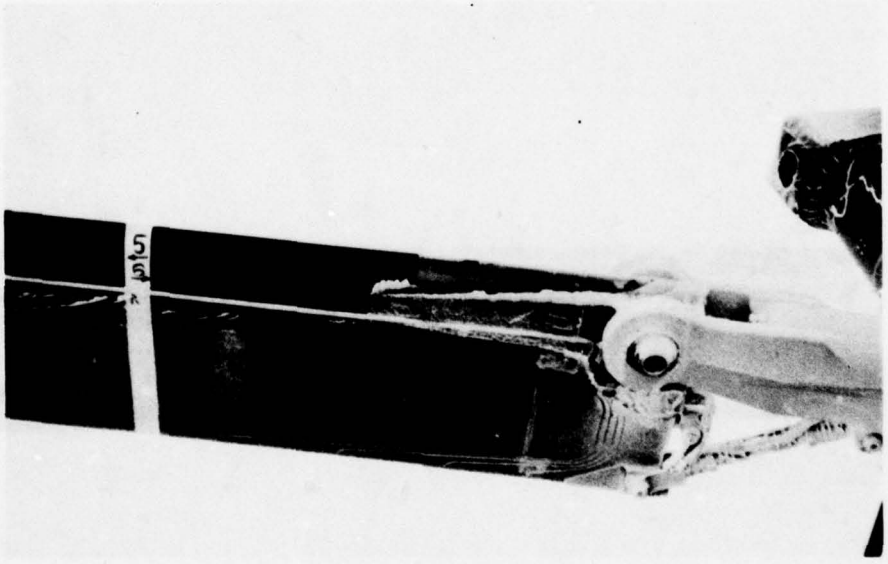

Flt. 87 630

Figure 59. Zone 6 Deicing Results Following 30-Minute Spray Rig Run (-11°C, 0.5 g/m^3) in Light Freezing Rain

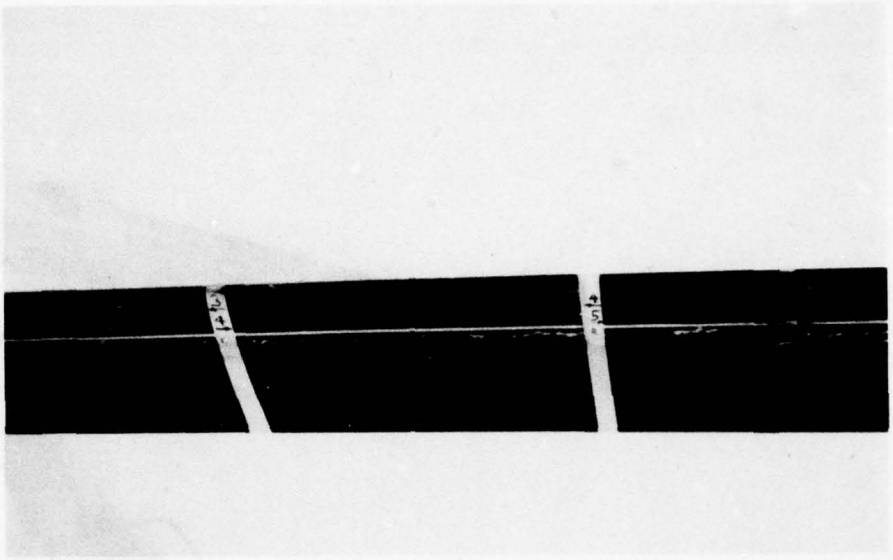

Flt. 87 628

Figure 60. Zone 5, 4, and 3 Deicing Results Following 30-Minute Spray Rig Run (-11°C, 0.5 g/m^3) in Light Freezing Rain

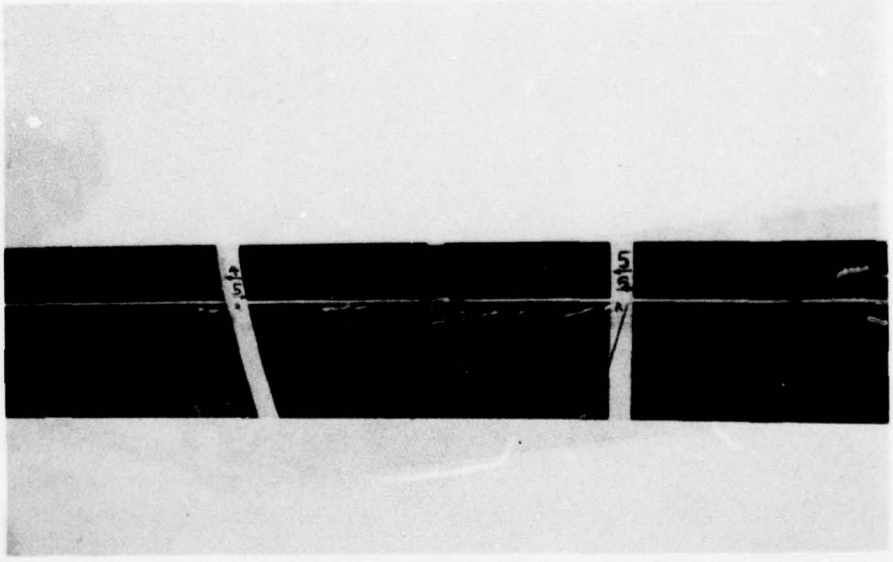

Flt. 87 629

Figure 61. Zone 6, 5, and 4 Deicing Results Following 30-Minute Spray Rig Run (-11°C, 0.5 g/m^3) in Light Freezing Rain

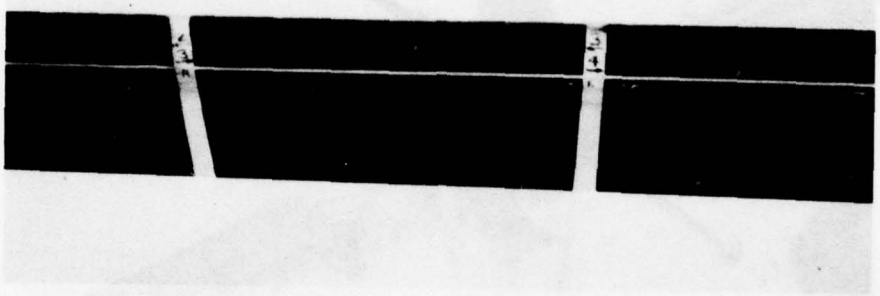

Flt. 87

627

Figure 62. Zone 3 Deicing Results Following 30-Minute Spray Rig Run (-11°C, 0.5 g/m^3) in Light Freezing Rain

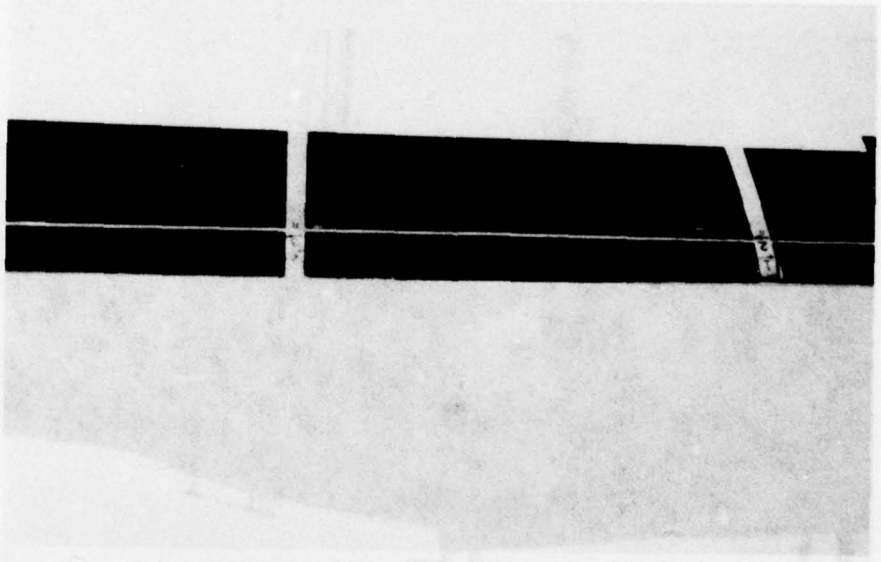

Flt. 87

626

Figure 63. Zone 2 Deicing Results Following 30-Minute Spray Rig Run (-11°C, 0.5 g/m^3) in Light Freezing Rain

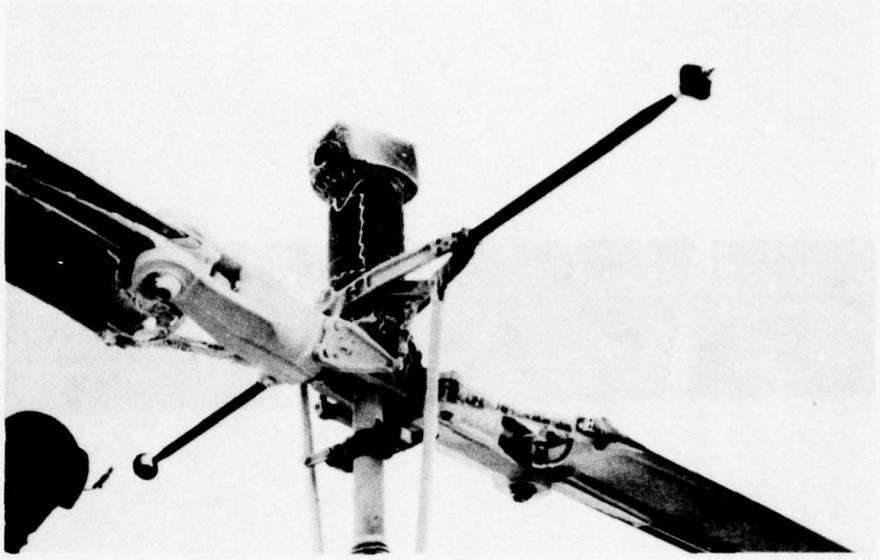

Flt. 87 644

Figure 64. Rotor Hub Area Following 30-Minute Spray Rig Run (-11°C, 0.5 g/m^3) in Light Freezing Rain

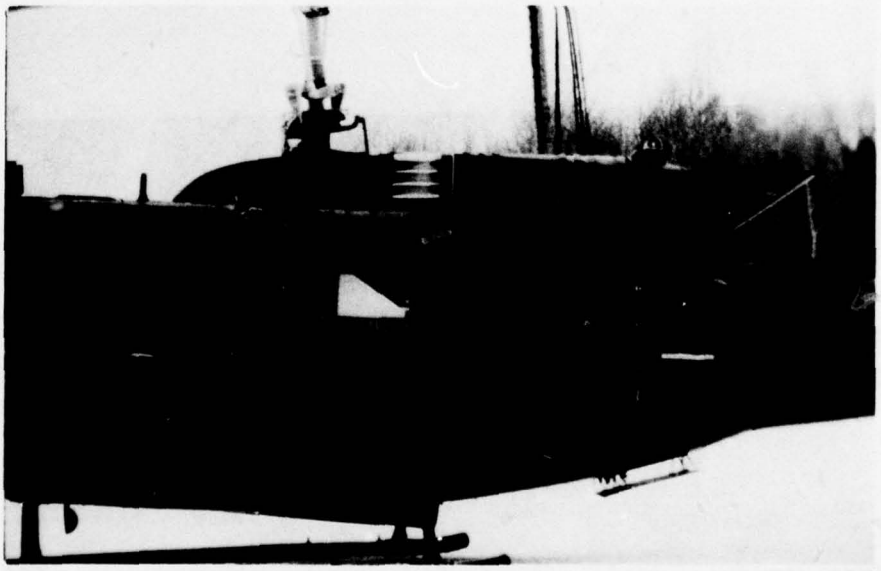

Flt. 87 655

Figure 65. Engine Air Inlet L.H. Screen and Mid-Fuselage After 30-Minute Spray Rig Run (-11°C, 0.5 g/m^3) in Light Freezing Rain (Measured ΔP Change = 5 Inches H_2O)

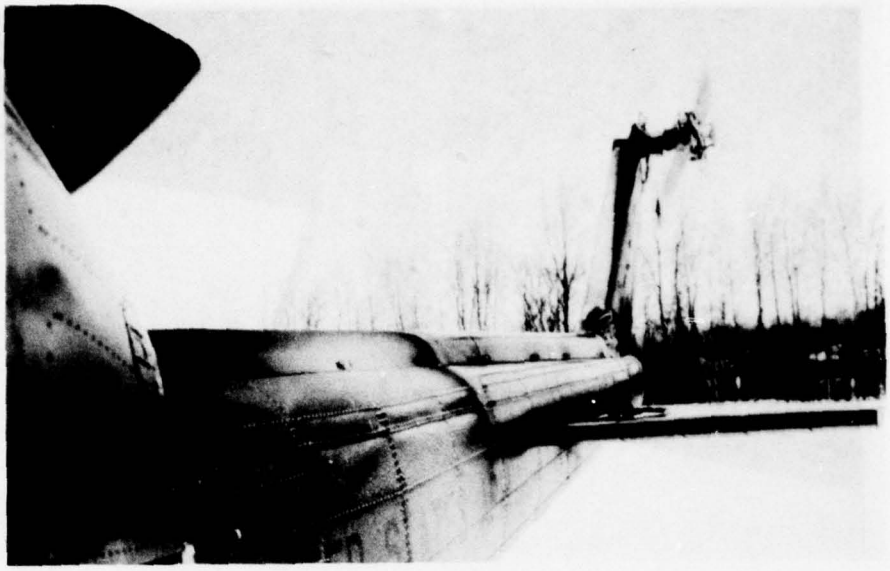

Flt. 87 661

Figure 66. Freezing Rain on L.H. Side of Aft Fuselage After 30-Minute Spray Rig Run - Note Engine Exhaust Heat Pattern on Fuselage (-11°C, 0.5 g/m^3)

Flt. 87 660

Figure 67. Freezing Rain on R.H. Side of Aft Fuselage After 30-Minute Spray Rig Run - Note Lack of Engine Exhaust Heat Pattern on Fuselage (-11°C, 0.5 g/m^3)

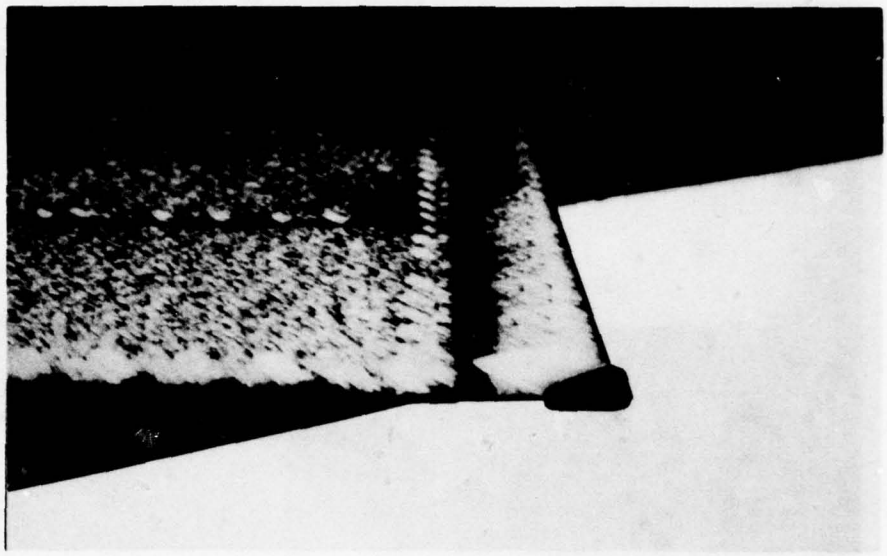

Flt. 87 663

Figure 68. Close-Up of Ice Formation on L.H. Synchronizing Elevator After 30-Minute Run in Freezing Rain (-11°C, 0.5 g/m^3)

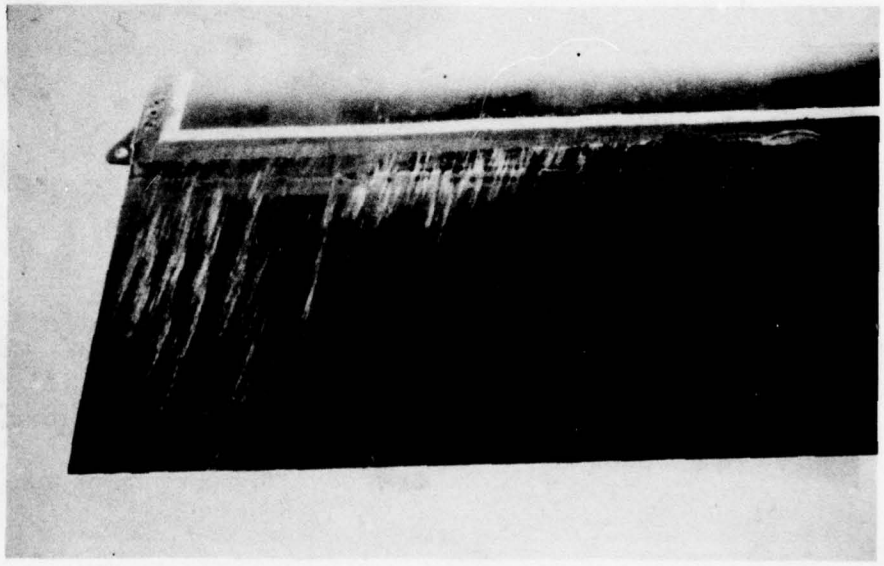

Flt. 82 433

Figure 69. Intentionally Induced Runback on Lower Blade Surface from Zone 1 Resulting From Insufficient Ice Thickness (3 Cycles at 1/2 the Proper Off-Time) (-14.4°C, 0.45 g/m^3)

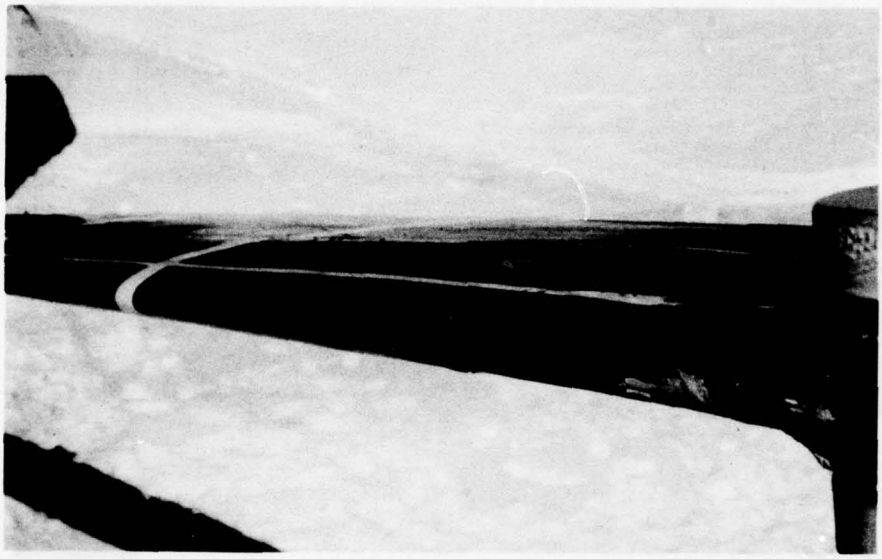

Flt. 81 409

Figure 70. Main Blade Upper Inboard Surface Deicing Results Following 30-Minute Spray Rig Run - Red Blade (-18°C, 0.35 g/m^3)

Flt. 81 411

Figure 71. Main Blade Upper Inboard Surface Deicing Results Following 30-Minute Spray Rig Run - White Blade (-18°C, 0.35 g/m^3)

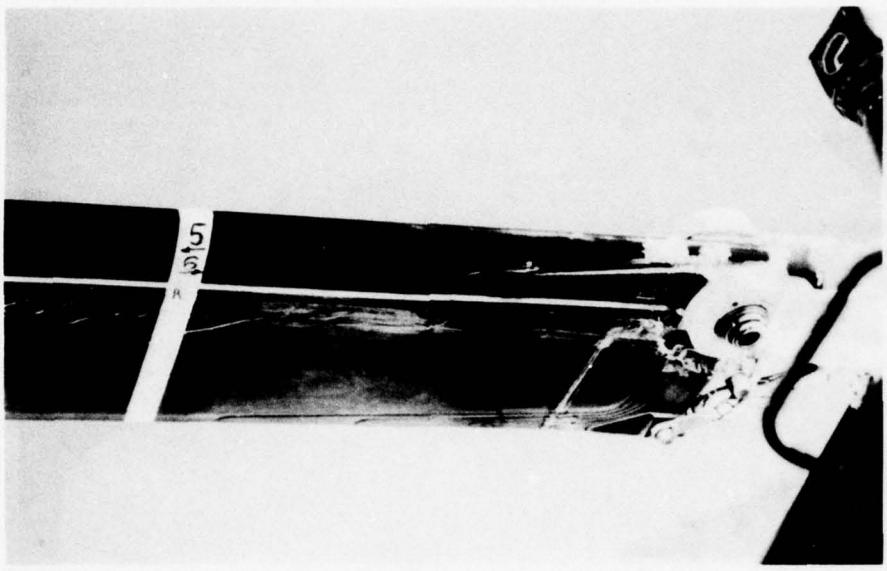

Flt. 81 408

Figure 72. Lower Inboard Surface Deicing Results Following 30-Minute Spray Rig Run - Red Blade (-18°C, 0.35 g/m^3)

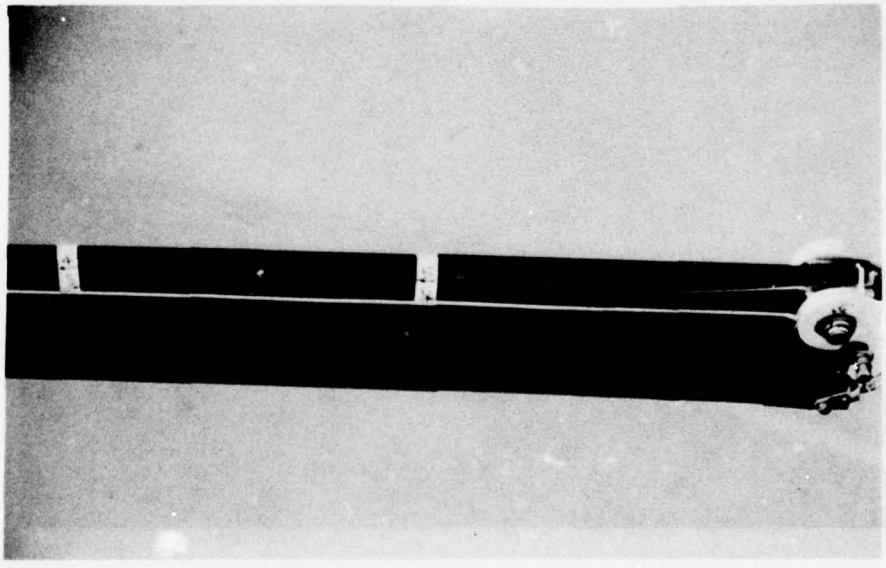

Flt. 81 412

Figure 73. Lower Inboard Surface Deicing Results Following 30-Minute Spray Rig Run - White Blade (-18°C, 0.35 g/m^3)

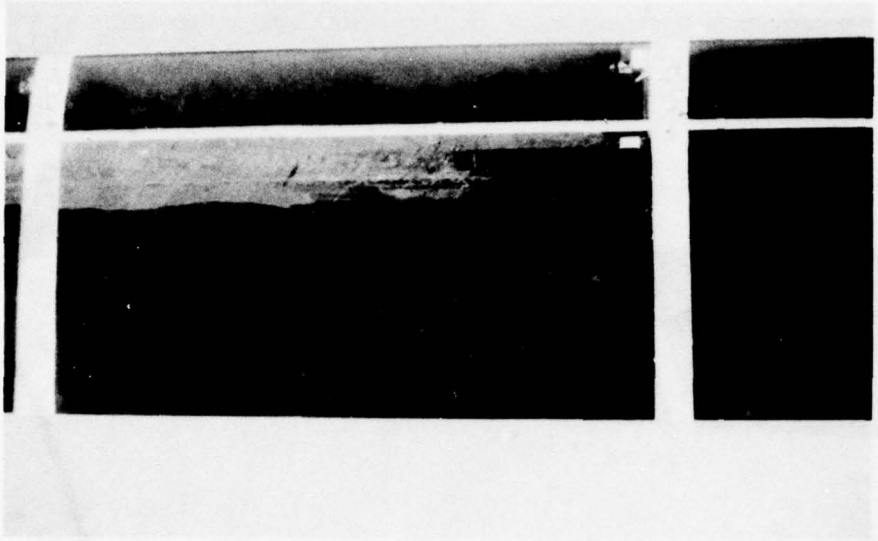

Flt. 81 405

Figure 74. Lower Surface Zone 4 Deicing Results Following 30-Minute Spray Rig Run - Red Blade (-18°C, 0.35 g/m^3)

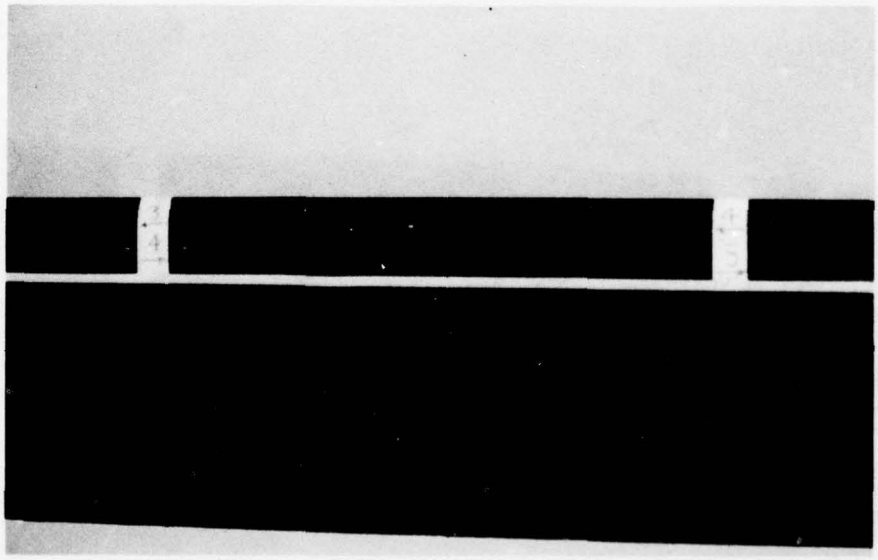

Flt. 81 413

Figure 75. Lower Surface Zone 4 Deicing Results Following 30-Minute Spray Rig Run - White Blade (-18°C, 0.35 g/m^3)

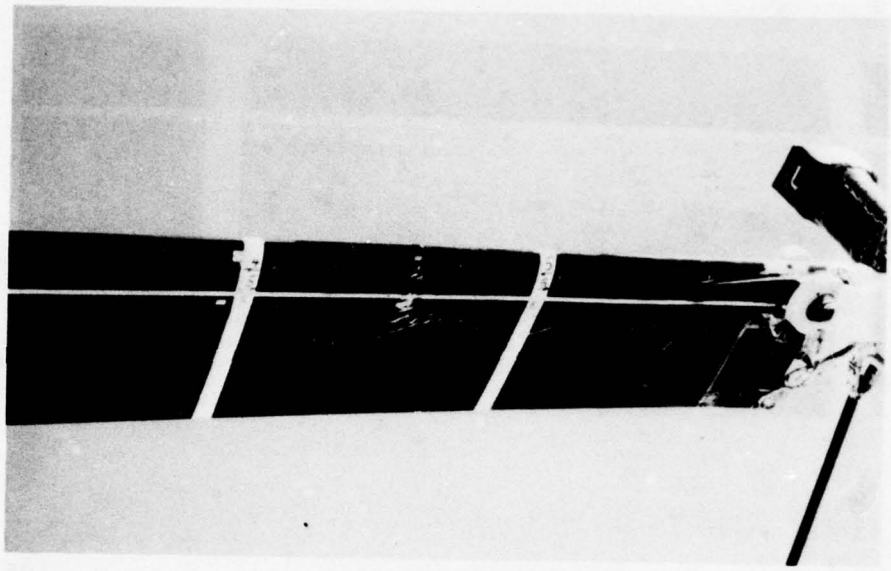

Flt. 81

406

Figure 76. Lower Inboard Blade Surface Runback Condition Following 30-Minute Spray Rig Run - Red Blade (-18°C, 0.35 g/m^3, 6 Deice Cycles)

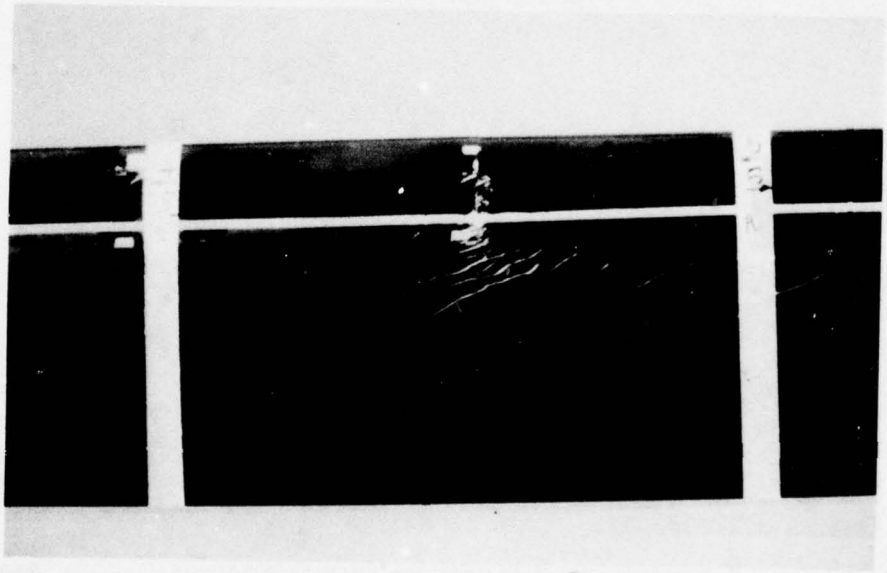

Flt. 81

404

Figure 77. Close-Up of Runback from Inboard Half of Zone 5 Following 30-Minute Spray Rig Run - Lower Surface, Red Blade (-18°C, 0.35 g/m^3, 6 Deice Cycles)

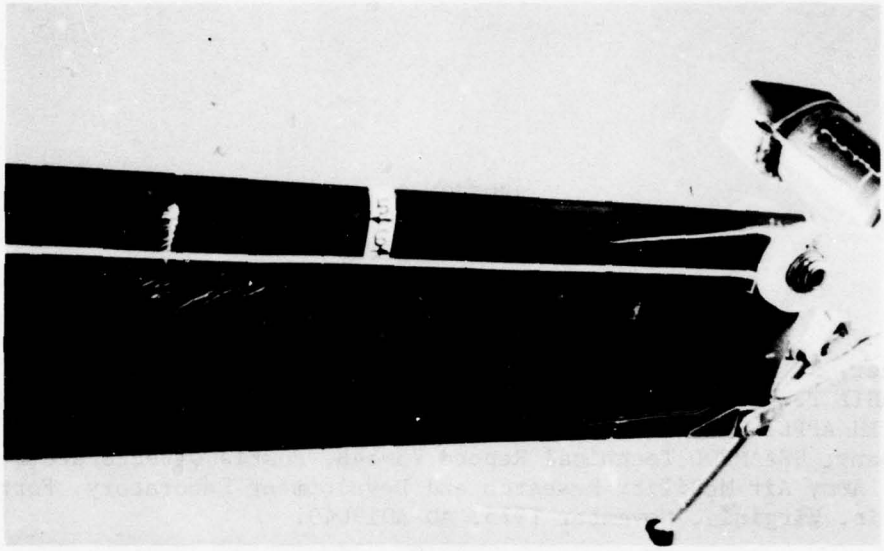

Flt. 81 410

Figure 78. Lower Inboard Blade Surface Runback Condition Following 30-Minute Spray Rig Run - White Blade (-18°C, 0.35 g/m^3, 6 Deice Cycles)

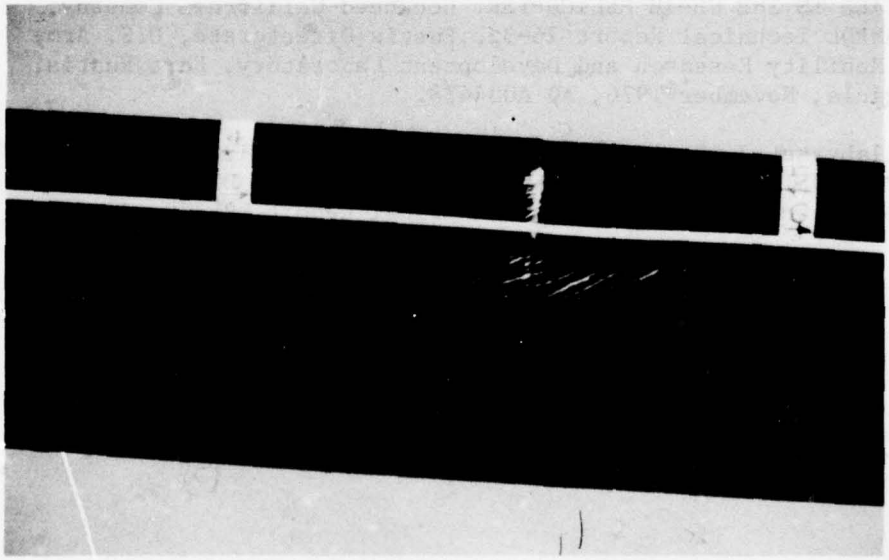

Flt. 80. 415

Figure 79. Close-Up of Runback from Inboard Half of Zone 5 Following 30-Minute Spray Rig Run - Lower Surface, White Blade (-18°C, 0.35 g/m^3, 6 Deice Cycles)

SECTION 9

LITERATURE CITED

1. Werner, J. B., THE DEVELOPMENT OF AN ADVANCED ANTI-ICING/DEICING CAPABILITY FOR U.S. ARMY HELICOPTERS, VOLUME II - ICE PROTECTION SYSTEM APPLICATION TO THE UH-1H HELICOPTER, Lockheed-California Company; USAAMRDL Technical Report 75-34B, Eustis Directorate, U.S. Army Air Mobility Research and Development Laboratory, Fort Eustis, Virginia, November 1975, AD A019049.

2. USAAEFA Project No. 74-13, Final Report, ARTIFICIAL ICING TESTS, LOCKHEED ADVANCED ICE PROTECTION SYSTEM INSTALLED ON A UH-1H HELICOPTER, U. S. Army Aviation Engineering Flight Activity, Edwards Air Force Base, California, June 1975.

3. Cotton, R. H., OTTAWA SPRAY RIG TESTS OF AN ICE PROTECTION SYSTEM APPLIED TO THE UH-1H HELICOPTER, Lockheed-California Company; USAAMRDL Technical Report 76-32, Eustis Directorate, U.S. Army Air Mobility Research and Development Laboratory, Fort Eustis, Virginia, November 1976, AD A034458.

4. Stallabrass, J. R. and Gibbard, G. A., A COMPARISON BETWEEN SPANWISE AND CHORDWISE METHODS OF HELICOPTER ROTOR BLADE DE-ICING, National Research Council of Canada Aeronautical Report LR-270, January 1960.

APPENDIX A. ICING WIND TUNNEL CALIBRATION OF A ROSEMOUNT ASPIRATED ICE DETECTOR

DIVISION OF MECHANICAL ENGINEERING

DIVISION DE GÉNIE MÉCANIQUE

CANADA

LIMITED

PAGES 8

FIG. DIAG. 27

REPORT RAPPORT

REPORT RAPPORT LTR-LT-76

DATE May 1977

SECTION

Low Temperature Laboratory

LAB. ORDER COMM. LAB. 21022X

FILE DOSSIER 3742-5

FOR POUR Department of the Army, U.S. Army Air Mobility Research and Development Laboratory, Eustis Directorate, Fort Eustis, Virginia 23604.

REFERENCE RÉFÉRENCE Purchase Order DAAJ02-77-M-0004 dated 14 February 1977

LTR- LT - 76

ICING WIND TUNNEL CALIBRATION OF A ROSEMOUNT ASPIRATED ICE DETECTOR

SUBMITTED BY PRÉSENTÉ PAR T. R. Ringer
SECTION HEAD CHEF DE SECTION

AUTHOR AUTEUR J. R. Stallabrass

APPROVED APPROUVÉ
DIRECTOR DIRECTEUR

TABLE OF CONTENTS

LIST OF ILLUSTRATIONS

LIST OF ILLUSTRATIONS (cont'd)

SUMMARY

Calibration of a Rosemount aspirated ice detector was made in an icing wind tunnel. Considerable improvement in the reliability and consistency of the icing rate indication over earlier tests was evident, but apparently at the expense of sensitivity. Some inadequacy in the anti-icing of the aspirator was still evident under higher heat loss situations, together with a tendency towards incomplete ice shedding from the sensor probe.

1.0 INTRODUCTION

At the conclusion of icing flight trials of a UH-1H helicopter at Ottawa in April 1977, the U. S. Army Air Mobility Research and Development Laboratory requested a calibration be made of the Rosemount aspirated ice detector and icing rate meter used on the helicopter.

Calibration was made in the high speed icing wind tunnel of the Low Temperature Laboratory in the presence of a U. S. Army observer on Rosemount Ice Detector Model No. 871FA121, Serial No. 7, complete with notched type aspirator, and in conjunction with Icing Rate Indicator Model No. 512P2, Serial No. 14.

2.0 CALIBRATION PROCEDURE

The ice detector complete with aspirator was mounted in a side wall of the wind tunnel test section. The pressure and temperature of the bleed air supplied to the aspirator were adjusted to 40 psig and 70°C respectively. Under these conditions the air consumption rate was 10.7 scfm.

With a given tunnel air velocity and temperature, the liquid water content of the tunnel airstream was adjusted until the meter of the Icing Rate Indicator unit indicated approximately L (light), M (moderate), or H (high). At each of these settings, the liquid water content (LWC) was measured using the rotating cylinder method (Ref. 1), and the voltage output on Pin G of the rate meter was noted and visually averaged. This voltage was also recorded on a pen recorder.

This procedure was followed for three different airspeeds (30, 90 and 150 knots T.A.S.) and at two different static air temperatures (-15°C and -5°C).

All tests were made at zero yaw angle.

3.0 TEST RESULTS

Details of all the calibration conditions at -15°C are presented in Table I, while those at -5°C are tabulated in Table II. Figures 4 through 24 show cuts from the recorder trace for each of the test conditions. It should be noted in these figures that time progression is from right to left at a scale of 10 seconds per cm. The voltage scale zero is at the bottom of the chart and the scale is 0.2 volts per cm.

It should also be noted that whenever a LWC measurement is made with the rotating cylinder, a decrease in the icing rate indication may be observed. This is because the rotating cylinder is placed directly ahead of the detector when the measurement is made. Such decreases during rotating cylinder measurements may be observed in Figs. 5, 10(a), 11, 14, etc.

The recordings demonstrate much greater consistency than those of the calibration tests reported in Ref. 2, in particular the large negative going voltage excursions have been eliminated, but apparently at the expense of the overall sensitivity of the device, since the cycle times between signals are now seen to be approximately double their previous values.

The greater consistency is demonstrated by the calibration curves of Fig. 1. The calibrations for static temperatures of -15°C and -5°C are seen to be essentially identical, although a velocity dependence is seen to exist.

The greater consistency also permitted calibration curves based on the cycle time between signals to be constructed for each airspeed as illustrated in Fig. 2. Again no significant temperature dependency is observable.

Fig. 3, which is crossplotted from Fig. 1, shows the liquid water content corresponding to the severity meter indications of L, M, and H as a function of airspeed. It may be noted that these indications corresponded to voltage outputs of 0.2, 0.4 and 0.8 volts, which in turn corresponded at 90 knots to LWC's of 0.15, 0.3 and 0.6 g/m^3 respectively.

It would appear that the expedient of notching the aspirator did not completely overcome the shortcoming of ice growth at the base of the probe such as experienced with the un-notched aspirator (Ref. 2). This problem, although particularly prevalent as a speed of 150 knots, also occurred at 90 knots with low air temperature (-15°C). Examples of these occurrences are seen in Figs. 7, 10(b), 11 and 20, and are categorized by an erratic output voltage followed, in most cases, by the output dropping to zero.

Photographs showing ice on the aspirator lip and at the base of the probe are reproduced in Figs. 25, 26 and 27(a) & (b).

4.0 REFERENCES

4.1 Rush, C. K.
Wardlaw, R. L.
Icing Measurements with a Single Rotating Cylinder. National Research Council of Canada, NAE Laboratory Report LR-206, September 1957.

4.2 Stallabrass, J. R.
Bailey, D. L.
Calibration of Rosemount Aspirated Ice Detector and Icing Rate Meter. National Research Council of Canada, DME Report LTR-LT-64, March 1976.

TABLE I -- TESTS AT -15°C

TUNNEL PARAMETERS			BLEED AIR TEMP. °C	RATE METER		ICE DET. CYCLE TIME Sec.	FIG. NO.	COMMENTS
True Airspeed kts.	Static Temp. °C	L.W.C. g/m^3		Icing Severity Reading	Voltage Output (Pin G)			
90	-15	0.29	70	M⁻ to M	0.4	150	4	Ice formed on corners of aspirator notch, but shed after 10 and 13 minutes.
90	-15	0.74	70	H^+	~1.2	64	5	Ice formed on corners of aspirator notch.
90	-15	0.18	70	L^+	0.25	255	6	
90	-15	0.31	70	M	0.4	145	7	After 12 min. ice on probe failed to shed fully, held by aspirator. Rate reading to zero.
90	-15	0.64	70	H	0.82	80	8	
150	-15	0.10	69	L	0.2	315	9	Ice on upper 1/2 of aspirator leading edge and on corners.
150	-15	0.22	69	M	0.41	145	10	3/8" ice built on upper 2/3 of aspirator lip. After 6 min. ice failed to shed from probe and reading zero. A minute later signal light flashing - 5 sec. on, 5 sec. off.
							25	Probe ice shed when run stopped to take photographs.
150	-15	0.40	70	H	0.82	80	11 26	After 5 min. ice failed to shed from probe resulting in erratic readings.
30	-15	0.29	71	L^+ to L	0.25	270	12	Aspirator lip remained free of ice.
30	-15	0.45	71	M⁻ to M	0.4	155	13	Dip in voltage after end of "hold". Voltage becomes slightly erratic towards end of icing period.
30	-15	0.84	71	H⁻	0.8	80	14	Voltage somewhat erratic.

TABLE II -- TESTS AT -5°C

TUNNEL PARAMETERS			BLEED AIR TEMP. °C	RATE METER		ICE DET. CYCLE TIME Sec.	FIG. NO.	COMMENTS
True Airspeed kts.	Static Temp. °C	L.W.C. g/m^3		Icing Severity Reading	Voltage Output (Pin G)			
30	-5	0.26	72	L	0.22	260	15	
30	-5	0.40	73	M^-	0.4	148	16	
30	-5	0.92	73	H to H^-	~0.8	80	17	Voltage becomes slightly erratic as ice thickness on probe approaches trip point.
90	-5	0.16	73	L to L^+	0.22	253	18	Large voltage dip (to zero) occurs when probe approx. 3/4 iced.
90	-5	0.26	72	M^-	0.4	156	19	
90	-5	0.62	70	H^+	0.89	72	20	
150	-5	0.10	73	L^+	0.24	286	21 27	At 3 min. ice was observed at base of probe. At 6 min. this ice prevented remainder of ice on probe from shedding when heat applied This ice refroze to probe with resultant large peak in output followed by fall to zero.
150	-5	0.22	73	M to M^+	~0.5	130	22	Fluctuating 0.45 to 0.55V.
150	-5	0.46	73	H to H^{++}	0.84 to 1.1	68	23	Reading climbs from 0.84V to 1.15V as probe ices.
150	-5	0.40	73	H^- to H^+	~0.9	75	24	Reading climbs from 0.75V to ~0.95V as probe ices.

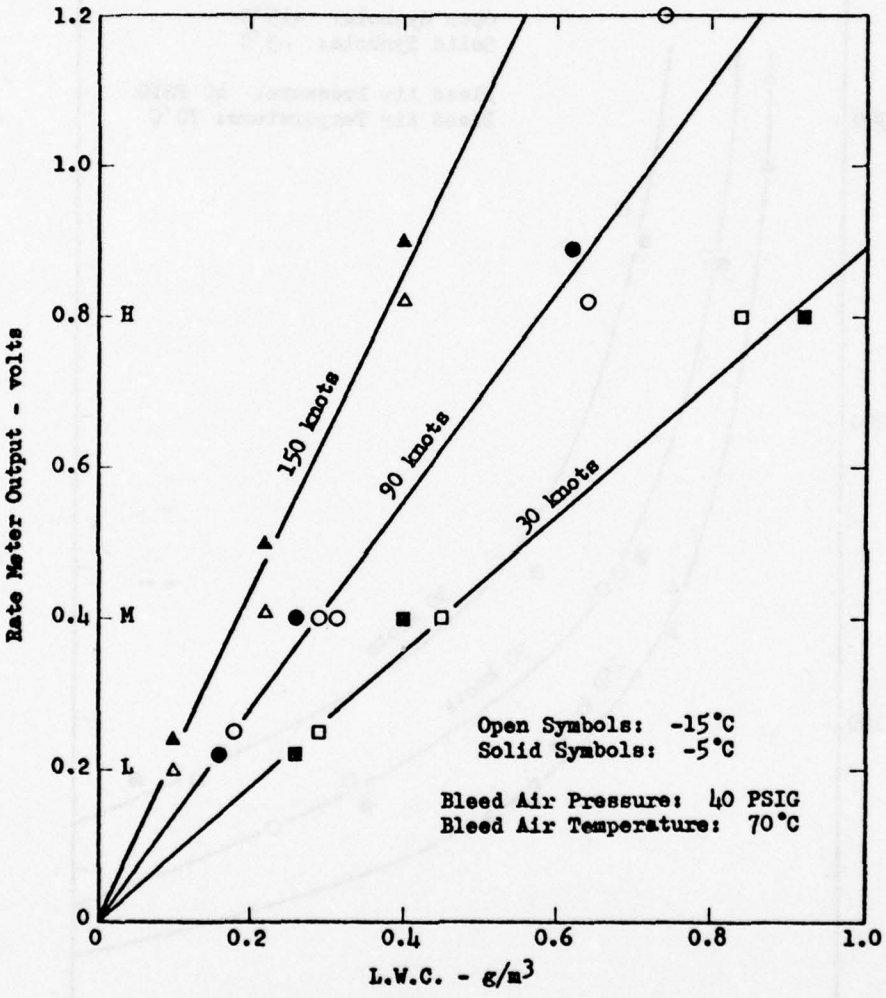

FIG. 1 RATE METER CALIBRATION

ROSEMOUNT ICE DETECTOR MODEL 871 FA 121, SER. 7
WITH NOTCHED ASPIRATOR

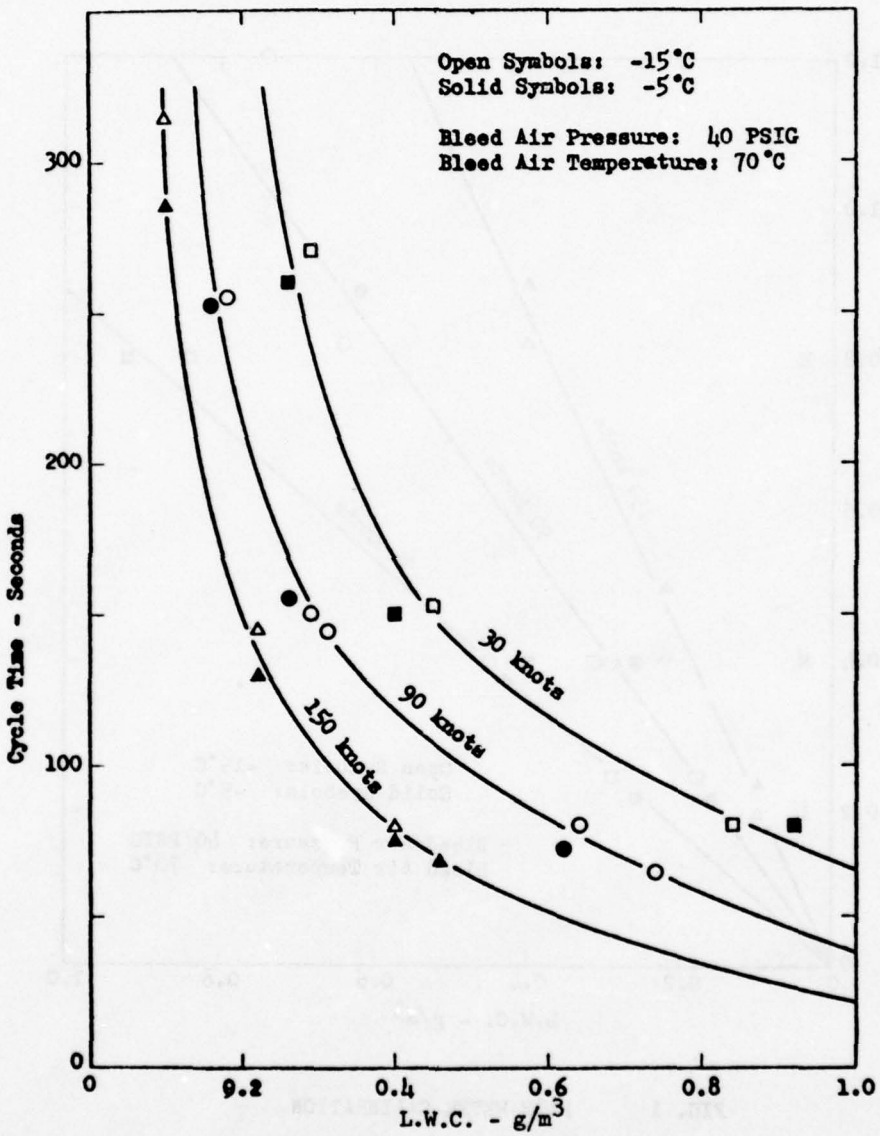

FIG. 2 CYCLE TIME CALIBRATION

ROSEMOUNT ICE DETECTOR MODEL 871 FA 121, SER. 7
WITH NOTCHED ASPIRATOR

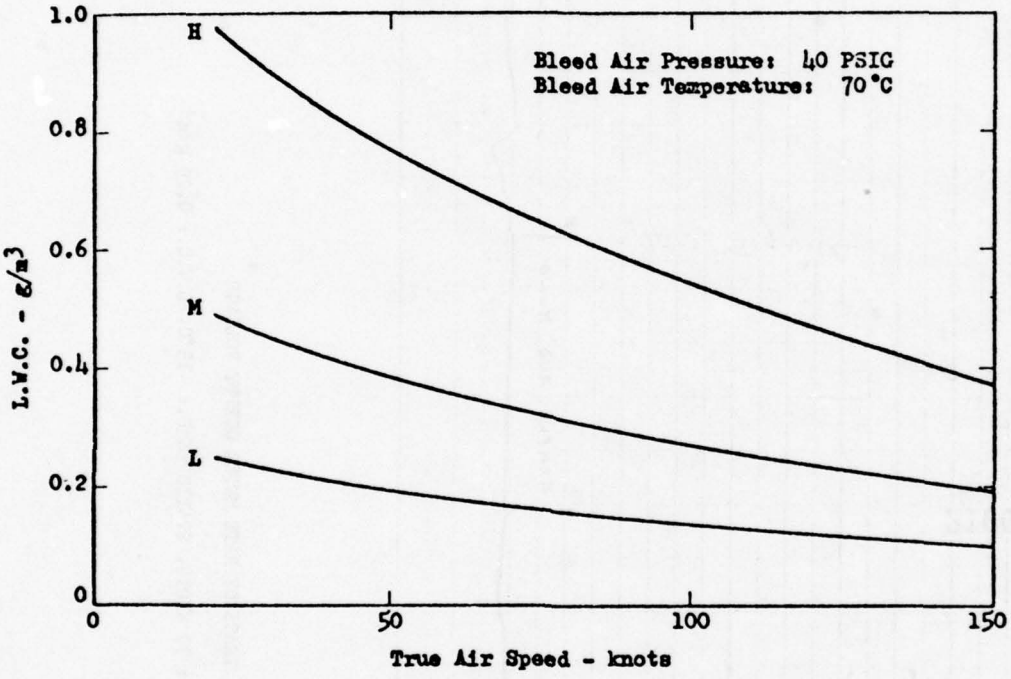

FIG. 3 L.W.C. CORRESPONDING TO ICING RATE METER INDICATIONS OF L, M and H AS A FUNCTION OF AIRSPEED

ROSEMOUNT ICE DETECTOR MODEL 871 FA 121, SER. 7
WITH NOTCHED ASPIRATOR

ICING RATE INDICATOR MODEL 512P2, SER. 14

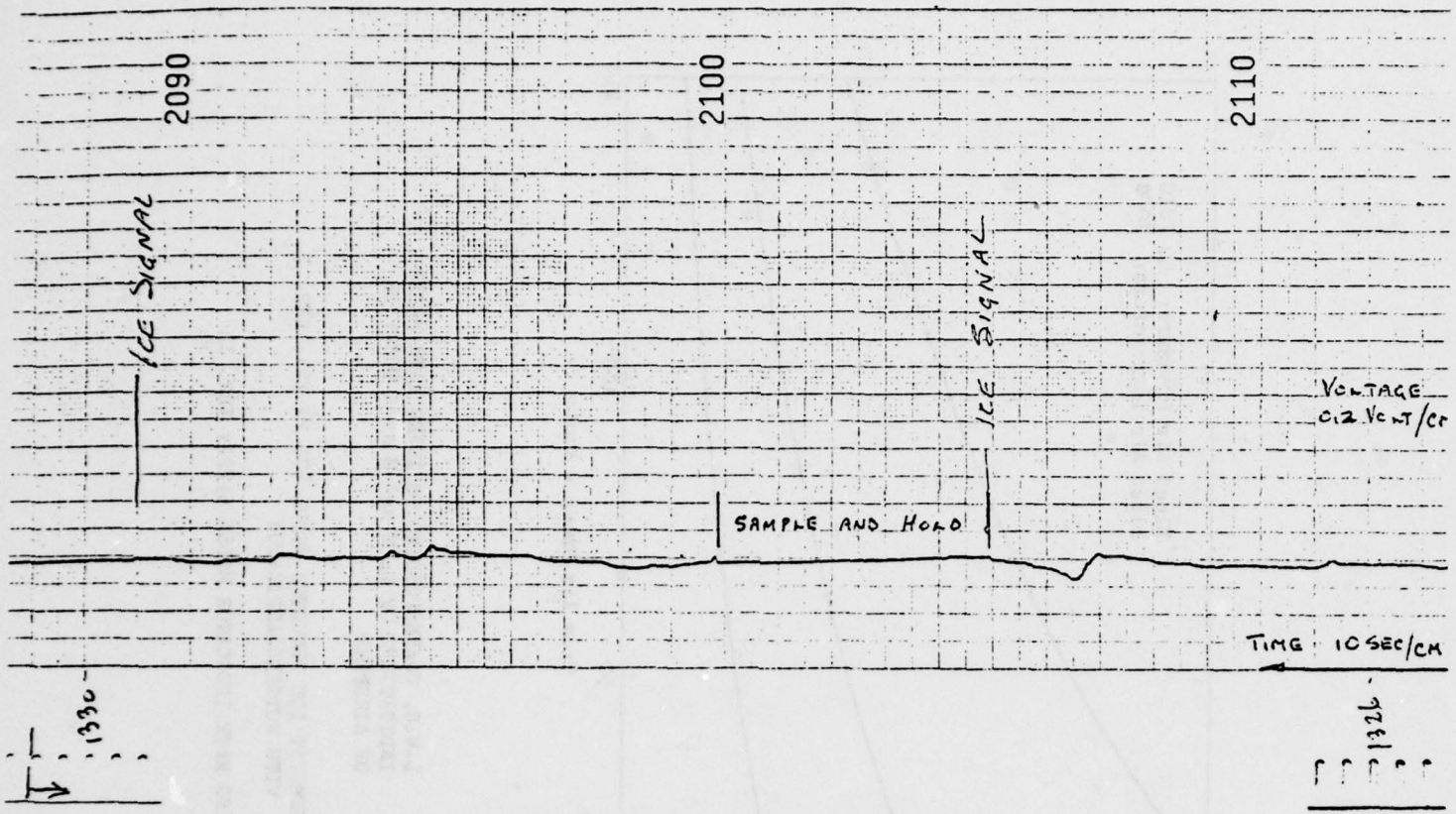

FIG. 4 RECORDER TRACE OF RATE METER OUTPUT VOLTAGE

AIRSPEED: 90 KNOTS, STATIC TEMP.: -15°C, L.W.C.: 0.29 g/m^3

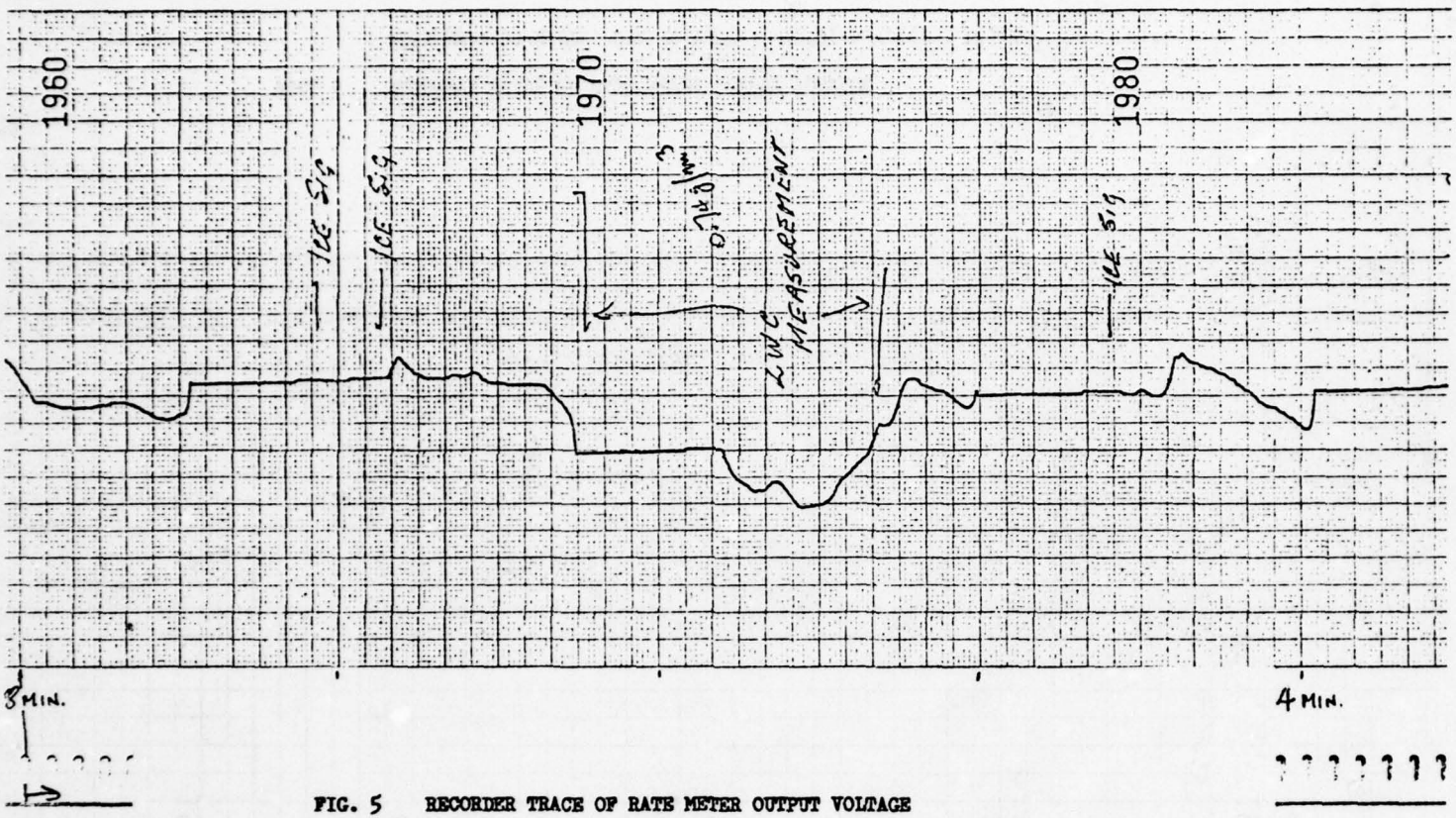

FIG. 5 RECORDER TRACE OF RATE METER OUTPUT VOLTAGE

AIRSPEED: 90 KNOTS, STATIC TEMP.: -15°C, L.W.C.: 0.74 g/m^3

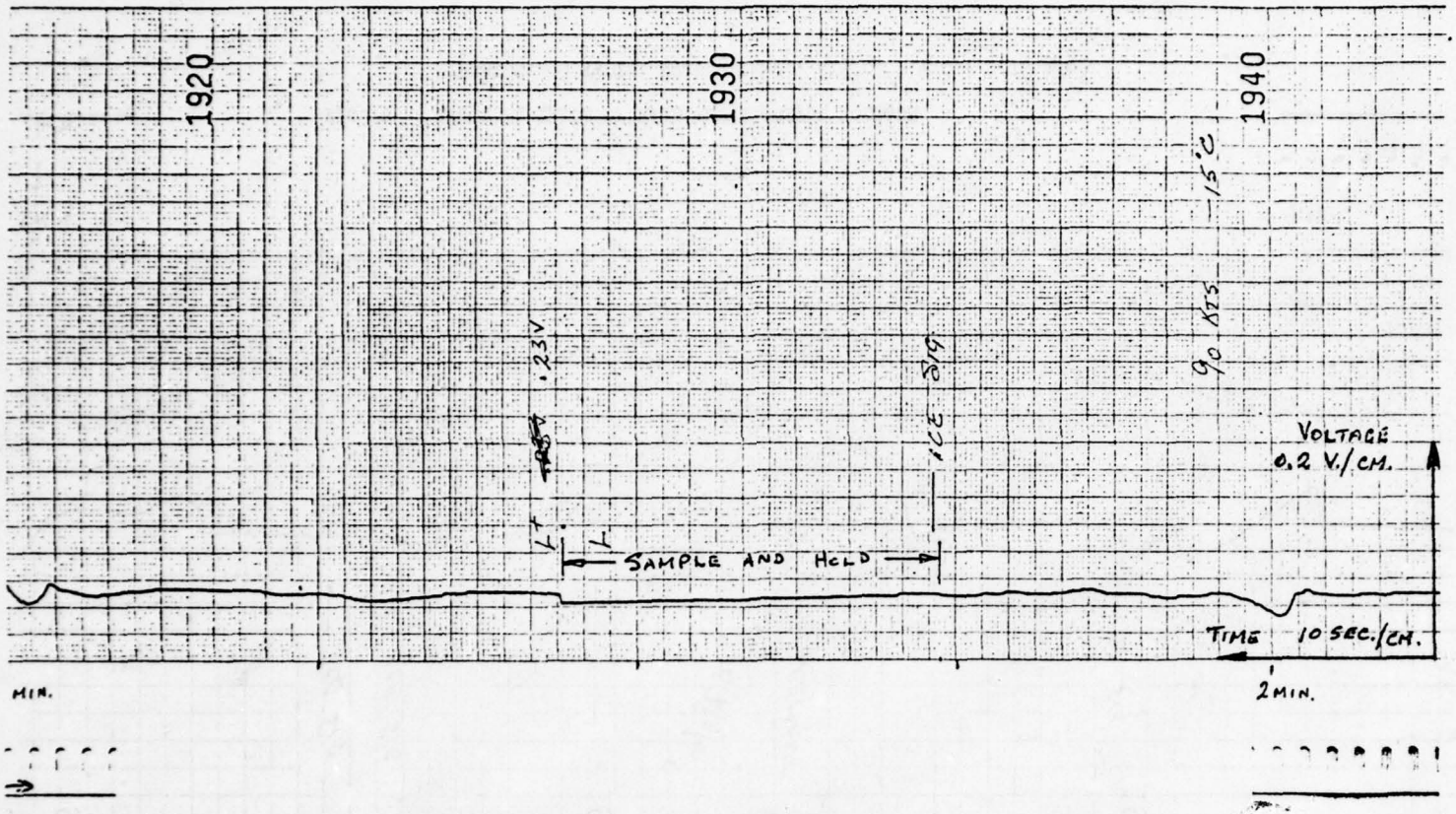

FIG. 6 RECORDER TRACE OF RATE METER OUTPUT VOLTAGE

AIRSPEED: 90 KNOTS, STATIC TEMP.: -15°C, L.W.C.: 0.18 g/m^3

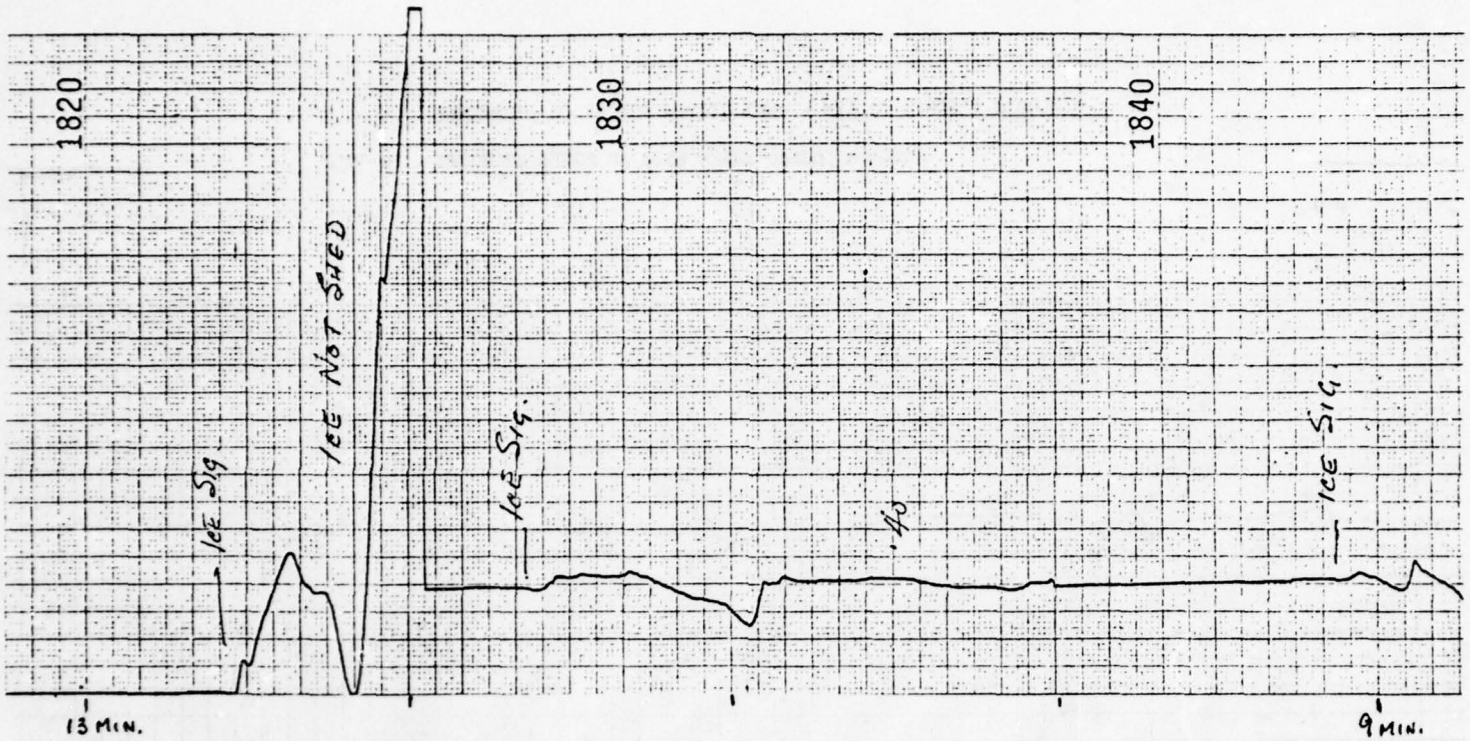

FIG. 7 RECORDER TRACE OF RATE METER OUTPUT VOLTAGE

AIRSPEED: 90 KNOTS, STATIC TEMP.: -15°C, L.W.C.: 0.31 g/m^3

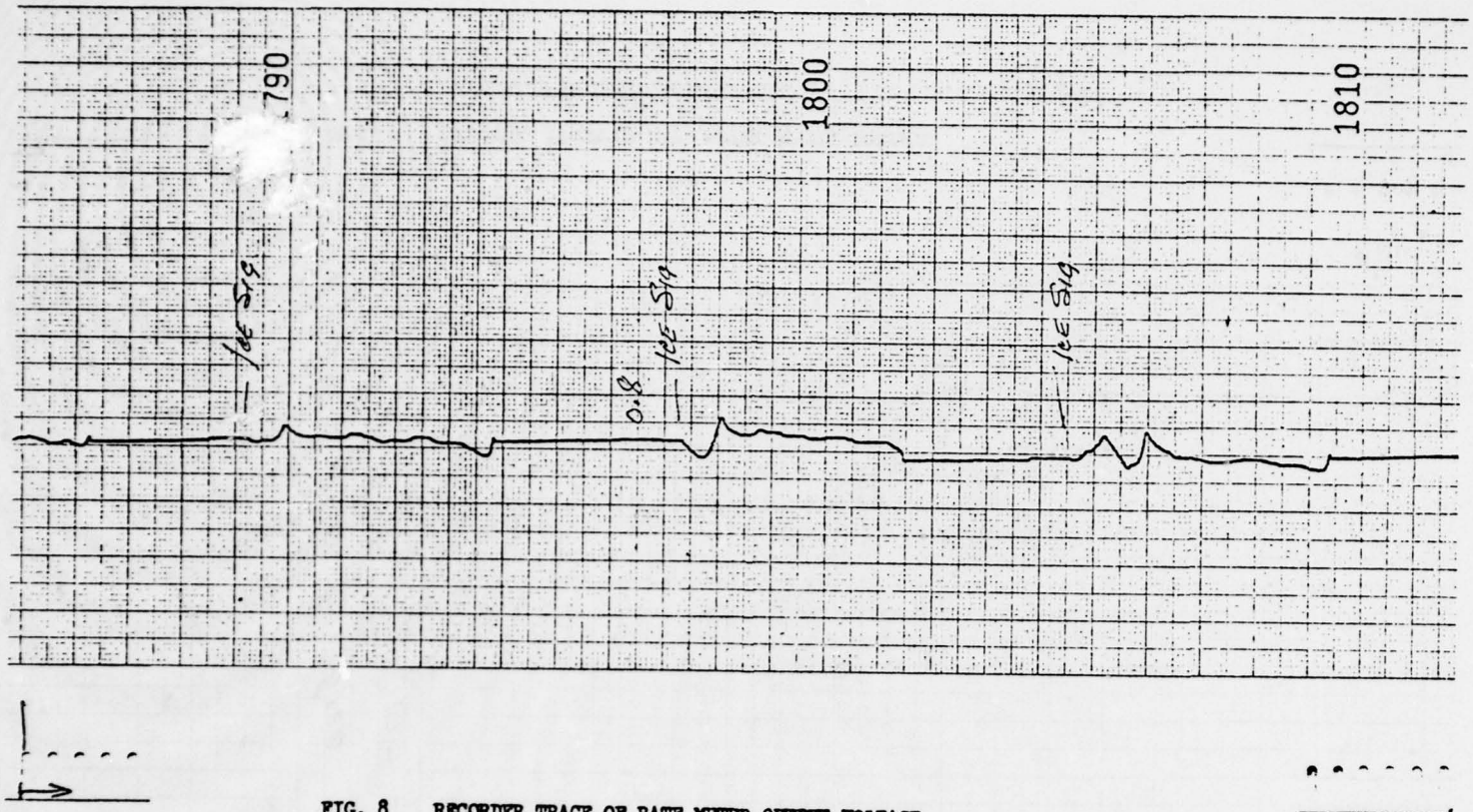

FIG. 8 RECORDER TRACE OF RATE METER OUTPUT VOLTAGE

AIRSPEED: 90 KNOTS, STATIC TEMP.: -15°C, L.W.C.: 0.64 g/m^3

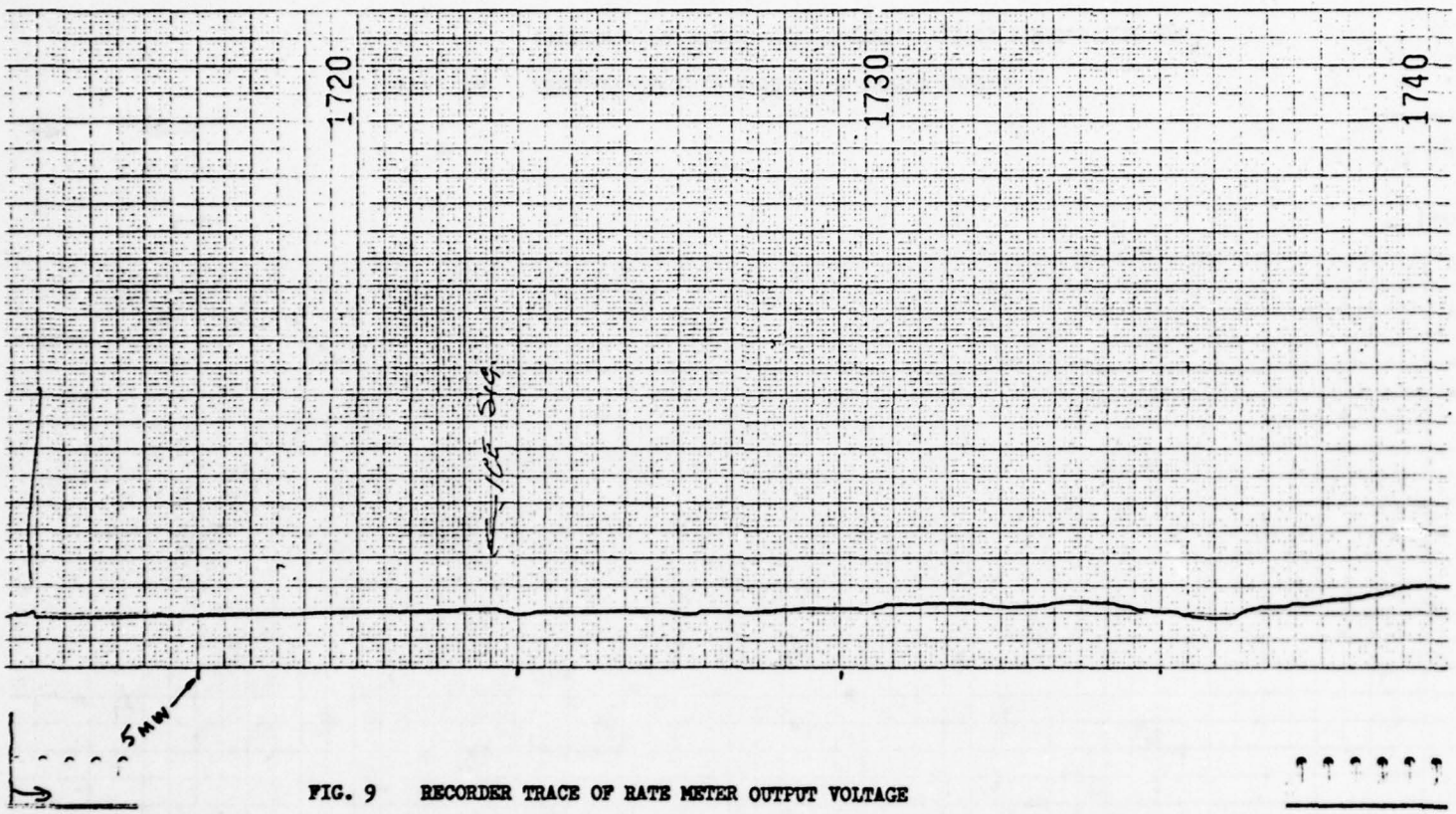

FIG. 9 RECORDER TRACE OF RATE METER OUTPUT VOLTAGE

AIRSPEED: 150 KNOTS, STATIC TEMP.: -15°C, L.W.C.: 0.10 g/m^3

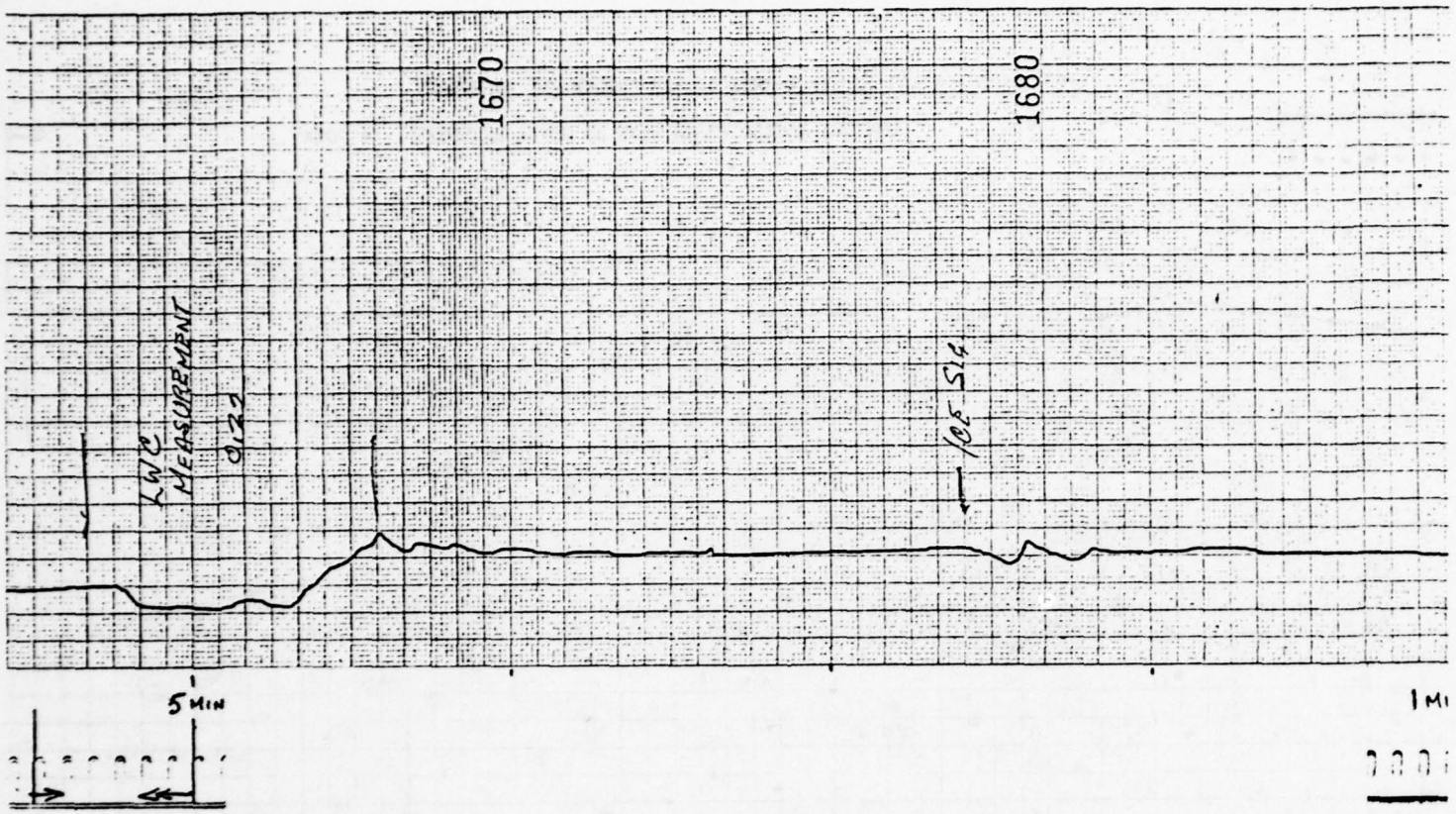

FIG. 10a RECORDER TRACE OF RATE METER OUTPUT VOLTAGE

AIRSPEED: 150 KNOTS, STATIC TEMP.: -15°C, L.W.C.: 0.22 g/m^3

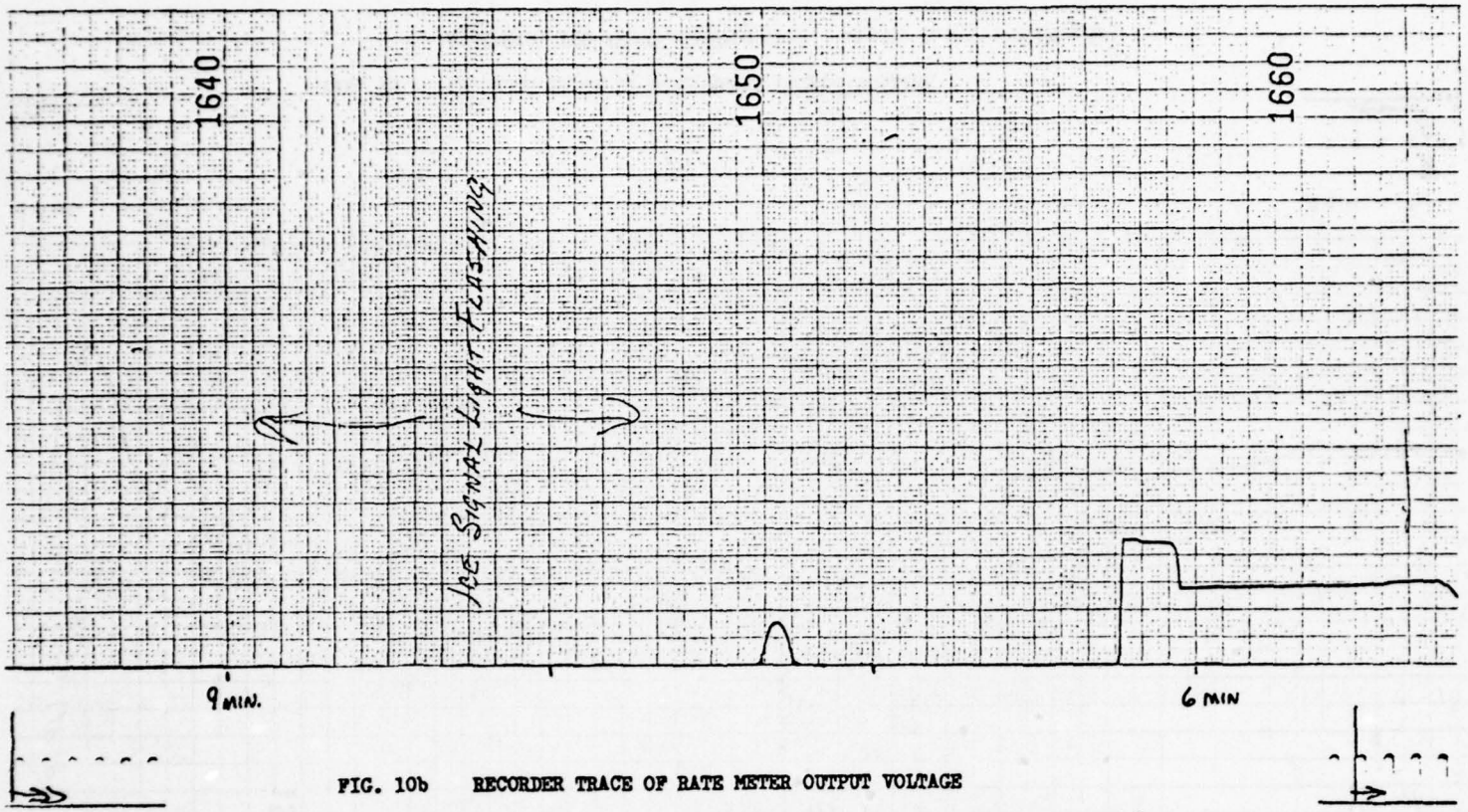

FIG. 10b RECORDER TRACE OF RATE METER OUTPUT VOLTAGE

AIRSPEED: 150 KNOTS, STATIC TEMP.: -15°C, L.W.C.: 0.22 g/m^3

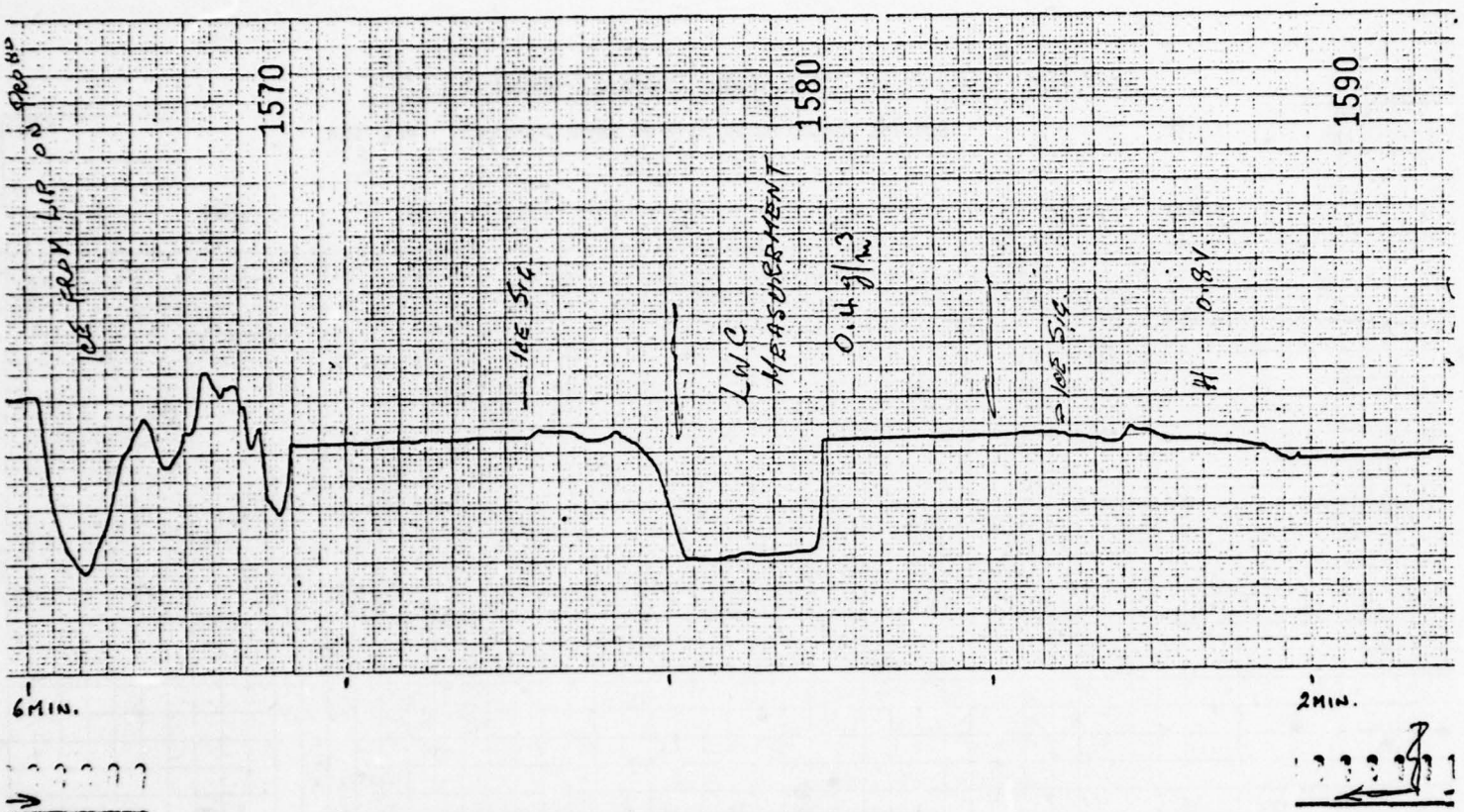

FIG. 11 RECORDER TRACE OF RATE METER OUTPUT VOLTAGE

AIRSPEED: 150 KNOTS, STATIC TEMP.: -15°C, L.W.C.: 0.40 g/m^3

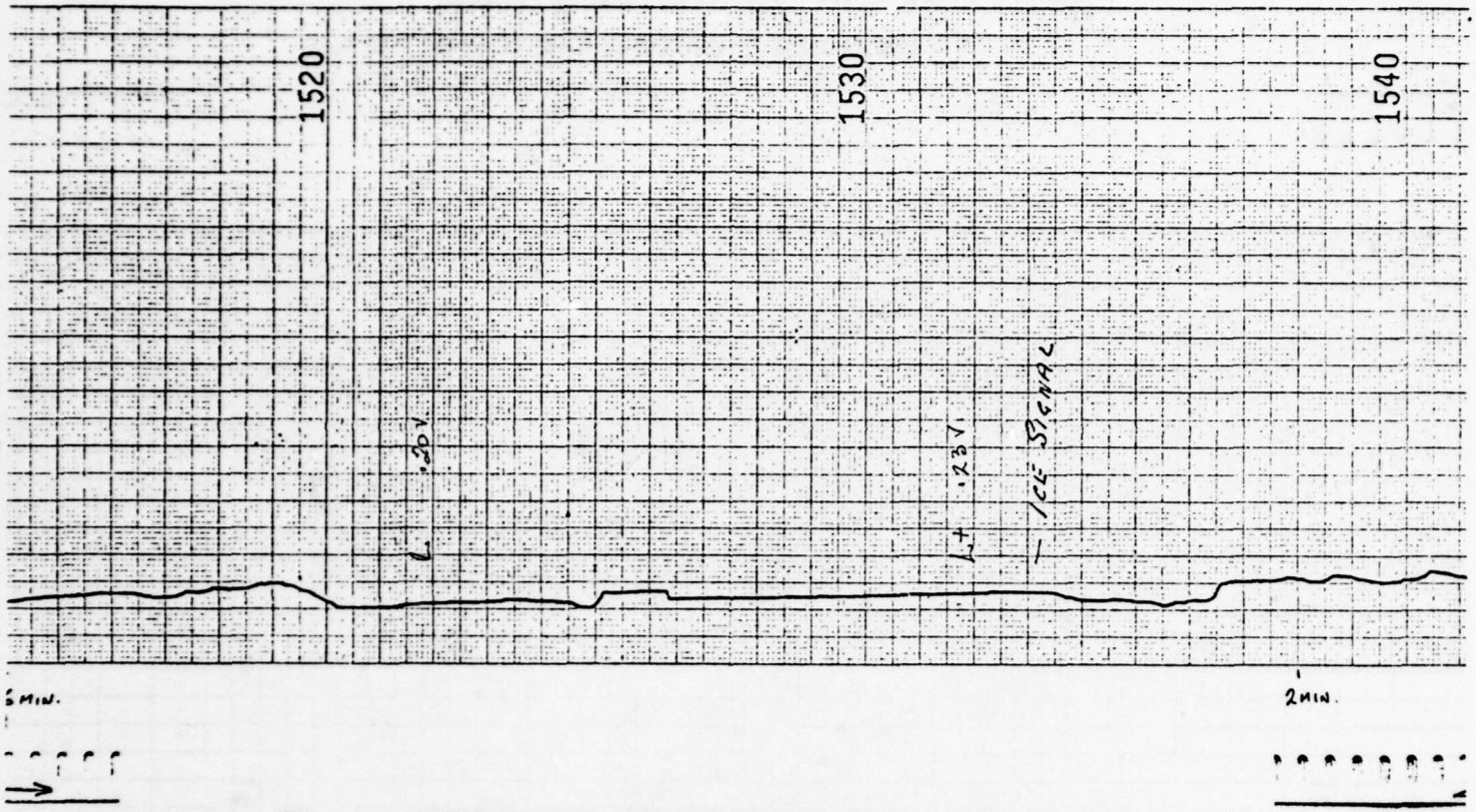

FIG. 12 RECORDER TRACE OF RATE METER OUTPUT VOLTAGE

AIRSPEED: 30 KNOTS, STATIC TEMP.: -15°C, L.W.C.: 0.29 g/m^3

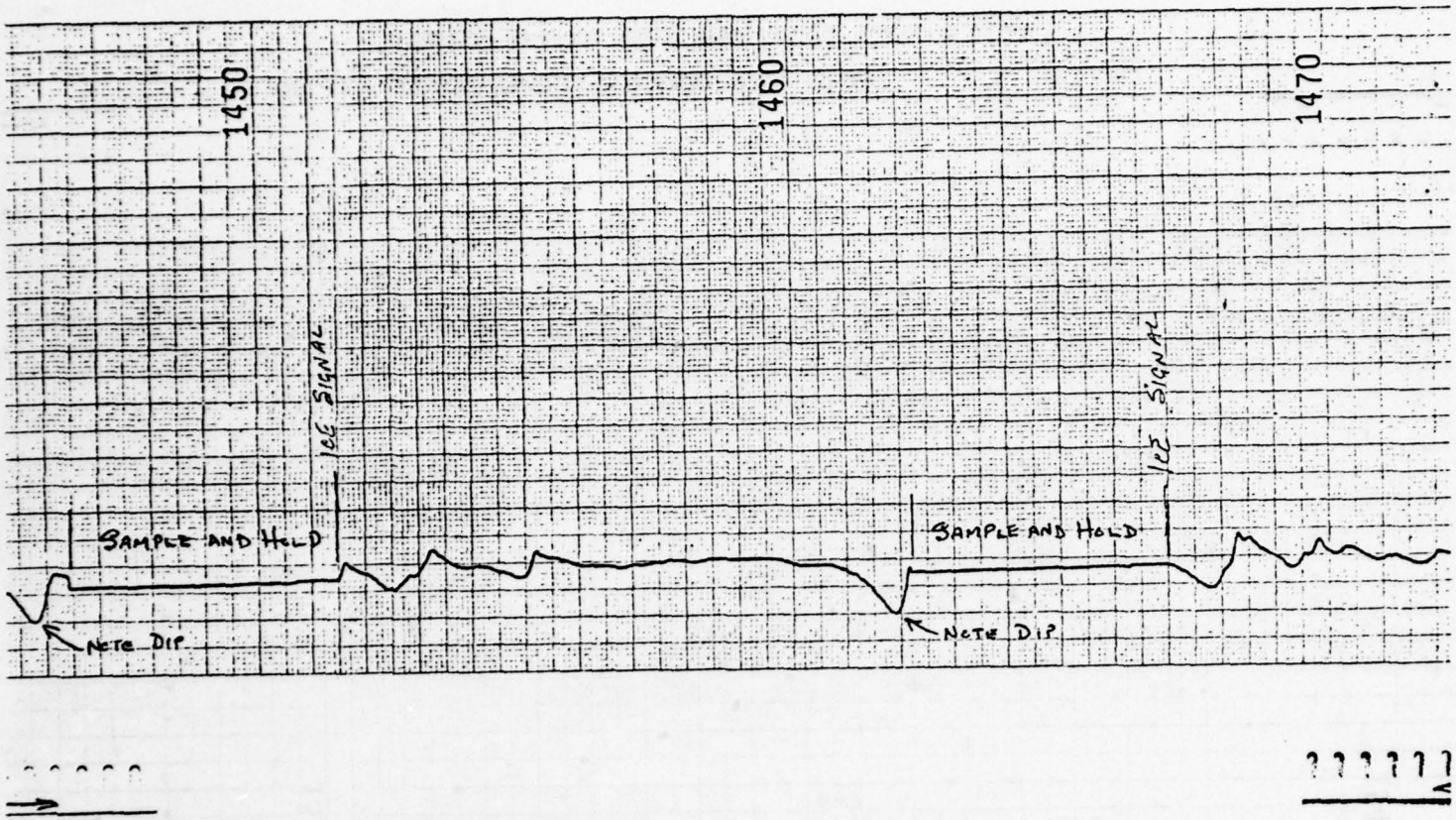

FIG. 13 RECORDER TRACE OF RATE METER OUTPUT VOLTAGE

AIRSPEED: 30 KNOTS, STATIC TEMP.: -15°C, L.W.C.: 0.45 g/m^3

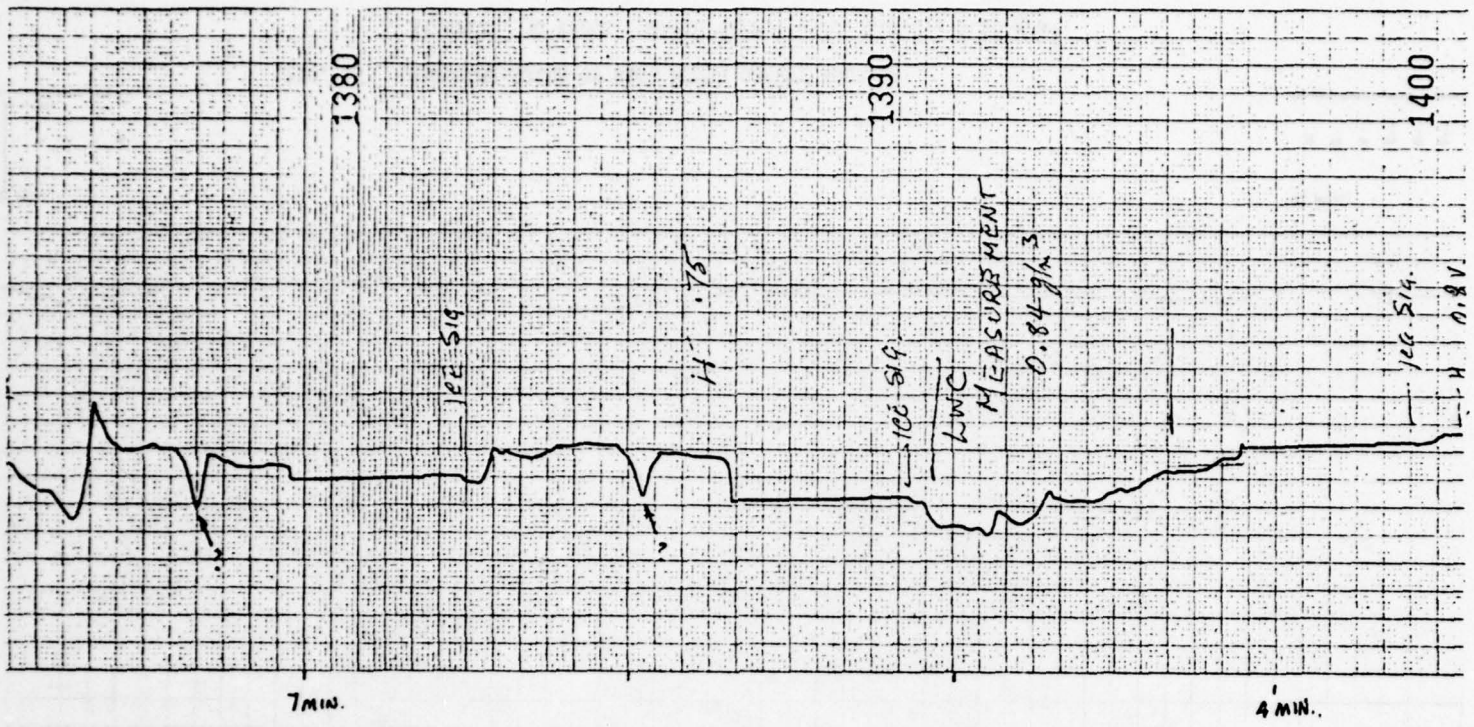

FIG. 14 RECORDER TRACE OF RATE METER OUTPUT VOLTAGE

AIRSPEED: 30 KNOTS, STATIC TEMP.: -15°C, L.W.C.: 0.84 g/m^3

FIG. 15 RECORDER TRACE OF RATE METER OUTPUT VOLTAGE

AIRSPEED: 30 KNOTS, STATIC TEMP.: -5°C, L.W.C.: 0.26 g/m^3

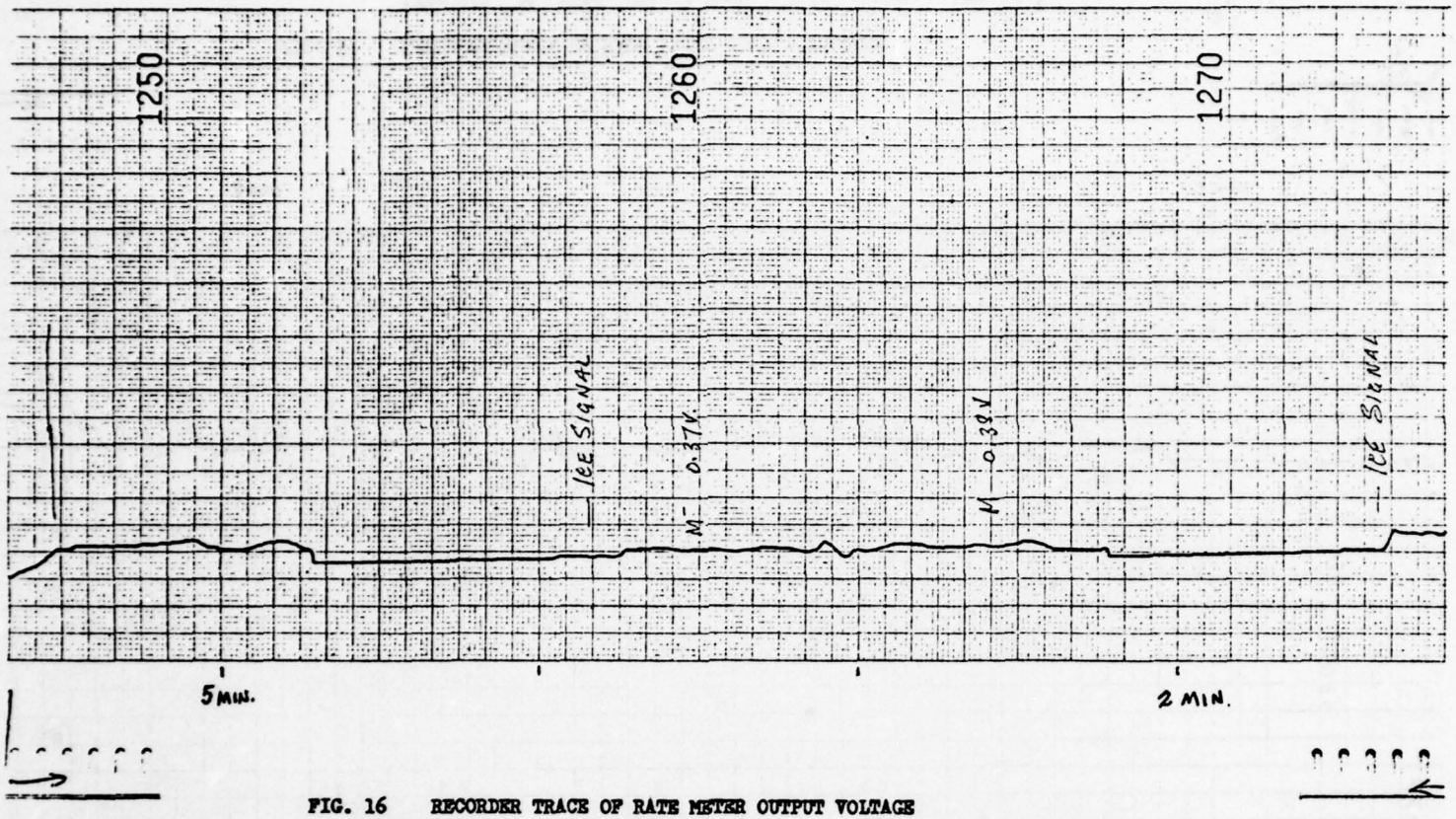

FIG. 16 RECORDER TRACE OF RATE METER OUTPUT VOLTAGE

AIRSPEED: 30 KNOTS, STATIC TEMP.: -5°C, L.W.C.: 0.40 g/m^3.

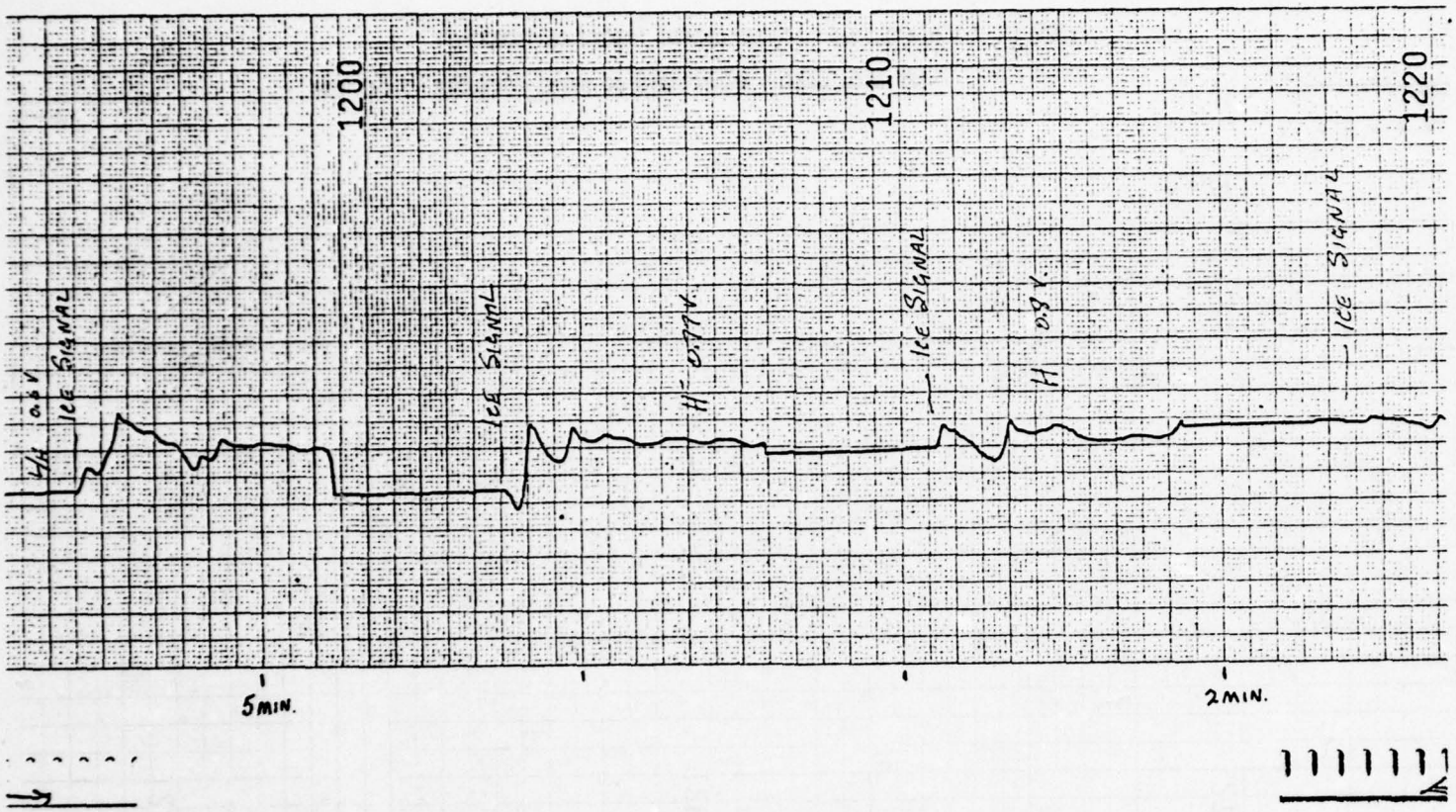

FIG. 17 RECORDER TRACE OF RATE METER OUTPUT VOLTAGE

AIRSPEED: 30 KNOTS, STATIC TEMP.: -5°C, L.W.C.: 0.92 g/m^3

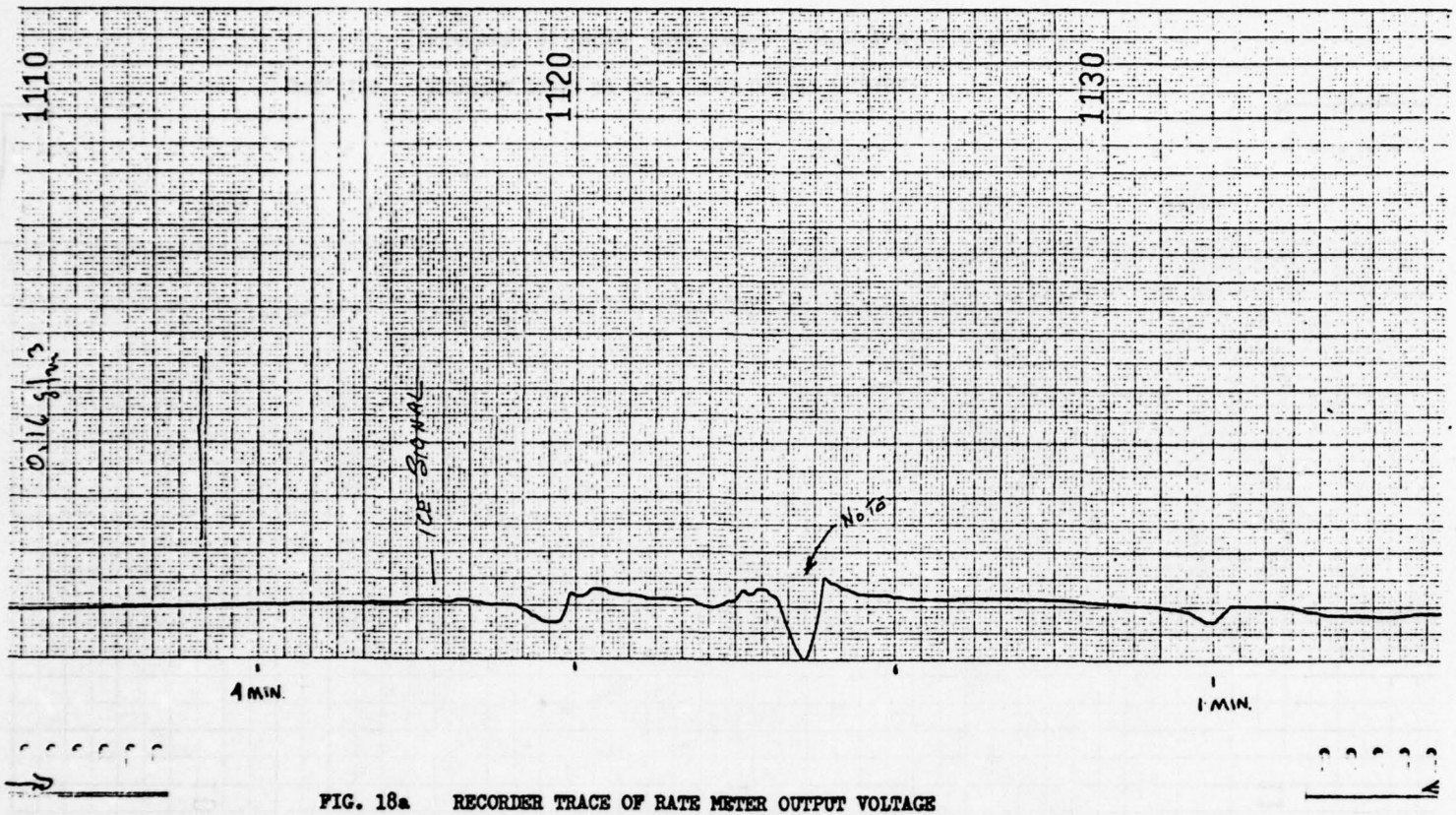

FIG. 18a RECORDER TRACE OF RATE METER OUTPUT VOLTAGE

AIRSPEED: 90 KNOTS, STATIC TEMP.: -5°C, L.W.C.: 0.16 g/m^3

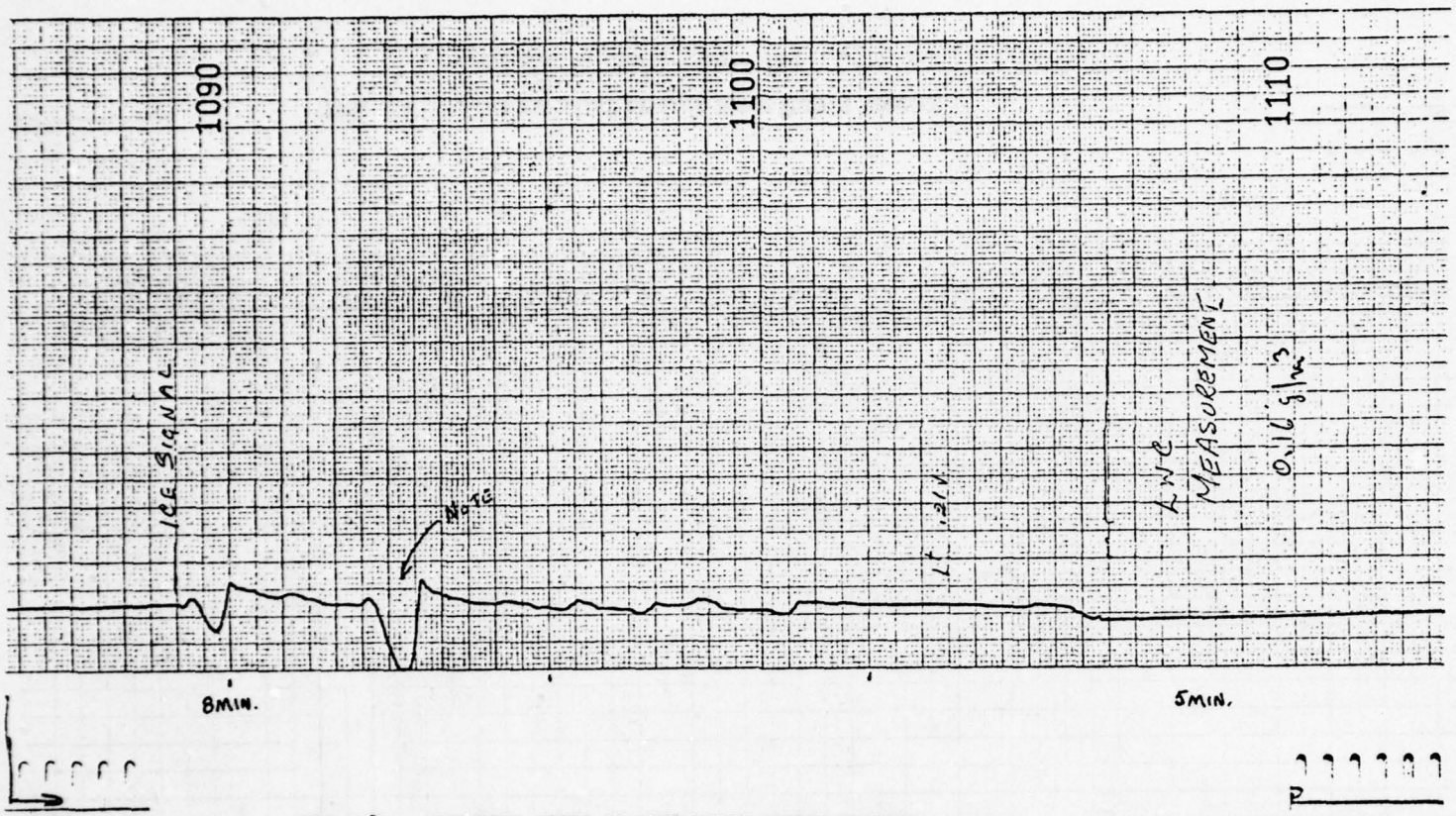

FIG. 18b RECORDER TRACE OF RATE METER OUTPUT VOLTAGE

AIRSPEED: 90 KNOTS, STATIC TEMP.: -5°C, L.W.C.: 0.16 g/m^3

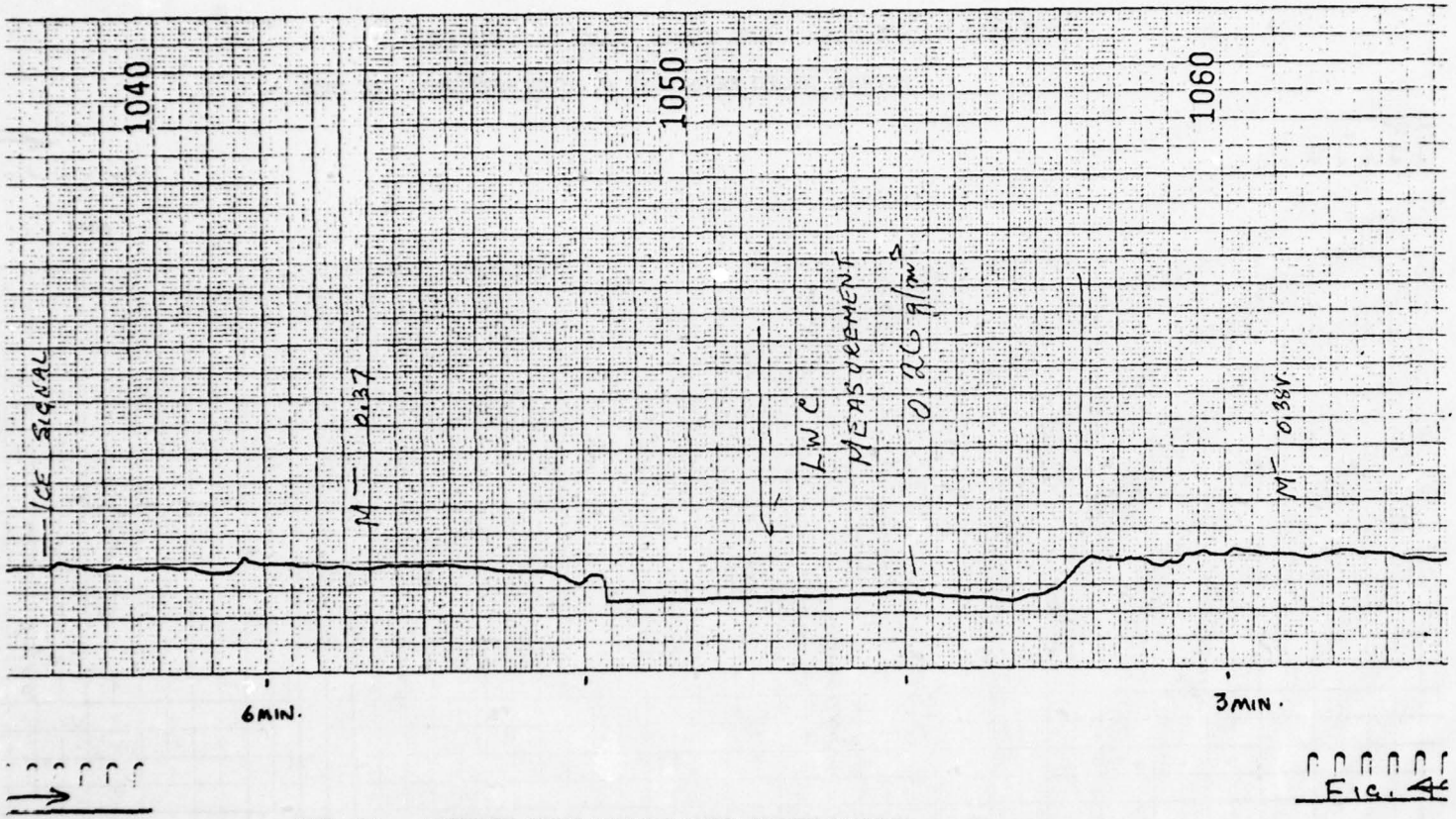

FIG. 19 RECORDER TRACE OF RATE METER OUTPUT VOLTAGE

AIRSPEED: 90 KNOTS, STATIC TEMP.: -5°C, L.W.C.: 0.26 g/m^3

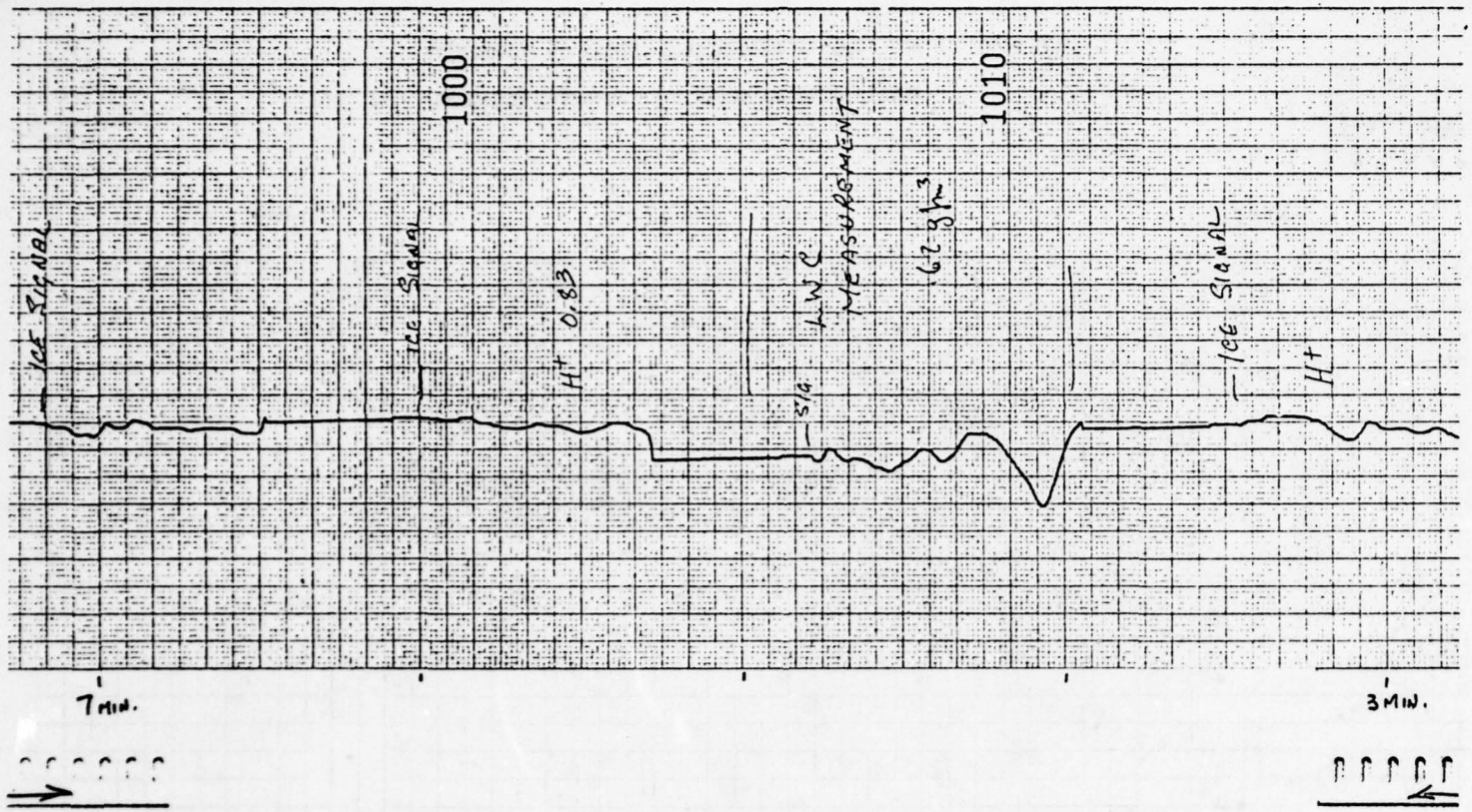

FIG. 20 RECORDER TRACE OF RATE METER OUTPUT VOLTAGE

AIRSPEED: 90 KNOTS, STATIC TEMP.: -5°C, L.W.C.: 0.62 g/m^3

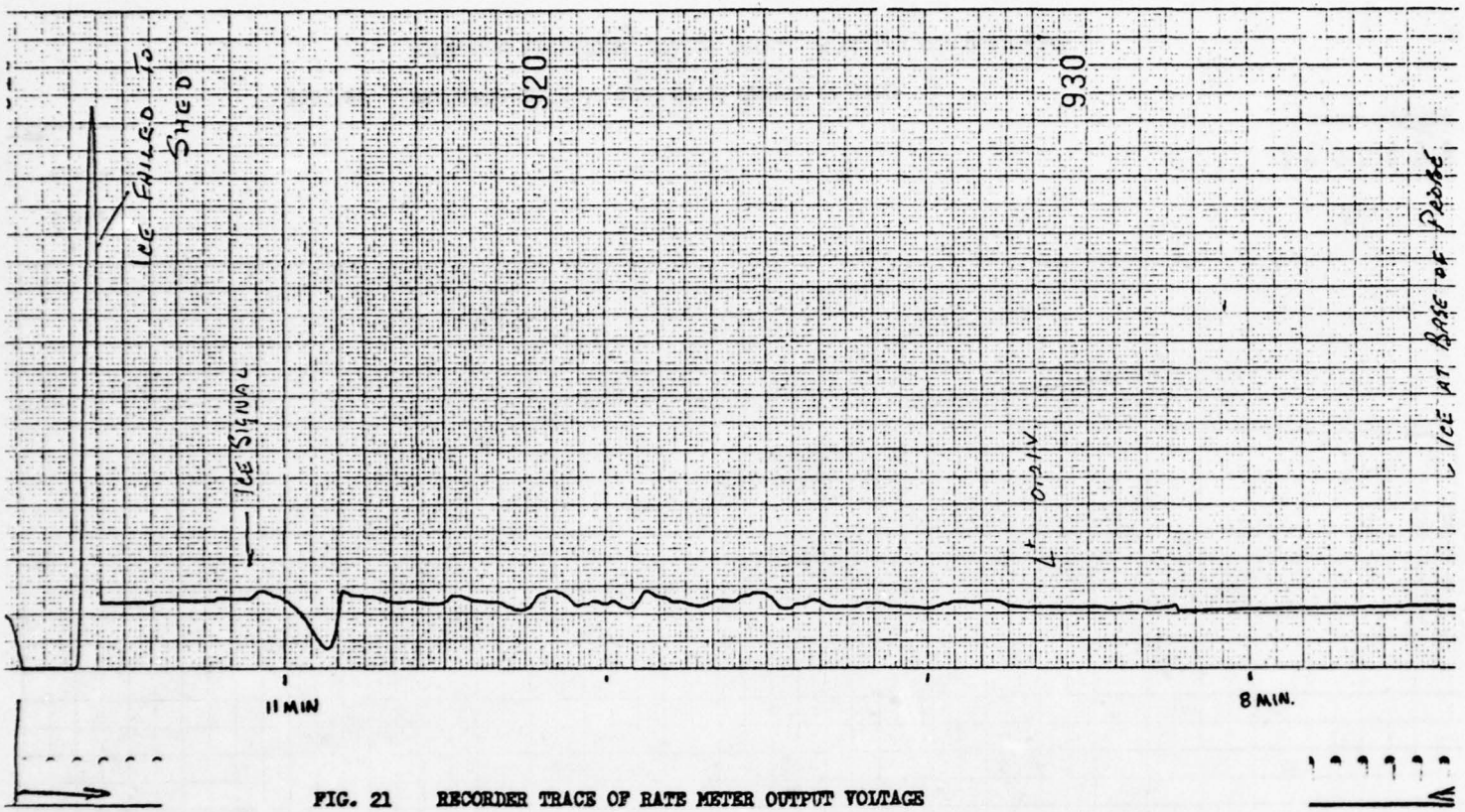

FIG. 21 RECORDER TRACE OF RATE METER OUTPUT VOLTAGE

AIRSPEED: 150 KNOTS, STATIC TEMP.: -5°C, L.W.C.: 0.10 g/m^3

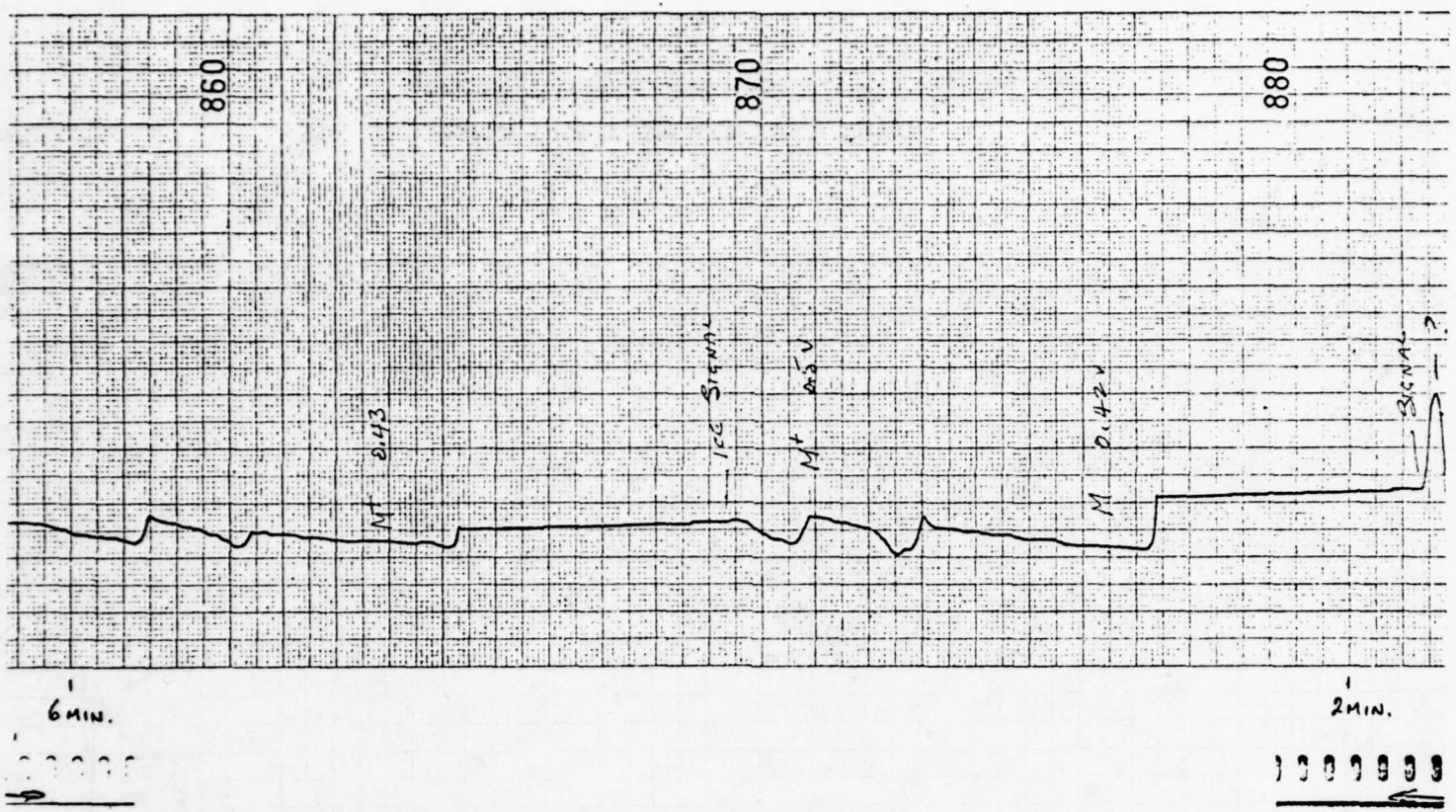

FIG. 22 RECORDER TRACE OF RATE METER OUTPUT VOLTAGE

AIRSPEED: 150 KNOTS, STATIC TEMP.: -5°C, L.W.C.: 0.22 g/m^3

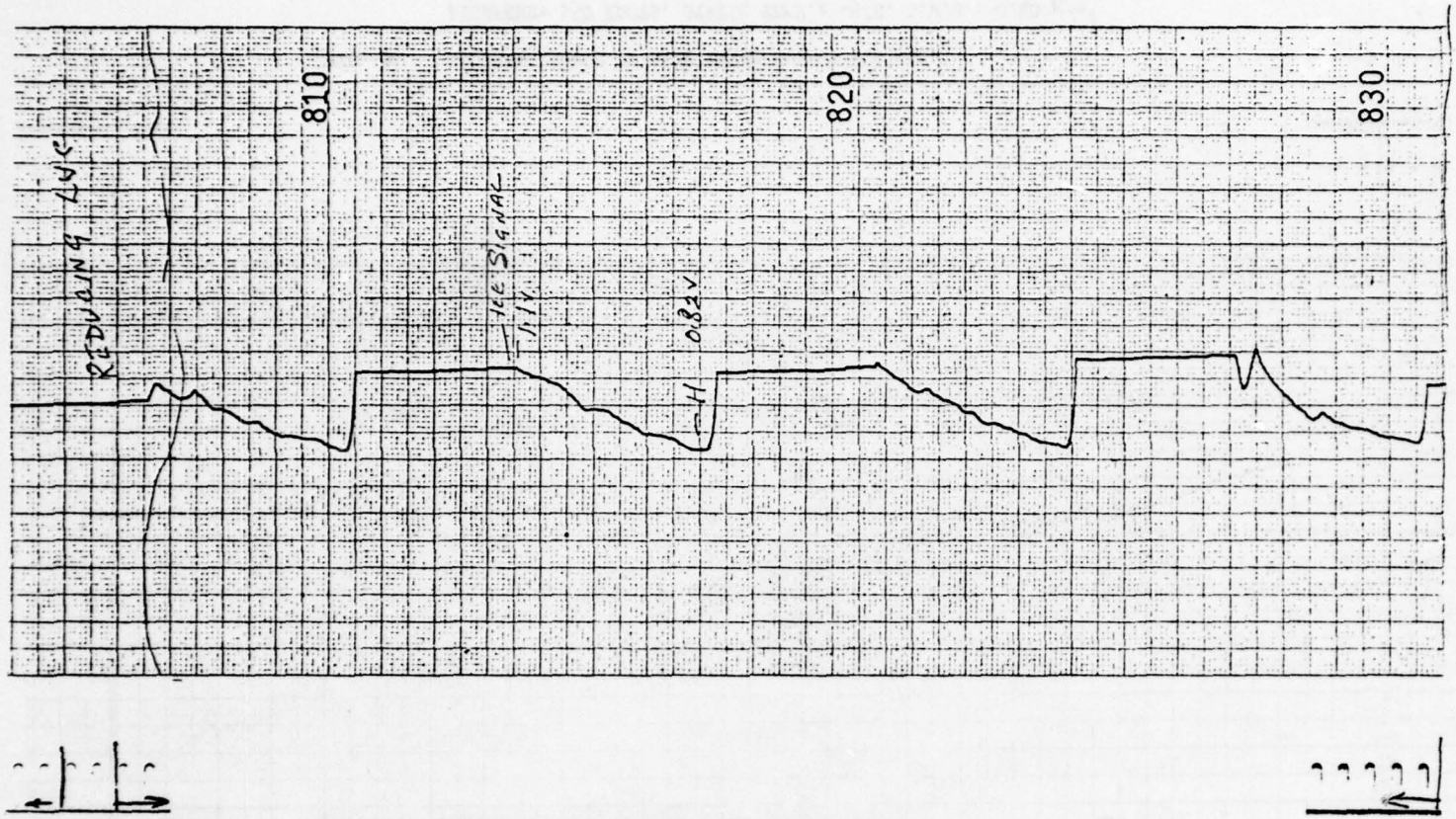

FIG. 23 RECORDER TRACE OF RATE METER OUTPUT VOLTAGE

AIRSPEED: 150 KNOTS, STATIC TEMP.: -5°C, L.W.C.: 0.46 g/m^3

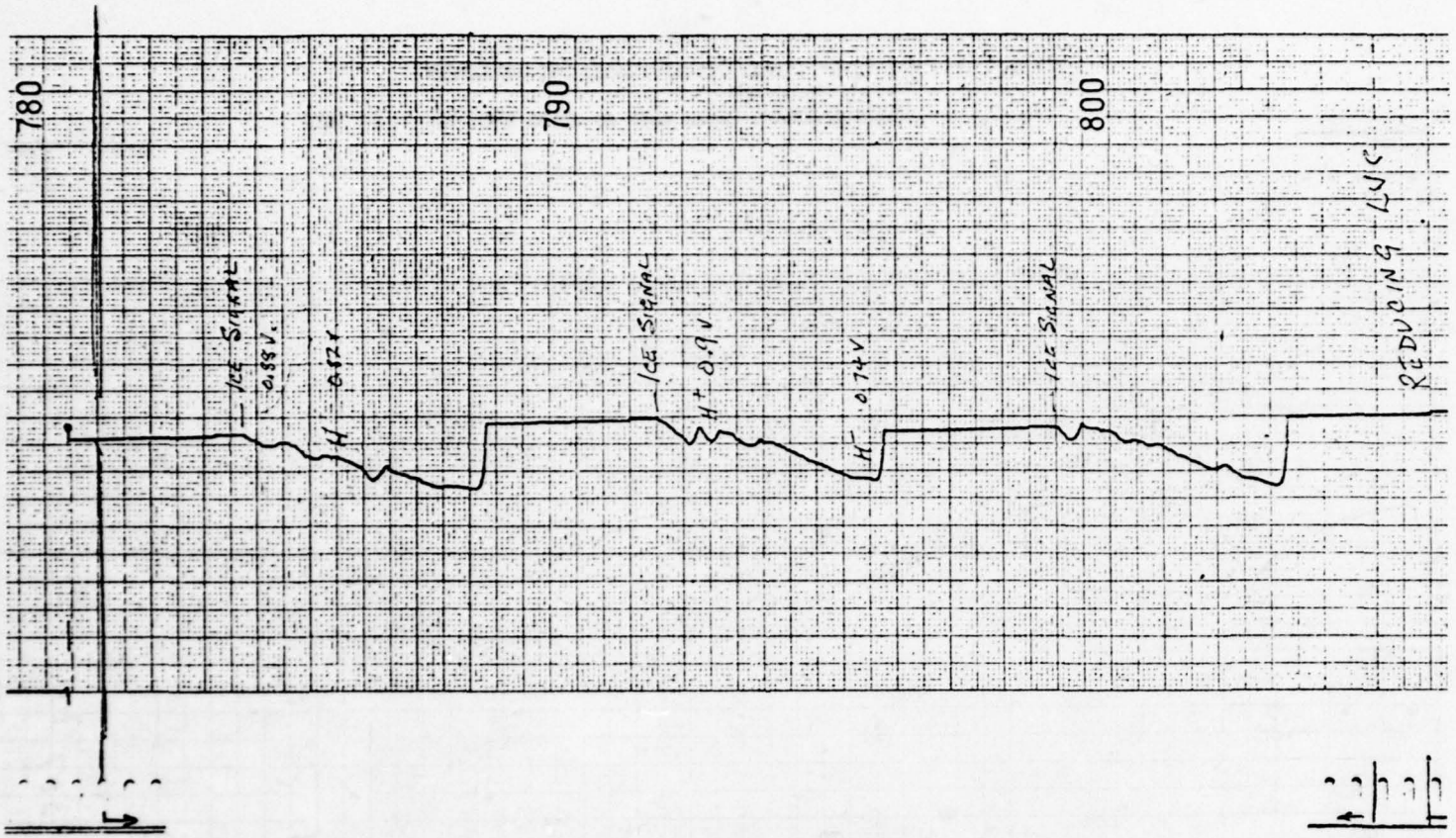

FIG. 24 RECORDER TRACE OF RATE METER OUTPUT VOLTAGE

AIRSPEED: 150 KNOTS, STATIC TEMP.: -5°C, L.W.C.: 0.40 g/m^3

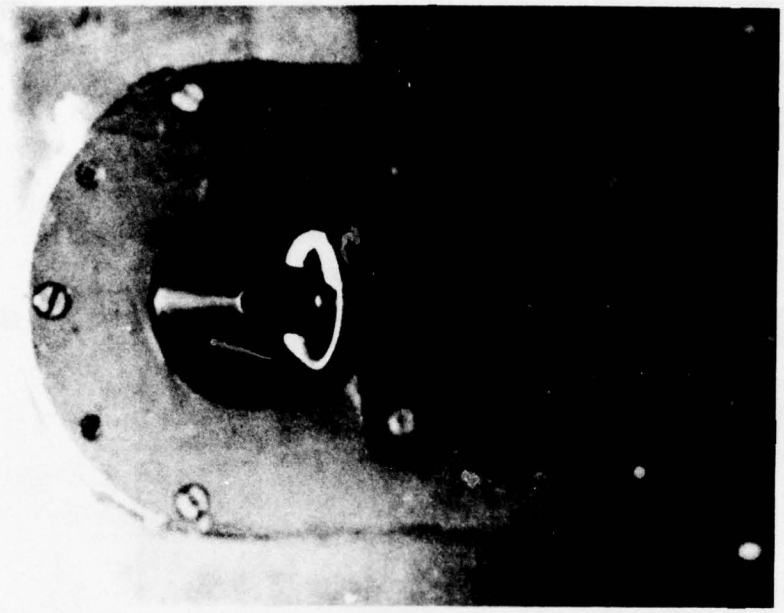

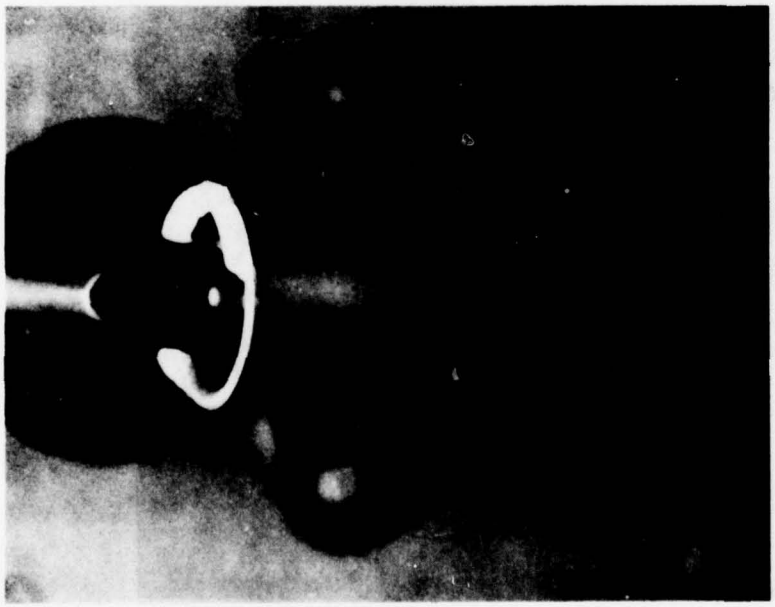

FIG. 25 SHOWING ICE ON ASPIRATOR LIP AND AT CORNERS OF NOTCH IN ASPIRATOR

AFTER 7 MINUTES AT 150 KNOTS, -15°C, 0.22 G/M^3

BLEED AIR PRESSURE 40 PSIG, TEMPERATURE 69°C

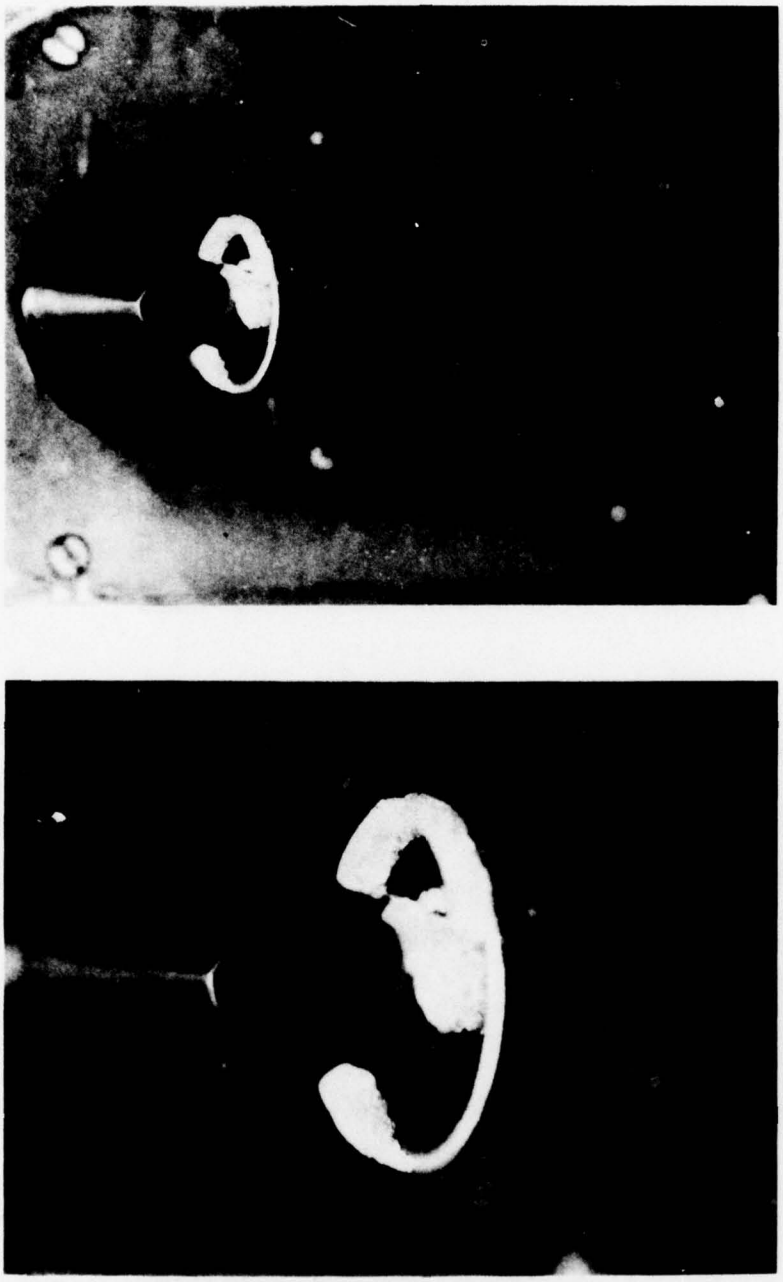

FIG. 26 SHOWING ICE ON ASPIRATOR LIP AND AT BASE OF SENSING PROBE

AFTER 5 MINUTES AT 150 KNOTS, -15°C, 0.4 G/M^3

BLEED AIR PRESSURE 40 PSIG, TEMPERATURE 70°C

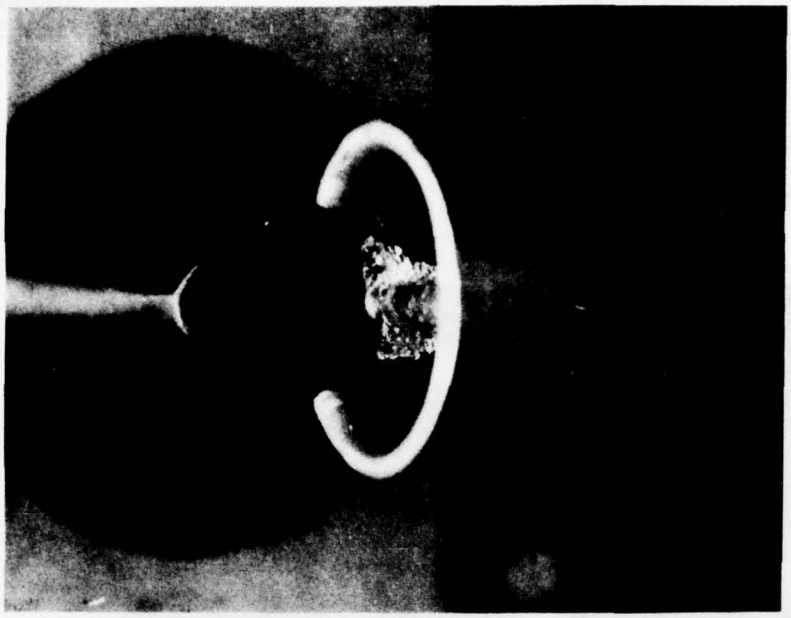

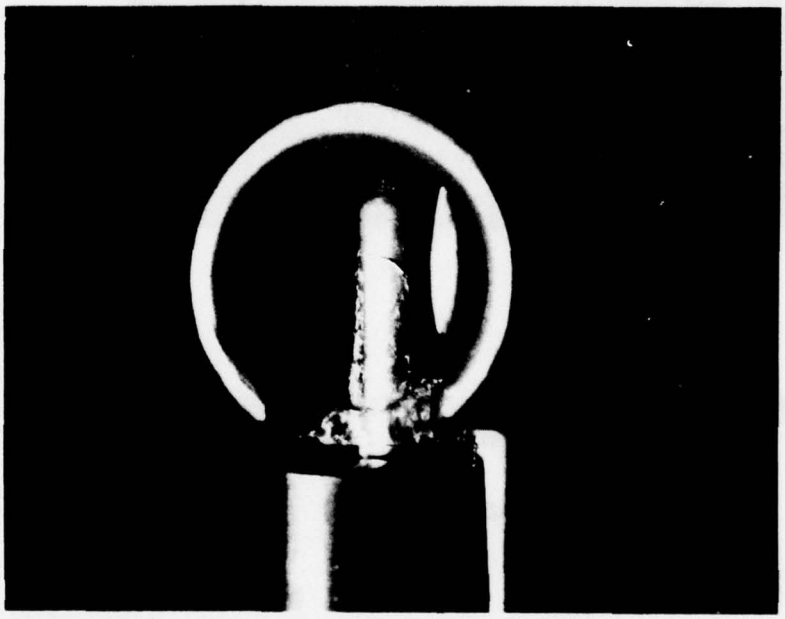

FIG. 27(a) SHOWING ICE THAT FAILED TO SHED FROM PROBE

AFTER 6 MINUTES AT 150 KNOTS, -5°C, 0.1 G/M^3

BLEED AIR PRESSURE 40 PSIG, TEMPERATURE 73°C

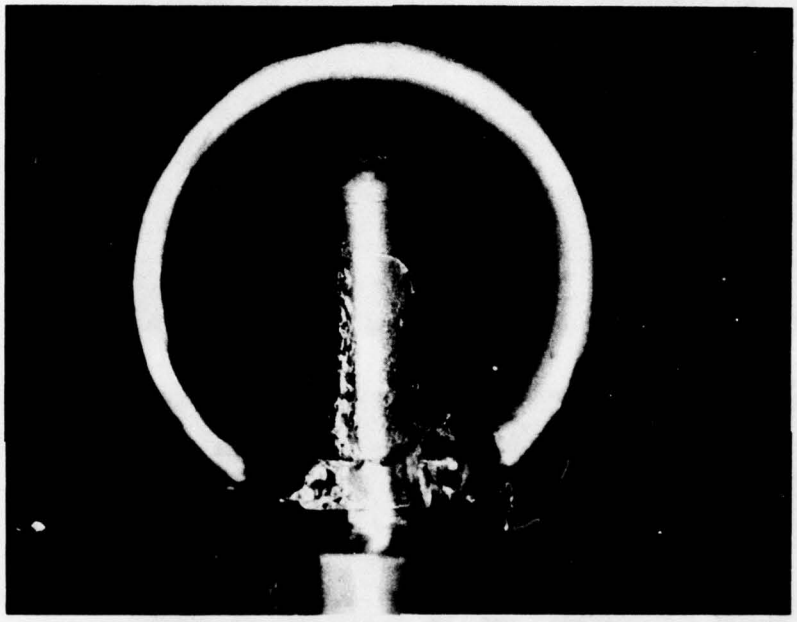

FIG. 27(b) SHOWING ICE THAT FAILED TO SHED FROM PROBE

CONDITIONS AS FIG. 27(a)

APPENDIX B. CONFIRMATORY CALIBRATION TESTS OF LEIGH INSTRUMENTS, LTD., ICE DETECTOR S/N 109

DIVISION OF MECHANICAL ENGINEERING

DIVISION DE GÉNIE MÉCANIQUE

CANADA

LIMITED

PAGES
PAGES 10

FIG.
DIAG. 7

REPORT
RAPPORT

REPORT
RAPPORT LTR-LT-77

DATE
DATE June 1977

SECTION

Low Temperature Laboratory

LAB. ORDER
COMM. LAB. 19478A

FILE
DOSSIER 3741-2

FOR
POUR Leigh Instruments Ltd., Carleton Place, Ontario.

REFERENCE
RÉFÉRENCE

LTR-LT-77

CONFIRMATORY CALIBRATION TESTS OF
LEIGH INSTRUMENTS LTD. ICE DETECTOR S/N 109

SUBMITTED BY
PRÉSENTÉ PAR T. R. Ringer
SECTION HEAD
CHEF DE SECTION

AUTHOR
AUTEUR J. R. Stallabrass

APPROVED
APPROUVÉ
DIRECTOR
DIRECTEUR

TABLE OF CONTENTS

LIST OF ILLUSTRATIONS

SUMMARY

Calibration tests of Leigh Instruments Ltd. Ice Detector S/N 109 were made to confirm and extend earlier calibration results provided by Leigh Instruments Ltd. No change in the basic calibration at 100 knots was evident; this calibration was extended to a liquid water content of 2.4 g/m^3. The effects due to changes in bleed air temperature, bleed air pressure, altitude and yaw were investigated, as well as low speed performance down to 10 knots.

1.0 INTRODUCTION

At the conclusion in April 1977 of the icing flight trials at Ottawa of a UH-1H helicopter conducted by the U. S. Army Air Mobility Research and Development Laboratory and Lockheed Aircraft Corporation, a confirmatory calibration was made of the Leigh Instruments Ltd. ice detector used on these trials.

Calibration was made in the high speed wind tunnel of the Low Temperature Laboratory on the Leigh Instruments Ltd. system comprising:-

Ice Detector Unit, Mk 10-3D	S/N 109
Icing Rate Circuit	S/N 001
Integrating Rate Unit	S/N IRU4

2.0 CALIBRATION PROCEDURE

The ice detector unit was mounted in a side wall of the wind tunnel test section. The signal (ramp) output from the detector was applied to the inputs of the Icing Rate Circuit (IRC) and the Integrating Rate Unit (IRU). This ramp voltage was also recorded on an analog pen recorder.

With the bleed air supply to the detector adjusted to the appropriate pressure and temperature, the wind tunnel velocity and air temperature set, the water sprays were adjusted to provide the approximate liquid water content (LWC) desired. When "on condition", eight (generally) consecutive readings of the indicated LWC displayed by the Integrating Rate Unit were recorded, followed immediately by a monitoring of the actual LWC by means of the rotating cylinder method (Ref. 1).

3.0 TEST CONDITIONS

The following calibrations or investigations were made:-

3.1 Basic Confirmatory Calibration. Made at 100 knots I.A.S., -10°C total temperature, and bleed air supply of 50 psig and 70°C, and at a series of liquid water contents up to about 2.5 g/m^3.

3.2 As 3.1, but for the 3 highest LWC's only, and at -20°C total temperature in order to improve the reliability of the rotating cylinder LWC measurements (i.e. to minimize exceeding the Ludlam limit).

3.3 As 3.1, but for the 3 highest LWC's only, and with a reduced bleed air temperature of 30°C.

3.4 Effect of Bleed Air Pressure. Conditions as in 3.1 except that the LWC was held constant at about 0.5 g/m^3, but with the bleed air pressure varied from 30 psig to 80 psig.

3.5 Effect of Bleed Air Pressure. Conditions as in 3.4 except LWC held at about 0.25 g/m^3.

3.6 Effect of Bleed Air Pressure. Repeat of 3.4.

3.7 Effect of Bleed Air Pressure. Conditions as in 3.4 except LWC held at about 0.75 g/m^3.

3.8 Effect of Bleed Air Pressure at Reduced Speed. Similar to Condition 3.4 except at 30 knots indicated airspeed.

3.9 Effect of Altitude. Conditions as in 3.1 except that the altitude was 10,000 ft., the LWC was 0.42 g/m^3, but at two bleed air pressures, i.e. 35.4 psig referenced to room pressure (approx. 14.7 psia) equivalent to 40 psig referenced to static pressure (10.1 psia) at 10,000 ft., and 40 psig referenced to room pressure.

3.10 Low Speed Performance. Made at a series of indicated airspeeds from 100 knots down to 10 knots at a static air temperature of -15°C, with bleed air at 50 psig and 70°C, and with a constant water flow rate to the spray nozzles (implying an approximately inverse relationship between LWC and airspeed).

3.11 Effect of Yaw. At an airspeed of 10 knots, air temperature -15°C, bleed air 50 psig and 70°C, and sprays set for a LWC of approximately 1 g/m^3, the detector head was set at yaw angles of 0°, 30° and 60°.

3.12 Anti-icing Performance. Three additional tests were run under severe conditions to check anti-icing performance and for photographic purposes.

4.0 TEST RESULTS

The various test conditions and the test results are tabulated in Table I. In addition to the average of the 8 (or sometimes more) indicated LWC readings, both the lowest and the highest indications are also shown.

Fig. 1 shows the results of the basic calibration at 100 knots (Test Conditions 3.1 and 3.2). The reduction in bleed air temperature (Condition 3.3) is seen from the Table to have no significant effect at the higher values of concentration employed, nor was any icing of the ejector duct apparent.

The effect of bleed pressure to the ejector is seen in Fig. 2 at an airspeed of 100 knots (Conditions 3.4, 3.5 and 3.7). The results of Condition 3.6 are not plotted in Fig. 2 for clarity and because of no significant difference from those of Condition 3.4.

The effect of bleed air pressure when operating at an airspeed of 30 knots (Condition 3.8) is shown in Fig. 3.

Fig. 4 demonstrates the low speed performance of the system. The sprays were set at about their lowest controllable flow rate, and this flow rate maintained at all speeds. Because of the resulting variation of LWC with

speed, the indicated LWC at each speed was divided by its corresponding true LWC and this ratio plotted against speed. A point at 100 knots was included to provide a reference.

Figs. 5a and 5b show the detector head at the conclusion of 3 minutes at 100 knots I.A.S., -11°C and 2.4 g/m^3. The head itself has remained free of ice apart from a few innocuous specks of ice on the trailing edge of the tail pipe. Runback ice has formed on the trailing edge of the strut, but does not affect the performance of the detector.

The static temperature was dropped to -18°C with the same airspeed and liquid water content. Figs. 6a and 6b show the result after 5 minutes. Ice has now formed on both the outside and inside of the tail pipe. However, in spite of the fairly considerable blockage of the tail pipe, no abnormal effect on the LWC indications resulted.

Fig. 7 shows the detector after 10 minutes at 150 knots I.A.S., -15°C and 0.56 g/m^3. No problems were encountered under these conditions, and normal LWC indications were given throughout the run.

5.0 DISCUSSION

5.1 Basic Calibration at 100 Knots. This series of points confirms and extends the previous calibration of this ice detector system. As Fig. 1 demonstrates, a 1:1 relationship exists between the indicated and true liquid water contents at 100 knots. At a static air temperature of -21°C, this correspondence holds good up to a LWC of 2.5 g/m^3, while at -11°C saturation occurs at LWC's in excess of about 1.8 g/m^3. The scatter in the indicated LWC readings is shown in Fig. 1 by the vertical bars. This scatter is due in part to variations in the spray density in the wind tunnel, and in part also to variations in the ice growth pattern on the ice detector probe. This latter effect can be seen in Fig. 1 by the increase in the spread that occurs as the Ludlam Limit is approached and/or exceeded as the LWC increases. Particularly apparent in this regard is the increase in spread at -11°C compared with that at -21°C at the LWC of 1.42 g/m^3.

5.2 Effect of Bleed Air Pressure. At an airspeed of 100 knots, the test results (Fig. 2) show no significant effect due to bleed air pressure variations between about 30 psig and 65 psig. Above 65 psig, however, an instability and some increase in the indicated readings are apparent, particularly at LWC's above about 0.5 g/m^3. To double check on this, Condition 3.6, a repeat of 3.4, was run with no significant difference. This peculiarity is currently unexplained, but since it lies outside the normal operating range of the device, it is considered to be largely of academic interest only.

At 30 knots (Fig. 3) the loss of ram effect results in a greater dependence on compressor bleed air pressure as is to be expected, and is the reason that a fairly close tolerance on the air supply pressure is desirable.

5.3 Effect of Altitude. Because the pressure of the compressor bleed air decreases with altitude such that a gauge pressure of 60 psig at sea level reduces to a gauge pressure of about 40 psig at 10,000 ft., it seemed desirable to check the performance of the detector at altitude with reduced supply pressure (i.e. Test Condition 3.9). The results (see Table) suggest no significant change in performance under altitude conditions.

5.4 Low Speed Performance. Reference to Fig. 4 shows that a minimum in the LWC ratio of about 0.65 occurs at about 40 knots airspeed, and that below this speed the ratio increases so that at speeds below about 20 knots and in the hover the instrument reads essentially the true LWC.

5.5 Effect of Yaw. These three runs (Condition 3.11) at minimum airspeed show a decided increase in the indicated value of LWC at a yaw angle of 30°, and a slight decrease at an angle of 60°. Thus, at speeds close to the hover, although some deviation from calibrated output may be expected, the instrument is still responsive even at considerable yaw angles.

5.6 Detector Head Anti-icing Performance. Three particularly severe conditions (Conditions 3.12) were run to investigate the anti-icing performance of the detector head. The first and third of these were completely satisfactory; the second, at conditions more severe than Intermittent Maximum, must be considered marginal in view of the ice that built up within the tail pipe even though no apparent abnormalities in LWC indication occurred in the five minutes of the run.

6.0 REFERENCE

1. Rush, C. K.
Wardlaw, R. L. "Icing Measurements with a Single Rotating Cylinder". NRC, NAE Lab. Rept. LR-206, 1957.

TABLE I - TEST RESULTS

Condition No.	WIND TUNNEL PARAMETERS						BLEED AIR		ICE DETECTOR SYSTEM INDICATED LWC			COMMENTS
	Ind. Airspeed kts.	True Airspeed kts.	Total Temp. °C	Static Temp. °C	Altitude ft.	LWC g/m³	Pressure psig	Temp. °C	Min. g/m³	Max. g/m³	Average g/m³	
3.1	100	96	-10	-11	650	0.26	50	69	0.22	0.24	0.23	Basic calibration
	"	"	"	"	"	0.55	"	70	0.51	0.55	0.54	@ 100 kt., 50 psig
	"	"	"	"	"	0.85	"	"	0.82	0.92	0.87	
	"	"	"	"	"	1.42	"	"	1.37	1.65	1.51	
	"	"	"	"	"	1.86	"	"	1.72	1.93	1.82	
	"	"	"	"	"	2.4	"	"	1.71	2.05	1.81	
3.2	100	94	-20	-21	640	1.42	50	70	1.46	1.56	1.50	
	"	"	"	"	"	1.86	"	"	1.84	2.00	1.92	
	"	"	"	"	"	2.4	"	"	2.23	2.54	2.42	
3.3	100	96	-10	-11	720	1.42	50	30	1.49	1.75	1.66	Reduced bleed air
	"	"	"	"	"	1.86	"	"	1.66	2.00	1.84	temperature
	"	"	"	"	"	2.4	"	"	1.73	2.08	1.91	16 readings made
3.4	100	96	-10	-11	720	0.52	70	69	0.58	0.74	0.65	Effect of bleed
	"	"	"	"	"	"	50	69	0.50	0.52	0.51	air pressure
	"	"	"	"	"	"	30	70	0.46	0.48	0.47	
	"	"	"	"	"	"	60	"	0.49	0.52	0.50	
	"	"	"	"	"	"	65	"	0.49	0.52	0.505	
	"	"	"	"	"	"	80	"	0.47	0.70	0.57	
	"	"	"	"	"	"	75	"	0.55	0.65	0.60	
	"	"	"	"	"	"	70	"	0.51	0.61	0.55	
	"	"	"	"	"	"	65	"	0.48	0.53	0.51	

TABLE I - TEST RESULTS (cont'd.)

Condition No.	WIND TUNNEL PARAMETERS						BLEED AIR		ICE DETECTOR SYSTEM INDICATED LWC			COMMENTS
	Ind. Airspeed kts.	True Airspeed kts.	Total Temp. °C	Static Temp. °C	Altitude ft.	LWC g/m³	Pressure psig	Temp. °C	Min. g/m³	Max. g/m³	Average g/m³	
3.5	100	97	-10	-11	1000	0.24	30	70	0.19	0.21	0.205	Effect of bleed air pressure
	"	"	"	"	"	"	50	"	0.22	0.23	0.22	
	"	"	"	"	"	"	60	"	0.22	0.23	0.23	
	"	"	"	"	"	"	70	"	0.21	0.22	0.22	
	"	"	"	"	"	"	80	"	0.21	0.22	0.215	
3.6	100	97	-10	-11	1000	0.52	50	70	0.49	0.52	0.505	Effect of bleed air pressure
	"	"	"	"	"	"	60	"	0.49	0.53	0.51	
	"	"	"	"	"	"	70	"	0.51	0.69	0.58	
	"	"	"	"	"	"	80	"	0.51	0.77	0.63	
3.7	100	97	-10	-11	1000	0.72	80	70	0.82	1.31	1.04	Effect of bleed air pressure
	"	"	"	"	"	"	70	69	0.77	0.96	0.86	
	"	"	"	"	"	"	60	69	0.70	0.73	0.72	
	"	"	"	"	"	"	50	70	0.71	0.75	0.73	
	"	"	"	"	"	"	30	71	0.67	0.70	0.69	
	"	"	"	"	"	"	80	70	0.80	1.05	0.94	
3.8	30	29	-10	-10	300	0.62	70	70	0.65	0.78	0.70	Effect of bleed air pressure @ reduced speed
	"	"	"	"	"	"	50	"	0.46	0.66	0.57	
	"	"	"	"	"	"	30	"	0.29	0.34	0.31	
3.9	100	115	-10	-12	9500	0.42	35.4	70	0.42	0.45	0.435	Effect of Altitude
	"	"	"	"	10000	"	40	69	0.41	0.45	0.43	

TABLE I - TEST RESULTS (cont'd.)

Condition No.	WIND TUNNEL PARAMETERS						BLEED AIR		ICE DETECTOR SYSTEM INDICATED LWC			COMMENTS
	Ind. Airspeed kts.	True Airspeed kts.	Total Temp. °C	Static Temp. °C	Altitude ft.	LWC g/m³	Pressure psig	Temp. °C	Min. g/m³	Max. g/m³	Average g/m³	
												Low speed performance
3.10	100	96	-14	-15	1000	0.14	50	70	0.11	0.12	0.12	LWC ratio = 0.86
	50	48	-15	"	600	0.32	"	"	0.20	0.22	0.21	LWC ratio = 0.66
	40	38	"	"	600	0.42	"	"	0.27	0.28	0.27	LWC ratio = 0.64
	30	29	"	"	550	0.56	"	"	0.35	0.39	0.38	LWC ratio = 0.68
	20	19	"	"	530	0.59	"	"	0.41	0.61	0.50	LWC ratio = 0.85
	10	9.5	"	"	520	1.2	"	"	1.07	1.36	1.16	LWC ratio = 0.97
												Effect of yaw
3.11	10.5	10	-15	-15	600	1.02	50	70	1.06	1.20	1.13	0° yaw
	11.5	11	"	"	"	0.95	"	"	1.53	1.84	1.71	30° yaw
	11	10.5	"	"	"	0.88	"	"	0.78	0.87	0.82	60° yaw
												Anti-icing performance
3.12	100	97	-10	-11	1000	2.4	50	70	1.77	1.92	1.84	See Figs. 5a & 5b
	"	96	-16.5	-18	"	2.4	"	"	1.93	2.22	2.07	See Figs. 6a & 6b
	150	146	-12	-15	1700	0.56	"	"	0.75	0.89	0.82	See Fig. 7

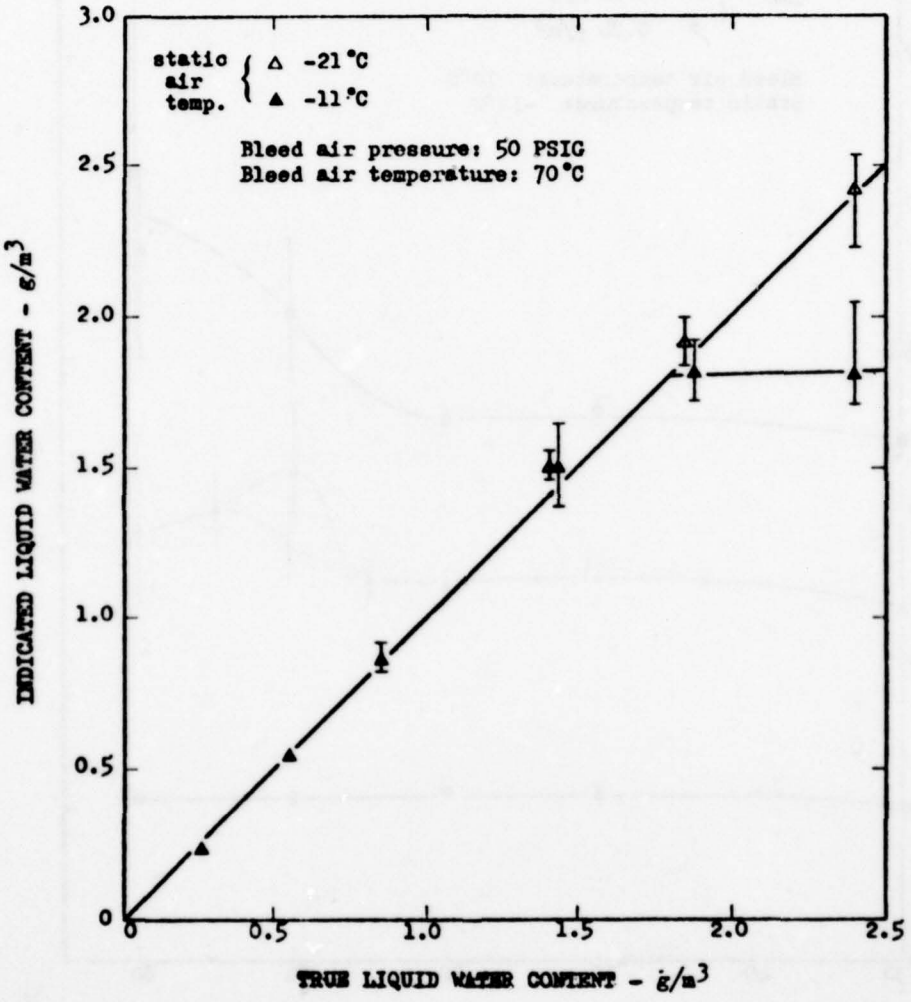

FIG. 1 BASIC CALIBRATION AT 100 KNOTS

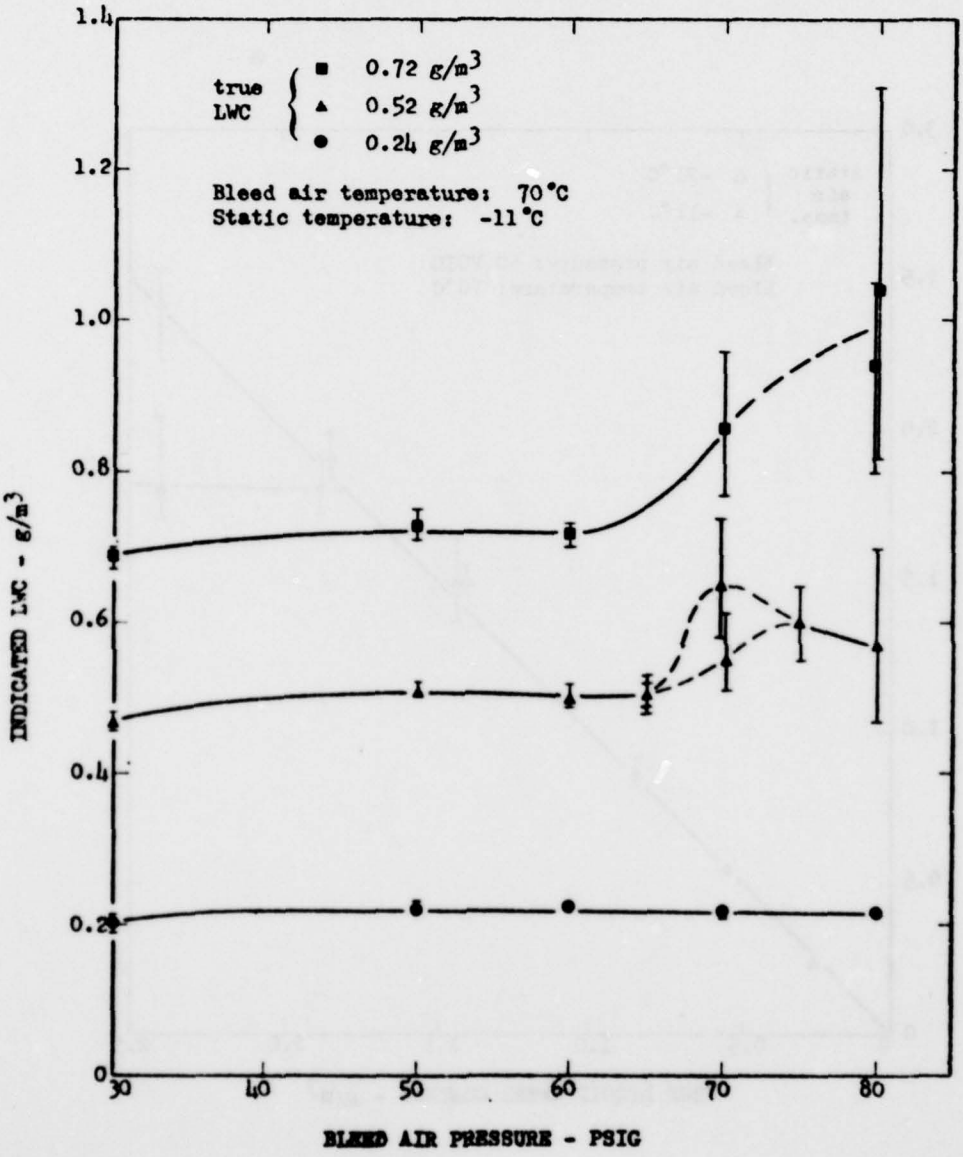

FIG. 2 EFFECT OF BLEED AIR PRESSURE AT 100 KNOTS

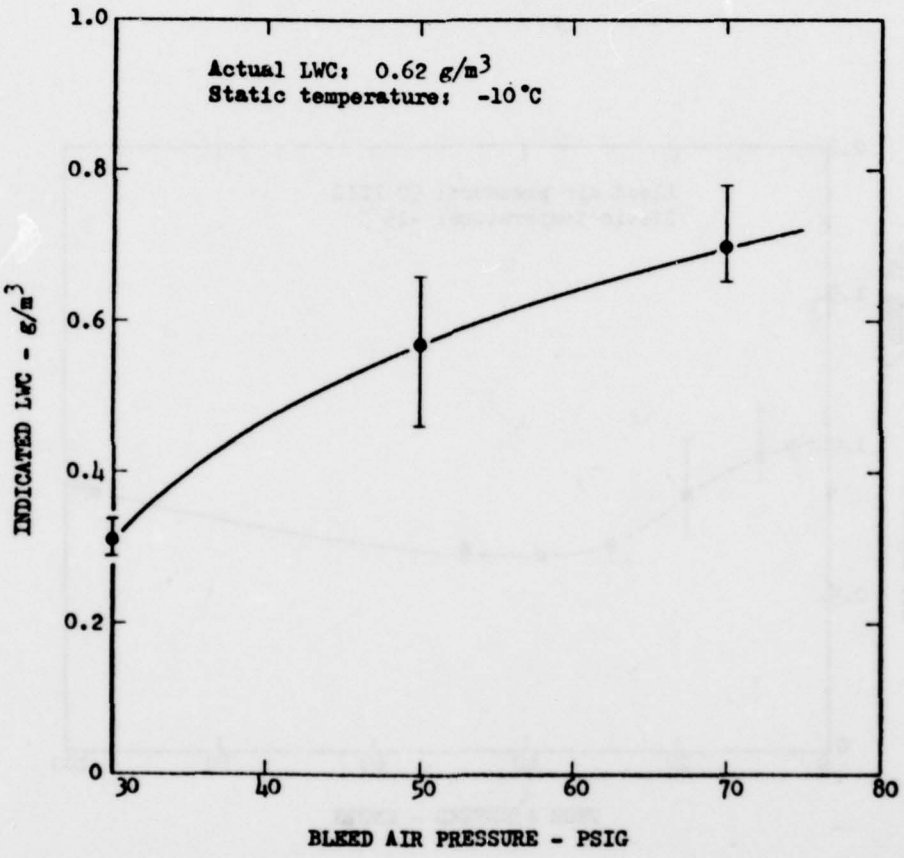

FIG. 3 EFFECT OF BLEED AIR PRESSURE AT 30 KNOTS

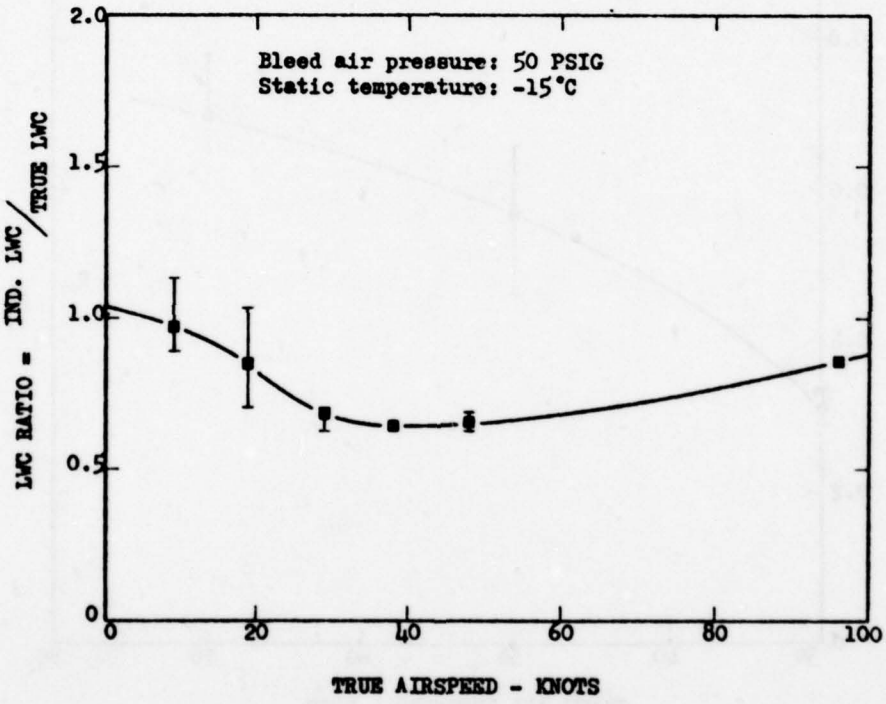

FIG. 4 LOW SPEED PERFORMANCE

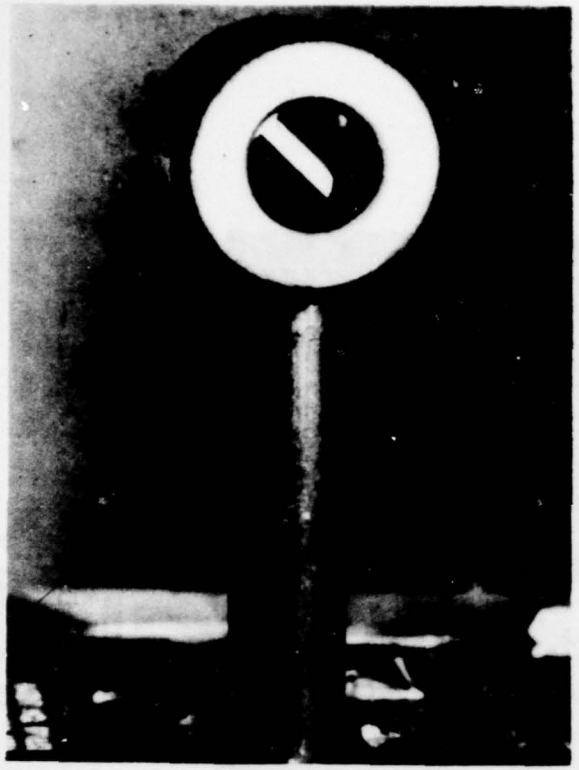

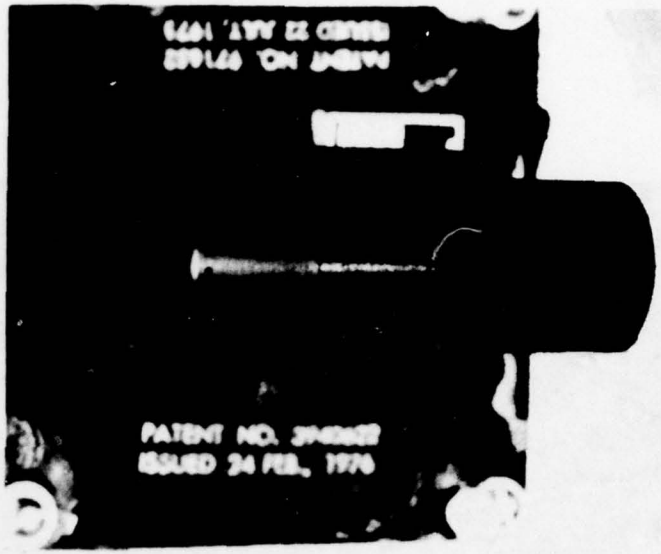

FIG. 5a ANTI-ICING PERFORMANCE

After 3 minutes at:
IAS 100 kts.
T_S -11°C
LWC 2.4 g/m^3

LTR-LT-77
Fig. 5a

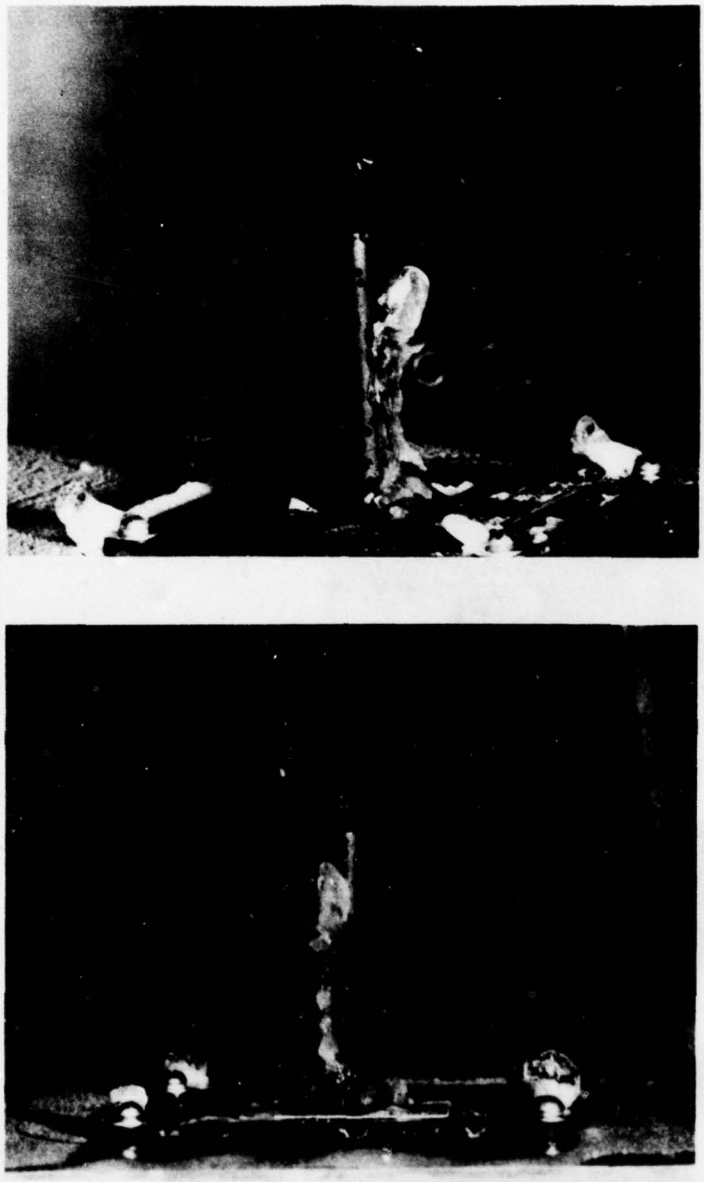

FIG. 5b ANTI-ICING PERFORMANCE

After 3 minutes at:

IAS	100 kts.
T_S	-11 °C
LWC	2.4 g/m^3

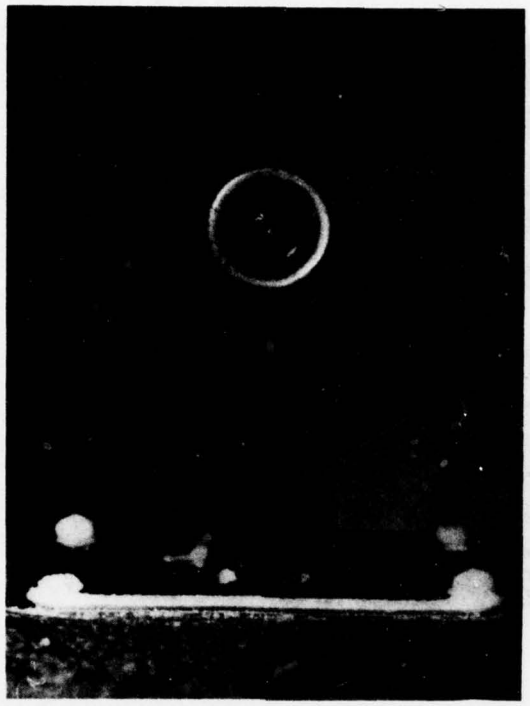

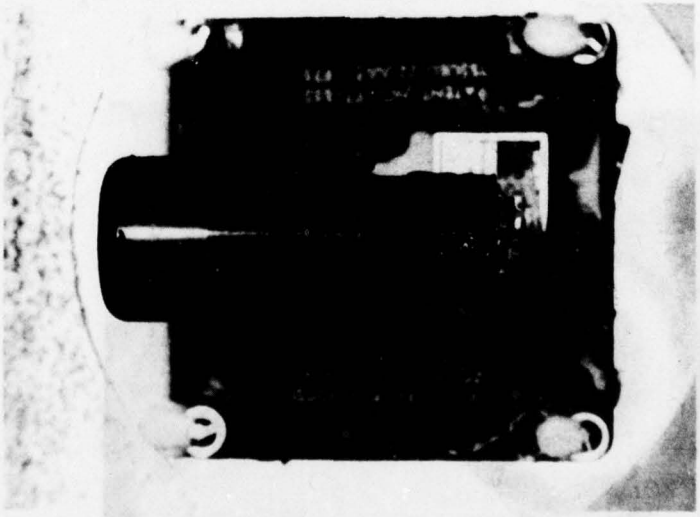

FIG. 6a ANTI-ICING PERFORMANCE

After 5 minutes at:

IAS	100 kts.
T_S	-18 °C
LWC	2.4 g/m^3

FIG. 6b ANTI-ICING PERFORMANCE

After 5 minutes at: IAS 100 kts.
T_S -18°C
LWC 2.4 g/m^3

LTR-LT-77
Fig. 6b

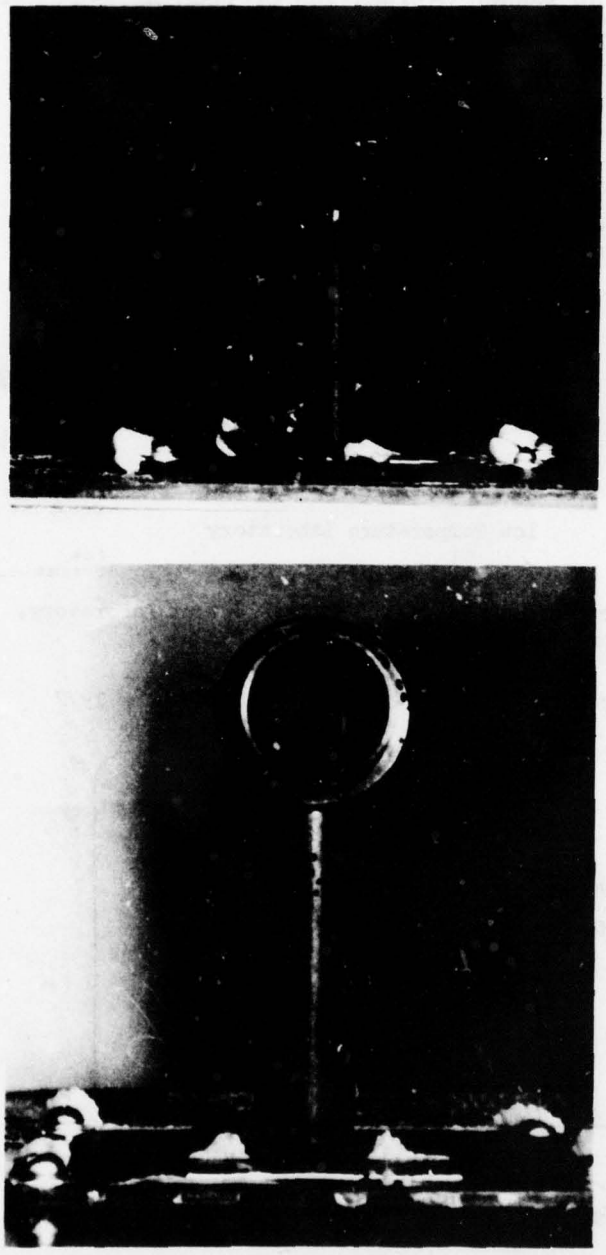

FIG. 7 ANTI-ICING PERFORMANCE

After 10 minutes at:
IAS 150 kts.
T_S -15°C
LWC 0.56 g/m^3

AD-A059 704 LOCKHEED-CALIFORNIA CO BURBANK F/G 1/3
NATURAL ICING FLIGHT TESTS AND ADDITIONAL SIMULATED ICING TESTS--ETC(U)
JUL 78 R H COTTON DAAJ02-77-C-0002
UNCLASSIFIED LR-28240 USAAMRDL-TR-77-36 NL

3 OF 3
ADA
059704

END
DATE FILMED
12-78
DDC

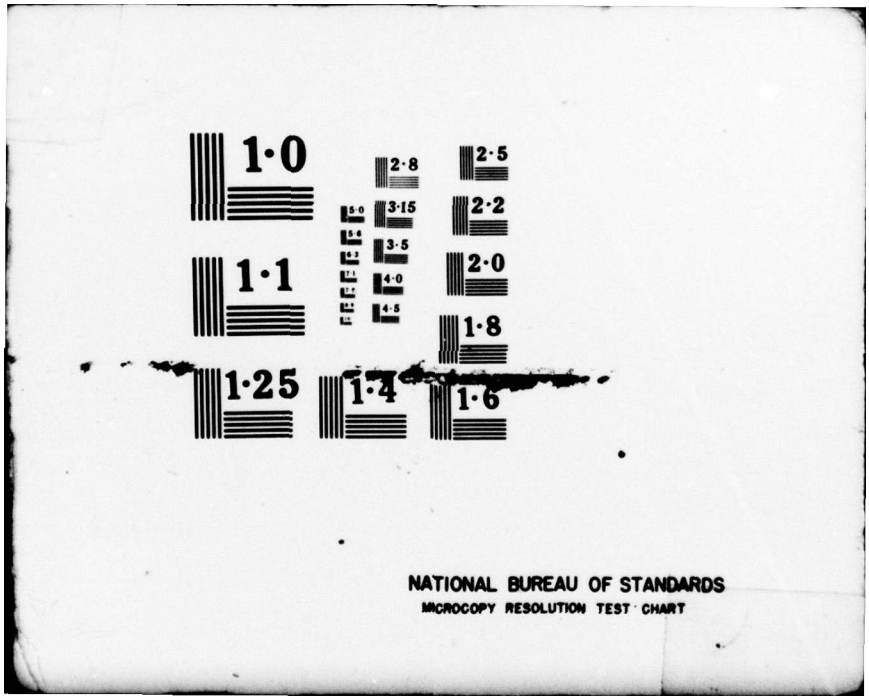
1·0
1·1
1·25
2·8
3·15
3·5
4·0
4·5
1·4
2·5
2·2
2·0
1·8
1·6
NATIONAL BUREAU OF STANDARDS
MICROCOPY RESOLUTION TEST CHART

APPENDIX C. ICING WIND TUNNEL CALIBRATION OF NORMALAIR-GARRETT, LTD., ASPIRATED ICING SEVERITY INDICATOR

DIVISION OF MECHANICAL ENGINEERING

DIVISION DE GÉNIE MÉCANIQUE

CANADA

LIMITED

PAGES 8

FIG. 5

REPORT RAPPORT

REPORT RAPPORT LTR-LT-75

DATE May 1977

SECTION

Low Temperature Laboratory

LAB. ORDER COMM. LAB. 21022X

FILE DOSSIER 3742-5

FOR POUR U. S. Army Air Mobility Research and Development Laboratory, Eustis Directorate, Fort Eustis, Virginia 23604.

REFERENCE RÉFÉRENCE Purchase Order DAAJ02-77-M-0004 dated 14 February 1977

LTR-LT-75

ICING WIND TUNNEL CALIBRATION OF NORMALAIR-GARRETT LTD. ASPIRATED ICING SEVERITY INDICATOR

SUBMITTED BY PRÉSENTÉ PAR T. R. Ringer
SECTION HEAD CHEF DE SECTION

AUTHOR AUTEUR J. R. Stallabrass

APPROVED APPROUVÉ
DIRECTOR DIRECTEUR

TABLE OF CONTENTS

LIST OF ILLUSTRATIONS

SUMMARY

Calibration of a Normalair-Garrett aspirated icing severity meter was made in an icing wind tunnel. Because of inadequate anti-icing of the aspirator, the instrument gave unreliable readings at temperatures of -10°C and below. At a temperature of -5°C the calibration at 90 knots was good for liquid water contents in excess of about 0.35 g/m^3, while at 30 knots the indicated LWC was about one half of the true value.

1.0 INTRODUCTION

At the conclusion of the icing flight trials at Ottawa in April 1977 of a UH-1H helicopter, the U. S. Army Air Mobility Research and Development Laboratory requested a calibration be made of the Normalair-Garrett Ltd. inferential icing severity indicator used on the helicopter.

Calibration was made in the high speed icing wind tunnel of the Low Temperature Laboratory in the presence of a U. S. Army observer on the Normalair Garrett Ltd. system comprising:-

Sensor Head	Dwg. 7726N000, Ser. NG2519
Aspirator	Dwg. 7722N000, Ser. NG2539
Controller	Dwg. 7266C000, Ser. NG2404
Meter	Dwg. 7598N000, Ser. NG2273
Pressure Regulator	Dwg. 3422B000, Ser. B1867

The system was wired in accordance with Fig. 1.

2.0 CALIBRATION PROCEDURE

The sensor head and aspirator were mounted on a side wall of the wind tunnel test section. The air to the pressure regulator was supplied at a pressure of 40 psig and at a temperature of 70°C. It was found that the pressure regulator reduced the air pressure supplied to the aspirator to 18 psig, and that the air consumption was 5 scfm.

Calibration was to be made at four combinations of airspeed and static temperature as follows:- Airspeed: 90 knots and 30 knots; Static Temperature: -15°C and -5°C. However, because of icing problems at -15°C, the lower test temperature was amended to -10°C during the course of the tests. At each of these conditions the liquid water content in the tunnel was adjusted to a series of values ranging from about 0.2 g/m^3 to about 1.5 g/m^3. At each value the exact LWC was measured using the rotating cylinder method (Ref. 1) and the reading of Normalair-Garrett icing severity meter was noted.

3.0 TEST RESULTS

As received, the meter had a mechanical zero error of about +0.02 g/m^3. The meter was mechanically re-zeroed before starting the tests.

A chronology of all the test conditions and the response of the ice detector (as indicated by the meter reading) is presented in the Table.

It was found that the heat capacity of the bleed air when supplied to the aspirator at 70°C was insufficient to maintain the aspirator anti-iced at or below the following conditions:-

1. 90 knots true airspeed, -10°C static air temperature.
2. 30 knots true airspeed, -15°C static air temperature.

It was also found that a bleed air temperature of 100°C was insufficient to clear the ice at 90 knots true airspeed and -15°C static air temperature.

Under any of these conditions, ice not only formed on the inlet lip of the aspirator (except in the area where the air entered the lip cavity), but also within the duct itself, where almost complete blockage occurred where the sensor head was located, as Figs. 3 and 4 illustrate.

The effect of this ice in the duct was to cause initially the meter reading to climb to a high value and thereafter to drop to a zero or near zero reading as the ice blockage became more complete. It was therefore not possible to relate the meter indication to the existing liquid water content under these conditions.

At 90 knots and -5°C, in spite of a little fluctuation, it was possible to relate the meter reading to liquid water content as Fig. 5 indicates. The meter indication appears to cut out at water concentrations below about 0.2 g/m^3, while calibration is good at about 0.35 g/m^3 and above.

At 30 knots and -10°C considerable time was required before a reasonably stable indication was given by the meter, and it seems possible that, although no ice formed on the inlet lip of the aspirator, some ice in fact formed within the duct, at least at liquid water contents in excess of 0.5 g/m^3. The sudden drop in reading from 0.7 g/m^3 to 0.1 g/m^3 half a minute after the water content had been reduced from 0.76 to 0.34 g/m^3 would be consistent with a piece of ice in the duct shedding. It would appear therefore that operation is marginal under these conditions of airspeed and ambient temperature.

At 30 knots and -5°C reasonably consistent operation resulted and the relation between indicated and actual liquid water content is shown in Fig. 5. Some increased fluctuation in indication was apparent at the LWC of 0.68 g/m^3, and this was thought possibly to be the result of the rather considerable amount of water flowing on the aspirator duct walls. At this speed (30 knots) the indication given was about one half of that at 90 knots.

4.0 REFERENCE

Rush, C. K.
Wardlaw, R. L. Icing Measurements with a Single Rotating Cylinder. National Research Council of Canada, NAE Laboratory Report LR-206, September 1957.

TABLE OF TEST CONDITIONS AND RESULTS

TUNNEL PARAMETERS			BLEED AIR		N.G.L. Meter Reading g/m^3	Fig. No.	Elapsed Time min.	Comments
True Airspeed kts.	Static Temp. °C	L.W.C. g/m^3	Pressure psig	Temp. °C				
90	-15	0.25	40	70	0		0	2/3 of aspirator nose icing over.
					~0.7		~1	Reading climbed to ~0.7 g/m^3.
					0		~5	Reading fell back to zero.
								Bleed air temperature increased.
90	-15	0.25	40	100	0.1 - 0.9		~10	Aspirator nose not de-icing, Meter reading fluctuating.
90	-15	0.25	40	75	0.1 - 0.9	2	~12	No change. Shut down. Ice on aspirator nose removed.
90	-10	0.25	40	72	0 - 0.05		0	Meter slowly came off zero.
					0.03 - 0.1 Av. 0.05		1	Reading fluctuating. Upper 1/2 of aspirator nose icing.
					0.17		6	Reading more steady. Ice removed from aspirator nose.
90	-10	0.37	40	72	0.75		11	L.W.C. increased. Reading slowly increased to 0.75.
					~0.5		16	Then decreased to ~0.5 g/m^3. Upper 1/2 of aspirator nose iced.
					0.4		20	Further slight decrease. Ice removed from nose.
90	-10	0.68	40	73	0.85		23	L.W.C. increased. Upper 1/2 of aspirator nose icing.
					1.5		24	Reading climbed.
					0		26	Reading dropped to zero.
					0	3	27	Shut down. Photographs taken. Ice in duct.
90	-5	0.23	40	70	0 - 0.1 (Av.0.05)		0	Reading fluctuating.
				73	0 - 0.1		5	Aspirator nose remaining free of ice.
90	-5	0.68	40	73	Av. 0.65		9	L.W.C. increased. Light on.
90	-5	0.37	40	73	0.32		13	L.W.C. decreased. Light off.
90	-5	0.25	40	73	0.1		15	L.W.C. decreased.
90	-5	0.8	40	73	0.75		17	L.W.C. increased. Light on.

TABLE OF TEST CONDITIONS AND RESULTS

TUNNEL PARAMETERS			BLEED AIR		N.G.L. Meter Reading g/m^3	Fig. No.	Elapsed Time min.	Comments
True Airspeed kts.	Static Temp. °C	L.W.C. g/m^3	Pressure psig	Temp. °C				
30	-15	0.23	40	69	0		0	Meter not moving off zero.
					0+		4	Needle just off stop.
					0.01 - 0.05		7	Ice on upper 1/4 of inlet lip.
30	-15	0.70	40	70	0.3 - 0.4 (Av. 0.35)		9	Meter reading fluctuating.
					0.4		13	
					0.55		15	Reading slowly climbing. Light on.
					0.65		16	Reading slowly climbing. Light on.
							17	Shut down. Ice cleared from duct.
30	-10	0.51	40	70	0.1		0	
					0.2		3	Inlet lip remaining clear of ice.
					0.25		4	
				69	0.3 - 0.35		6	
					0.35 - 0.4		8	
					0.35 - 0.4		10	
30	-10	0.76	40	69	0.5		11	L.W.C. increased.
					0.55		14	Light on.
					0.7		16	Reading climbing. L.W.C. reduced.
30	-10	0.34	40	69	0.1		16½	Reading dropped suddenly.
					0.2		18	Reading steady.
					0.2		22	Reading still steady. Shut down.
30	-5	0.35	40	69	0.15		0	Reading moderately steady.
					0.2		3	
					0.2		4	
					0.15		5	
30	-5	0.52	40	70	0.2 - 0.3		6	L.W.C. increased.
					0.25		12	
30	-5	0.68	40	70	0.4 -		13	L.W.C. increased.
					0.35 - 0.4		17	Reading made a momentary drop to 0.2 g/m^3
					0.1 - 0.4		19	Reading fluctuating. Considerable water flowing on aspirator surface. Shut down.

TABLE OF TEST CONDITIONS AND RESULTS

TUNNEL PARAMETERS			BLEED AIR		N.G.L. Meter Reading g/m^3	Fig. No.	Elapsed Time min.	Comments
True Airspeed kts.	Static Temp. °C	L.W.C. g/m^3	Pressure psig	Temp. °C				
30	-5	1.4	40	73	0.8		0	Light on at 0.55 g/m^3. Occasional fluctuations in reading.
							6	Dropping temperature to take rotating cylinder L.W.C. measurement.
30	-16	1.4	40	72	increasing to ~1.1		8	Ice forming on and in aspirator.
	-16.5						9	
					Av. 0.8		10	Reading fluctuating between 1.1 & 0.6.
30	-16.5	1.4	40	72	0		11	Reading dropping to zero.
90	-18	0.8	40	70	0.7 - 0.8		0	
					~1.4		2	3/4 of aspirator nose iced.
90	-18	0.8	40	70	~1.7		7	
						4	8	Shut down.

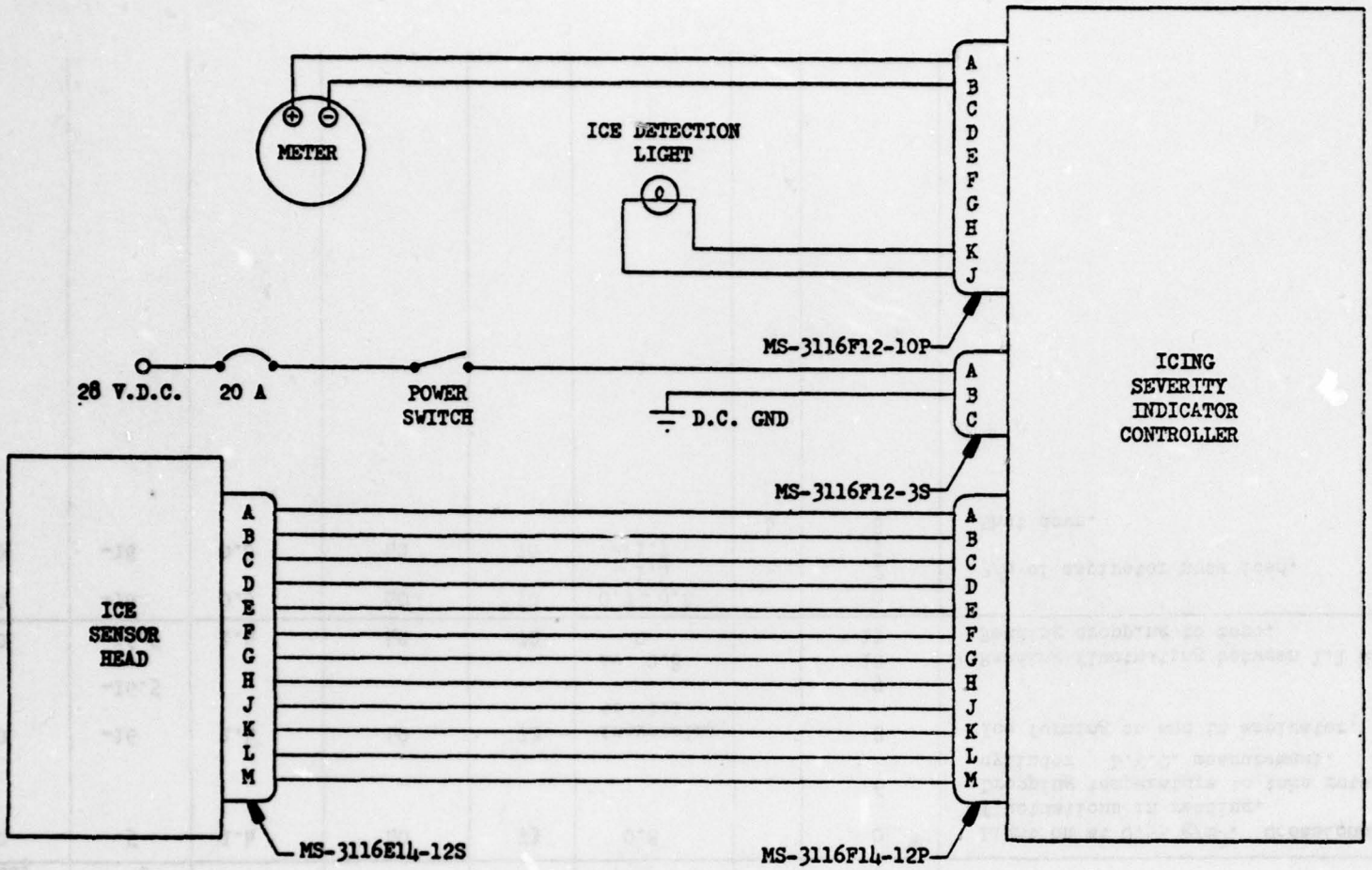

FIG. 1. NGL ICE DETECTOR SYSTEM WIRING DIAGRAM-ICING TUNNEL TEST

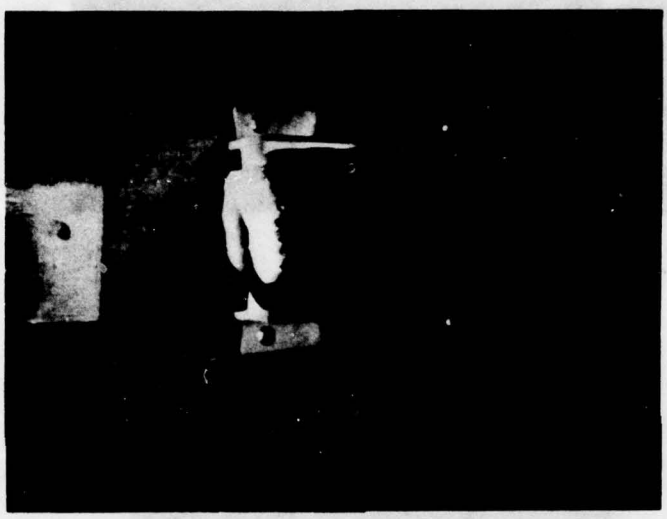

FIG. 2 ICE ON ASPIRATOR NOSE

12 MINUTES AT 90 KNOTS, -15°C, 0.25 G/M^3

BLEED AIR PRESSURE 40 PSIG, TEMPERATURE 70 - 100°C

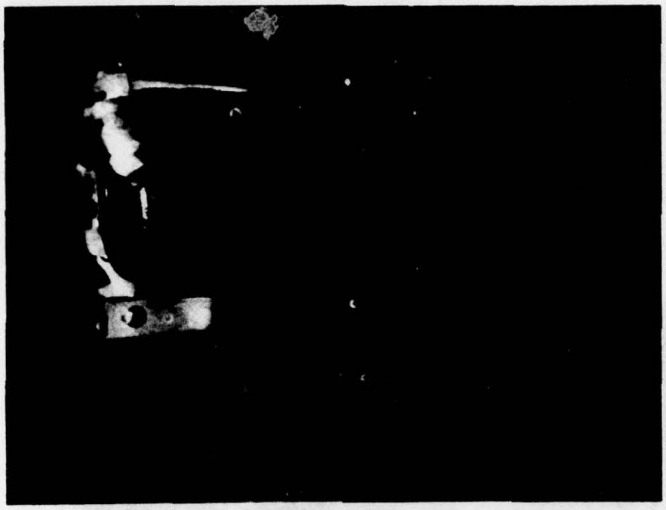

FIG. 3 ICE ON ASPIRATOR LIP AND WITHIN DUCT

AT COMPLETION OF 27 MINUTE RUN AT 90 KNOTS, -10°C WITH LWC'S OF 0.25, 0.37 AND 0.68 G/M^3.

BLEED AIR PRESSURE 40 PSIG, TEMPERATURE 72°C

FIG. 4 ICE ON ASPIRATOR LIP AND WITHIN DUCT
8 MINUTES AT 90 KNOTS, -18°C, 0.8 G/M^3
BLEED AIR PRESSURE 40 PSIG, TEMPERATURE 70°C

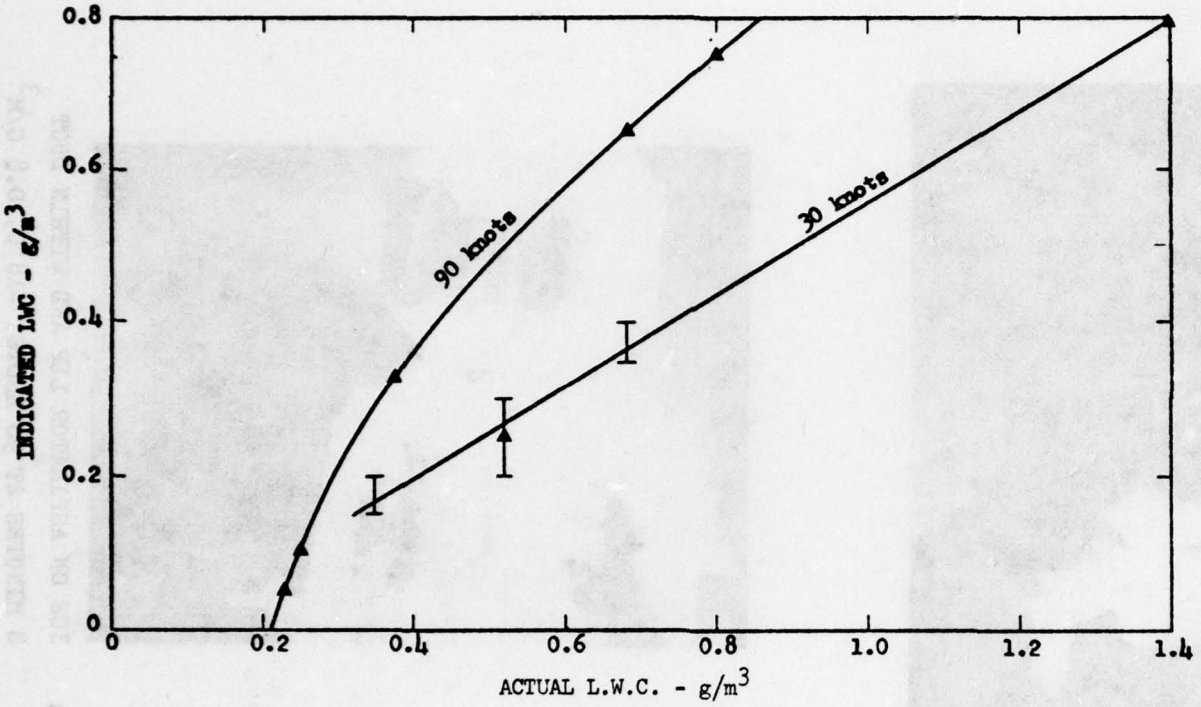

FIG. 5 RESULTS OF TESTS AT -5°C